

The correlation of keratin expression with in-vitro epithelial cell line differentiation

Aden, Deeqo

The copyright of this thesis rests with the author and no quotation from it or information derived from it may be published without the prior written consent of the author

For additional information about this publication click this link.

<https://qmro.qmul.ac.uk/jspui/handle/123456789/308>

Information about this research object was correct at the time of download; we occasionally make corrections to records, please therefore check the published record when citing. For more information contact scholarlycommunications@qmul.ac.uk

**The correlation of keratin expression with
in-vitro epithelial cell line differentiation**

Deeqo Aden

Thesis submitted to the University of London
for Degree of Master of Philosophy (MPhil)

Supervisors:

Professor Ian. C. Mackenzie
Professor Farida Fortune

Centre for Clinical and Diagnostic Oral Science
Barts and The London School of Medicine and Dentistry
Queen Mary, University of London

2009

Contents

Content pages	2
Abstract	6
Acknowledgements and Declaration	7
List of Figures	8
List of Tables	12
Abbreviations	14
<u>Chapter 1: Literature review</u>	16
1.1 Structure and function of the Oral Mucosa.....	17
1.2 Maintenance of the oral cavity.....	20
1.2.1 Environmental Factors which damage the Oral Mucosa.....	21
1.3 Structure and function of the Oral Mucosa	21
1.3.1 Skin Barrier Formation.....	22
1.4 Comparison of Oral Mucosa and Skin.....	24
1.5 Developmental and Experimental Models used in Oral mucosa and Skin.....	28
1.6 Keratinocytes.....	29
1.6.1 Desmosomes.....	29
1.6.2 Hemidesmosomes.....	30
1.6.3 Tight Junctions.....	32
1.6.4 Gap Junctions.....	32
1.7 Keratinocyte Differentiation.....	34
1.7.1 Molecules Involved in Transition from Basal to Suprabasal Differentiated Cells of the Epidermis	36
1.7.2 Factors influencing Keratinocyte Differentiation.....	38
1.8 Intermediate Filaments Proteins (IFPs).....	40
1.9 Intermediate Filament Structure.....	42
1.10 Keratins.....	43
1.11 Keratin Function.....	47
1.12 Mechanisms of Transcriptional Regulation of Keratin Gene Expression.....	48
1.13 Transcriptional regulation of keratin gene expression.....	49
1.13.1 Transcriptional regulation of K12 Gene.....	49
1.13.2 Transcriptional Regulation of K14, K3, K15 and K6 Genes.....	49
1.13.3 Transcriptional Regulation of K19 Gene.....	49
1.13.4 Transcriptional Regulation of K4 Gene.....	50
1.13.5 Transcriptional Regulation of K17 Gene	50
1.13.6 Transcriptional Regulation of K3 Gene	50
1.13.7 Using Proximal Promoters.....	51
1.14 Post-translational Modification of Keratin Proteins.....	52
1.14.1 Phosphorylation Modification of Other IFPs.....	54
1.15 Keratin Expression in Normal Epithelia.....	55
1.15.1 Hair-Specific Keratins.....	56
1.16 Keratin Expression in Pathology.....	58
1.17 Keratins Implicated in Genetic Diseases.....	59
1.17.1 Keratin Mutations and Overlapping Phenotypes	60
1.18 Keratin 13.....	61
1.18.1 Factors influencing K13 expression.....	62
1.18.2 K13 Expression in Development and Experimental Models.....	62

1.18.3 Epigenetic Control of Gene Expression.....	63
1.19 Keratin 15.....	65
1.19.1 K15 and 13 Expression as Models of <i>in-vitro</i> Epithelial Differentiation.....	65
1.19.2 Factors and Regulatory Elements influencing K15 Expression.....	66
1.20 Hypothesis and Aims of the Study.....	67
Chapter 2: Methods and Materials	69
2.1 Reporter Gene Assays	70
2.1.1 Wild-Type GFP to Variant EGFP.....	71
2.1.2 Control Plasmid Constructs used for Transfection.....	72
2.2 Cloning strategy for K15 and K13 Promoter Constructs.....	73
2.2.1 Construction of K15 and K13 Promoter Reporter Gene Plasmids.....	74
2.3 Polymerase Chain Reaction (PCR).....	74
2.4 pEGFP-N3B Vector.....	75
2.4.1 Abolishing AseI restriction site in pEGFP-N3 vector.....	75
2.4.2 Making the K13 and K15 Promoter Construct.....	78
2.5 Agarose Gel.....	82
2.5.1 Isolation of DNA from Agarose gel and DNA Purification.....	82
2.5.2 Ligation of Insert to Vector.....	82
2.5.3 Bacterial Strains used for Transformation in this Study.....	83
2.5.4 Plasmid Transformation using Competent Bacterial Cells.....	83
2.5.5 Restriction Digestion	83
2.6 Purification of Plasmid DNA from 3-10ml Bacterial Culture.....	84
2.6.1 Purification of Plasmid using Qiagen Maxiprep Kit.....	84
2.6.2 DNA Precipitation.....	84
2.7 Spectrophotometer.....	85
2.8 Cell Culture Media and Types of Cell.....	85
2.8.1 Cell Seeding and Counting using a Haemocytometer.....	86
2.9 DNA Transient transfection into adherent cell lines using Fugene 6.....	87
2.9.1 DNA Transient Transfection into Adherent Cell Lines using Lipofectamine.....	88
2.10 Fluorescence Activated Cell-Sorting (FACS) Analysis.....	88
2.10.1 Visualization of EGFP and DsRed Labelled Promoters.....	89
2.10.2 Flow Cytometry Data Analysis.....	89
2.10.3 Flow Cytometry.....	90
2.11 Addition of Pharmacological Agents to K13 and K15 Promoter Constructs.....	90
2.12 DNA Sequencing.....	91
2.13 Transcription Factor Database.....	91
2.14 Isolating and Truncating the Human K13 Promoter Construct.....	92
2.14.1 Designing Primers for pEGFP-N3BK13Pro-7.117kb.....	96
2.14.2 Designing Primers for Sequencing of pEGFP N3BK13Pro Deletion Series.....	98
2.14.3 Site-Directed Mutagenesis Kit.....	98
2.14.4 Quick-change Multi-site Directed Mutagenesis Kit (Stratagene).....	99
2.15 Immunocytochemistry.....	101
2.16 MTT Assay.....	102
2.16.1 MTT Assay procedure.....	103
2.17 Western Blot.....	103
2.17.1 Sample Collection.....	103
2.17.2 SDS PAGE.....	104
2.17.3 Protein Transfer Membrane using Semi-dry Method.....	104
2.17.4 Membrane Staining.....	104
2.17.5 Blocking Membrane.....	105

2.17.6 Antibody Binding.....	105
2.17.7 ECL Detection and Protein Exposure.....	105
2.17.8 Densitometry	106
2.18 Stable Transfection	106
2.18.1 K13 or K15 Promoter linked GFP Expression in Oral SCC25 Cells.....	106
2.18.2 Analysis of K13 and K15 Promoter expression by FACS.....	106
2.18.3 Analysis of K13 or K15 Promoter Expression using Colony Forming Assay.....	107
Chapter 3: Comparative bioinformatics analysis of keratin promoters	108
3.1 Introduction.....	109
3.2 Computational Approach to Identifying Transcription Factor Binding Sites.....	109
3.2.2 Technical Approach used to Identify Regulatory Elements.....	111
3.2.3 Computational Databases used to Identify Keratin Tissue-Specific.....	113
3.3 Aims.....	115
3.4 Materials and Methods.....	115
3.5 Results.....	116
3.5.1 5'-upstream region of Keratin Genes.....	116
3.5.2 Data Organisation and Analysis.....	118
3.5.3 Transcription Factor Selection.....	121
3.5.4 Tfbs in skin suprabasal keratins promoters.....	125
3.5.5 Tfbs in pathological suprabasal keratins promoters.....	127
3.5.6 Tfbs in palm and sole suprabasal keratins promoters.....	128
3.5.7 Tfbs in oral mucosa suprabasal keratins promoters.....	129
3.5.8 Tfbs in cornea suprabasal keratins promoters.....	130
3.5.9 Tfbs in simple epithelia suprabasal promoters.....	131
3.5.10 Comparison of Tfbs in basal and suprabasal promoters.....	131
3.6 Discussion.....	136
Chapter 4: Isolation and tissue specific expression of K13 promoter	138
4.1 Introduction.....	139
4.2 Aims.....	141
4.3 Materials and Methods.....	141
4.4 Results.....	143
4.4.1 Restriction Analysis of K13 and K15 Promoter Constructs	143
4.4.2 Restriction Digestion Analysis of K13 Promoter Deletion Fragments.....	145
4.4.3 K13 FL Promoter Sequence Information and Transcription Factor Database.....	148
4.4.4 DNA Sequencing Result.....	151
4.4.5 GFP Expression can be used to Quantify K13 Promoter Activity.....	154
4.4.6 Qualitative data of K13 promoter linked GFP specific expression.....	156
4.4.7 FACS analysis of K13 Promoter Expression.....	158
4.4.8 K13 Protein Expression using Western Blot.....	161
4.4.9 FACS Data.....	162
4.4.10 FACS Analysis of FL K13 promoter and R1 and R2 Deletion Fragments.....	163
4.4.11 Truncated K13 Promoter and R1 to R6 Deletion Fragments	167
4.4.12 Pathways involved in the Induction of K13 Expression.....	170
4.4.13 MTT Assay Result.....	170
4.4.14 Induction of K13 Expression by TPA.....	171
4.4.15 MEK 1/ 2 and PI3K/Akt pathways.....	174
4.4.16 Inhibition of MEK 1/ 2 Pathway and K13 FL Promoter Expression.....	175
4.4.17 Inhibition of PI3K/Akt Pathway and K13 FL Promoter Expression.....	178
4.4.18 Post-transcriptional Regulation of K13 Protein Expression.....	180
4.4.19 K13 Protein Expression in Epithelial Cell Lines.....	182

4.4.20 The effect of TSA and SB on K13 Expression in HeLa Cell Line.....	185
4.5 Discussion.....	187
Chapter 5: K15 and K13 expression with oral cell line maturation	193
5.1.Introduction.....	194
5.2 Aims.....	197
5.2.1 Hypothesis.....	197
5.2.2 Materials and Methods.....	197
5.3 Results.....	198
5.3.1 Affymetrix HG-U133A Arrays RNA extracts of K15 and K13.....	198
5.3.2 K15 and K13 Promoter Expression in SCC25, H357 and A431 Lines.....	199
5.3.3 Stably Transfecting and Selecting the K15 and K13 Promoter.....	202
5.3.4: K15 or K13 expression and Colony Forming Assay.....	204
5.3.5 K15 or K13 GFP Expression and Intensity Scoring Method.....	206
5.3.6: K15 or K13 Expression and FACS.....	213
5.3.7 Staining of K15 or K13 in SCC25 and A431 Cell Lines.....	215
5.4 Discussion.....	218
Chapter 6: General discussion and Futures	221
6.1 General discussion.....	222
6.2 Chapter 3 Discussion.....	222
6.2.1 TFsearch and Suprabasal Keratin Promoters.....	223
6.3 Chapter 4 Discussion.....	224
6.3.1 K13 FL Promoter and Deletion Fragments (R1-R6).....	225
6.3.2 Important Pathways Involved in K13 Induction in Oral SCC25 Cells.....	225
6.3.3 Altered Chromatin Structure Induced K13 Expression in RTS3b cells.....	227
6.4 Chapter 5 Discussion.....	227
6.4.1 K15 or K13 Expression using FACS and Colony Forming Assay.....	228
6.4.2 Use of Q-PCR for K15 or K13 Expression in Oral SCC25 cells.....	229
6.5 Limitations of the study.....	229
6.6 Future studies.....	231
6.7 Conclusion.....	232
References	234-251
Appendices	252-262

Abstract

The mechanism of transcriptional regulation which allows oral mucosal-specific expression of the human keratin 13 (*K13*) gene remains unknown. The pattern of expression of keratin genes in the oral mucosa shows sequential synthesis of specific basal and suprabasal keratins. *K15* and *K13* are respectively basal and suprabasal markers of buccal epithelial tissue. *K15* and *K13* expression are known to alter in oral squamous cell carcinoma. When differentiation occurs basal cells migrate to the suprabasal layer and *K15* synthesis stops and the synthesis of suprabasal markers like *K13* begins. The aims of the study are to determine whether the *K13* promoter can confer 1) oral mucosal cell-specific differentiation in *in-vitro* culture, 2) understand the mechanism by which different positive or negative regulators impose basal cell-specific promoter expression and how this differs from suprabasal promoter expression and 3) whether *K15* and *K13* expression can be correlated with *in-vitro* cell differentiation stage. To provide insight into the basal and suprabasal expression of *K15* and *K13*, their 5'-upstream sequence regions were linked to EGFP. The results show that the expression of *K15* and *K13* can be correlated with *in-vitro* cell differentiation stages in malignant epithelial cell lines. The full length *K13* promoter construct drove negligible GFP expression in the human foreskin fibroblast cell line and had a greater expression in the oral SCC25 cell line than the epidermal-derived RTS3b cell line. Therefore, the *K13* promoter sequence appears to contain suppressor elements conferring oral cell-specificity. The expression patterns of truncated *K13* promoter fragments after transient transfection into permissive, non permissive and non-epithelial cell lines, suggest binding of a negative regulatory element to the full length *K13*-3089bp promoter. *K13* expression is induced by pharmacological alteration of chromatin structure in non-permissive skin-derived RTS3b cells. The MEK 1/2 pathway seems not necessary for the expression of *K13*, but PI3K/Akt pathway is important for expression of *K13* in oral mucosa. In conclusion, the results suggest that keratin gene promoter expression can be correlated with *in-vitro* cell differentiation stages and these restricted differences in keratin expression might be co-ordinated by the synergistic action of transcription factors.

Acknowledgements

I would like to thank my supervisor professor Ian Mackenzie, Dr Peter Forbes and Dr Andriana Magariti, Dr Lesley Bergmeier for advising me on the write up and proof reading the thesis. I am also very grateful to both Dr Ahmad Waseem and Dr Hong Wan for their help with technical assistance in the project. I would also like to thank Dr Lisa Harper for teaching me about cell culture, Dr Felix Schnappauf, Dr Lisa Harper and Dr Gary Warnes for their tremendous help with the FACS machine, Dr Stuart Fawell for his initial help in the project and later on his help in keratin promoter sequence search, and Dr Ian McKay for his introduction on how use the transcription factor search database once the keratin promoter sequence was obtained. I would also like to thank Dr Muy-Teck Teh for his general help in the day to day life of the laboratory and for answering many of my endless questions. Special thanks to Adegun Oluyori, Adiam Bahta, Nagihan Bostanci and Sangeetha Thomson for being helpful to me on so many occasions and for their wonderful friendship. Last but not least I would like to say a big thank you to my mother and sister who have taught me the art of patience and the courage to see things through despite adversities.

This project was funded by the Medical Research Council.

Declaration

I declare that the majority of the work in this thesis submitted for MPhil degree is my own and anything else is either cited or individuals whose work I have used in this thesis are clearly acknowledged.

List of Figures

Chapter 1

- Figure 1.1 Keratin specific expression in keratinized and non-keratinized epithelia
- Figure 1.2 The anatomical location of three types of epithelia in the oral mucosa
- Figure 1.3 A cross section of the oral mucosa
- Figure 1.4 The symmetric and asymmetrical division pattern of epithelial stem cells
- Figure 1.5 Haematoxylin and eosin (H&E) staining of skin cross section
- Figure 1.6 Components of the stratum corneum layer of adult epidermis
- Figure 1.7 Schematic representations of skin and its associated appendages
- Figure 1.8 Desmosome structure
- Figure 1.9 Hemidesmosome structure
- Figure 1.10 The three types of cellular junctions (adhesion, gap and tight junction)
- Figure 1.11 Terminal differentiation processes in the epidermis
- Figure 1.12 Structure of Intermediate Filament Proteins (IFPs)
- Figure 1.13 The formation of keratin polypeptide into 12nm IF
- Figure 1.14 The number of exons and introns in K1 to K20 gene
- Figure 1.15 Function of keratins and other intermediate filament proteins
- Figure 1.16 Posttranslational mechanisms which regulate keratin expression
- Figure 1.17 Histone acetylation and DNA methylation in gene regulation
- Figure 1.18 Simplified diagram illustrating the overall aim of the study

Chapter 2

- Figure 2.1 Schematic showing how GFP expression was measured
- Figure 2.2 The four different types of constructs used in this study
- Figure 2.3 C-F Diagram showing steps taken to abolish AseI site from pEGFP-N3
- Figure 2.3 A-B Diagram showing steps taken to abolish AseI site from pEGFP-N3
- Figure 2.4 Details of human K13 or K15 promoter constructs
- Figure 2.5 Details of cloning K13 or K15 promoter into pEGFP-N3B vector
- Figure 2.6 A-C amplifying K13 or K15 and cloning into TOPO TA
- Figure 2.6 D-G Details of sub-cloning K13 or K15 promoter into pEGFP-N3B vector
- Figure 2.6 H-N PCR against different regions of the K13 FL promoter truncated
- Figure 2.6 H1-N1 Different constructs made from K13 FL promoter
- Figure 2.7 Diagrammatic representation of K13 gene and nucleotide sequence
- Figure 2.8 Overview of the Quick-change multi site directed mutagenesis method

Chapter 3

- Figure 3.1 Interdependence of the use of techniques and computational approach
- Figure 3.2 DNA sequence into transcription factor database
- Figure 3.3 Transcription factors binding basal K15 and suprabasal K13 promoters
- Figure 3.4 Diagram showing the location of intergene regions in genes
- Figure 3.5 TFsearch database result
- Figure 3.6 Transcription factor binding sites (Tfbs) in basal and skin suprabasal promoters.
- Figure 3.7 Tfbs in basal and pathological suprabasal promoters.
- Figure 3.8 Tfbs in basal and palm and sole suprabasal promoters
- Figure 3.9 Tfbs in basal and oral mucosa suprabasal promoters
- Figure 3.10 Tfbs in basal and cornea suprabasal promoters
- Figure 3.11 Tfbs in simple epithelia suprabasal promoters
- Figure 3.12 Overall Tfbs in basal and suprabasal keratin promoters
- Figure 3.13 Common Tfbs in basal and suprabasal keratins

Figure 3.14 Computer analysis of Tfbs which bind to basal/suprabasal keratins

Figure 3.15 Computer analysis of Tfbs which bind to suprabasal promoters

Chapter 4

Figure 4.1 Sizes of K13-FL promoter deletion constructs.

Figure 4.2 Restriction analysis of K13 and K15 promoter constructs

Figure 4.3 Restriction maps of enzymes used within insert and pEGFP-N3B vector

Figure 4.4 Restriction analysis of pEGFP-N3B containing K13 FL and inserts of various sizes

Figure 4.5 Analysis of 3kb K13 FL and inserts of various sizes religated back to pEGFP-N3B vector

Figure 4.6 Restriction analysis of pEGFP-N3B containing 3kb K13 FL and inserts of various sizes

Figure 4.7 K13 FL promoter DNA sequence

Figure 4.8 K13 deletion fragments (R1-R6) sequencing result

Figure 4.9 Entrez pubmed taxonomy blast result of sequenced K13 fragments

Figure 4.10 GFP and DsRed fluorescence in SCC25 cells

Figure 4.11 GFP reporter gene fluorescence versus CMV, K13 and K13 DNA conc

Figure 4.12 GFP fluorescence in oral SCC25 cells transfected with CMV or K13

Figure 4.13 GFP fluorescence in RTS3b cells transfected with CMV or K13

Figure 4.14 GFP/DsRed fluorescence in HeLa cells transfected with CMV or K13

Figure 4.15 GFP fluorescence in HFF cells transfected with CMV or K13 promoter

Figure 4.16 GFP expression of K13 FL promoter construct in various cell lines

Figure 4.17 GFP expression of CMV promoter in various cell lines

Figure 4.18 K13 protein expression in various cell lines

Figure 4.19 Evaluation of band density of K13 protein expression

Figure 4.20 Typical FACS dot plot data

Figure 4.21 The expression pattern of K13-FL, K13-R1, K13-R2 constructs

Figure 4.22 FACS dot plot expression of K13-FL, K13-R1, K13-R2 constructs in SCC25 cells

Figure 4.23 FACS dot plot expression of K13-FL, K13-R1, K13-R2 constructs RTS3b cells

Figure 4.24 FACS dot plot expression of K13-FL, K13-R1, K13-R2 constructs in HeLa cells

Figure 4.25 FACS dot plot expression of K13-FL, K13-R1, K13-R2 constructs in HFF cells

Figure 4.26 GFP expression of K13 FL, R1 to R6 constructs in SCC25, RTS3b, HeLa and HFF cell lines

Figure 4.27 MTT results of various pharmacological inhibitors

Figure 4.28 The effects of 100nM TPA on K13 FL, K13-1901bp promoter constructs

Figure 4.29 The effect of TPA on CMV promoter in pEGFP-N3B vector

Figure 4.30 The effect of TPA on K13 protein expression in oral SCC25

Figure 4.31 Evaluation of band density of K13 expression in the presence of TPA in oral SCC25 cells

Figure 4.32 The effect of MEK 1/2 pathway inhibitor PD98059 on K13 FL promoter

Figure 4.33 The effect of MEK 1/2 pathway inhibitor PD98059 on CMV promoter

Figure 4.34 Effect of MEK 1/2 inhibitor PD98059 on K13 protein expression

Figure 4.35 Evaluation of band density of K13 expression in the presence of inhibitor PD98059 in oral SCC25 cells

Figure 4.36 The effect of PI3K/Akt pathway inhibitor LY294002 effect on K13 FL promoter
Figure 4.37 The effect of PI3K/Akt pathway inhibitor LY294002 effect on CMV promoter
Figure 4.38 Effect of PI3K/Akt pathway inhibitor LY294002 on K13 protein
Figure 4.39 Evaluation of band density of K13 expression in the presence of PI3K-Akt pathway inhibitor LY294002 on K13 protein
Figure 4.40 K13 protein expression in various epithelial cell lines.
Figure 4.41 Evaluation of band density of K13 expression in epithelial cell lines cell line
Figure 4.42 Effect of TSA and SB on K13 protein expression in RTS3b cells
Figure 4.43 Evaluation of band density of K13 expression in presence of TSA and SB in RTS3b cells
Figure 4.44 The of effect of TSA and SB on K13 protein expression in HeLa cells
Figure 4.45 Evaluation of band density of K13 expression in the presence of TSA and SB in HeLa cells
Figure 4.46 Schematic diagrams showing negative regulatory elements which bind K13 FL promoter deletion fragments.

Chapter 5

Figure 5.1 Differentiation specific keratins expression in buccal, palate and epidermis
Figure 5.2 Maturation specific keratin specific expressions in normal oral epithelium
Figure 5.3 K15 RNA expressions in paraclone and holoclone formed by SCC25 cells
Figure 5.4 K13 RNA expressions in paraclone and holoclone formed by SCC25 cells
Figure 5.5 GFP fluorescence in A431 cells stably transfected with CMV, K13 and K15 promoter
Figure 5.6 GFP expression in H357 cells stably transfected with CMV, K13 and K15 promoter
Figure 5.7 GFP expression in SCC25 cells stably transfected with CMV, K13 and K15 promoter
Figure 5.8 EGFP expression of K15 and K13 promoter construct in SCC25 cells
Figure 5.9 Representative typical FACS data obtained for K13 promoter construct
Figure 5.10 GFP expression of FACS sorted K15, K13 and CMV promoters in SCC25 cells
Figure 5.11 Brightfield and fluorescence images of K15 promoter constructs stably transfected into SCC25 cells
Figure 5.12 Representative image colony forming assay in six well plate
Figure 5.13 Number of colonies formed by K15 and K13 promoter constructs
Figure 5.14 Brightfield and fluorescence images of K15 promoter constructs expression holoclone colony formed by SCC25 cells
Figure 5.15 Brightfield and fluorescence images of K15 promoter constructs expression paraclone colony formed by SCC25 cells
Figure 5.16 Brightfield and fluorescence images of K13 promoter constructs expression holoclone colony formed by SCC25 cells
Figure 5.17 Brightfield and fluorescence images of K13 promoter constructs expression paraclone colony formed by SCC25 cells
Figure 5.18 K15 and K13 promoter linked GFP intensity in holoclone and paraclone colony formed by SCC25 cells

Figure 5.19 Brightfield images of scraped holoclone and paraclone formed by SCC25 cells transfected with K15 and K13 promoter construct
Figure 5.20 GFP expression of K15 and K13 promoter construct in holoclone and paraclone colony formed by SCC25 cells
Figure 5.21 Immunofluorescence staining of K15 protein expression in SCC25 cells
Figure 5.22 Immunofluorescence staining of K15 protein expression in A431 cells
Figure 5.23 Immunofluorescence staining of K13 protein expression in SCC25 cells
Figure 5.24 Immunofluorescence staining of K13 protein expression in A431 cells

Chapter 6

Figure 6.1 process of keratinocyte differentiation and death and involvement of PI3K/Akt pathway

Appendice

Figure 7.1 Agarose gel of K13 and K15 promoter PCR product
Figure 7.2 K13 / K15 promoter before ligation to transfer vector
Figure 7.3 K13 and K15 promoter after ligation to pRRL/m Cherry and pRRL/GFP
Figure 7.4 Laser capture microdissection on holoclone and paraclone colonies transfected with K15 promoter construct in SCC25 cells
Figure 7.5 Laser capture microdissection on holoclone and paraclone colonies transfected with K13 promoter construct in SCC25 cells
Figure 7.6 Intergene upstream size of K13 and K15 gene
Figure 7.7 K15 3kb upstream from ATG site and downstream nucleotide sequence

List of Tables

Chapter 1

- Table 1.1 Summary of differences and similarities between oral mucosa and epidermis
- Table 1.2 Summary of differences and similarities between oral mucosa and epidermis
- Table 1.3 New nomenclatures for keratin type I gene and protein
- Table 1.4 New nomenclatures for keratin type II gene and protein
- Table 1.5 The function of epithelial keratins
- Table 1.6 Transcription factors involved in conferring keratin epithelial and tissue specific expression
- Table 1.7 Keratin expressions in simple and stratified epithelia
- Table 1.8 Keratin mutations and their associated keratinopathies

Chapter 2

- Table 2.1 Standard 50µl reaction for polymerase chain reaction (PCR)
- Table 2.2 Vectors used and to be used in the study
- Table 2.3 Ligation of K13 and K15 promoter into TOPO TA vector
- Table 2.4 Ligation of K13 and K15 promoter (Insert) into pEGFP-N3B vector
- Table 2.5 The names of cell lines used in this study and where they derived from
- Table 2.6 Master Mix for transfection
- Table 2.7 Mutagenesis Reactions
- Table 2.8 Control Reactions
- Table 2.9 The primary antibody used in the study
- Table 2.10 The secondary antibody used in the study

Chapter 3

- Table 3.1 Size of keratin upstream promoter region analysed by TFsearch database
- Table 3.2 An example of information on the selected transcription factor binding sites (Tfbs) within basal K5 promoter sequence
- Table 3.3 An example of information on the selected Tfbs within suprabasal K2P promoter sequence
- Table 3.4 Site of keratin expression in normal and diseased state
- Table 3.5 The raw data of Tfbs in basal versus suprabasal keratin gene promoters
- Table 3.6 Tfbs in basal versus suprabasal keratin gene promoters
- Table 3.7 The function of C/EBP, Sp1, USF and GATA 1,2,3 transcription factors
- Table 3.8 The function of AP-1, STATx, c-Rel and NF-κB transcription factors
- Table 3.9 the number of Tfbs in basal keratin versus suprabasal keratin promoter

Chapter 4

- Table 4.1 Transcription factors which bind the sequence of K13 FL promoter
- Table 4.2 The expression of K13 promoter epithelial and non-epithelial cell lines
- Table 4.3 FACS data obtained for truncated K13 full length promoter fragments

Chapter 5

- Table 5.1 The score allocated to K15 and K13 promoter intensity

Appendices

- Table 7.1 Primer for K13 and K15 promoter sequences in PCR amplification
- Table 7.2 Primers for K15 and K13 gene in quantitative Polymerase chain reaction

Table 7.3 Molecules in each mole of K13 promoter deletion fragments
Table 7.4 The sequence of K13 promoter fragments
Table 7.5 pEGFP-N3B Vector sequence used for DNA sequencing
Table 7.6 Standard solution and Media
Table 7.7 Standard solution and Media
Table 7.8 Standard solution and Media
Table 7.9 Standard solution and Media
Table 7.10 Materials used in the study and company of purchase

Abbreviations

α = alpha

AKT= a serine/threonine kinase also known as protein kinase B (PKB)

AP-1= activator protein 1

β =beta

bp= base pair

BP180 /BPAG2=Bullous Pemphigoid antigen 180kDa

BP230 /BPAG2=Bullous Pemphigoid antigen 230kDa

$^{\circ}\text{C}$ = centigrade

Ca^{2+} = calcium

CAT= Chloramphenicol acetyl transferase

C/EBP= CAAT/ enhancer binding protein

CMV= cytomegalovirus

C-terminal= Carboxyl terminus

DAG= diacylglycerol

DAPI= 4',6 diamidino-phenylindole clyglycerol

Dsc1-3=desmocollins

Dsg1-3=desmogleins

DNA= deoxyribonucleic acid

DMBA= 9, 10-dimethylbenz[*a*]anthracene

E.coli= Escherichia coli

EBS= epidermolysis bullosa simplex

EGFP= enhanced green fluorescent protein

EtoH= ethanol

FACS= fluorescence activated cell sorter

FCS= foetal calf serum

FL= full length

GFP= green fluorescent protein

GKLF= gut-enriched Kruppel like factor

HFF= Human foreskin fibroblast

IFs=intermediate filaments

IFPs=Intermediate Filament Proteins

K=keratin

KGF= keratinocyte growth factor

KLF= Kruppel like factor

L=litre

LRC= Label retaining cells

MAPK= mitogen activated protein kinases

MCF-7= simple breast epithelia carcinoma

μg = micrograms

μl = microlitre

Mins=minutes

MEK 1/ 2= mitogen and extracellular signal regulated kinase

Mol=molar

Mr= molecular weight

MTT= Methylthiazolyldiphenyl-tetrazolium bromide

NIH3T3= mouse embryonic fibroblast

nM= nanomolar

N-terminal= amino terminus

OL= oral leukoplakia

OLP= oral lichen planus
OSF= oral submucous fibrosis
OSCC= oral Squamous cell carcinoma
pEGFP-N3B= enhanced green fluorescent protein (**B**=new BstZ171 restriction site introduced)
PI3K= phosphatidylinositol 3' kinase
PKC= protein kinase C
PL=promoter less
PMA= Phorbol 12-myristate 13-acetate
4- α -PMA= 4 alpha Phorbol 12-myristate 13-acetate
QLB= quick Ligation buffer
RA= retinoid acid
RARE= retinoid acid response element
RPM= Revolution per minute
SCC25= Squamous cell carcinoma of the tongue
SDM= site directed mutagenesis
Secs=Seconds
Sp1= stimulator protein 1
STATs= Signal transducer and activator of transcription
STDEV=Standard deviation
Tfbs= Transcription factor binding sites
TGF- β = transforming growth factor beta
Thiazolyl Blue Tetrazolium Bromide=3-(4,5-Dimethyl-2-thiazolyl)-2,5-diphenyl-2H-tetrazolium bromide
TJs=Tight junctions
TPA=12-0-tetradecanoylphorbol 13-acetate also known as PMA
WSN= white sponge nevus

Chapter 1

Literature Review

1.1 The Structure and Function of the Oral Mucosa

Different types of epithelial tissue can be classified according to their morphology and differentiation-specific protein expression patterns. Various epithelial types include simple epithelia such as those found in trachea, non-keratinized epithelia such as the oesophagus and buccal mucosa, and the keratinized epithelia found in the skin and palate and gingival tissue of the oral cavity (Figure 1.1). The oral mucosa, unlike the skin contains both keratinized and non-keratinized epithelium (Presland and Dale, 2000). The oral mucosa can be divided into three anatomical regions based on their pattern of keratinisation: masticatory, lining and specialized mucosa as listed below (Smart, 2004).

- The masticatory mucosa covers about 50% of the oral mucosal surface and is found in regions of high compression and friction, such as the gingiva and hard palate (Seoane et al, 2002). The masticatory mucosa is characterised by a keratinised or parakeratinised epithelium and a thick lamina propria. The masticatory mucosa of the gingiva and hard palate are bound directly to the underlying bone (Smart, 2004).
- The lining mucosa, which is mobile and distensible, which has a non-keratinised epithelia and a loose lamina propria and covers the cheeks, lips, floor of the mouth, ventral surface of the tongue and the soft palate. The lining mucosa occupies about 30% of the oral mucosal surface (Smart, 2004).
- The specialized regions of the oral cavity are the vermillion border of the lips and the dorsum of the tongue. The vermillion border of the lips is special because it represents a change from non-keratinized internal oral mucosa to the highly keratinized external skin (Figure 1.2). The dorsum of the tongue contains different types of papillae and taste bud receptors which enable distinction of four different types of taste: salty, sour, and sweet and bitter (Berkovitz and Moxham, 2002).

Mucosal functions include protection against both mechanical and compressive shearing forces, forming a barrier to microorganisms, toxins and various antigens and also providing an immunological defence, both humoral and cell mediated (Berkovitz and Moxham, 2002).

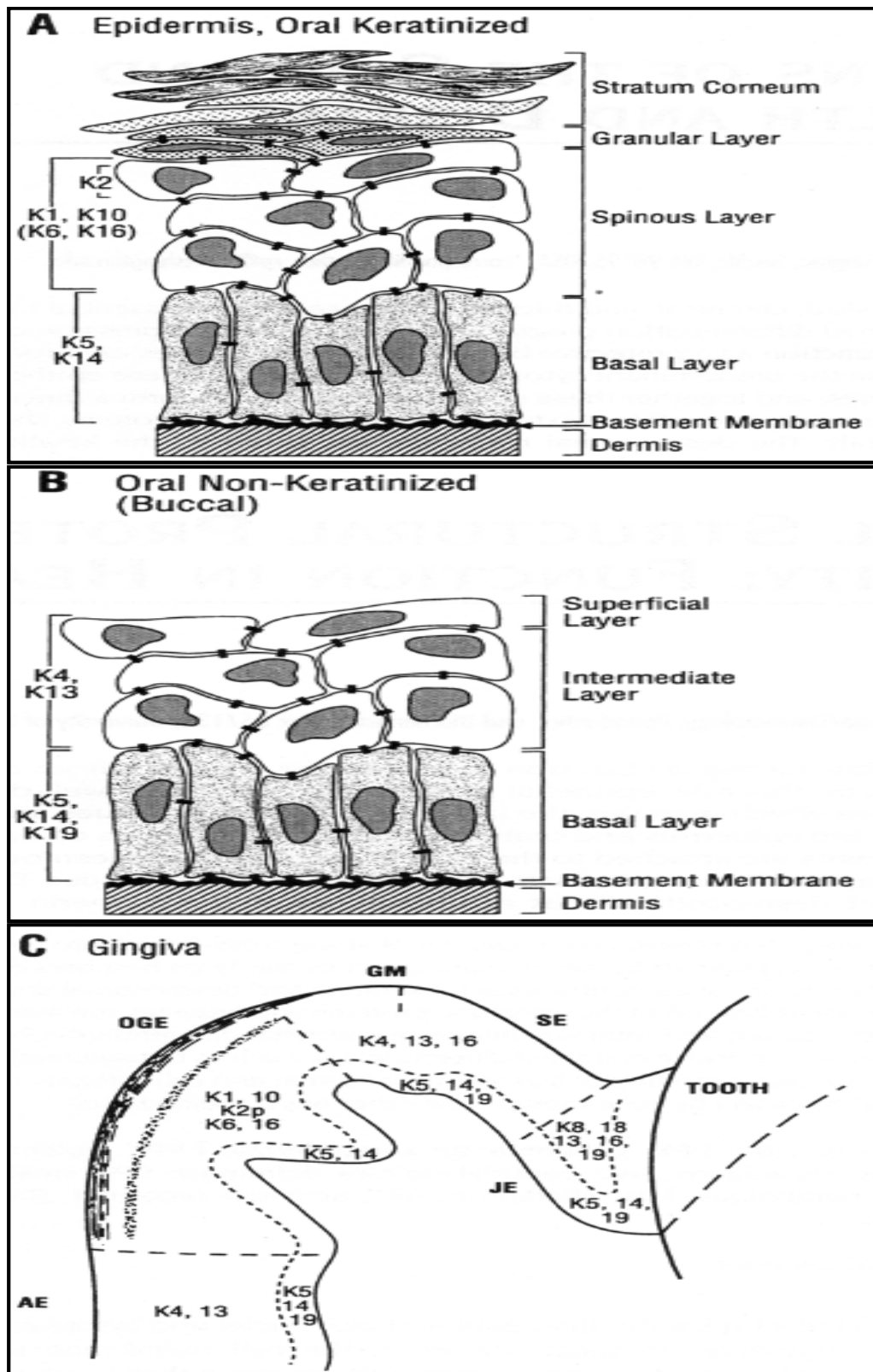


Figure 1.1: Differentiation programmes of the keratinizing epithelium of the epidermis and the oral mucosal (A), non-keratinizing buccal oral mucosa (B) and gingival epithelium, which is composed of keratinized and non-keratinized epithelia (C). The keratin pairs expressed by each layer are indicated. In panel C the following abbreviations are used: AE =alveolar epithelium, OGE=oral gingival epithelium, GM=gingival margin, SE=sulcular epithelium and JE=junctional epithelium (adapted from Presland and Dale, 2000).

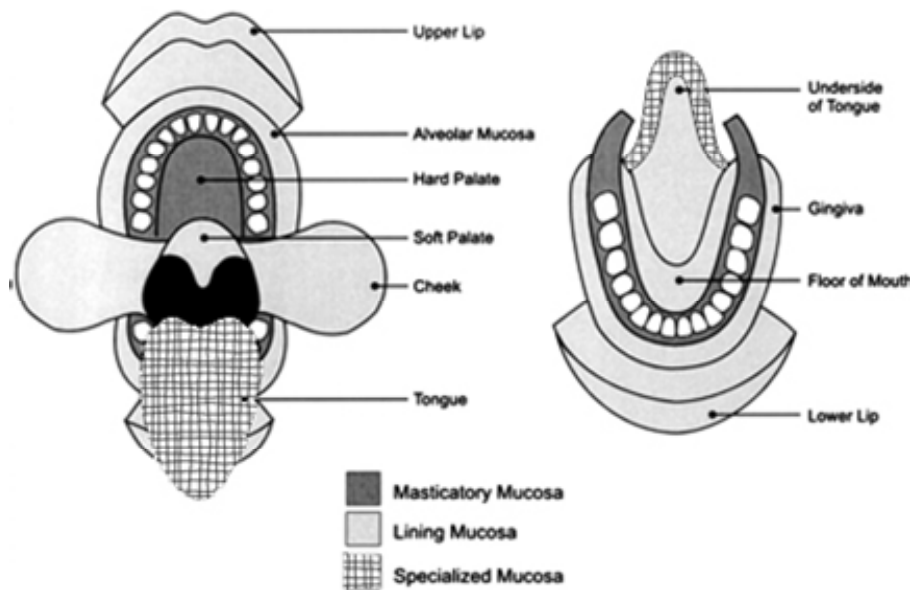


Figure 1.2: The anatomical location of the three types (masticatory, lining, and specialized mucosa) of epithelial covering of the oral cavity (adapted from Squier and Kremer, 2001).

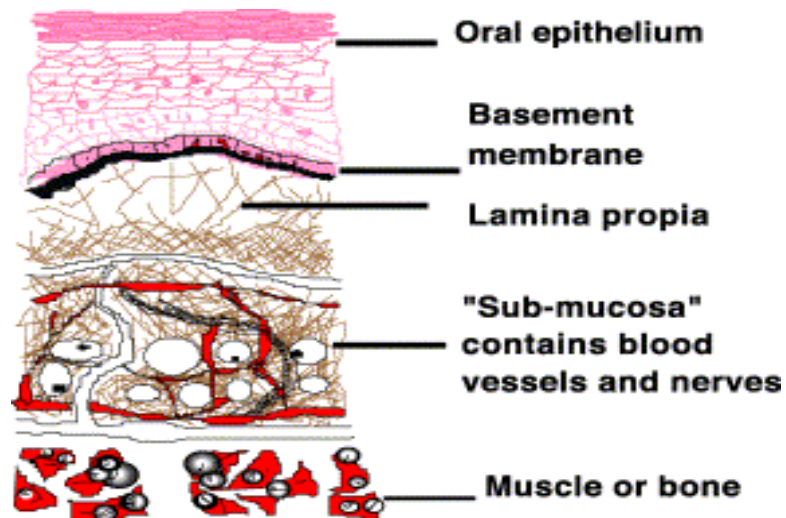


Figure 1.3: A cross section of the oral mucosa. The oral mucosa is comprised of stratified epithelium, a basement membrane, lamina propria and sub-mucosa containing blood vessels and nerves which are directly attached to bone or muscle depending on the site of the oral mucosa (adapted from Smart, 2004).

1.2 Maintenance of the Oral Mucosa

When the oral epithelium is faced with injuries that compromise its barrier function, it rapidly undergoes an epithelial repair programme, which includes the movement of cells to cover defects and a rapid production of cells that differentiate to repopulate the injured epithelium. The source of these differentiated cells within the injured tissues are stem cells which reside in the basal layer and have the ability to repopulate the injured epithelia and aid in oral epithelial homeostasis (Beachy et al, 2004). When stem cells divide, they can give rise to two identical daughter cells that retains the characteristics of its parent – this process is termed symmetric division (Mackenzie, 2005). Stem cells can also divide to produce one daughter cell that retains the characteristic of the parent and another daughter cell that known as a transient amplifying cell that embarks on a specific-differentiation program; this process is termed asymmetric division or fate (Alonso and Fuchs, 2003). These different types of stem cell fate patterns in epithelia are useful for the expansion of the stem cell population in the case of symmetric division and for maintaining the process of homeostasis, in the case of asymmetric stem cell division (Mackenzie, 2005) as shown in Figure 1.4.

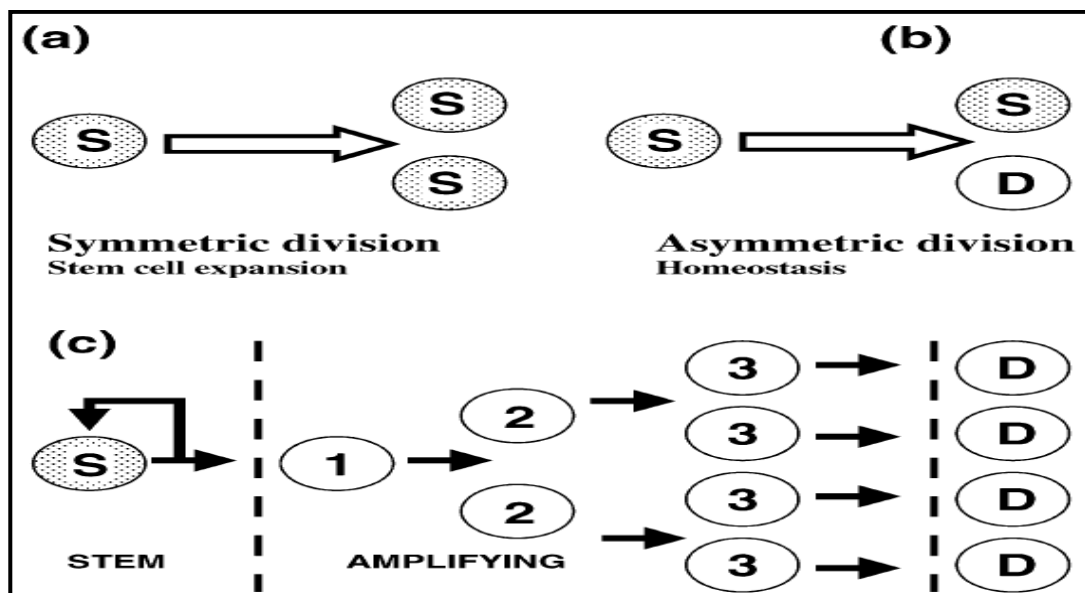


Figure 1.4: The division pattern of epithelial stem cells: a) shows a stem cell dividing to produce two daughter cells which are identical to itself and this type of division is termed symmetric division. Whereas in b) a stem cell divides to produce one cell, which is identical to the parental stem cell and another, which differentiates. This type of stem cell division is termed asymmetric division. c) shows a non-stem cell daughter cell giving rise to transit amplifying cells to expand the differentiating cell population (adapted from Mackenzie, 2005)

1.2.1 Environmental Factors which Damage the Oral Mucosa

The oral epithelium is damaged by chronic infections such as those caused by the fungal organism *Candida albicans*, eating foods which cause abrasion, habits such as drug use, tobacco smoking, alcohol consumption and chewing Betel Quid (Shieh et al, 2003). A study by Lee et al, (2003), investigated the effect of the use of betel quid, tobacco smoking and alcohol consumption on the risk of developing oral precancerous lesions, such as oral leukoplakias (OL) and oral submucous fibrosis (OSF). The study showed people who chew betel quid significantly increase their risk of developing OL and OSF. Cigarette smoking was also reported to potentiate the effect of betel quid on causing OL (Lee et al, 2003). Arecoline, the alkaloid in areca nut of betel quid has been shown to have cytotoxic effects and increase the synthesis of double stranded polynucleic acid of human buccal fibroblasts, which eventually causes OL (Lee et al, 2003).

1.3 Structure and Function of the Skin

The skin covers the entire body and is a large organ, extending to approximately 2m² in area and it is around 2.5 mm thick on average (Tobin, 2006). Some of the skin associated appendages include the hair, hair follicles, sebaceous and sweat glands (Figure 1.7). The skin has many functions, including forming a protective barrier, enabling sensory perception, and thermoregulation (Heath et al, 2000). The skin epithelium not only forms a barrier against the environment, but also aids in preventing the entry of toxic substances, bacteria, viruses and preventing dehydration by controlling the loss and gain of body fluids (Gibbs and Ponc, 2000). The skin is divided into two types: hairy skin and the glabrous non-hairy skin found on the palm of the hands and sole of the feet (Presland and Jurevic, 2002). The skin comprises three main layers: the epidermis, dermis and hypodermis as shown in Figure 1.5 (Heath et al, 2000). The epidermal and dermal skin layers are embryologically derived from ectoderm and mesoderm respectively (Heath et al, 2000). The epidermal layer consists of five layers: 1; Stratum corneum, 2; Stratum lucidum, 3; Stratum granulosum, 4; Stratum spinosum and 5; Stratum basale, (Section 1.7), and with the exception of stratum lucidum, these layers are also present in the oral mucosa. The stratum lucidum layer is histologically visible in palm and sole skin. Although the stratified epithelium is largely composed of keratinocytes, there are also other cell populations, namely melanocytes, Langerhans cells (which have

immunological function) and Merkel cells (Presland and Jurevic, 2002). Melanocytes give pigment to the keratinocytes; this process involves melanosomes that transporting melanin granules and fuse with keratinocytes to release the melanin granules (Gu and Coulombe, 2007). The melanin pigment is then transported to the supernuclear region of the keratinocytes, where they are able to impart protection of the nuclear genome against UV irradiation (Gu and Coulombe, 2007).

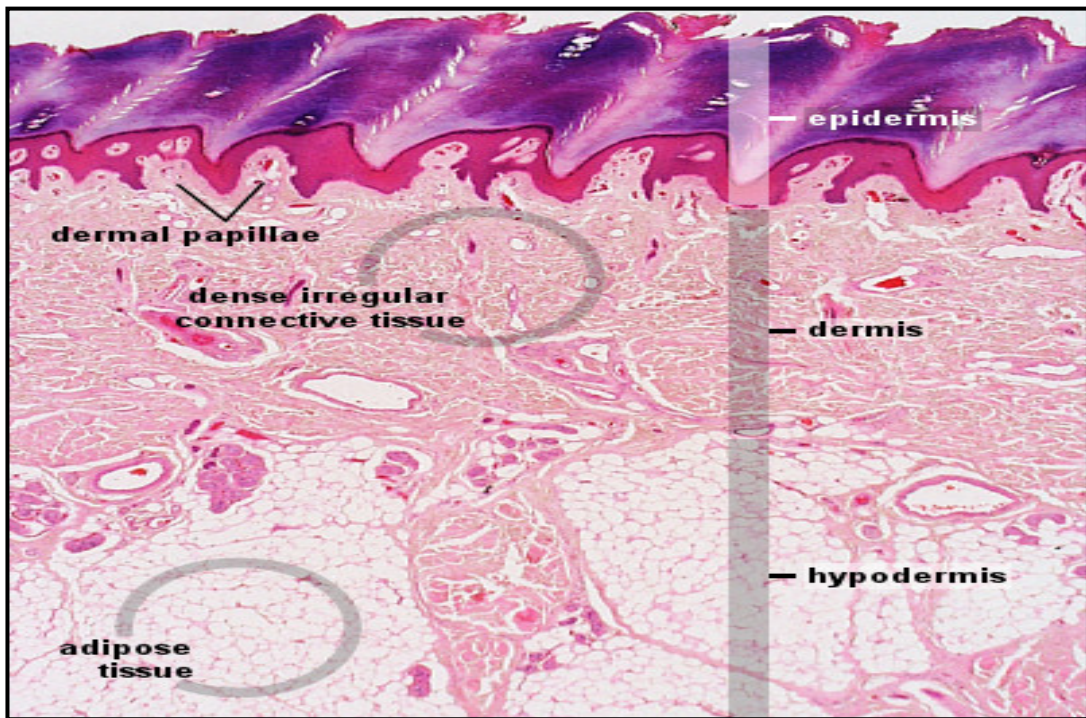


Figure 1.5: Haematoxylin and eosin (H&E) staining of thick skin of palmar and plantar epidermis, dermis and hypodermal layers (adapted from website number 8 in the reference section).

1.3.1 Skin Barrier Formation

The primary role of the epidermis is to provide protection for the organism against the external environment; the epidermis does this by constructing an elaborate and highly organised outer surface area, called the stratum corneum (Byrne et al, 2003). The essential component of the epidermal barrier is the keratinocyte cornified envelope (CE) (Marshall et al, 2001). The CE is a specialized structure which is formed in the inside of the plasma membrane of terminally differentiating cells (Steinert and Marekov, 1999). The CE is an insoluble 15nm thick structure, which is composed of two parts: the protein envelope and the lipid envelope (Nemes and Steinert, 1999). The protein envelope is coated by a 5nm thick lipid envelope, which

is covalently attached to the exterior part of the protein envelope (Nemes and Steinert, 1999). Many components make up the macromolecular assembly of the highly insoluble CE; these include: small proline-rich proteins (SPRs and also known as cornifin), loricrin, filaggrin, type II keratin proteins, trichohyalin as well as various cell junctional proteins which include envoplakin (Figure 1.6), periplakin and desmoplakin (Steinert and Marekov 1999). These insoluble proteins are interlinked together by disulfide bonds and isopeptide bonds formed by the action of transglutaminases (Steinert and Marekov, 1999). Transglutaminases (TGases), are Ca^{2+} dependent enzymes which are involved in the transfer of an acyl group between the γ -carboxamide group of protein-bound glutamine and the ϵ -amino group of lysine residues (Nemes et al, 1999). There are seven types of human TGases, of which only four (TGases 1, 2, 3 and X) are expressed in stratified epithelia of the epidermis (Nemes et al, 1999). TGase 1 and 3 enzymes are important for the cross-linking of trichohyalin, small proline-rich proteins and loricrin substrates (Nemes et al, 1999). Involucrin and the desmosomal related proteins like envoplakin and desmoplakin together function as early scaffolding components of the CE (Steinert et al, 1998). SPRs serve as cross-bridging proteins and directly modulate the biochemical properties of CE (Nemes and Steinert, 1999). Filaggrin is released by proteolysis from profilaggrin, a major differentiation product of orthokeratinizing epithelia (Nemes and Steinert, 1999). Filaggrin functions by binding to keratins and forming a tight array which is typically seen in corneocytes (Nemes and Steinert, 1999). Loricrin is by far the most abundant protein in CE and accounts for over 70% of protein mass of CE and both TGase 1 and 3 use loricrin for CE assembly *in-vivo* (Nemes and Steinert, 1999). Moreover, the amount of structural proteins which constitute CE and the presence or absence of the lipid envelope differs between various stratified squamous epithelium, according to the different protective function required (Steinert et al, 1998). For example, in orthokeratinizing epithelia, such as that of epidermis, there is an additional water barrier function, which is imparted by a 5nm thick lipid envelope and this is not present in internal oral epithelia (Steinert and Marekov, 1999). In addition, there is increased loricrin protein mass in CE of the epidermis in comparison to the palate and buccal mucosa (Nemes and Steinert, 1999). Also the amount of SPR proteins in different epithelia differs in relation to resistance of the epithelia to physical trauma or in response to chemical insults. For example the SPR proteins in CE of the trunk epidermis is about 5% of total protein

content, while human buccal epithelia contains about 50% SPR3 protein (Steinert et al, 1998).

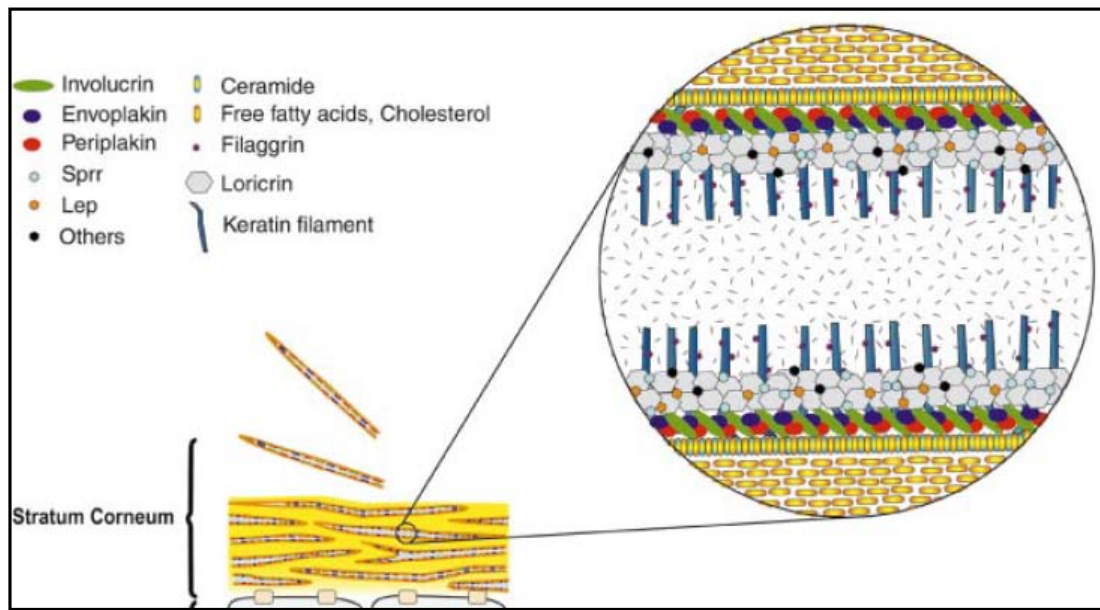


Figure 1.6: Diagrammatic representation of stratum corneum layer of adult epidermis. The stratum corneum is composed of keratinocytes which have undergone the process of terminal differentiation, this process results in the production of the cornified envelope. The cornified envelope is surrounded by a lipid capsule, shown in diagram as ceramide, free fatty acids and cholesterol. The cornified envelope is composed of many structural proteins such as involucrin, envoplakin, periplakin, filaggrin, loricrin, SPRs and Lep (adapted from Byrne et al, 2003)

1.4 Comparison of the Oral Mucosa and Skin

Different epithelial tissues show variation in their differentiation pattern and this contributes to some of the structural and functional differences in the oral mucosa and skin (Gibbs and Ponec, 2000). Generally, the oral mucosa contains more cell layers and hence is a thicker epithelium than to epidermal equivalent (Gibbs and Ponec, 2000). Although there is absence of hair follicles in oral mucosa, it does contain minor salivary glands and occasional sebaceous glands, known as Fordyce spots or granules, which are found in the upper lip and cheeks and appear as yellow spots protruding from the pink coloured mucosa (Winning and Townsend, 2000). Other phenotypic differences between oral mucosa and skin include the colour and melanin content; and the oral mucosa is more pink/reddish in colour because of the increased concentration of blood vessels in the connective tissue (Winning and Townsend, 2000). The melanin content in skin varies between individuals and is

correlated with the level of skin pigmentation (Winning and Townsend, 2000). Table 1.1 and 1.2 highlight some the structural developmental differences and similarities in both differentiation markers and cell to cell adhesion molecules of the oral mucosa and the skin (Figure 1.7).

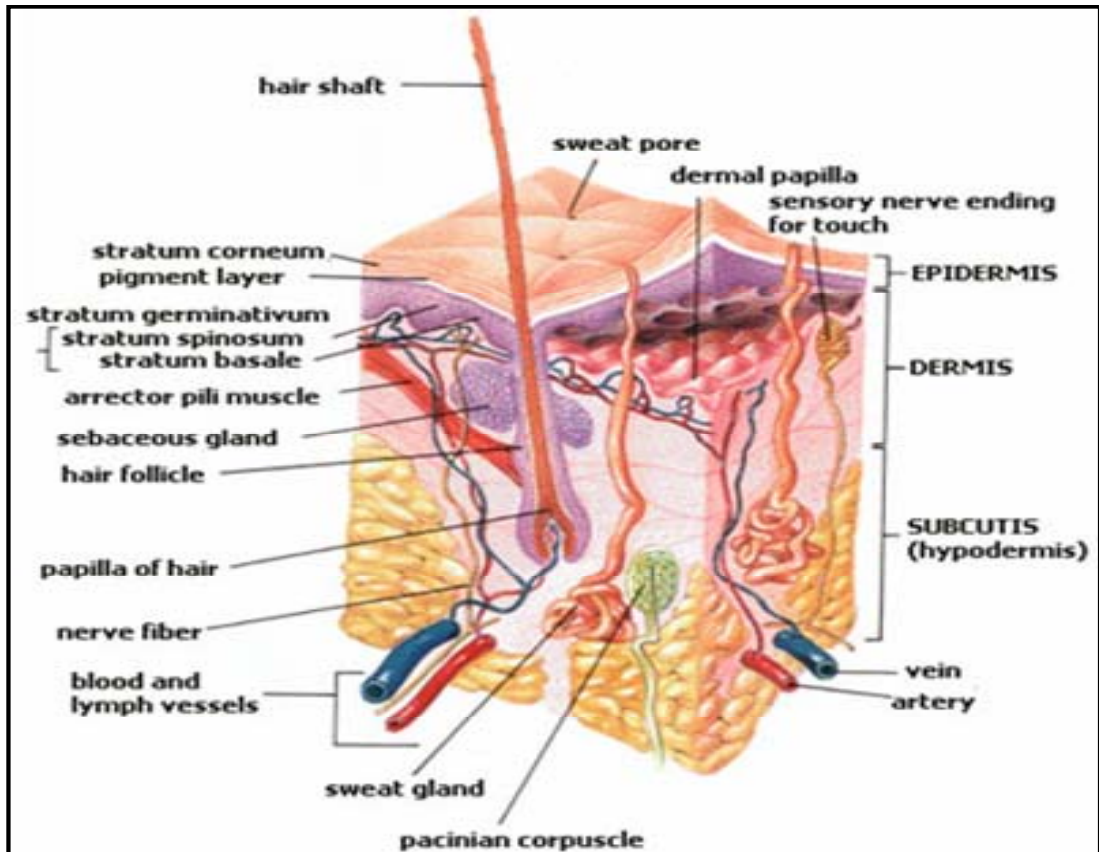


Figure 1.7: Schematic representation of skin and its associated appendages (adapted from website number 3 in the Reference).

Table 1.1: Summary of similarities and difference between the oral mucosa and skin differentiation markers.

Similarities of oral and Skin differentiation markers and their function	Differences of oral mucosa from Skin
Both the oral mucosa and skin express intermediate filament associated proteins and cornified envelope proteins such as involucrin, loricrin, cornifin- α /small profile-rich proteins.	Cornifins consist of two isoforms, β and α which act as precursor proteins for the cornified envelope protein. Both β and α isoforms are expressed in oral mucosa but only cornifin- α is found in normal skin (Fujimoto et al, 1997).
Transglutaminase is expressed by both epidermis and keratinized oral mucosa.	The non-keratinized oral mucosa expresses the filaggrin (although very weak patchy staining), involucrin, cornifin- α transglutaminase.
K5, K14, K1 and K10 proteins are respectively found in basal and suprabasal layers of keratinized oral mucosa and the epidermis.	Only the mRNA for K1 and K10 are expressed in the non-keratinized buccal mucosa. K19 is expressed in basal layer and K4/K13 pair is expressed in the suprabasal basal layer of non-keratinized oral mucosa.
Cytokines such as interleukins, tumor necrosis factors, colony stimulating factors, chemokines, growth factors, interferon and associated receptors are produced by both the oral mucosa and epidermis under various conditions such as inflammation.	K76 is expressed in keratinized oral mucosa, while K2 is expressed in skin.
Chymotryptic protein is expressed in the stratum corneum of both epidermis and keratinized oral mucosa	The membrane coating granules in the nonkeratinizing epithelial do not contain acylceramides and also contain only very small amounts of ceramides. The membrane coating granules have no lamellate contents (Lesch et al, 1989).
	The palate oral mucosa is 10 times more permeable and floor of the mouth is 20 times more permeable than the skin.

(adapted from Winning and Townsend, 2000)

Table1.2: Summary of the differences between expression of cell to cell and cell matrix adhesion molecules in Oral mucosa and Skin.

Similarities of Oral mucosa and Skin cell-cell and cell matrix adhesion molecules	Differences of Oral mucosa from Skin
Both skin and oral mucosa epithelia express integrins in the their basal layer.	In suprabasal layer of floor of the mouth and lateral border of the tongue, integrins $\alpha 2$, $\alpha 3$ and $\beta 1$ are expressed, but not in skin does not.
The transmembrane binding glycoprotein CD44 which is involved in cell to cell adhesion is expressed in all layers of epithelial lining both oral mucosa and skin.	Desmoglein-1 expression is less in the oral mucosa in comparison to the skin.
The intracellular desmosomal proteins desmoplakins are involved in mediating the interaction of keratin filaments to the cytoplasmic domain of desmoglein and desmocollin. Both the skin and the oral mucosa express transmembrane and desmosome associated proteins such as desmoglein-3 and desmocollin.	
In spinous layers of both epidermis and buccal epithelium connexin-43 expression occurs.	In the spinous layer of the buccal epithelium Connexin-26 expression occurs.
The constituent of hemidesmosomes proteins such as BP230, ladinin, BP180, laminin-5, collagen IV and VII and other lamina densa proteins are expressed by both the oral mucosa and skin.	Cell surface carbohydrates (ABO and Lewis blood group antigens) show differential expression related to tissue differentiation status e.g. keratinized and non-keratinized epithelium, epithelial wounds, or malignant epithelium.

(adapted from Winning and Townsend, 2000)

1.5 Developmental and Experimental Models used in Oral mucosa and Skin

The functional demands and tissue features of the skin and oral mucosa are reflected by the structure and biology of the tissue and the cellular products which make them up (Winning and Townsend, 2000). Interactions between the epithelium and mesenchyme are essential for epithelial repair, homeostasis and morphogenesis (Costea et al, 2003). Although much is now known about the role of epithelial-mesenchymal interactions, much controversy still exists regarding which layer causes the phenotypic differences observed in oral mucosa and skin (Costea et al, 2003). Some groups argue that the properties of the keratinocyte making up the overlying oral mucosa and skin epithelium are innate or intrinsic to that epithelium, while others argue that the mesenchymal tissue influences growth and differentiation of overlying epithelium through providing a suitable biomatrix environment or by synthesis of diffusible factors (Costea et al, 2003). However, a large body of literature has attempted to address whether the variability in structure and functions of skin and oral mucosa are inherent or whether extrinsic stromal factors can regulate it (Compton et al, 1998). Early experiments have shown that by using a co-culture of the epidermis and buccal mucosa epithelia grown on top of uterine connective tissue have a normal histo-differentiation pattern (Squier and Kammeyer, 1983). This includes the formation of thick keratinized surface of the epidermis and skin appendages such as hair and the buccal epithelium which appeared slightly thinner than normal (Squier and Kammeyer, 1983). These results suggest that the oral mucosa and epidermis have some intrinsic capacity to develop normally and show significance of connective tissue for normal histo-differentiation patterns, given the fact that buccal mucosa was slightly thinner than normal (Squier and Kammeyer, 1983). Other studies have used human cultured epithelial autografts (CEA) of sole skin transplanted to non-sole derived connective tissue from various other body sites of pediatric patients treated for acute burns (Compton et al, 1998). Sole skin transplanted to non-sole derived connective tissue was then compared to biopsies of sole derived for amputated specimens and non-sole derived skin of age matched controls. The results have shown that the site specific K9 expression in sole skin is innate to keratinocytes which make up this epithelium and can be maintained in the absence of site specific dermal tissue (Compton et al, 1998). Studies by Okazaki et al, (2003) looking at the influences of underlying mesenchymal tissues, using organotypic co-cultures of normal buccal mucosal epithelium and abdominal skin

have shown that skin differentiation is intrinsically controlled, however epithelial keratin specific differentiation and phenotype can be extrinsically modified by underlying mesenchymal fibroblast (Okazaki et al, 2003).

Taken together, most of these studies suggest that although the connective tissue and mesenchymal fibroblasts are important, the intrinsic control innate to the keratinocytes of the skin and oral mucosa may play a more significant role in determining epithelial phenotype.

1.6 Keratinocytes

The stratified squamous epithelial surface lining the oral mucosa, oesophagus, cervix, cornea and the epidermis are predominantly made up of keratinocytes (Leask et al, 1991). In order for the epithelia to provide an effective cohesive barrier, keratinocytes are linked by several types of cellular junctions (Presland and Jurevic, 2002). The adhesion structures and cellular junctions include desmosomes and hemidesmosomes, adherens junctions, gap junctions and tight junctions. Together these adhesion and cellular junctions have a role in mechanical, biochemical and signalling interaction between cells (Presland and Jurevic, 2002; Burns, 2004).

1.6.1 Desmosomes

Desmosomes consist of products of three gene families: the desmosomal cadherins, the armadillo family of nuclear and junctional proteins, and the plakins (Burns et al, 2004). The desmosomal cadherins family of transmembrane proteins are made up of desmogleins (Dsg1-3) and desmocollins (Dsc1-3), which show epidermal differentiation specific expression. Dsg1 and Dsc1 are expressed in the superficial layer of the epidermis, whereas Dsg3 and Dsc3 are expressed in the basal layer of the epidermis (Burns et al, 2004). The intracellular part of desmogleins and desmocollins are attached to keratin filaments via desmoplakins and plakoglobin as shown in Figure 1.8. The armadillo protein plakophilin 1 has an essential role in the adhesiveness of the site specific plakin cell envelope proteins, such as envoplakin and periplakin in differentiated keratinocyte (Burns et al, 2004).

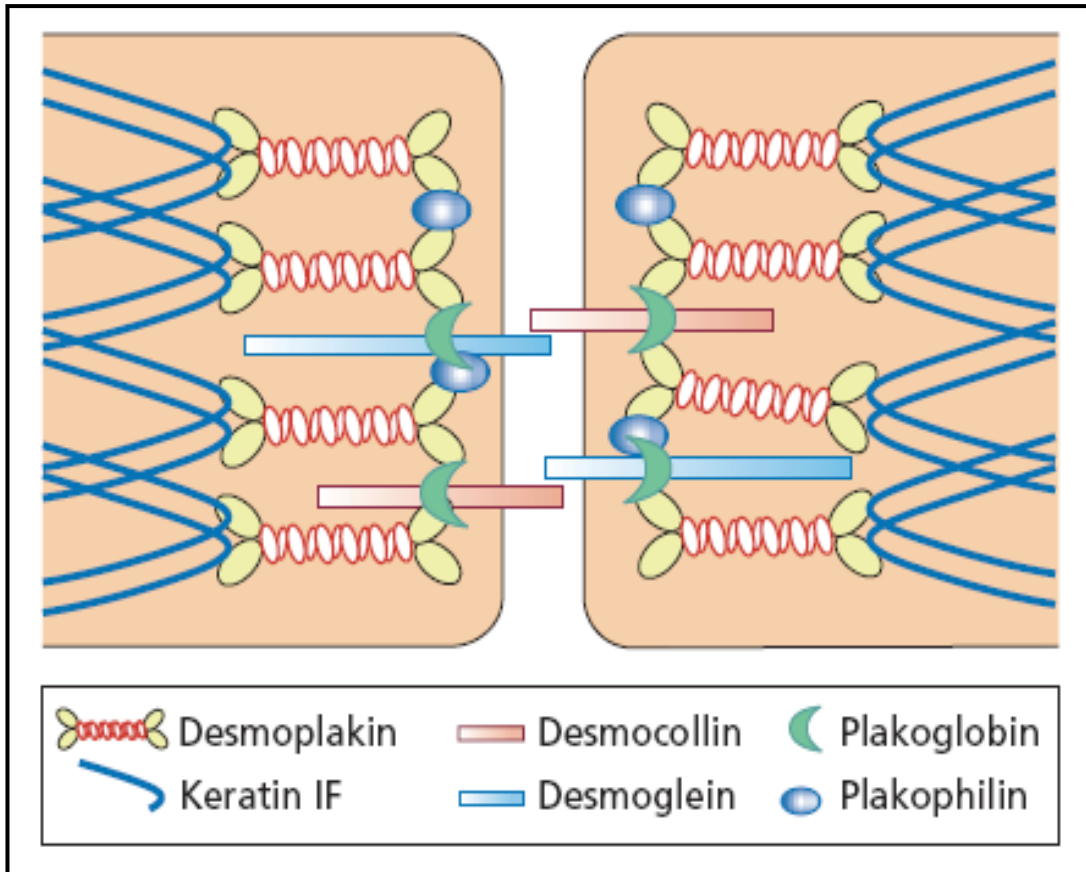


Figure 1.8: Macromolecular constitution of desmosomes, which link adjacent keratinocytes together. Keratinocytes are connected through the transmembrane cadherin glycoproteins known as desmogleins and desmocollins. Attachment of desmogleins and desmocollins to keratin filaments occurs via desmosomal plaque proteins known as desmoplakins, plakoglobin and plakophilin (adapted from Burns et al. 2004)

1.6.2 Hemidesmosomes

Hemidesmosomes are adhesion structures that attach keratinocytes to the basement membrane, as shown in Figures 1.9 (Presland and Jurevic, 2002). Hemidesmosomes are a multiprotein complex which consist of six proteins, the basal keratinocytes specific subunit of $\alpha 6$ and $\beta 4$ integrin (Hatakeyama et al, 2004), the Bullous Pemphigoid antigen 180 (BP180 or BPAG2) and 230 (BP230 or BPAG1), CD151 and plectin (Raymond et al, 2005). In addition there is also laminin 5, which mediates the attachment to basement membrane by traversing the lamina lucida and interacting with other extracellular matrix components (Hatakeyama et al, 2004). The $\beta 4$ subunit of integrin is large and thus acts as a scaffolding for the binding of other hemidesmosomal components (Raymond et al, 2005). BP230 is an intracellular electron-dense plaque that acts as an auto-antigen in Bullous Pemphigoid (Hatakeyama et al, 2004). The cytolinker plectin protein located in the cytoplasm

mediates the binding of $\alpha 6\beta 4$ integrin to the intermediate filament system. Both BP180, a collagen protein that extends from the intracellular to the extracellular space (Hatakeyama et al, 2004) and the CD151 hemidesmosomal components are transmembrane proteins (Raymond et al, 2005).

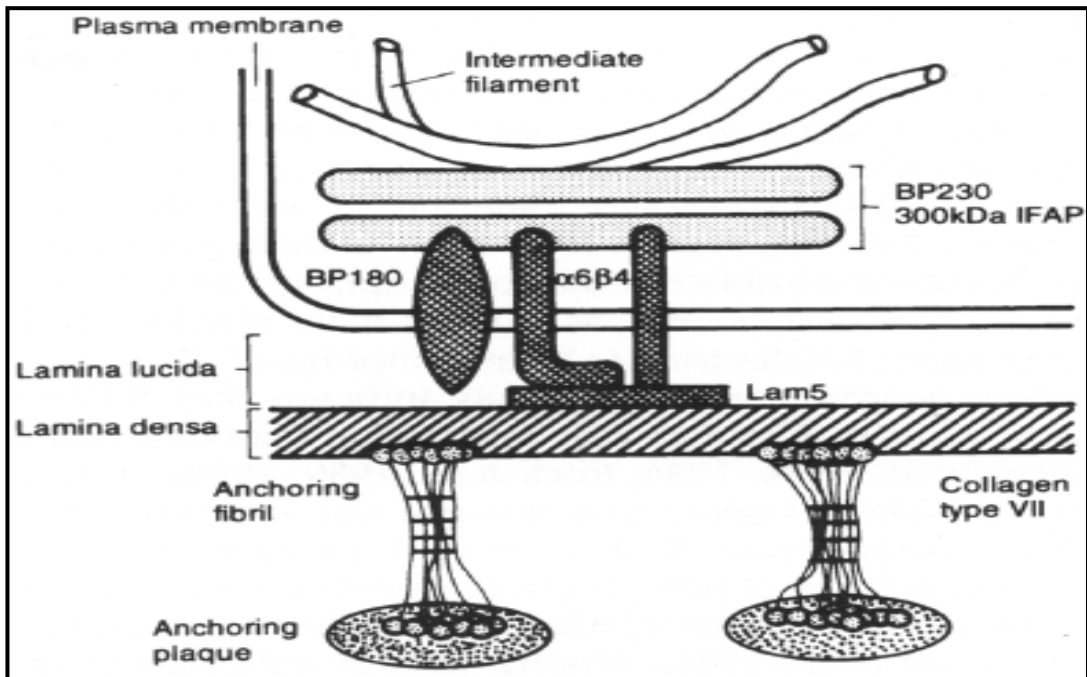


Figure 1.9: Diagram showing hemidesmosomes components, which mediate attachment of basal keratinocytes to the extracellular matrix by connecting the keratin intermediate filaments with transmembrane proteins. The transmembrane proteins then interact with extracellular matrix. The $\alpha 6$ and $\beta 4$ integrin subunit interacts with extracellular matrix. The $\alpha 6\beta 4$ integrin subunit also interact with laminin-5 in the lamina lucida and the anchoring fibrils attach and interlink the lamina densa and anchoring plaque (adapted from Dabelsteen, 1998).

1.6.3 Tight Junctions

Tight junctions (TJs) form a diffusion barrier (Figure 1.10C) which coordinates the influx of hydrophilic molecules through a paracellular pathway (the movement of ion through the intercellular space between epithelial cells) (Yuki et al, 2007). TJs regulate cell permeability in both simple and stratified epithelia and have an essential role in skin barrier integrity and in maintaining cell polarity (Burns et al, 2004). The TJ which link keratinocytes to one another are composed of transmembrane and intercellular molecules that include occludin, junction adhesion molecule and claudins (Burns et al, 2004). A single occludin gene exists, unlike claudins which forms a multi-gene family with 24 or more possible members (Yuki et al, 2007).

Claudin is thought to regulate epidermal permeability by directing the formation of TJs (Burns et al, 2004). Occludin was originally considered to be a structural protein that contributes to the formation and sealing of TJs, but was later found not to be essential to the formation of TJ strands, which indicates that it has a regulatory function as opposed to structural function (Yuki et al, 2007). An increase in extracellular Ca^{2+} in epidermal keratinocyte cultures was shown to induce the formation of desmosomes, adherens junctions, causing cells to stratify, and also to cause an increase in zonulae occludentes 1 (ZO-1), occludin and claudin-1 expression (Yuki et al, 2007).

1.6.4 Gap Junctions

Cell to cell communication is controlled through gap junction proteins and this is vital for the development and maintenance of the tissues (Burns et al, 2004). Gap junction proteins are known as connexins and form surface structures which permit the diffusion of low molecular mass substances directly between the cytoplasm of adjacent cells (Shore et al, 2001). Gap junctions regulate the electrical and metabolic activities of cells (Shore et al, 2001) and each gap junction is made up of two hemichannels or connexons, which are themselves each composed of six connexin molecules. The assembly of connexins takes place within the Golgi network and these connexins are then transported to the plasma membrane (Burns et al, 2004). Once the connexins are at the plasma membrane, the connexons from adjacent keratinocytes interact to form a complete intercellular channel (Essenfelder et al, 2005). More than 20 different mammalian connexins have been described and show tissue specific distributions and different regulatory properties (Essenfelder et al, 2005). Once a gap junction is formed either from homotypic or heterotypic connexins it can be regulated by protein kinase C, Src kinase, the local pH, calmodulin and calcium concentration (Burns et al, 2004). Connexin 30 (Cx30) is a family member that is expressed in the brain and in rat and human epidermis (Essenfelder et al, 2005). A point mutation and several deletion mutations in the human Cx30 gene have been shown to cause non-syndromic autosomal profound hearing loss and also cause Hidrotic Ectodermal Dysplasia, which affects the nails, hair and skin. The association of Cx30 with loss of hearing and skin disease indicates the essential role of Cx30 in auditory signal transduction and epidermal differentiation (Essenfelder et al, 2005).

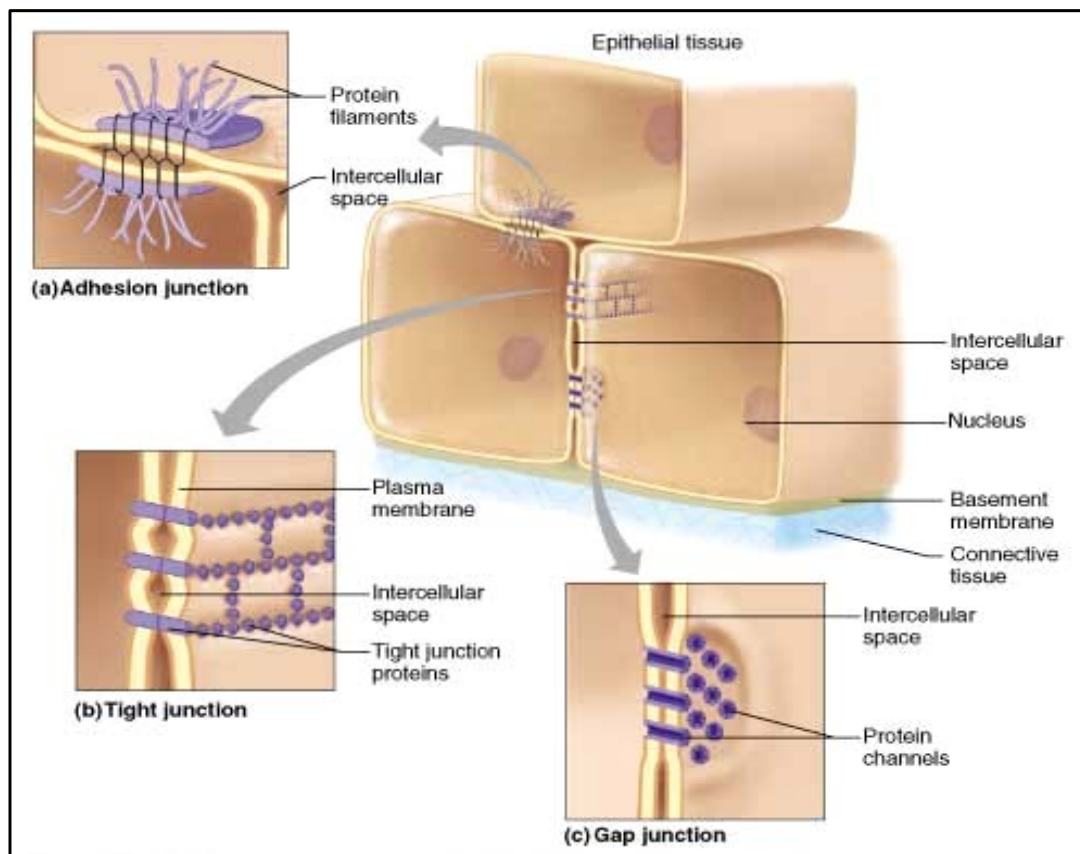
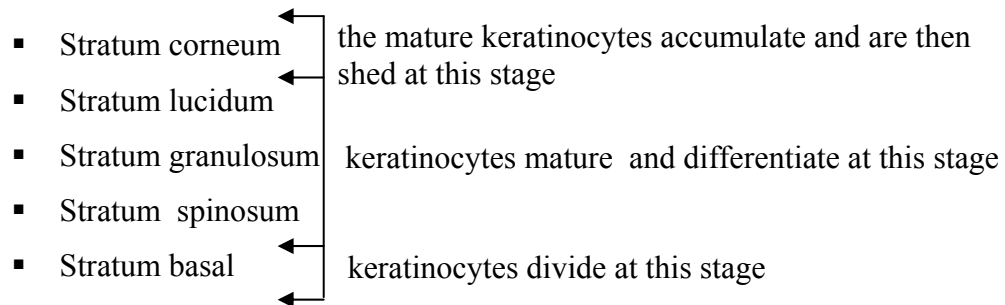


Figure 1.10: The picture shows the three types of cellular junctions, which enable cells to connect with one another to form a tissue. A given cell type may have more than one type of junction. (a) Adhesion junctions which acts as a staple like structure to hold the cells together in the tissue. (b) Tight junctions, these junctions as the name implies join the cells very tightly. (c) Gap junction aids in the flow of molecules such as calcium between cells (adapted from website number 7 in the Reference section).

1.7 Keratinocyte Differentiation

Differentiation is a process whereby cells undergo a change to become specialized cells within a particular tissue (Alberts et al, 1994). Keratinocyte differentiation can be recognized by the expression of differentiation markers characteristic for each stage of differentiation (Plachot and Lelievre, 2004). The oral mucosal epithelia and the skin consist of defined layers, each of which contains keratinocytes expressing specific keratin gene pairs, for example K1/K10 are expressed in the epidermis. Most keratins are in pairs of type I and II, except for a few keratin genes such as K15 and K19 which do not have a keratin partner, due to the lack of a proper tail domain, but rather compensate for decreased or absent keratin genes (Owens and Lane, 2003; Radoja et al, 2004). For example in Epidermolysis Bullosa Simplex, K15 compensates for the absence of K14 in the basal layer of the skin and pairs with K5

(Radoja et al, 2004). The scheme below shows the various stages a keratinocyte undergoes in the process of keratinization (Figure 1.2A) before being shed from the surface (Whyte et al, 2002).



Differentiation involves the detachment of basal keratinocytes and migration away from their basement membrane (Alt et al, 2004). Migration into the suprabasal layer is associated with selective loss of the $\alpha 6\beta 4$ integrin complex (Alt et al, 2004). During the migration of keratinocytes into the spinous and granular layers, changes in keratinocyte cell structure occur, in which the keratinocytes become enlarged, flattened, lose organelles and nuclei; the cytoplasm becomes condensed and the cytoskeletal proteins become cross-linked to the cornified envelope (Waseem et al, 1999). This is followed by stacking of multiple keratinocytes in the stratum corneum. In the final stage of differentiation, the keratinocytes transform into a rigid cornified cell and the flattened dead keratinocytes, are known as squames (Figure 1.11), that are eventually shed from the epithelial surface (Eckert et al, 2002). What triggers the differentiation process is now becoming better understood. Loss of integrins, which are receptors for extracellular matrix proteins such as collagens, laminins and fibronectins was initially hypothesised to cause the detachment of keratinocytes from the basal layer (Janes and Watt, 2006). This mechanism involves the loss of $\alpha 6\beta$ -integrin, which leads to loss of keratinocyte adhesiveness and hence detachment. However, it is now known that the start and stop signals for induction of keratinocyte differentiation mechanism is through integrin receptors and their ligand (Janes and Watt, 2006). When primary human keratinocytes were placed in cell suspension, they initiated the terminal differentiation process through integrin signalling. The cue for integrin to initiate differentiation was established by the use of anti- $\beta 1$ integrin antibodies against the cell suspension (Janes and Watt, 2006). The mechanism through which integrin receptors and their ligand regulate differentiation initiation are through two types of signals (Janes and Watt, 2006). The ‘do not differentiate’

signal is induced by ligand occupied receptors, while the ‘do differentiate’ signal is induced by unoccupied integrin receptors (Janes and Watt, 2006).

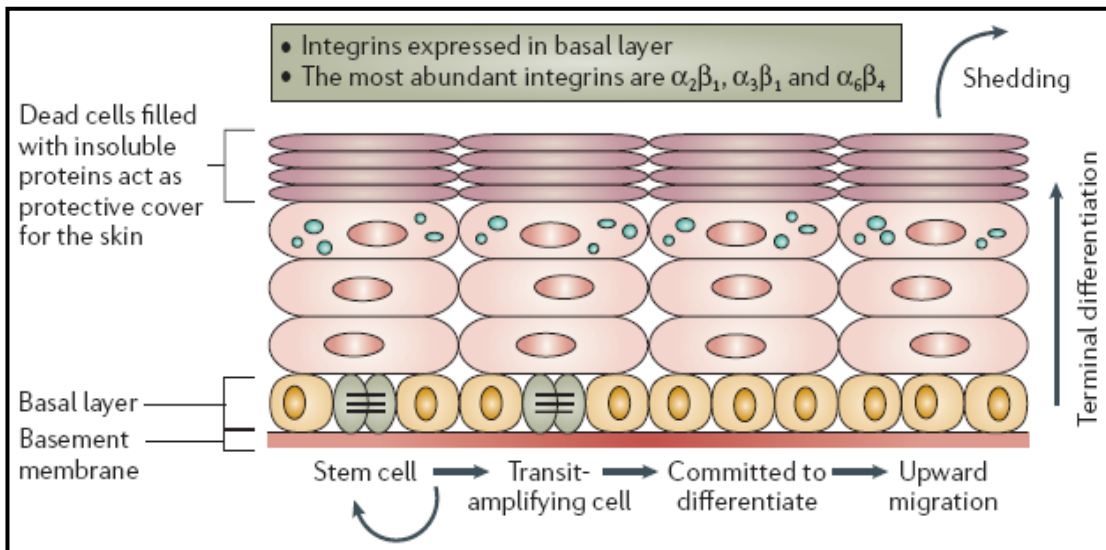


Figure 1.11: The normal differentiation processes in the human interfollicular epidermis. The $\alpha_2\beta_1$, $\alpha_3\beta_1$ and $\alpha_6\beta_4$ integrin subunits are expressed in the basal layer, which is attached to the basement membrane. The basal layer also contains stem cells, that give rise to transit amplify cells and cells which have lost the ability to divide and therefore become committed to terminal differentiation (adapted from Janes and Watt, 2006).

1.7.1 Molecules Involved in Transition from Basal to Suprabasal Differentiated Cells of the Epidermis

There are many molecules such as cell cycle regulators and transcription factors, which regulate the process of terminal differentiation in the epidermis. Cdc42 protein is a small GTPase belonging to the Rho family and is constitutively expressed protein which is involved in the regulation of cell cycle (Wu et al, 2006). Cdc42 is essential for differentiation of skin progenitor cells into hair follicle lineage (Wu et al, 2006). The differentiation of skin stem cell into hair follicles requires the inhibition of β -catenin degradation, which is controlled by a complex of axin and protein kinase GSK3 β (Wu et al, 2006). This control involves the phosphorylation of β -catenin in the cytosol by GSK3 β , which marks β -catenin for proteasomal degradation (Wu et al, 2006). Cdc42 stabilizes β -catenin and prevents its degradation, by binding to the cytosolic complex of Par6, Par3 and PKC ζ , which in turn inhibits GSK3 β activity. (Wu et al, 2006). Inhibition of GSK3 β activity leads to reduced phosphorylation of axin and degradation of β -catenin (Wu et al, 2006). This free β -catenin enters the nucleus together with LEF and TCF transcription factors

and thus induces hair follicle specific gene expression. The absence of Cdc42 results in increased GSK3 β activity and increased axin phosphorylation and subsequent degradation of β -catenin, such that there is a reduced level of β -catenin in the nucleus and thus β -catenin is unable to induce hair follicle gene-specific expression (Wu et al, 2006). Therefore the loss of β -catenin during hair follicle development leads to progenitor follicular cells changing their fate from hair follicle to epidermal differentiation (Wu et al, 2006). This finding indicates that Cdc42 is essential for terminal differentiation of hair follicle progenitor cells by regulating β -catenin turnover (Wu et al, 2006). p63 is a member of the p53 family of DNA-binding factors and has essential role in epidermal differentiation (Kashiwagi et al, 2007). The ectopic expression of p63 in simple epithelia has caused the induction of epidermal differentiation related keratin expression and thus it was suggested that p63 might be important for determining the squamous cell fate (Kashiwagi et al, 2007). It also been reported that the retinoblastoma (Rb) family of proteins, which includes pRb, p130 and p107, are specifically expressed during epidermal keratinocyte differentiation in both *in-vivo* and *in-vitro* (Paramio et al, 2000). When different combinations of the retinoblastoma proteins are ectopically expressed, this triggers different stages of the differentiation program, which highlights the importance of retinoblastoma proteins in regulating differentiation process (Paramio et al, 2000). The E2F transcription factor family are also involved in regulating different stages of the differentiation process in the epidermis (Paramio et al, 2000). This was demonstrated by transfecting HaCaT keratinocytes cells with E2F1 or EF24 plasmid constructs (Paramio et al, 2000). E2F1 transfected cells were unable to differentiate, which correlates with E2F1 been uniformly present throughout the epidermal keratinocyte layers (Paramio et al, 2000). Whereas E2F4 transfected cells show increase differentiation, which correlates with E2F4 been expressed at the onset of human epidermal keratinocyte differentiation (Paramio et al, 2000). It was suggested that both Rb and E2F transcription factor families interact to modulate the process of epidermal differentiation (Paramio et al, 2000). c-Myc is a member of the Myc transcription factor family, which plays an essential role in cell proliferation, apoptosis and cell differentiation (Gandarillas, 2000). In cultured keratinocytes, c-Myc promotes differentiation, while in other cell types, activity of c-Myc promotes proliferation and apoptosis (Gandarillas, 2000). In cultured keratinocytes, c-Myc is able to promote differentiation, by driving the keratinocytes out of the stem cell

compartment and into transit amplification (Gandarillas, 2000). Furthermore, cycle cell inhibitors such as the cyclin dependent kinase inhibitors including p16, p21 and p27 as well as the pocket protein p130, are all up-regulated during keratinocyte differentiation, leading to suppression of proliferation (Gandarillas, 2000). Positive cycle cell regulators, such as the cyclin A, cdk2, and cdc2 are all down-regulated during keratinocyte differentiation (Gandarillas, 2000). Analysis of epidermal specific promoters has revealed a common set of transcription factors such as AP-1 and Sp1, which regulate the expression of epidermal keratin differentiation markers (Smith et al, 2004). It was also suggested that tissue-specific and ubiquitously expressed transcription factors synergistically interact to regulate numerous genes expressed in different layers of the epidermis (Smith et al, 2004). The importance of specific transcription factors such as POU domain, NFkB and C/EBP in the normal epidermal differentiation process was demonstrated when these transcription factors were either ectopically expressed or mutated (Smith et al, 2004). This resulted in non-functional transcription factors, which in turn led to abnormal differentiation process in the epidermis (Smith et al, 2004).

1.7.2 Factors influencing Keratinocyte Differentiation

There are many factors which influence keratinocyte differentiation and these include epidermal growth factor (EGF), keratinocyte growth factor (KGF), transforming growth factor (TGF), retinoic acid, thyroid hormone and calcium (McBride et al, 1999). In adult epidermis, EGF receptor (EGFR) is mainly expressed in the basal layer and to a lesser extent in the suprabasal layer (Tomic-Canic et al, 1998). The binding of the ligand to EGFR causes keratinocyte activation, proliferation, degradation of extracellular matrix and subsequent keratinocyte migration to different layers (Tomic-Canic et al, 1998). In the human epidermis there is a calcium gradient being lowest in the basal layer and the highest in the granular layer, and this gradient is essential for *in-vivo* differentiation (Bikle, 2004). Keratinocytes grown at low calcium concentration (below 0.07mM) undergo cell proliferation, in which there is a slow development of intercellular contact and slow formation of the cornified envelope. Increasing the calcium concentration (above 0.1Mm) causes a number of changes including switching from the expression of proliferation markers to the expression of epidermal K1/K10 differentiation markers and elevated expression of transglutaminase and involucrin (Yang et al, 2003). The

basal keratinocytes contain vitamin D receptors, which allow keratinocytes to produce their own supply of the active metabolite of vitamin D, 1,25 (OH)₂ D₃, which causes keratinocyte differentiation (Bikle, 2004). Study looking at the effect of fibroblast secreted KGF on the morphogenesis of reconstituted human oral epithelium has shown that although KGF promoted epithelial growth, it did not significantly increase epithelial differentiation (Costea et al, 2003).

Transforming growth factor-beta (TGF- β) is multifunctional cytokine which plays an important role in cutaneous wound repair and also has regulatory role in both epithelial proliferation and differentiation (Karatsaidis et al, 2003). Of the three TGF- β isoforms, TGF- β 1 inhibits epithelial cell growth by up regulating cyclin-dependent kinase inhibitors such as p15 and p21 and also by transcriptionally repressing the expression of *c-myc* gene, which normally promotes cell growth (Karatsaidis et al, 2003). In addition, TGF- β 1 causes keratinocyte apoptosis and regulates keratinocyte differentiation by increasing keratin expression (Karatsaidis et al, 2003). Retinoic acid (RA) is the active form of vitamin A found in epithelia (Kautsky et al, 1995). Using an air-liquid interface culture system which was adapted for growth and differentiation of oral keratinocytes, the effect of RA on morphological differentiation and expression markers of keratinized oral epithelia was investigated (Kautsky et al, 1995). The results have shown that a specific range of RA concentration (10^{-9} to 10^{-8} mol/L) was required for epidermal differentiation, whereas lower (10^{-10} mol/L) RA concentration was shown to cause oral keratinocyte differentiation (Kautsky et al, 1995). The results have shown that RA works via two mechanisms to induce differentiation; 1) via direct RA dependent concentration and 2) sub-epithelial fibroblasts mediate the affects of RA on differentiation markers (Kautsky et al, 1995). RA induces differentiation via concentration dependent mechanism, whereby low RA concentration causes decreased expression of K13 and K19, whereas proflaggrin and K1 expression was increased (Kautsky et al, 1995). 2) The effect of RA on differentiation markers is partially mediated by sub-epithelial fibroblasts and this regulation is more indirect, given that the fibroblast influences the apparent RA exposure of the keratinocytes independently of the actual RA concentration in the culture medium (Kautsky et al, 1995). Furthermore, recent work by Hatakeyama et al, (2004) on the affect of RA on cell-cell and cell-matrix connections of gingival epithelial cells in a multilayered culture system, has shown

that RA disintegrated desmosomes by depriving the cells of desmoglein I. In addition, RA also dissociated desmocollin I, K13, K4, reduced the expression of hemidesmosome components BGAGI, and K14 expression in basal keratinocytes (Hatakeyama et al, 2004). Using gel mobility assay with purified receptors and transient transfection assays with vectors expressing various mutant and K5, K14 and K17 promoter-CAT constructs, the affect of Thyroid hormone (T3R) on markers of epidermal differentiation was investigated (Tomic-Canic et al, 1996). The results have shown that epidermal differentiation markers were constitutively activated by unoccupied T3R receptors, while suppression of epidermal differentiation marker expression occurred in presence of T3R occupied with ligand. T3R regulates epidermal keratin gene expression by directly binding to its response element present in keratin gene promoters (Tomic-Canic et al, 1996).

1.8 Intermediate Filament Proteins (IFPs)

Eukaryotic cells contain a cytoskeleton composed of three types of structural protein that continuously reorganize the cell as it changes shape, proliferates and responds to its environment (Purves et al, 1998). These structural proteins are actin, which forms microfilaments, tubulin which forms microtubules and the intermediate filament proteins (IFPs) (Paramio and Jorcano, 2002). Actin and tubulin are important for cell shape, mobility and cell division, whereas IFPs have a role in cell and tissue strength. There are six types of IF proteins, which are categorized according to their sequence and pattern of expression (Hesse et al, 2001). One type of protein is nuclear, while the other five are cytoplasmic and differentially expressed in tissues at various stages of embryonic and adult development (Fuchs, 1994). Type I and II IFPs are known as keratins and comprise 49 proteins expressed in epithelium, hair and nail. Type III IF proteins include vimentin (normally expressed in mesenchymal cells), desmin (expressed in muscle cells), glial fibrillary acidic protein (expressed in glial cells) and peripherin (expressed in the peripheral nervous system). Type IV IF proteins include the neurofilament specific proteins (NF-L, NF-M, and NF-H) and Internexin which are found in neurones. Type V are the nuclear lamins A, B, B2 and C which are found in the nuclear lamina (Paramio and Jorcano, 2002). The rod domain of most cytoplasmic IF proteins is approximately 310 amino acids long, while the rod domain of nuclear lamins is slightly larger with approximately 352 amino acids (Depianto and Coulombe, 2004). The main criteria used to assign a particular protein

to the IF family is its ability to polymerize either alone or with other IF proteins into a 10-12nm filament. IF proteins possess several conserved features that are essential for filament polymerization (Depianto and Coulombe, 2004). The structure of IF proteins show that they are composed of three domains: amino-terminal head domain, central rod domain and carboxyl-terminal tail domain. The head and tail domains differ from the rod domain in many respects, they are smaller in size, differ in primary structure and do not adopt a rigid structure like the rod domain (Figure 1.12). The rod domains are well conserved throughout the IF proteins and are essential for keratin filament stability. The ends and middle of the rod domain are the sites of most keratin mutations that are responsible for disease (Richard et al, 1995). However, mutation involving a single amino acid substitution in a highly conserved residue of the amino end of helix 1A of the K14 α -helical rod domain leads to a subtype of epidermal bullosa simplex known as Dowling-Meara (Fuchs, 1994). EBS Dowling-Meara, is characterised by severe intra-epidermal blistering and clumping of keratin filaments in the basal cell cytoplasm (Fuchs, 1994). The rod domain is predominantly α -helical in nature, which is interrupted by non-helical linker regions at conserved locations. Moreover, the N and C-terminals, which respectively correspond to the head and tail portions of the rod domain, possess conserved signature motifs that are vital to the formation of biologically functional filaments (Depianto and Coulombe, 2004). The above sub-families of IF proteins together form the intermediate filaments, but a particular emphasis on type I and type II keratins will be the focus of this study.

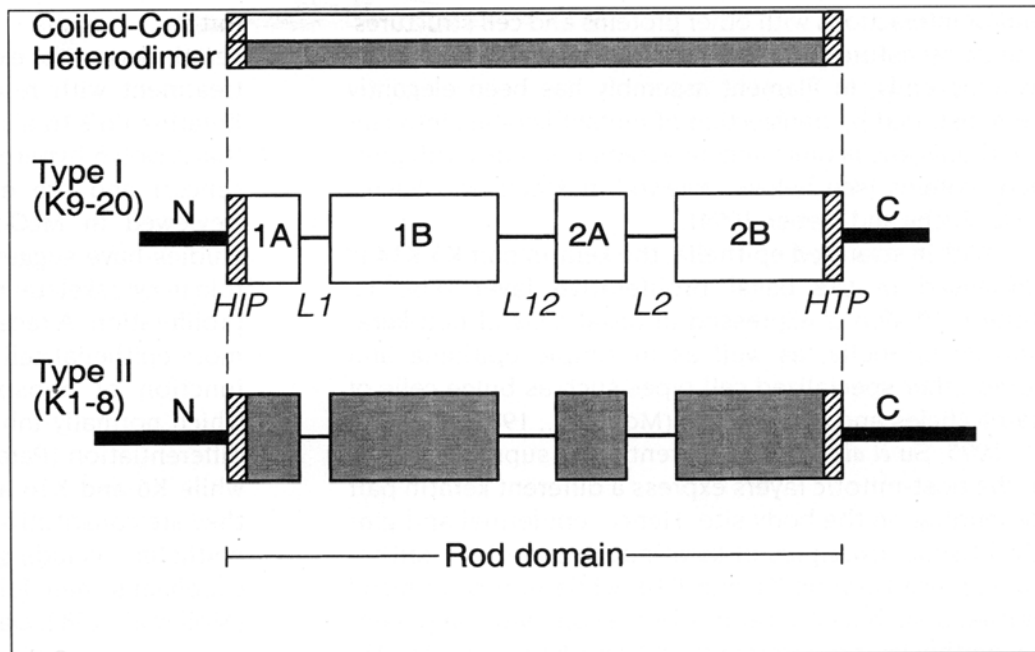


Figure 1.12: Structure of IF proteins. Type I and type II keratins consist of a central α -helical rod domain flanked by non-helical N and C terminal segments. The rod consists of 4 consecutive α -helical segments (1A, 1B, 2A and 2B), which are interrupted by helix breaking linker (L) regions. A coil-coil heterodimer, consisting of type I and type II polypeptide, aligned in parallel, is shown above. The most severe keratin mutation occurs as single amino acid substitution in the helix initiation peptide (HIP) and helix terminal peptide (HTP) (adapted from Presland and Dale, 2000).

1.9 Intermediate Filament Structure

Keratins are the building blocks of IFs and they go through a series of stages to form a functional 10-12nm IFs, these stages are as follows:

- **Monomer:** keratins are initially synthesized as single proteins.
- **Dimers:** keratins then form a pair of type I and type II.
- **Anti-parallel tetramer:** keratins then form into a twisted rope-like structure.
- **Protofilament:** the tetramers then link in head to tail fashion to form linear chains.
- **Protofibril:** two protofilament intertwine to form a protofibrils, and then groups of four protofibrils intertwine.
- **Intermediate filament 10-12nm,** produced from intertwined protofibrils as shown in Figure 1.13 (Chu and Weiss 2002).

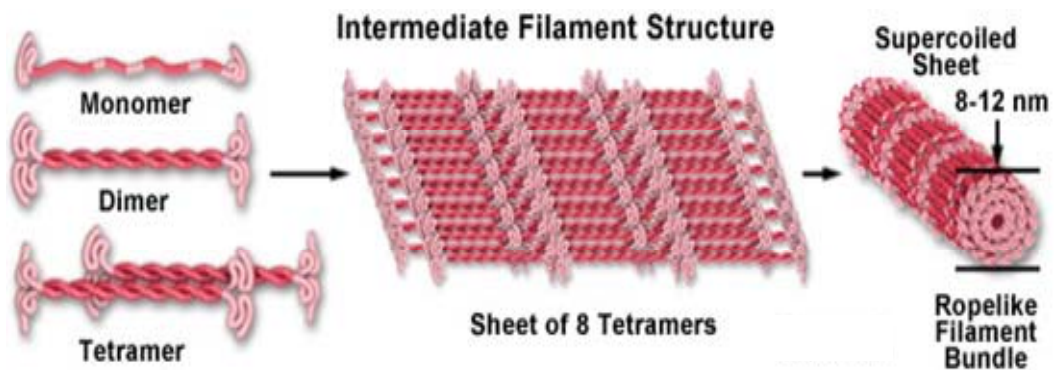


Figure 1.13: The formation of keratin polypeptide into intermediate filaments, (adapted from website number 13 in the reference section).

1.10 Keratins

Keratins are insoluble structural proteins that are a major constituent of the epithelial cells and their products such as hair, nails, horns and hooves (Reference: website 6). Keratin expression in epithelial tissue generally occurs as pairs of type I and II heteropolymer (Waseem et al, 1998). Type I keratins of soft epithelia (K9-K23) and hair-specific keratins (Ha1-Ha8), are more acidic and smaller than type II keratins, having molecular weight range of 40–56.5kDa. Type II keratins of soft epithelial tissues (K1-K8) and hair (Hb1-Hb6) are basic to neutral and are larger in size: 53–67kDa (Waseem et al, 1998). To date there are a total of 33 type I and 34 type II keratin genes known. In type I, 5 are pseudogenes, 17 are epithelial keratin genes and 11 are hair-specific keratins genes. In type II, there are 8 pseudogenes, 20 epithelial keratin genes and 6 hair-specific keratins genes. (Schweizer et al, 2006). Type I human keratin genes are located on chromosome 17, with the exception of keratin 18 which is located on chromosome 12, while type II keratin genes are located on chromosome 12 (Hesse et al, 2004). The number of exons and introns in type I and II keratin genes are normally 8 and 7 respectively, while the type II K8 (Figure 1.14) has intron 5 missing (Krauss and Franke, 1990). Therefore, it seems that keratin gene structure is conserved and this conservation is important for filament formation. Certain keratin pairs are expressed at certain stage of embryonic development such that expression of type I and type II keratins are tissue specific, maturation dependent and developmentally regulated (Lu et al, 2006). Keratins can be identified by the following properties:

- they are water insoluble
- molecular weight range between (40-70kDa)
- ability to reconstitute into 10-12nm filaments
- they show epithelial tissue specificity
- association with desmosomal protein (Sun et al, 1983).

The original and most widely used classification of keratins is that proposed by Moll et al, (1982), in which keratins were classified according to molecular weight as well as into acidic and basic proteins based on their isoelectric properties. However, keratin nomenclature has been recently reviewed by Schweizer et al, (2006), as shown in the Tables 1.3 and Table 1.4.

Table 1.3: New Type I Keratin Nomenclature

Old protein designation	Old gene designation	Current protein designation	Current gene designation
Type I human epithelial keratins			
K9	<i>KRT9</i>	K9	<i>KRT9</i>
K10	<i>KRT10</i>	K10	<i>KRT10</i>
K12	<i>KRT12</i>	K12	<i>KRT12</i>
K13	<i>KRT13</i>	K13	<i>KRT13</i>
K14	<i>KRT14</i>	K14	<i>KRT14</i>
K15	<i>KRT15</i>	K15	<i>KRT15</i>
K16	<i>KRT16</i>	K16	<i>KRT16</i>
K17	<i>KRT17</i>	K17	<i>KRT17</i>
K18	<i>KRT18</i>	K18	<i>KRT18</i>
K19	<i>KRT19</i>	K19	<i>KRT19</i>
K20	<i>KRT20</i>	K20	<i>KRT20</i>
K21 Rat	no designation	-	-
K23	<i>KRT23</i>	K23	<i>KRT23</i>
K24	<i>KRT24</i>	K24	<i>KRT24</i>
K25irs1, K10C, HIRSa1	<i>KRT25A</i>	K25	<i>KRT25</i>
K25irs2, K10D	<i>KRT25B</i>	K26	<i>KRT26</i>
K25irs3, K10C, HIRSa1	<i>KRT25C</i>	K27	<i>KRT27</i>
K25irs4, HIRSa2	<i>KRT25D</i>	K28	<i>KRT28</i>
Type I hair-specific keratins			
Ha1	<i>KRTHA1</i>	K31	<i>KRT31</i>
Ha2	<i>KRTHA2</i>	K32	<i>KRT32</i>
Ha3-I	<i>KRTHA3A</i>	K33a	<i>KRT33A</i>
Ha3-II	<i>KRTHA3B</i>	K33b	<i>KRT33B</i>
Ha4	<i>KRTHA4</i>	K34	<i>KRT34</i>
Ha5	<i>KRTHA5</i>	K35	<i>KRT35</i>
Ha6	<i>KRTHA6</i>	K36	<i>KRT36</i>
Ha7	<i>KRTHA7</i>	K37	<i>KRT37</i>
Ha8	<i>KRTHA8</i>	K38	<i>KRT38</i>
-	-	K39	<i>KRT39</i>
-	-	K40	<i>KRT40</i>

(adapted from Schweizer et al, 2006).

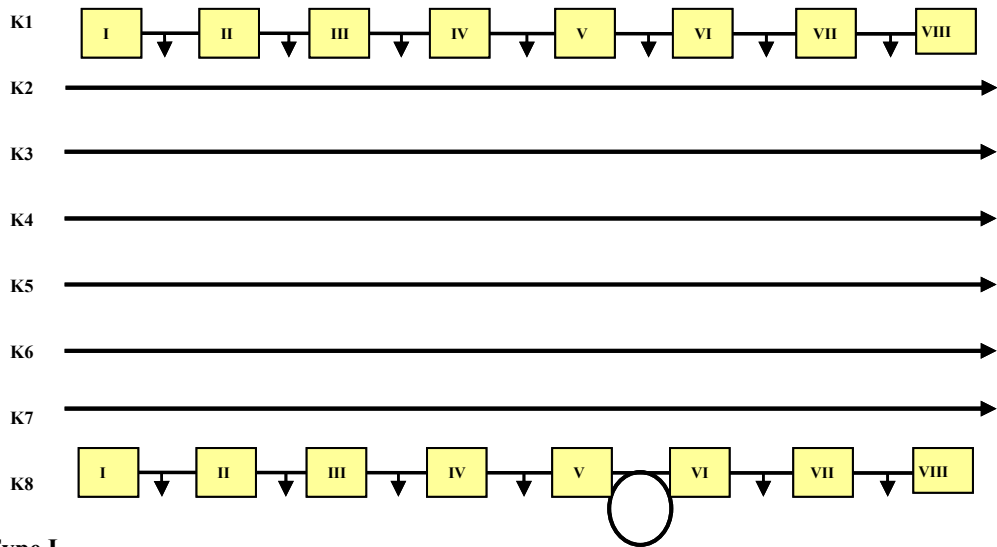
Table 1.4: New Type II Keratin Nomenclature

Old protein designation	Old gene designation	Current protein designation	Current gene designation
Type II human epithelial keratins			
K1	<i>KRT1</i>	K1	<i>KRT1</i>
K2e	<i>KRT2A</i>	K2	<i>KRT2</i>
K3	<i>KRT3</i>	K3	<i>KRT3</i>
K4	<i>KRT4</i>	K4	<i>KRT4</i>
K5	<i>KRT5</i>	K5	<i>KRT5</i>
K6a	<i>KRT6A</i>	K6a	<i>KRT6A</i>
K6b	<i>KRT6B</i>	K6b	<i>KRT6B</i>
K6e/h	no designation	K6c	<i>KRT6C</i>
K7	<i>KRT7</i>	K7	<i>KRT7</i>
K8	<i>KRT8</i>	K8	<i>KRT8</i>
K6irs1	no designation	K71	<i>KRT71</i>
K6irs2	no designation	K72	<i>KRT72</i>
K6irs3	no designation	K73	<i>KRT73</i>
K6irs4	no designation	K74	<i>KRT74</i>
K6hf	no designation	K75	<i>KRT75</i>
K2p	<i>KRT2B</i>	K76	<i>KRT76</i>
K1b	no designation	K77	<i>KRT77</i>
K5b	no designation	K78	<i>KRT78</i>
K6l	no designation	K79	<i>KRT79</i>
Kb20	no designation	K80	<i>KRT80</i>
Type II hair-specific keratins			
Hb1, K2.9	<i>KRTHB1</i>	K81	<i>KRT81</i>
Hb2	<i>KRTHB2</i>	K82	<i>KRT82</i>
Hb3, K2.10	<i>KRTHB3</i>	K83	<i>KRT83</i>
Hb4	<i>KRTHB4</i>	K84	<i>KRT84</i>
Hb5, K2.12	<i>KRTHB5</i>	K85	<i>KRT85</i>
Hb6, K2.11	<i>KRTHB6</i>	K86	<i>KRT86</i>

(adapted from Schweizer et al, 2006).

Keratin family exon and intron conservation

Type II



Type I

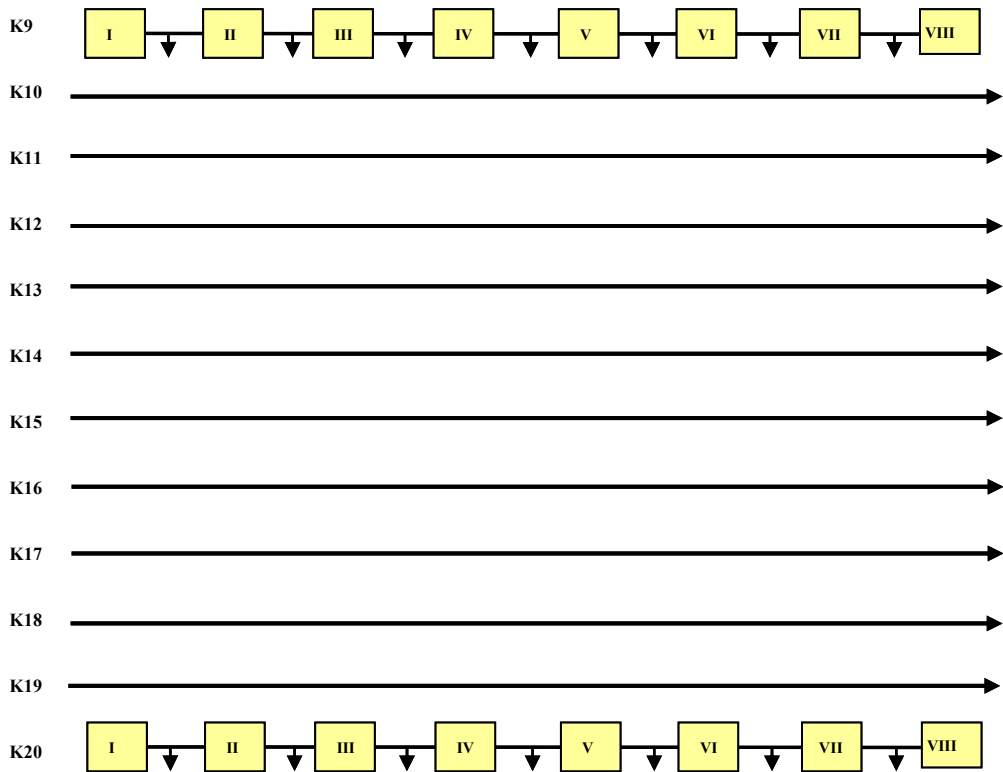


Figure 1.14: Exon and intron conservation among the keratin gene family, light yellow boxes with roman numerals represent the number of exons and small tiny arrows facing down indicate the number of introns. The black circle shows type II K8 is missing intron five. The bold long arrow facing right indicates the conserved number of exons and introns among keratin type I and type II (adapted from Krauss and Franke, 1990).

1.11 Keratin Function

The main function of keratins in epithelial tissue is to provide the cell with mechanical support and maintain cell integrity, by imparting strength to the cell and prevent it from collapsing. The function of keratins was first discovered in the early 1990's when mutations affecting some basal keratins K5/K14 were shown to correlate with a type of skin blistering disorder, Epidermolysis Bullosa Simplex (Meleady and Clynes, 2001). Another mechanical function of keratin includes protecting the cell from apoptosis (Zhou et al, 2006). Recently observed non-mechanical functions of keratin gene (Figure 1.15) include protecting the cell from injury, tissue specific expression, involvement in cell signalling, maintaining the position and function of sub-cellular organelle (Zhou et al, 2006).

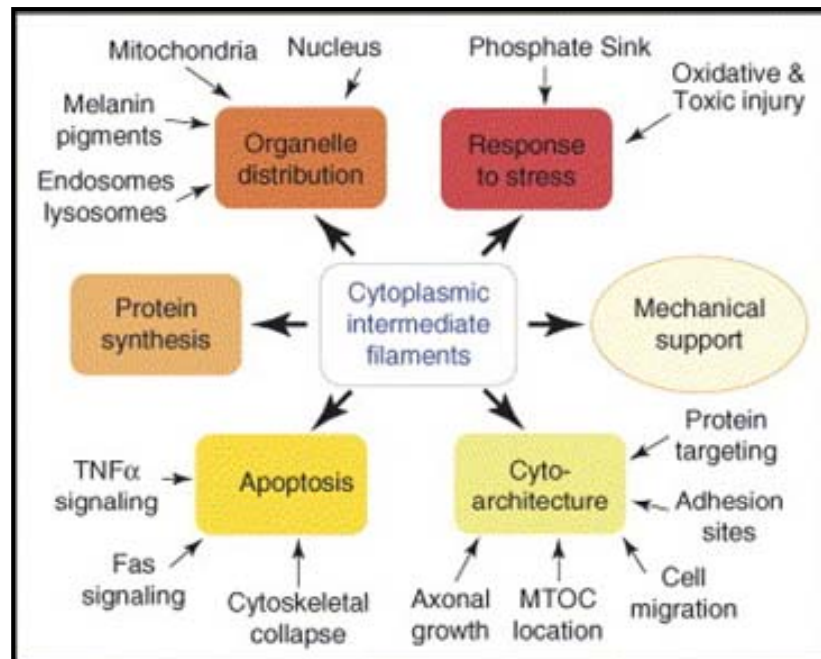


Figure 1.15: Function of keratins and other intermediate filament proteins. The arrows protruding from the centre box point to the six major cellular functions of keratins and other intermediate filament proteins, which are 1; mechanical support 2; cyto-architecture 3; regulation and execution of apoptosis 4; regulation of protein synthesis 5; organelle distribution and 6; response to stress. The smaller arrows are a summary of experimental studies supporting the specific function within the broad category of cellular functions (adapted from Gu and Coulombe, 2007).

Table 1.5: The function of epithelial keratins

Keratins are involved in cell signalling
Keratins act as stress proteins (for example in protecting liver cells from toxins).
Keratins are involved in the regulating the availability of cellular proteins (such as keratin associated proteins by either providing anchoring or by maybe effecting the enzymatic activity of keratin associated proteins).
Keratins are involved in aiding the targeting of protein to polarized epithelia (apical destined membrane markers are either rearranged or absent in villus of intestine keratin null mice models).
Keratins are involved in tissue-specific expression in differentiation dependent functions (the head and tail domains which shows heterogeneity in its sequence among different keratins, contributing to tissue-specific expression and function of keratins genes.

(adapted from Coulombe and Omary, 2002)

1.12 Mechanisms of Transcriptional Regulation of Keratin Gene Expression

A transcription factor is defined as any molecule participating alone or as apart of a complex, in binding to a gene response element with the ultimate outcome of either up or down regulation of that gene (Nebert, 2002). Eukaryotic genes show differentiation specific expression patterns, which are regulated by cis-acting elements (Huff et al, 1993). The two types of positive cis-acting DNA elements are described as enhancers and promoters. Promoters by definition are gene region that initiates gene transcription, and they are normally only functional when placed immediately upstream from the region to be transcribed (Jiang et al, 1990). An enhancer can act at a distance, regardless of position or orientation (Jiang et al, 1990). Such cis-acting elements often serve as the binding sites for transcription factors and the cis-elements which regulate keratin gene expression are said to reside in the 5'-upstream region or the 3'-downstream of the gene and sometimes in the introns (Huff et al, 1993). To account for the tissue specific expression of keratin genes, two mechanisms have been suggested: 1) a positive regulatory mechanism with an epithelial specific activator or 2) a negative regulatory mechanism which involves a reducer of signal strength in non-epithelial cells or cells which do not express the endogenous keratin gene (Jiang et al, 1990).

1.13 Transcriptional Regulation of Keratin Gene Expression

Several studies have identified an increasing number of transcription factors implicated in the regulation of keratin gene expression (Leask et al, 1990; Chen et al, 1997; Wang et al, 2002). The control of cell specific gene transcription plays a central role in the formation and maintenance of various tissues, including the oral mucosa (Wu et al, 1993). Structural variation in the oral mucosa is governed by keratinocyte-specific gene expression (Leask et al, 1990), but to date no specific set of transcription factors is known to govern tissue-specific expression of keratin genes, despite the fact that the 5'-upstream sequences of many keratin genes have been cloned and found to function in a tissue specific manner in cultured keratinocytes (Wang et al, 2002).

1.13.1 Transcriptional Regulation of K12 Gene

Important cis-regulatory elements of the mouse K12 gene serve as cornea epithelial cell specific factors, these factors include AP-1, C/EBP and KLF6 and has been found to bind in between -0.4Kb to -0.6Kb of the K12 promoter region (Wang et al, 2002). The defining DNA sequence of the K12 promoter regions has been found by deletion analysis of promoter in plasmid constructs either transfected into cultured cells or studied *in-vivo* by the use of transgenic mice (Wang et al, 2002).

1.13.2 Transcriptional Regulation of K14, K3, K15 and K6 Genes

The AP-2 transcription factor has been implicated in epidermal K14 gene regulation. The 5'-upstream sequences of several other keratin gene promoters, including the K3, K15 and K6a are also known to harbour AP-2 binding motifs. However, with K5 and K14 genes, AP-2 alone does not seem to be sufficient for epithelial specific expression (Chen et al, 1997). The 5'-upstream region of bovine K6a gene confers tissue-specific expression and hyper-proliferation related induction in transgenic mice (Ramirez et al, 1995).

1.13.3 Transcriptional Regulation of K19 Gene

The K19 promoter has been shown to be active in a subset of gastrointestinal cancer cells derived from the oesophagus and pancreas (Opitz and Rustgi, 2000). This activity was mapped to a short region containing an overlapping binding site for gut-

enriched-Kruppel-like-factor (GKLF/KLF4) and Sp1 in these cells, which leads to aberrant K19 gene expression (Opitz and Rustgi, 2000).

1.13.4 Transcriptional Regulation of K4 Gene

K4 shows tissue specific expression in cornea, oral mucosa and oesophagus, the tissue specific transcriptional regulation of K4 expression in the cornea is mediated by the binding of Sp1 to two independent Sp1 cis-acting elements. However, the transcriptional control of K4 expression in the oesophagus is regulated by GKLF oesophageal-specific transcription factor (Opitz and Rustgi, 2000)

1.13.5 Transcriptional Regulation of K17 Gene

K17 is not normally expressed in the skin, but it is expressed under numerous pathological conditions which affect the skin such as cutaneous allergic reactions and psoriasis (Milisavljevic et al, 1996). The mechanism involved in the transcriptional regulation of K17 is not understood, but in an attempt to unravel the molecular mechanism which regulates the expression of K17 gene expression, a 0.45Kb promoter region of K17 gene was used (Milisavljevic et al, 1996). The results have shown that there is an interferon responsive element, nuclear factor 1 (NF1), AP-2 and Sp1 binding sites in K17 promoter. Site-directed mutagenesis and electrophoretic mobility shift assays were used to demonstrate the importance of these transcription factors binding sites to the K17 promoter and their functional involvement in both the interferon-gamma induced and constitutive K17 expression (Milisavljevic et al, 1996).

1.13.6 Transcriptional Regulation of K3 Gene

K3 is expressed in the basal layer of the corneal epithelium and in the suprabasal layer of the peripheral cornea (Wu et al, 1993). Using 3.6Kb of K3 upstream promoter sequence linked to chloramphenicol acetyl transferase (CAT) reporter gene, the K3 promoter construct showed corneal and esophageal cell specific expression, but was not expressed in fibroblasts (Wu et al, 1993). This keratinocyte specific expression of K3 was localized to 0.3Kb in the upstream sequence and this sequence was also shown to contain a cluster of NFkB transcription factors binding sites, which is thought to confer the K3 keratinocyte differentiation specific expression (Wu et al, 1993).

1.13.7 Using Proximal Promoters

Some studies are subject to methodological criticism of their use of a small promoter fragment for investigating vital regulatory sequences. Larger fragments maybe essential for a better picture of overall suppressor and enhancer elements important for the expression of keratin genes. In addition, experiments with larger fragments have produced results with closer to the *in-vivo* levels of keratin gene expression. This is exemplified by K1, the first suprabasal keratin to be investigated as a transgene, in which a 10.8Kb fragment containing the human K1 (HK1) coding region, 1.2Kb of upstream sequence and 4.4Kb of downstream sequence, is used to generate transgenic mice (Blomhoff, 1994). The results have shown that 1) 10.8Kb HK1 fragment might be missing sequence information required for correctly regulating tissue and developmental specific expression in transgenic mice. 2) The Ca^{2+} concentration in the medium caused induction of both mouse keratin 1 (MK1) and HK1 fragment, while other agents such as retinoic acid suppressed MK1 but not HK1 (Rosenthal et al, 1991). This data suggest that neither the 10.8Kb (Blomhoff, 1994), nor 12Kb HK1 fragment contain the important cis-acting elements which may function to regulate the suppressive action of RA on HK1 (Rosenthal et al, 1991). In an attempt to support the hypotheses that 1) HK1 can show tissue and developmental specific expression in transgenic mice and 2) a further upstream regulatory element might be required to enable the observation of the suppressive effect of RA on HK1 (Blomhoff, 1994). Transgenic mice were generated from a larger HK1 fragment containing the coding region, 13Kb of upstream sequence and 3.4Kb of downstream sequence (Blomhoff, 1994). As a result of generating this larger HK1 fragment, the staining pattern of HK1 was absent in epidermal basal layer and the same expression as the endogenous HK1 protein was found (Blomhoff, 1994). Retinoic acid suppressed expression of larger HK1 fragment in transgenic mice (Blomhoff, 1994). Taken together, these results emphasize the importance of using larger upstream and downstream sequences of the gene in order to show correct regulation with regards to tissue and developmental specific expression of keratin genes. Although in this thesis, a larger K13 and K15 promoter (3Kb) sequence is used in comparison to other studies (Wang et al, 2002), nevertheless the maximum promoter size was estimated to be around 8Kb for K13 and 4.6Kb for K15 (Appendix: Figure 7.6). Thus, this thesis could have benefited from using the complete upstream sequence as opposed to the 3Kb used. As highlighted above with

HK1, larger fragments are more likely to show correct regulation and thus are closer to resembling the *in-vivo* differentiation-specific expression of keratin genes.

Table 1.6: Summary of studies showing type I and II keratin epithelial specific expression and the transcription factors involved.

Name of Keratin	Normally areas of expression	Notes	Transcription factor	Reference
K5	The basal layer of all stratified epithelia	Analysis of 5.2Kb5' upstream region of the K5 gene was able to confer corneal specific expression	Most of the transcriptional activity is located to an enhancer - 762-1009 which was shown to bind AP-1	(Casatorres et al, 1994)
K14	K14 is basal marker in all stratified epithelia	K14 expression is up-regulated in oral squamous cell carcinoma and dysplastic tissue.	Luciferase reporter gene assay has shown that the -1759 to -1629 of the K14 promoter caused a substantial increase of K14 promoter in several OSCC cell lines. There are several SP-1 and SP-3 complex binds to that region of the promoter.	(Ohkura et al, 2005)

Table 1.6 shows summary of keratins that show epithelial specific expression and the transcription factors which are implicated in conferring this specific expression.

1.14 Post-translational Modification of Keratin Proteins

Keratin proteins can intrinsically regulate their own function by undergoing bundling, which enables them to acquire greater elasticity to withstand experimentally induced deformation and thus show enhanced mechanical resilience (Coulombe and Omary, 2002). Keratin protein function can also be regulated extrinsically by their interaction or association with other non-keratin proteins, which results in keratin phosphorylation, glycosylation, transglutamination, ubiquitination (Figure 1.16) and proteolytic cleavage (Coulombe and Omary, 2002). Amongst all the post-translational modifications which regulate keratin protein expression, phosphorylation is the most studied (Zhou et al, 2006). Keratin phosphorylation involves the addition or removal of a phosphate group which commonly occurs in heterogenic sequences present in the head and tail domain of keratins (Zhou et al,

2006). Phosphorylation and de-phosphorylation of keratin and other intermediate filament proteins are required for transient assembly and disassembly during mitosis, leading to remodelling of the epithelium (Owens and Lane, 2003). Hyperphosphorylation of keratin causes the assembled keratin filaments to irreversibly depolymerize, while specific phosphorylation causes reversible remodelling of keratin filaments (Owens and Lane, 2003). For example as result of ser52 site phosphorylation in K18, the importance of this site in filament reorganisation was recognised; also another phosphorylation site ser33 in K18 was identified as been essential for the binding of 14-3-3 protein (Ku et al, 1998). The function of keratin associated proteins such as 14-3-3 is to regulate the enzymatic activity of the protein to which it is bound to (Ku et al, 1998). For example, when 14-3-3 protein reversibly associates with K18/K8 in cultured cells, this leads to 14-3-3 induced keratin subcellular distribution (Ku et al, 1998). Another posttranslational modification of keratins is glycosylation (Omary et al, 1998). Glycosylation is the addition of polysaccharides to target proteins, this addition of polysaccharides serves various function for the protein, including the correct folding of proteins such that they are not degraded rapidly (Omary et al, 1998). Glycosylation of K18, K8, and K13 occurs via O-GlcNac (Omary et al, 1998). Three serine glycosylated sites were identified in the head domain of K18 protein and, although the function of this posttranslational modification is unknown, it is thought that all keratins are glycosylated (Omary et al, 1998). Transglutamination occurs in both stratified epidermal and simple epithelial keratins (Omary et al, 1998). Transglutamination of keratin proteins occurs during normal physiological and diseases state (Coulombe and Omary, 2002). Transglutamination modification of keratin protein occurs in the cornified envelope (CE) and links, a few type II keratins (K6, K5, K2 and K1) proteins to other structural CE proteins like loricrin, involucrin and envoplakin, by the highly conserved lysine in the head domain (Coulombe and Omary, 2002). Use of fractionated mouse epidermis for analysis of keratin expression, has led to the identification of a 67kDa protein (K1) and another smaller protein product of 65.5kDa (K1a) which arose by proteolytic cleavage in the granular layer of the epidermis (Bowden et al, 1987). In addition, further proteolytic modulation of the 58kDa (K10), has led to the production of another smaller product of 55.5kDa (K10a) in extracts derived from stratum corneum of fractioned mouse epidermis (Bowden et al, 1987). This proteolytic modification is thought to take place in the

lower and upper stratum corneum of the epidermal environment (Bowden et al, 1984). The proteolytic modification of K1 and K10 is thought to permit the tight packing of filaments in the stratum corneum and thus contribute to the specific protective function of the epidermis (Bowden et al, 1984).

1.14.1 Phosphorylation Modification of Other IFPs

Other intermediate filament proteins (IFPs) such as vimentin, have been reported to be regulated by p21-activated kinase (PAK), a downstream target of Cdc42 or Rac (Goto et al, 2002). As result of PAK enzyme binding to vimentin, the following serine sites, ser25, ser38, ser50, ser65 and ser72 in the amino terminal head domain of vimentin are phosphorylated by PAK (Goto et al, 2002). It was suggested that vimentin phosphorylation by PAK in COS-7 cells might regulate the reorganisation of vimentin filament (Goto et al, 2002).

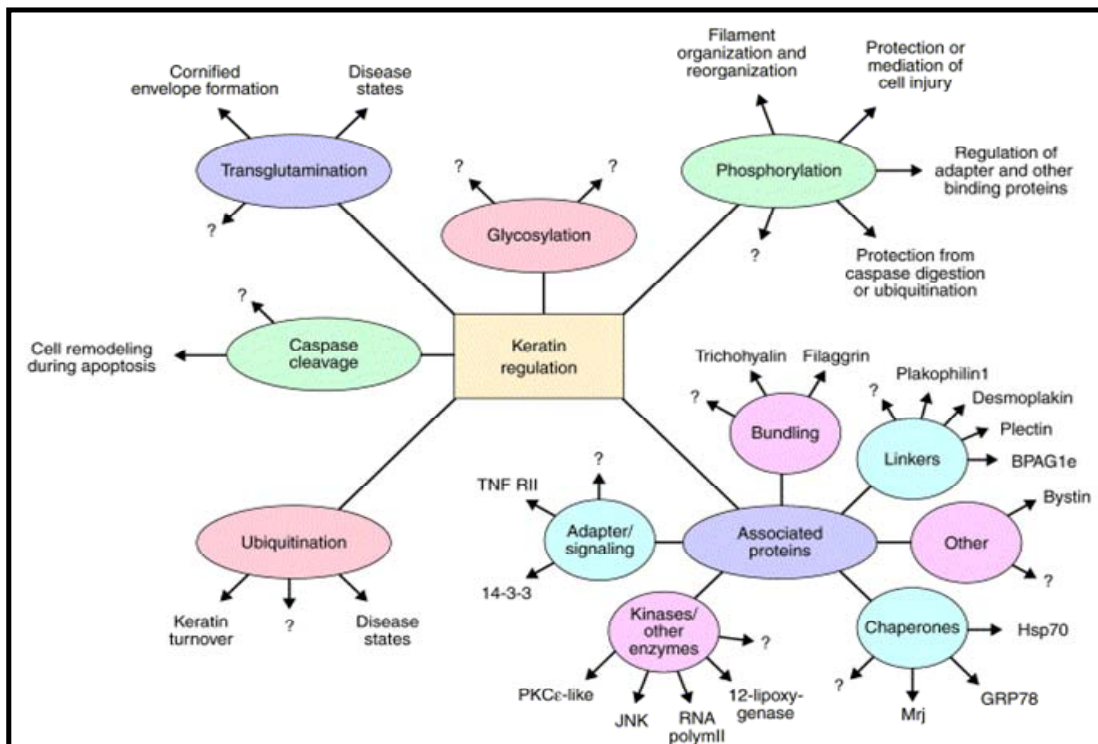


Figure 1.16: Various post-translational mechanisms which regulate the expression of keratin and keratin associated proteins (adapted from Coulombe and Omary, 2002).

1.15 Keratin Expression in Normal Epithelia

The expression of a specific pair of keratins (Table 1.7) begins in the basal layer of the stratified squamous epithelium, which typically expresses K5, K14 and to a lesser extent, K15 (Radoja et al, 2004). However, in the basal layer of the oesophageal epithelium K14 is substituted by K15 (Brembeck et al, 2001). The expression of the K5/K14 pair is down-regulated when keratinocytes detach from the basement membrane. This is followed by the expression of a suprabasal keratin pair, which differs between epithelial tissues; for example, in keratinizing epithelia of the epidermis, gingiva and hard palate, the K1/K10 are expressed (Waseem et al, 1998). However, in non-keratinizing buccal and oesophagus epithelium K4/K13 are expressed. In the more differentiated central cornea K3/K12 are expressed in both the basal and suprabasal layers, but in the stem cell rich peripheral cornea (the limbus), K12/K3 are expressed only in the suprabasal layer (Jiang et al, 1991) The adult tongue expresses K1, K2, K4, K5, K6a, K10, K13, K14, and K16 and infrequently expresses K17. In the basal layer of both the fungiform and filiform papillae K5 and K14 are expressed (Vaidya et al, 2000). K6a and K16 are usually expressed in the outer root sheath of hair follicles, the gingiva and hard palate, oesophagus, and female genital tract (Waseem et al, 1999). K6a and K16 are also expressed in the nail bed and the epidermis covering the palms and the soles (Rothnagel et al, 1999). Other keratins that are normally expressed in palm and sole skin include K1, K5, K9, K10, K14 and K17 (Rugg et al, 2002). The suprabasal layer of the hard palate and gingiva express K76 which distinguishes it from the epidermal K2 (Presland and Dale, 2000). K11, which was identified in the original keratin cataloguing by Moll et al, (1982), was later identified as a modified form of K10 and thus K11 does not exist in the human genome (Bowden, 2005). K7 and K17 are expressed in simple epithelial, for example the kidney (Jiang et al, 1991). K8 and K18 are normally expressed in the simple epithelia of the liver, small and large intestine and the pancreas which particularly expresses high levels of K8 and K18 (Brembeck et al, 2001). K8 and K19 are normally expressed in glandular and in foetal buccal and tongue epithelium until 27 weeks of gestation (Fillies et al, 2006). Sites of K19 expression include the oesophagus, stomach, pancreas, small intestine, colon in human adults, outer root sheath of the hair follicle and foetal liver, which expresses particularly high levels of K19, but this is not normally expressed in adult liver cells

or epidermis (Brembeck and Rustgi, 2000; Chu and Weiss, 2002). K20 is normally expressed in gastrointestinal epithelia and urothelia (Owens and Lane, 2003).

Table 1.7: Keratin expression in simple and stratified epithelia

Epithelial type	Keratins		Distribution
	Type II	Type I	
Simple epithelial	K8	K18	Most secretory and parenchymatous cells
	K7	K19	Ductal epithelia (bile and pancreatic, renal collecting duct) and gastrointestinal epithelia.
		K20	Gastrointestinal epithelia, Merkel cells of the skin and taste buds of the oral mucosa
Stratified squamous epithelial	K5	K14	Basal cells of the squamous and glandular epithelia, myoepithelia, and mesothelium.
		K15	Squamous epithelia.
Suprabasal cells	K1	K10	Epidermis (entire suprabasal compartment)
		K9	Epidermis of the palms and soles
	K2		Epidermis (high layers)
	K76		Gingiva, hard palate
	K3	K12	Corneal epithelium
	K4	K13	Non-keratinizing stratified squamous epithelia of internal organs.
	K6a, K6b	K16, K17	Hyperproliferative squamous epithelia

(adapted from Chu and Weiss, 2002).

1.15.1 Hair-Specific Keratins

The hair keratins were originally designated as hard keratins and the epithelial keratins as soft keratins (Langbein et al, 2001). The hard keratins are involved in the formation of keratinized structures such as nails, claws and hair (Langbein et al, 2001). Like the soft keratins, the hard keratins are also divided into an acidic (Ha) type I (44-48kDa), whose genes are located in chromosome 17, and a basic (Hb) type II (55-60kDa) keratins, whose genes are located in chromosome 12 (Langbein et al, 2001). Using two-dimensional gel electrophoresis and Coomassie blue, stained proteins of each hair keratin subfamily were numbered 1 to 4 (Langbein et al, 2001).

These type I hair keratins were designated as hHa1 to hHa4, while the type II were designated hHb1 to hHb4. In addition, a subsequent characterisation of type I and II hair keratins has led to the discovery of 7 type I and 4 type II keratins proteins (Langbein et al, 2001). Based on sequence characteristics, the type I hair keratins have been divided into 3 distinct groups (Cribier et al, 2001). Group A, which includes hHa1, hHa3-I, hHa3-II and hHa4, is expressed in the hair cortex; group B members, which include hHa7 and hHa8, are expressed in the vellus hair and in the cortex of terminal hair. Group C members, which include hHa6, hHa5 and hHa2, are expressed in the cuticle and matrix or the cortex (Cribier et al, 2001). However, recent studies have shown that the type I and II hair keratins comprise exactly 11 and 6 members of hair keratins and are designated as K31 to K40 for type I and K81 to K86 for type II as shown in Tables 1.3 and 1.4 (Schweizer et al, 2006).

1.16 Keratin Expression in Pathology

Epithelia are the origin of most human cancers, and are located at sites where cell division is high and epithelial cells are environmentally stressed, these factors make the proliferating cells more prone to oncogenic transformation (Owens and Lane, 2003). Importantly, the epithelia also interface with the environment. The causes of epithelial cancer can be both genetic and environmental, such as smoking (Reibel, 2003). Studies on various populations have reported that smokers have higher risks of getting oral cancer than non-smokers (Reibel, 2003). Although the exact mechanism through which smoking causes oral cancer remains unknown, it is thought that the carcinogens in tobacco smoke can cause changes in DNA (Reibel, 2003). Markers used for determining future cancer development in oral pre-malignant lesions are divided into three categories, 1) genomic markers including chromosome aberrations (which cause loss or gain of allele), 2) proliferation markers and 3) differentiation markers (Reibel, 2003). Keratins are differentiation markers of oral mucosa and can also be utilized for characterization of malignant tumours, since expression of a particular keratin in tumour cells is dependent on the degree of differentiation (Kim et al, 1996). Furthermore, in oral squamous cell carcinoma (OSCC), there is marked reduction of K13 and K4 expression, with the appearance of K1 and K10 as well as K2 (Boisnic et al, 1995). OSCC accounts for 90% or more of all oral malignant neoplasms, but with respect to all cancers, oral cancer accounts for appropriately 4% (Soames et al, 2005). OSCC is the sixth most frequent cancer in

the world with approximately 30,000 new cases diagnosed annually (Nagler 2002). The incidence of oral cancer varies enormously around the world and it is most prevalent in India and south East Asia (Soames et al, 2005). The overall 5 year survival rate for patients with oral squamous cell carcinoma is among the lowest for major cancers, despite progress in therapeutic and diagnostic oncology in the past two decades (Nagler, 2002). Prognosis remains poor owing to continued diagnosis of the disease only at an advanced stage (Nagler, 2002) and a major area of improvement should be aimed at promoting awareness of OSCC by educating the general public about signs, symptoms and aetiological factors which increase the risk of oral cancer. This would assist early detection of oral cancer when treatment is most effective (Gervasio et al, 2001). The finding of biological tumour markers might increase the early diagnosis and treatment rates of OSCC (Nagler, 2002). Epithelial tumours retain specific features of keratin expression patterns of their cell type of origin, and in cases where clinical data or conventional histopathology remain unclear, keratin proteins can be used to aid in identifying and classifying the tumour (Moll et al, 2008). Keratins are thought to be a good biological tumour marker because they are stable and effective immunogens for generating monoclonal antibodies (Owens and Lane, 2003). Staining for keratins in epithelial tumours, indicated patterns of keratin expression associated with:

- Expression of new subsets of keratins not expressed by normal tissue.
- Lack of expression of the original keratins (Kim et al, 1996).

OSCC originates from different sites and is normally characterised by stratified epithelial-specific keratins, which might be co-expressed with simple epithelial-specific keratins (Moll et al, 2008). Of all the known keratin genes to date, only a few have been used as a diagnostic markers (Moll et al, 2008). An example of expression of new subsets of keratins not expressed by normal tissue, has recently been reported in SCC of the oral cavity whereby the expression of simple epithelial-specific K8/K18 expression was used as an independent prognostic marker and has been shown to correlate with decreased overall and progression free survival (Fillies et al, 2006).

1.17 Keratins Implicated in Genetic Diseases

A link between keratins and their inherited mutations which lead to skin fragility and oral mucosa disorders was discovered in the early 1990s; this proved to be a valuable discovery in the understanding of intermediate filament function (Lane and McLean, 2004). K5 or K14 gene mutations in mouse and human epidermis have been shown to cause a skin blistering disorder known as epidermolysis bullosa simplex (EBS) (DePianto and Coulombe, 2004). EBS is a genetic skin disease affecting approximately 1:2000 of the population (Csikos et al, 2004). Almost all cases of EBS are characterized by mechanical-stress-induced blistering of the skin and, in severe cases, the oesophagus and oral mucosa may also blister (Csikos et al, 2004). This is a result of keratin filament bundle degeneration in the basal keratinocytes which begins within a few days after birth (Csikos et al, 2004). Furthermore, a common phenomenon occurring in keratin gene families is substitution for one member of the keratin family by another mutated or missing one (Radoja et al, 2004), which leads to a lack of phenotype in gene knock-out. An example of the above was observed in mutant K14 gene in EBS patients, which was counteracted by increasing the cellular content of K15 using thyroid hormone and IFN- γ agents, in an attempt to compensate for the mutant K14 and thus ease the skin blistering in EBS patients (Radoja et al, 2004). Mutations in palm and sole skin associated K1, K5, K6b, K10, K14, K16, K17 and K9 genes are thought to cause palmoplantar keratodermas (PPKs), which involves thickening and hyperkeratosis of palmoplantar skin (Rugg et al, 2002). Furthermore, mutation of epidermal suprabasal markers K1 and K10 results in a condition known as epidermolytic hyperkeratosis, a blistering of the suprabasal layer caused by cell lysis, degeneration and basal cell hyperplasia (Brembeck et al, 2001). Additionally, keratins have been implicated in functional roles beyond that of mechanical resistance. For example, the K8 and K18 filaments network found in the simple epithelia of the liver contributes to the resistance of hepatocytes to chemical and osmotic stress (DePianto and Coulombe, 2004). K8 or K18 gene knockout mice experiment has demonstrated a predisposition of mice to liver cirrhosis (DePianto and Coulombe, 2004).

1.17.1 Keratin Mutations and Overlapping Phenotypes in Skin and Oral Mucosa Epithelia

Some of the mutations in keratin genes can cause overlapping phenotypes in different tissues which expresses the keratin gene. An example of this is a 3bp deletion in exon 1 of *KRT6A*, which leads to removal of asparagine from position 8 in the conserved 1A helical domain. This results in a rare autosomal dominant condition known as Pachyonychia Congenita (PC) (Bowden et al, 1995). PC is more common in Slovenian and Croatian families who are from specific locations having isolated populations where family members intermarry (Bowden et al, 1995). K6a and K16 are normally expressed in palm and sole epidermis, hair follicle, nail and oral epithelia of the tongue (Bowden et al, 1995). Thus mutations in *KRT6A*, results in thickened nails, palmoplantar keratoderma and leukokeratosis of the tongue (Bowden et al, 1995). In addition, mutation in the *KRT13* and *KRT4* genes has been shown to cause a benign autosomal dominant disorder known as White Sponge Nevus (WSN), which is characterized by thick, white spongy fold in the oral mucosa, and to a lesser extent in the mucosal membrane of the nose, oesophagus and the rectum (Opitz et al, 1998). Histological analysis of the white spongy plaque shows evidence of acanthosis, hyperproliferation and tonofilament aggregation and these pathological changes are also associated with many epidermal keratin disorders (Rugg et al, 1995). Furthermore, a three-base-pair deletion in the helix initiation peptide of K4 was discovered in some families affected by WSN (Rugg et al, 1995), while a substitution mutation has been found in one allele of K13 gene leading to substitution of conserved leucine for proline (Richard et al, 1995). This substitution mutation occurred in the conserved 1A region of the helical rod domain which is important for keratin filament stability and is the site which corresponds to most keratin mutations that causes disease (Richard et al, 1995).

Table 1.8: Keratin proteins and associated Keratinopathies of Epidermis and Oral mucosa

Tissue	Keratin proteins expressed	Associated Keratinopathies
Epidermis	K5, K14 (basal)	EB simplex (K5,K14)
	K1, K10	Epidermolytic hyperkeratosis
	K2	Ichthyosis bullosa of Siemens
Palm and Sole skin	K9	Epidermolytic PPK
	K16	Non-Epidermolytic form of PPK
	K6a, K16, K19	Pachyonychia congenita
	K1, K10	Epidermolytic hyperkeratosis 2
Gingiva/hard palate	K5, K14 (basal)	EB simplex
	K6a, K16,	Pachyonychia congenita
	K1, K10	None reported
	K76	None reported
Buccal/soft palate	K5, K14, K19 (basal)	EB simplex
	K4, K13	White sponge nevus

(adapted from Presland and Dale, 2000).

1.18 Keratin 13

Human keratin 13 (K13) is a type I acidic keratin with a molecular weight of 54kDa. The K13 gene (*KRT13*) is 4601 nucleotides long and contains seven introns and eight exons (Waseem et al, 1998). Human *KRT13* has been mapped to the long arm region of chromosome 17 (Romano et al, 1992). Although there are pseudogenes or functional isoforms of some keratins such as K14 (in the human genome there are three K14 pseudogenes), only one appears to be functional (Vassar et al, 1989) and there is no evidence of multiple *KRT13* genes (Richard et al, 1995; Waseem et al, 1998). K13 is heavily *O*-glycosylated in certain cultured keratinocytes but not in mucosal tissues of human or mouse origin. Although *N*-acetylglucosamine is the residue involved in K13 glycosylation, neither the site of this sugar attachment nor the function of this post-translational modification has been clarified (King and Hounsell, 1989). K13 is one of the most abundant filament proteins in buccal non-stratified epithelia (Kim et al, 1996) and together with K4, its type II basic keratin partner, it forms the major keratin network of most internal stratified epithelia (Waseem et al, 1998). Furthermore, in most stratified squamous epithelia K13 is expressed in suprabasal layers, although in human urothelium K13 has been

identified in basal as well as in suprabasal layers (Kuruc et al, 1989). Using immunohistochemistry to stain for K13, expression was found in buccal, soft palate, gingiva and conjunctival mucosa (Brysk and Tyring, 1995). K13 is also strongly expressed in the ventral surface of the tongue (Sawaf et al, 1990). The epidermis does not normally express K13, but exceptions are the penile foreskin, the anus and regenerating epidermis (Waseem et al, 1998).

1.18.1 Factors influencing K13 Expression

The reported factors which influence K13 expression are retinoic acid and calcium (Waseem et al, 1998). The expression of K13 has been shown to be elevated in presence of 1.2mM calcium in comparison to keratinocyte growth medium without calcium (Brysk and Tyring, 1995). Retinoic acid (RA), the active form of vitamin A, has been reported to directly and indirectly modulate the growth and differentiation of various normal and malignant cells (Kim et al, 1996). The direct effects of retinoic acid are thought to be mediated by changes in K13 expression, since the K13 promoter has been reported to contain an retinoic acid responsive element (RARE) consensus sequence (GGTTCA(N)₅TGTTCT). This sequence has homology to the natural RARE of the β 2 retinoic acid receptor gene (Winter et al, 1994). Using differential cDNA cloning, 10 genes were identified as being regulated by retinoic acid in a head and neck squamous carcinoma cell line (MDA886Ln). Among the 10 genes identified, K13 gene expression was most related to the degree of sensitivity of growth to RA, as K13 was not expressed in a series of RA-resistant cell lines tested and it was suggested that low K13 expression might be mechanistically related to resistance to RA-induced growth inhibition (Kim et al, 1996). Furthermore, RA regulates oral epithelial differentiation by effecting gene transcription via interaction with specific nuclear receptor proteins that function as retinoid activated transcription factors (Kautsky et al, 1995).

1.18.2 K13 Expression in Development and Experimental Models

K13 is expressed by foetal epidermis and cultured epidermal keratinocytes, but it is seen in adult skin only as occasional patches in the basal-cell layer. It was suggested that the association of K13 expression with mucosal surfaces and with submerged keratinocyte cultures may be linked to its expression in foetal skin (Brysk and Tyring, 1995). However, human K13 is only transiently expressed in keratinocytes

of foetal epidermis, and is replaced by K10 later in adulthood (Kuruc et al, 1989). Furthermore, the normal pattern of K13 expression and other keratins is altered in the presence of chemically and virally induced tumours. For example, the expression of K1 and K10 in DMBA and TPA-induced epidermal tumours is suppressed, with an increase in K13, which is considered to be an early marker of carcinoma progression. Nevertheless, although K13 expression is induced by DMBA and TPA in epidermal tumours, K13 is not normally expressed in human epidermis (Waseem et al, 1998).

1.18.3 Epigenetic Control of Gene Expression

Epigenetic refers to features of chromatin and DNA modification that are stable over many rounds of cell division but do not involve changes in the underlying DNA sequence of the organism (Bird, 2007). Epigenetic control of gene expression (Figure 1.17) occurs in two ways: modification of the state of histone proteins, or chemical alteration of the DNA (Qiu, 2006). The histone proteins determine whether the chromatin is tightly packed, so transcription factors cannot have access to the DNA and gene transcription is silenced; or whether the chromatin is in a relaxed state and thus the gene can be transcribed (Qiu, 2006). Chemical DNA alteration occurs by methylation, that is the addition of methyl group by DNA methyltransferase to the cytosine base when it is followed by guanine in the DNA (Qiu, 2006). The addition of methyl groups to DNA attracts proteins that specifically bind methylated DNA, and this results in blocking access of transcription factors required for the induction of gene expression (Curradi et al, 2002). These proteins contain a methylated-DNA binding domain (MBD) and have been implicated in gene transcriptional repression (Curradi et al, 2002). In addition, when the MBD proteins were biochemically characterised they were found to exist in complexes with histone deacetylase, which indicates that methylated CpGs (mCpGs) suppress transcription by establishing a repressive chromatin environment (Curradi et al, 2002). Thus Curradi et al, (2002) have proposed that CpG methylation and histone deacetylation act synergistically to silence gene expression. Both DNA methylation and histone modification are important for genome reprogramming during development, large-scale gene silencing and tissue specific expression (Beri et al, 2007).

Tissue-specific expression of murine K13 in internal stratified squamous epithelia and its abnormal expression during two-stage mouse skin carcinogenesis is

associated with the methylation state of the remote 5'-flanking region of the gene (Winter et al, 1990). The murine K13 gene CpG methylation site termed M1 is located -2.3Kb upstream from the transcriptional start site, is involved in controlling the tissue specific K13 expression in stratified squamous epithelium. The methylated M1 site was observed in both basal and suprabasal cells of the epidermis (Winter et al, 1990) and thus correlated with the lack of K13 expression in the epidermis. On the other hand, the M1 site is unmethylated in the cells of internal stratified squamous epithelia of the tongue and oesophagus, which leads to K13 expression in these tissues (Winter et al, 1990). However, unlike its mouse counterpart, human K13 (Waseem et al, 1998) expression is not regulated by DNA methylation.

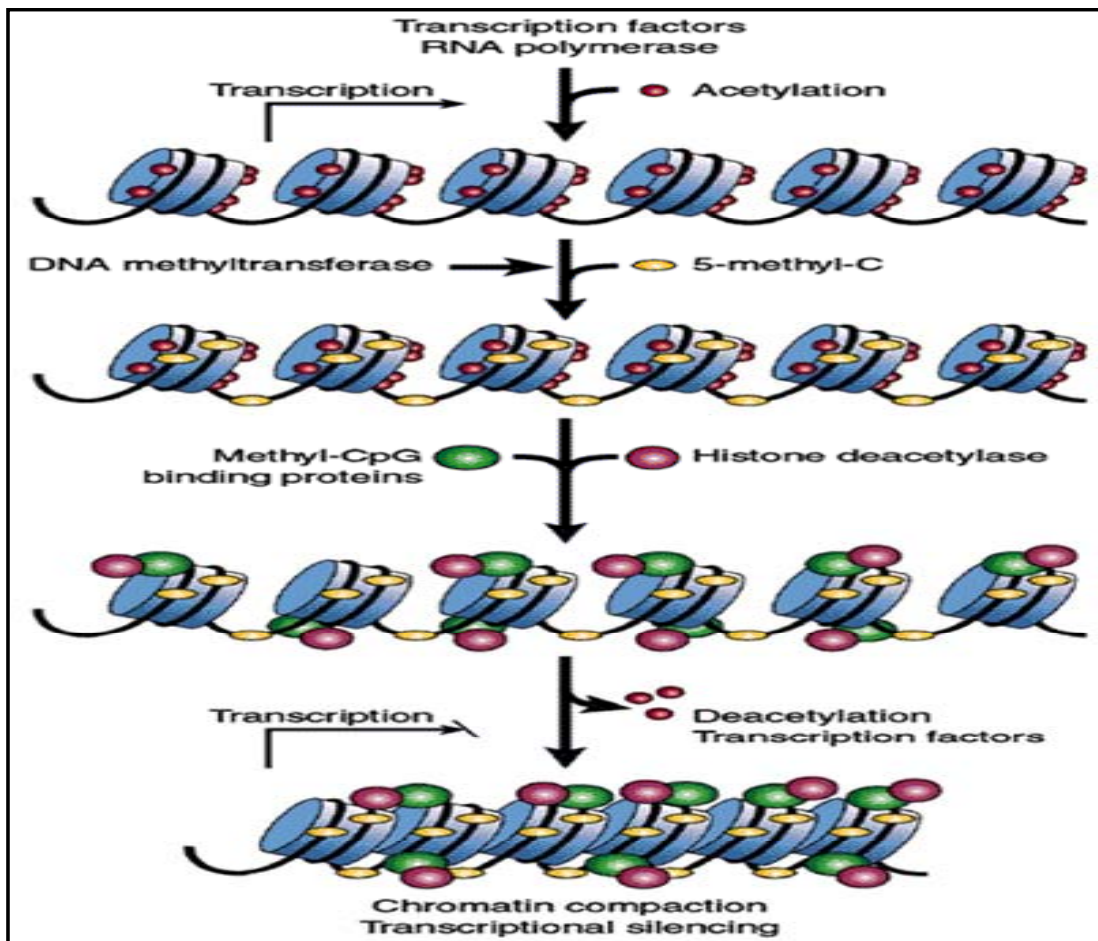


Figure 1.17: The epigenetic control of gene expression by DNA methylation and histone acetylation. Both mechanisms synergistically act together to either cause gene expression or silence gene expression such that lack of protein expression in tissues which do not endogenously express the gene occurs (adapted from website 9 in Reference).

1.19 Keratin 15

Human keratin 15 (K15) is a 57kDa protein which belongs to the acidic or type I keratin family and assembles into keratin filament network paired with K5, its basic type II partner (Romano et al, 1992). The K15 gene comprises 8 exons spanning appropriately 5.1Kb (Whittock et al, 2000). K15 is located in the q12-q24 region of chromosome 17 (Romano et al, 1992). The proliferating basal keratinocytes of all stratified squamous epithelial are characterized by their attachment to the basement membrane and expression of K14/K5 and to a lesser extent K15 (Radoja et al, 2004). K15 is normally expressed in basal cells of many epithelial tissues, such as those of the oral mucosa and the epidermis. In the epidermis, K15 is present in higher amounts in basal cells of thin skin than in the rapidly turning over thick sole plantar skin (Porter et al, 2000). In cultured keratinocytes, K15 levels are suppressed until the stratification of cultures, whereas K14 is constitutively expressed (Porter et al, 2000). In mouse and sheep K15 is expressed in the outer root sheath cells of hair follicle bulb and is restricted to the basal layer of the oesophagus. However, in human oesophagus, K15 is expressed throughout the epithelium (Whitbread and Powell, 1998). K15 is also weakly expressed in the ventral surface of the tongue (Sawaf et al, 1990).

1.19.1 K15 and K13 Expression as Models of *in-vitro* Epithelial Differentiation.

The K15 promoter was incorporated into this study for the following reasons: unlike K13 which is expressed in the suprabasal layer, K15 is expressed in the basal layer of both epidermis and oral mucosa (Porter et al, 2000). Furthermore, when basal cells differentiate, they migrate to the suprabasal compartment and during this process, the tissue stops synthesizing K5, K14 and K15 and induces other keratin pairs, characteristic of each tissue type (Casatorres et al, 1994). Thus to understand cell-specific keratin expression, it is necessary to study the mechanism by which the K15 gene promoter will enable positive or negative regulation in different environments (Casatorres et al, 1994) in comparison to suprabasal expressed K13 gene promoter. In addition, of the entire human type I keratin group, K13 shows the closest relationship to K15, since both K13 and K15 are characterized by relatively short tail domains of 46 and 43 amino acid residues respectively and are generally rich in hydroxyl-amino acids (Kuruc et al, 1989). While the location of stem cells can be related to the anatomic structure of some tissues (such as intestine, tongue papillae,

and hair follicles), stem cells are not easily identifiable morphologically in most areas of skin and oral mucosa. The presence of adhesion molecules such as the β 1-integrins and β -catenin were reported to be stem cell markers (Squier and Kremer, 2001). Staining for K15 and K19 has been used to identify stem cells in hair follicle, skin and in oral mucosa and are reported to be putative “stem cell markers” in these regions (Tudor et al, 2004). The utilization of K15 as a stem cell marker in the oral mucosa may enable researchers to identify the properties of stem cells *in-vitro* more easily and may lead to elucidating the molecules that coordinate specific developmental programs important in determining the influences of the environment on stem cell regulation and differentiation (Alonso and Fuchs, 2003).

1.19.2 Factors and Regulatory Elements Influencing K15 Expression

Analysis of murine K15 regulation has shown that the 5'-upstream region of the promoter may possess inhibitory cis-acting elements. Promoter sequences have exposed numerous potential cis-regulatory elements such as AP-1 and Sp1 binding sites, which are also important for regulation of numerous keratin genes. The AP-1 and Sp1 regulatory elements which bind the promoter region of the K15 gene are thought to inhibit K15 expression at some level and could be important for the basal specific expression of K15 gene (Liu et al, 2003). In addition, the manipulation of a cloned human K15 promoter with transcription factor and extracellular agents has shown that retinoic acid, glucocorticoid receptors and NF- κ B suppressed K15 expression, while C/EBP- β and AP-1 induced K15 gene expression (Radoja et al, 2004). However, thyroid hormone and IFN- γ are the only agents which potently increased the K15 promoter expression (Radoja et al, 2004). Other factors reported to downregulate K15 gene expression include TGF- β and tumour necrosis factor- α (TNF- α). K15 expression was suppressed by TGF- β and TNF- α , but to a lesser extent than epidermal growth factor (EGF) and keratinocyte growth factor (KGF) (Werner and Munz, 2000). Unlike K15, K14 has been shown to be upregulated by TGF- β . K15 mRNA was also reduced in expression after skin injury, whereas K14 expression increased during wound healing process (Werner and Munz, 2000). Using immuno-staining, K15 was localized to basal layer of the epidermis next to the wound, but not in the hyperproliferative epidermis (Werner and Munz, 2000). K15 exclusion from activated keratinocytes of the thickened wound epidermis was

explained by the increase of growth factor expression in injured skin leading to the absence of K15 expression (Werner and Munz, 2000).

1.20 Hypothesis and Aims of the Study

As outlined in this review, very little is known about K15 and K13 transcriptional regulation during differentiation-specific expression in the oral mucosa. In order to shed light on the molecular mechanism governing oral mucosa basal and suprabasal marker expression, this study will use K15 and K13 promoter-linked GFP reporter assays.

1) The mechanisms which regulate tissue specific expression of K13 are unknown. Therefore, the first hypothesis is that the expression of K13 promoter is regulated by suppressor elements rather than enhancer elements. This will be investigated by using a human K13 promoter linked GFP reporter gene construct and 5'-end truncated K13 promoter constructs which will be transiently transfected into permissive and non-permissive cell lines. Also, the importance of PKC, MEK 1/2 and PI3K/Akt pathways for the expression of K13 will be tested. This will be done by using transient transfection of a full length K13 promoter construct and Western blot to detect K13 protein expression in the presence or absence of PKC, MEK 1/2 and PI3K/Akt pathway inhibitors or activators.

2) The second hypothesis to be tested is that isolated human K13 and K15 promoter-linked GFP reporter gene expression is correlated with heterogeneous morphologically-distinct subpopulations present in oral mucosal cell lines. This will be investigated by transfecting the K15 and K13 promoter constructs into epithelial cell lines and using FACS to measure GFP expression. Colony assay will also be used to count the number of colonies formed by cells counting K15 or K13 FACS sorted promoter constructs. Immunocytochemistry will also be used to detect K15 and K13 protein expression in oral epithelial cell lines.

3) The third hypothesis is that the use of a transcription factor database is likely to reveal that suprabasal keratin promoters are governed by a set of transcription factors which are different from those governing basal keratin promoters. This hypothesis will be addressed by the use of a transcription factor database to see if transcription

factors which confer tissue specific expression in the basal and suprabasal layer are the same or different.

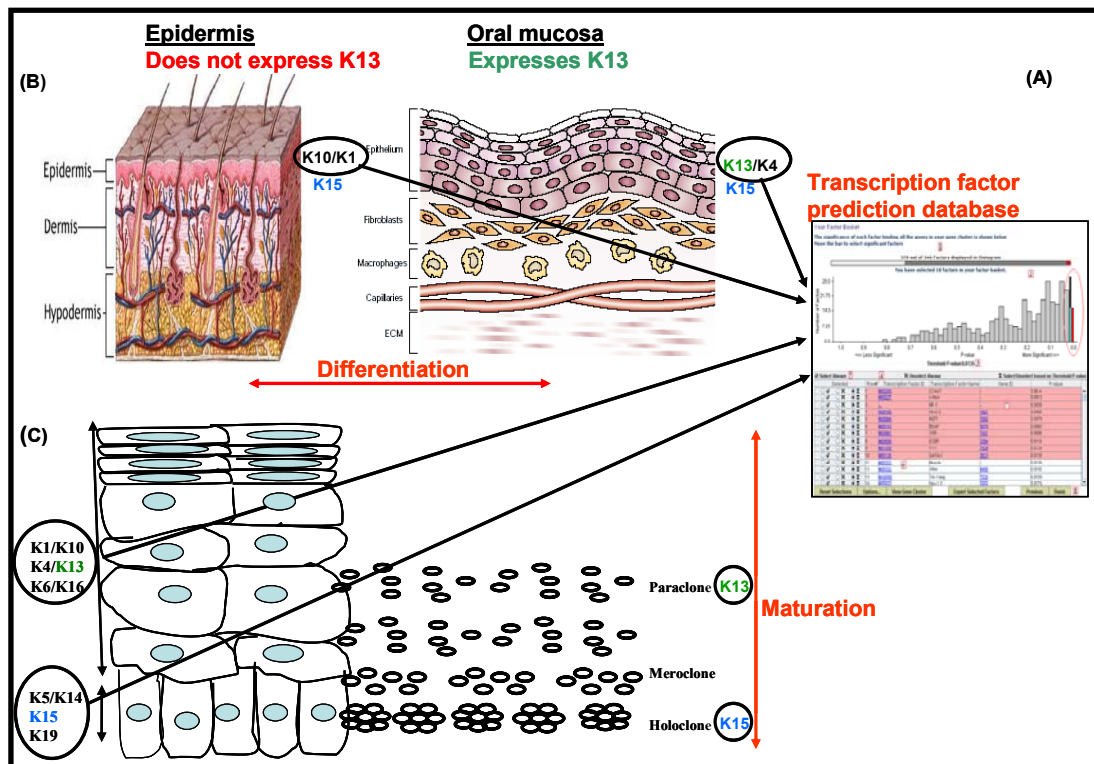


Figure 1.18: Diagram illustrating the overall aim of the study: the use of a transcription factor database (A) to detect putative transcription factor binding sites in keratin gene promoters as described in chapter 3 and how this chapter interlinks with chapter 4 and 5 is shown. (B) Shows the tissue specific differentiation as marked by K13 expression in the oral mucosa but not in the epidermis, as described in chapter 4. (C) Shows the correlation of K15 and K13 expression with oral mucosa maturation as described in chapter 5 (pictures were taken from website 1, 4 and 5 in the Reference section).

Chapter 2

Materials and Methods

2.1 Introduction to the use of Reporter Gene Assays and the Advantages of using a GFP Reporter Gene.

Analysis of individual cells at the molecular and physiological levels requires establishment of *in-vitro* culture systems whereby individual cells can be separately identified and investigated. In order to follow a particular gene of interest in a culture system it would be useful to develop methods of foreign gene transfer which make it possible to change cellular physiology or functions (Kishi et al, 2001). There are several ways to study signal transduction, promoter activity and gene expression, and one way is using an *in-vivo* reporter system. The reporter gene is placed downstream of a regulatory DNA sequence of interest (for example a promoter), and changes in reporter gene activity reflect changes in regulatory signals received by the promoter (Furtado and Henry, 2002). There are many reporter genes available today to study gene expression and promoter activity in eukaryotic cells (Furtado and Henry, 2002). These reporter genes include: *uidA* encoding β -glucuronidase, *LacZ* encoding β -galactosidase, *cat* encoding chloramphenicol acetyltransferase (CAT) and *luc* encoding luciferase reporters whose activities can be detected by measuring the product of an enzymatic reaction. However, green fluorescent protein (GFP) from jelly fish (*Aequorea Victoria*) is the only reporter which can be used for quantitative as well as qualitative assays. It is widely used as a reporter to study gene expression and protein localization in mammalian, bacterial and plant systems. The *gfp* gene encodes a green fluorescent protein (GFP), which emits green fluorescence (500-510nm) when exposed to 488nm blue/green visible light. The use of GFP has the following advantages: addition of substrate or cofactor in *in-vivo* or *in-vitro* is not required, it is resistant to photo bleaching and it remains stable under a wide variety of conditions. In addition, the GFP fluorescence can be detected with minimal handling and, in particular, no preparation of lysate is required and a fluorescence microscope, a fluorometer, a fluorescence-activated cell sorting machine, or an imaging microplate reader can be used to either quantify or visualize GFP expression (Furtado and Henry, 2002).

2.1.1 From Wild-Type GFP to Variant EGFP and Dual Coloured Fluorescent Proteins

The wild-type GFP protein has the undesirable property of low fluorescent intensity, when excited by blue light, which is due to lag in the development of fluorescence after the GFP has been synthesized (Zhang et al, 1996). The low fluorescent intensity of the wild-type GFP leads to poor expression in different mammalian cells and insensitivity of GFP, such that the GFP is below the standard for reporter proteins (Zhang et al, 1996). In an attempt to overcome this problem and thus improve GFP expression and detection in transfected mammalian cells, a mutation in the chromophore (the primary structure of GFP protein) was created, to make a EGFP protein which is 35 times more brighter than wild-type GFP protein (Zhang et al, 1996). The other alteration in the EGFP variant is codon optimization, whereby, in place of the jellyfish codon, favoured codons of highly expressed human proteins are used (Zhang et al, 1996). The GFP variants, which differ in their excitation and emission spectra, have been created by site-directed mutagenesis of the Serine, Tyrosine and the Glycine sequences which make up the amino acid that interact with the fluorophore (Ellenberg et al, 1999). As result of the original GFP gene mutation, the protein has been optimized for better expression and emission of fluorescent light. The variant fluorescent proteins include enhanced blue fluorescent protein (EBFP, which has an excitation and emission of 380/440nm), enhanced cyan fluorescent protein (ECFP, which has an excitation and emission of 433/453 and 380/440nm respectively) and also enhanced yellow fluorescent protein (EYFP, which has an excitation and emission of 488/509nm).

Figure 2.1 illustrates how the procedure of transient transfection experiments was carried out using pEGFP-N3 vector, whereby the CMV promoter of the vector was replaced with K13 or K15 promoter. These promoter constructs were then transfected into different pre plated epithelial and non-epithelia cells (6 well dishes) (Fisher, Leicestershire, UK). The cells were then harvested and the K13 and K15 promoter linked GFP fluorescence was analysed using a FACS machine.

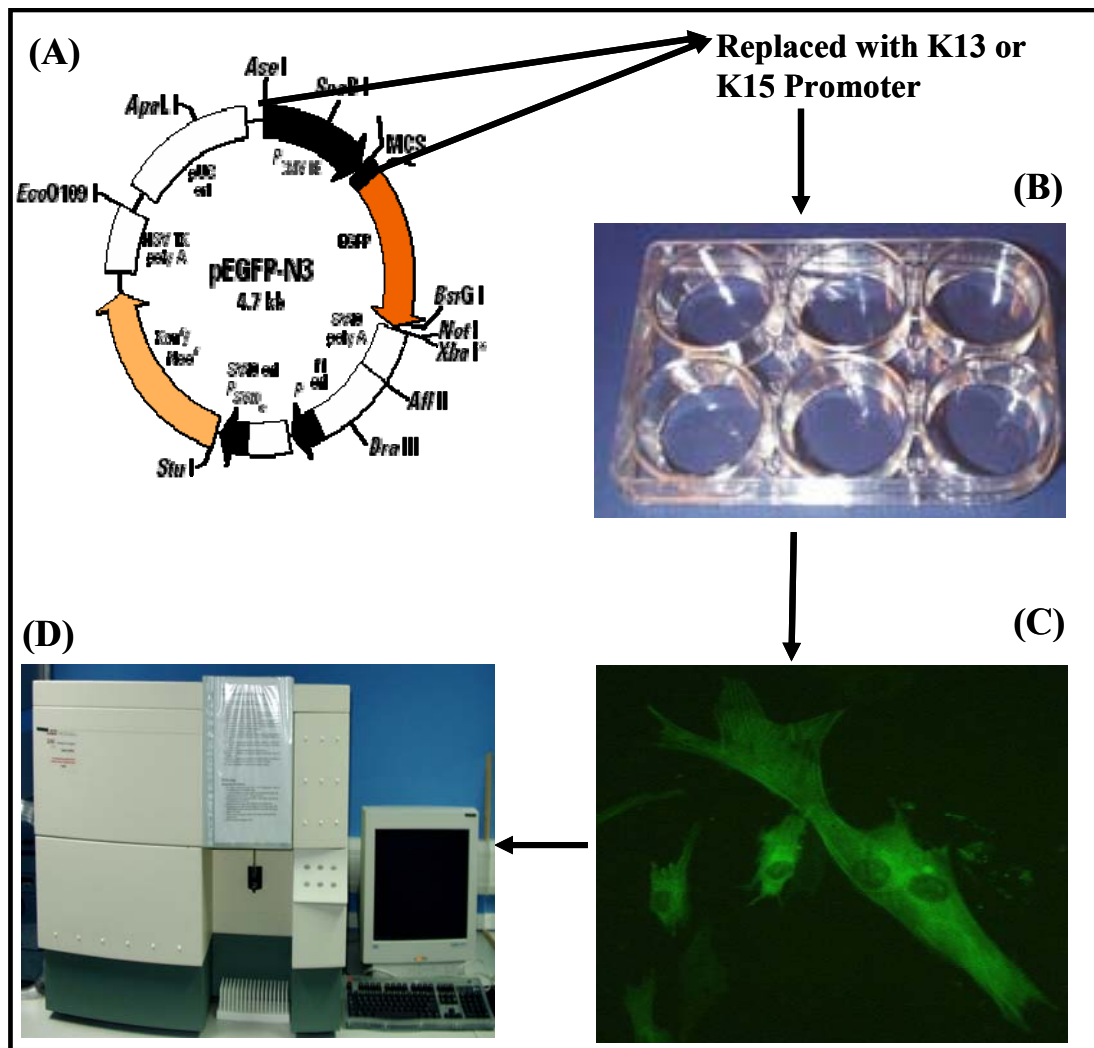


Figure 2.1: Schematic diagram showing a simple overview of how CMV promoter of pEGFP-N3B vector was replaced with K13 and K15 promoter (A). These promoter constructs were transfected into epithelia and non-epithelia cells pre-plated in a 6 well plate (B). The cells were then harvested and K13 and K15 promoter linked-GFP fluorescence (C) was quantified using FACS (D) machine (adapted from website number 10, 11 and 12 (pictures A-C) in the reference section and the pEGFP-N3 vector was adapted from the BD Bioscience Clontech Ltd, Oxford, UK, website 21 in the Reference section)

2.1.2 Control Plasmid Constructs used for Transfection

Gene transfer experiments in cell lines often benefit from the use of very active constitutive promoters, which cause transgenes to be expressed strongly at all times. Such promoters are generally derived from viruses, which have evolved to express their genes in many cell types (Strachan and Read, 2004). pEGFP-N3 encodes for a wild type GFP which has been optimized for a brighter fluorescence and higher expression (EGFP) in mammalian cells. The pEGFP-N3B parental vector (BD Bioscience Clontech Ltd, Oxford, UK) was used as positive control for all

transfection experiments. To make the promoterless (negative control) vector, the CMV from the pEGFP-N3B parental vector was removed to make a promoterless pEGFP-N3B vector (PL). pDsRed1-N1 vector (BD Bioscience Clontech Ltd, Oxford, UK) was used as an internal control for transfection efficiency and to take into account the biological variation which occurs from day to day, the pDsRed1-N1 vector (Figure 2.2) was co-transfected with each construct.

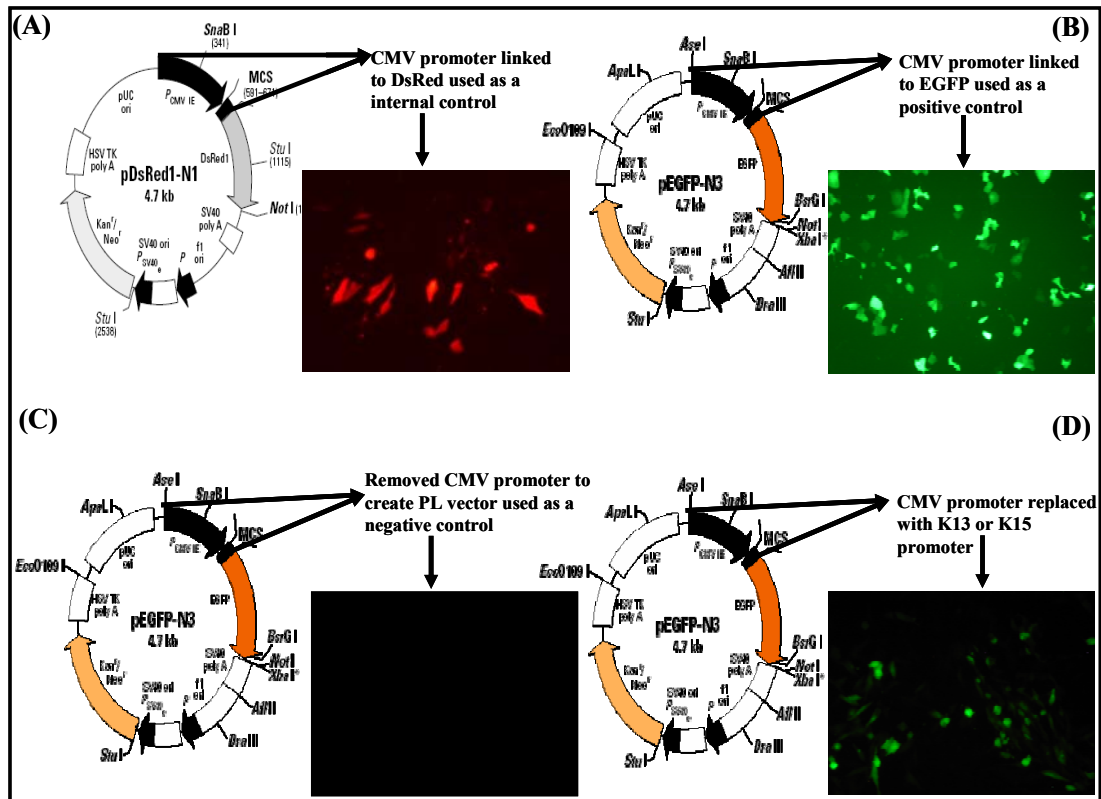


Figure 2.2: Constructs used in the study: (A): the CMV promoter linked to DsRed in pDsred1-N1 vector was used as an internal control for the transfection efficiency. (B): the CMV promoter linked to EGFP in pEGFP-N3 vector was used as positive control for the transfection efficiency. (C): the EGFP fluorescent protein was removed to create the promoterless (PL) vector, which was used as a negative control for the transfection experiments. (D): the CMV promoter was replaced with K13 or K15 promoter linked to EGFP in pEGFP-N3 vector (pDsred1-N1 and pEGFP-N3 vectors were adapted from the BD Bioscience Clontech Ltd, Oxford, UK, website 21 and 22 of the reference section)

2.2 Cloning strategy for K15 and K13 Promoter Constructs

3.018kb of the 5'-flanking region of the human K15 and K13 genes was amplified using a standard PCR protocol. The PCR product obtained was initially cloned into the pCR2.1-TOPO vector. The amplified DNA fragments were sub-cloned into BstZ17I and EcoRI for the K15 and K13 promoters; they were cloned into BstZ17I

and KpnI. Once the K13 and K15 promoters were completely digested with the appropriate enzyme for each promoter, a ligation reaction was set up to clone the K13 and K15 promoters into pEGFP-N3B vector to generate the K15 and K13 promoter driven GFP reporter constructs. Then utilizing site-directed mutagenesis, a 5'-end deletion series of K13 promoter constructs were generated.

2.2.1 Construction of K15 and K13 Promoter Reporter Gene Plasmids

The 3.018Kb K15 and K13 5'-upstream regions of the gene were obtained from the Ensemble genome browser database where all gene sequence are stored. Forward and reverse primer sequences (Appendix: table 7.1) were manually designed to amplify a 3.018Kb fragment for both the K13 and K15 promoter sequences using human genomic DNA.

2.3 Polymerase Chain Reaction (PCR)

The PCR reactions were carried out using standard protocols. Briefly, all PCR reactions were carried out using a thermal cycler block (Hybaid, Ashford, Middlesex, UK). The optimal annealing temperature was determined for each set of primers across a gradient of 50 to 65°C. The cycling conditions were as follows: an initial denaturing at 95°C for 2 minutes, followed by 35 cycles at 95°C for 30 seconds of denaturing. This was then followed by an annealing time of 30 secs at 56°C and 5 mins of final per cycle extension time at 72°C. The samples were then left to cool at 4°C over night. The standard PCR reaction was set up as in table 2.1. Many thermostable polymerases including Taq polymerase have a terminal deoxynucleotidyl transferase activity which selectively modifies PCR generated restriction fragments by adding single nucleotides (usually adenine), which is added onto the 3'-end of the amplified DNA fragment (Strachan and Read, 2004). This resulting overhang can make PCR product cloning difficult and in an attempt to overcome this difficulty, several approaches have been used (Strachan and Read, 2004). The first is the use of vectors such as TOPO TA vectors with overhanging T residues in the multiple cloning site. The second approach is to use enzymes such as Pfu which remove the overhanging single nucleotide (Strachan and Read, 2004). Thirdly, when designing the primers for the K15 and K13 PCR product a few extra extension nucleotides can be added onto the designed primer containing a suitable

restriction site at the 3'-end to generate an overhang ends and thus facilitating subsequent sub cloning into the pEGFP-N3 vector (Strachan and Read, 2004).

Table 2.1: Standard 50 μ l reaction for polymerase chain reaction (PCR)

Stock concentration	Final concentration used	Volume used
50-100ng template DNA	1-2ng/ μ l	1 μ l
50mM MgCl ₂	1mM	1 μ l
100mM dNTP mix	200nM of each dNTP	1 μ l
10x reaction buffer	1x	5 μ l
50 μ g/ml forward primer	100nM	5 μ l
50 μ g/ml reverse primer	100nM	5 μ l
4 u/ μ l Bio Taq polymerase	1.25 units	0.25 μ l
Water	x	31.75 μ l
Total	50 μ l	50 μ l

2.4 pEGFP-N3B Vector

The pEGFP-N3 vector expresses enhanced green fluorescent protein (EGFP) under the control of a human cytomegalovirus (CMV) immediate early promoter with pUC and SV40 origins of replication for prokaryotic and eukaryotic cells respectively. It expresses a kanamycin resistance gene, which enables selection of transformed bacteria, and a neomycin resistance gene, which allows stably transfected eukaryotic cells to be selected using G418. This information is presented on the vector map of pEGFP-N3 (Figure 2.2 A-B).

2.4.1 Abolishing AseI restriction site in pEGFP-N3 vector to replace with BstZ17I site to create pEGFP-N3B vector

In the pEGFP-N3B vector, the AseI restriction site was abolished and replaced with a unique BstZ17I (GTA/TAC) restriction site (Figure 2.2 A-B to 2.2 C- F). In addition, when designing the primer sequence in the 5'-end region of the forward primer used to amplify the K13 and K15 promoter sequence, BstZ17I site was incorporated into the DNA sequence. BstZ17I cuts at a GTA/TAC blunt sequence. There are two ways the DNA sequence can be cut, depending on the location of the cleavage sites produced by the restriction nucleases, and therefore the resulting restriction fragment

might have an overhang or a blunt end (Strachan and Read, 2004). Blunt end involves cleavage points which occur on the axis of symmetry, while overhanging ends involve cleavages that do not fall on the symmetry axis, such that the resulting restriction fragments either possess a 5'-end or 3'-end overhangs (Strachan and Read, 2004). Some of the disadvantages associated with blunt end restriction sites are that ligation efficiency with a blunt end is less than with a 3'-end overhang (Sanchez et al, 1996). In addition, the other disadvantages associated with blunt end ligation are that when using a DNA ligase to join two molecules into one, the amount of ligation product is significantly lower with blunt ends, and thus a higher concentration of plasmid DNA and DNA ligase enzyme is required (References: website 15). In addition, when sub-cloning, blunt end ligation has the disadvantage of potentially inserting the DNA insert in the opposite orientation to that desired. The advantage of blunt end ligation is that the strand ends are always compatible with each other (References: website 15).

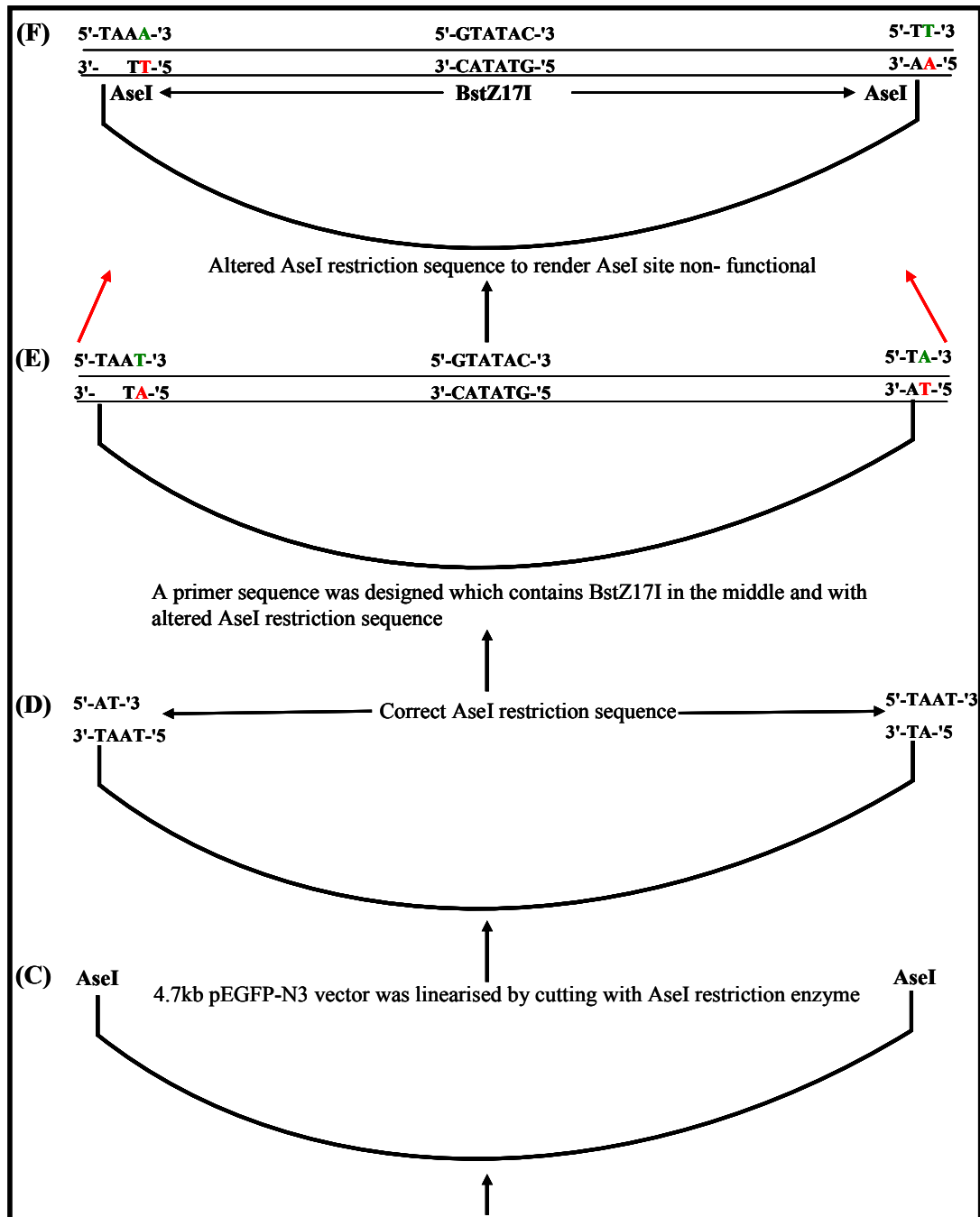


Figure 2.3 C-F: Abolishing AseI restriction site in pEGFP-N3 Vector:

C: shows the circular pEGFP-N3 vector linearised by digesting the 4.7kb pEGFP-N3 vector with AseI enzyme. E: shows the linearised 4.7kb pEGFP-N3 vector. D: shows the linearised 4.7kb pEGFP-N3 vector with AseI restriction enzyme and its correct nucleotide sequence. E: a primer (straight lines) was then designed which contains the BstZ17I site in the middle and AseI sites on other side of the linearised pEGFP-N3B vector, the highlighted 5' → 3' T and A (green) and A and T on 3' → 5' (red) either side of the vector sequence indicate the nucleotides to be changed. F: shows a designed primer sequence used to ligate to the pEGFP-N3 vector with non-functional AseI sites, this was done by replacing A with T and replacing T with A on either side of the pEGFP-N3 vector, such that AseI site is non-functional and BstZ17I restriction site is used instead.

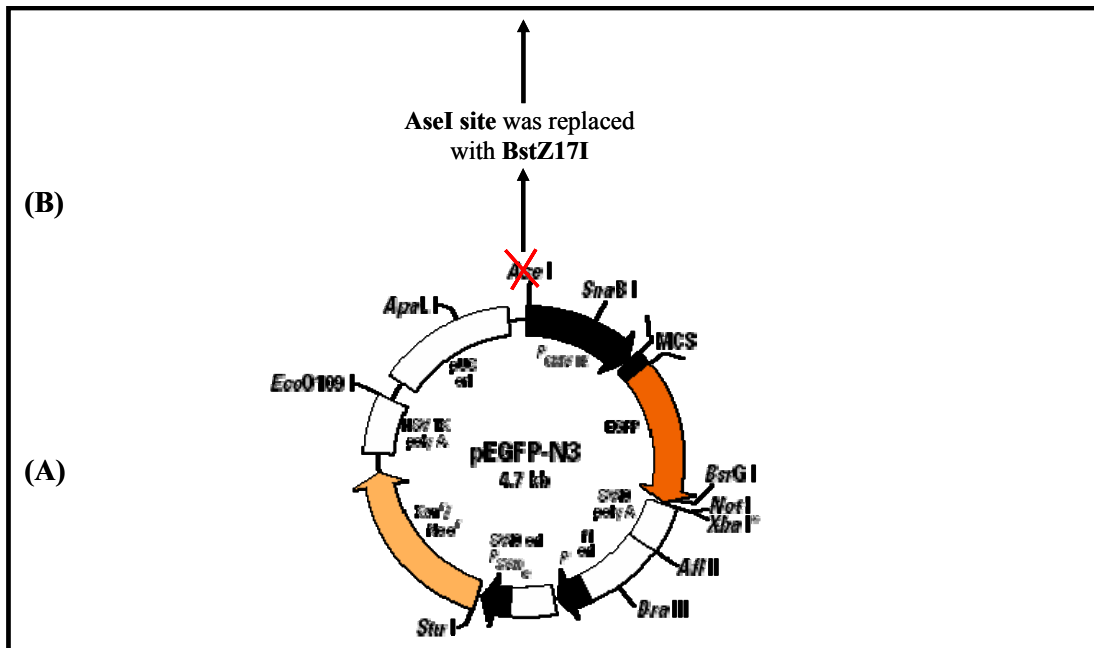


Figure 2.3 A-B: Vector Map of pEGFP-N3 and abolishing AseI restriction site: A: shows the features of pEGFP-N3 vector which includes the CMV promoter, the multiple cloning sites (MCS) and the antibiotic selection marker gene. B: shows AseI restriction site in pEGFP-N3 vector replaced with BstZ17I restriction to generate a pEGFP-N3B vector, instead of the original pEGFP-N3 vector.

2.4.2 Making the K13 and K15 Promoter Constructs using pEGFP-N3B expression vector

The K13 and K15 promoter fragments were amplified from human genomic DNA using PCR. The BstZ17I/KpnI or BstZ17I/EcoRI restriction promoter fragment for K13 and K15 was then cloned into TOPO TA cloning vector (Invitrogen Ltd, Paisley, UK, Figure 2.4 and Table 2.1). Then using several molecular biology techniques such as transformation, colony selection, mini and maxi-preparation a large scale of K13 and K15 DNA promoter fragments were made. The BstZ17I/KpnI or BstZ17I/EcoRI restriction promoter fragment for K13 and K15 was then cloned into a pEGFP-N3B expression vector (Figure 2.5 and Table 2.1). This was done by removing the CMV promoter (0.583kb) and replacing it with the K13 and K15 promoter fragment (3.018kb insert). The cloning of the K13 and K15 promoter fragment (3.018kb insert) into a pEGFP-N3B expression vector (Figure 2.5), started with the linearization of the pEGFP-N3B expression vector by using BstZ17I/KpnI or BstZ17I/EcoRI restriction enzymes (Figure 2.5 and Table 2.1). The same was also done for the K13 and K15 promoter fragments, whereby each PCR product was initially digested overnight with BstZ17I/KpnI or BstZ17I/EcoRI restriction enzymes for K13 and K15 promoter respectively. Then both vector and insert DNA were run

on 1% agarose gels, and then purified using the Qiagen purification kit (Qiagen Ltd, Crawley, UK). The pEGFP-N3B vector and K13 or K15 promoter insert were both digested, then ligated to the pEGFP-N3B vector.

Table 2.2: Vectors used in the Study

Name of Vector	Size	Resistance	Comment	Source of Vector
Topo TA	3.9kb	Ampicillin/ Kanamycin	Used to facilitate subsequent cloning of both of K13 and K15 promoter into pEGFP-N3B.	Invitrogen
pEGFP-N3B	4.7Kb	Kanamycin	Vector designed for high level expression of recombinant proteins in mammalian cell (expression rate 10-20%)	Clontech

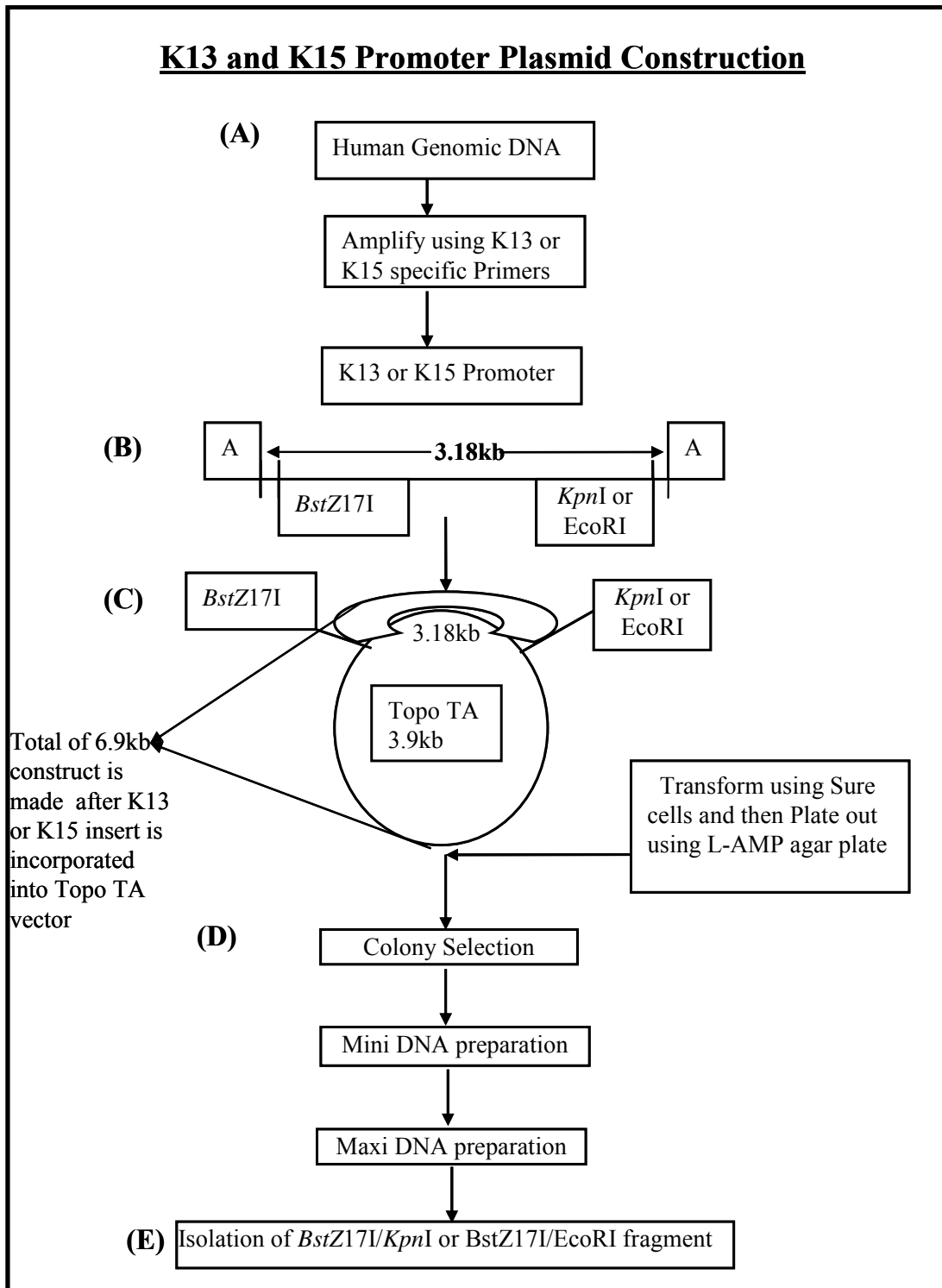


Figure 2.4: Diagram illustrating how both human K13 and K15 promoters were constructed. A: illustrates the initial amplification of K13 and K15 promoters from human genomic DNA using a specific set of primers. The letter A in the diagram B: represents the amplified fragment and the size of BstZ171/KpnI or BstZ171/EcoRI fragment for K13 and K15 promoter. C: shows BstZ171/KpnI or BstZ171/EcoRI fragment for K13 and K15 promoter (3.018kb insert) ligated to the Topo Ta vector (3.9kb vector), the size of the whole plasmid becomes 6.9kb, as the size of the vector is 3.9kb and that of K13 and K15 insert is 3.018kb. D: shows the procedure for making large scale K13 and K15 DNA fragments using colony selection, mini and maxi-preparation of K13 and K15 promoter. E: shows the isolated K13 and K15 fragments.

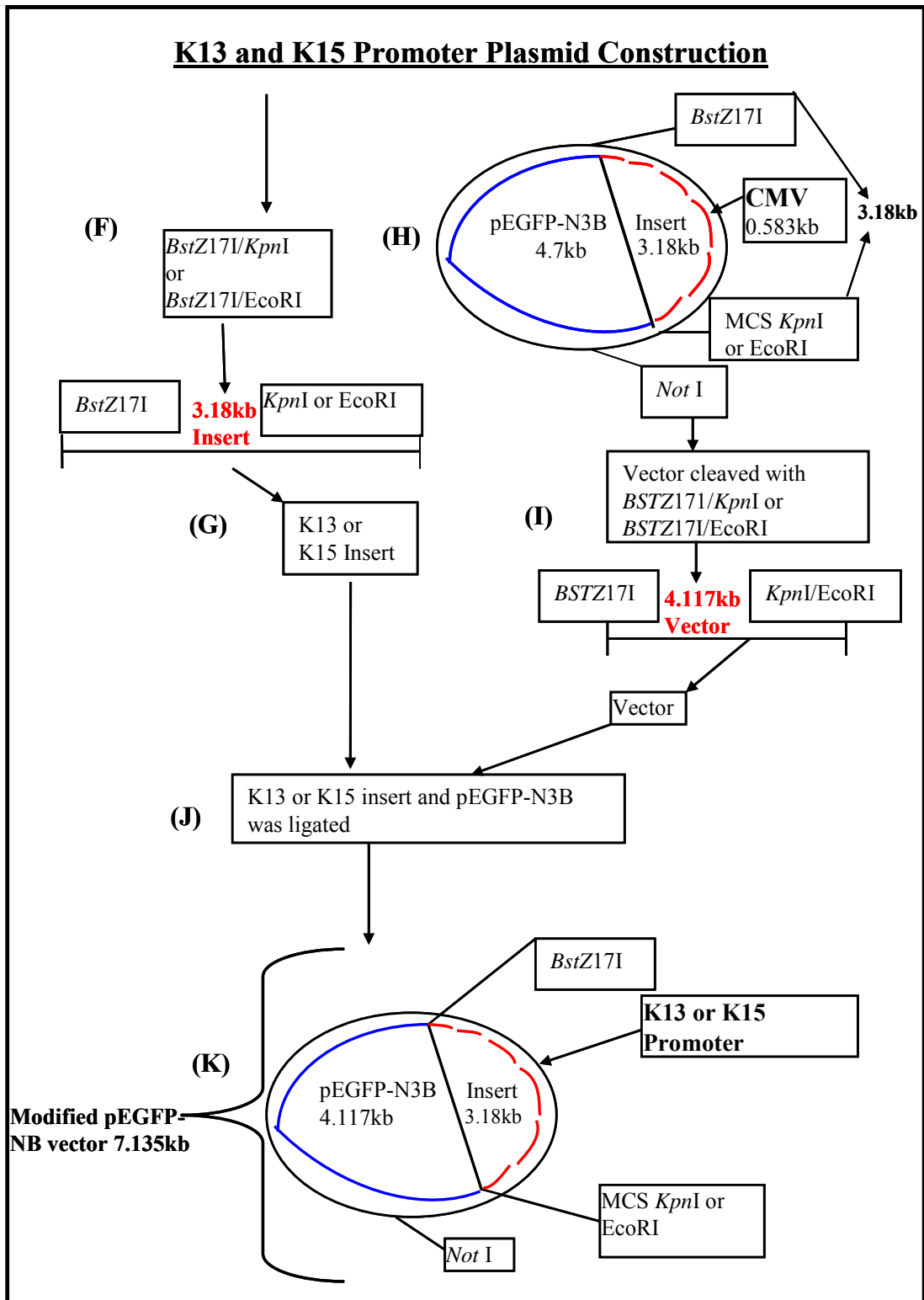


Figure 2.5: Diagram illustrating how both human K13 and K15 promoters were constructed. F: illustrates the full length isolated *BstZ171/KpnI* or *BstZ171/EcoRI* fragment for K13 and K15 promoter (insert). G: shows K13 and K15 promoters (3.018kb insert) H: shows how the pEGFP-N3B vector was modified, by removing the CMV promoter (0.583kb) and ligating the K13 or the K15 promoter. I: shows the pEGFP-N3B vector been cleaved with *BstZ171/KpnI* or *BstZ171/EcoRI* fragment for K13 and K15 promoters, in an attempt to linearise the vector. J: shows the K13 and K15 insert ligated to the pEGFP-N3B vector. K: shows the final modified pEGFP-N3B vector (4.117kb) containing the K13 and K15 insert (3.018kb).

2.5 Agarose Gel

The PCR products were fractionated on 0.8-2% (W/V) agarose gel (electrophoresis Grade, sepharose) using 1X TBE buffer containing 1µg/ml ethidium bromide. Double digested the DNA with BstZ17I/KpnI or BstZ17I/EcoRI using DNA ladder ([Fermentas, Inc.](#), Glen Burnie, [USA](#)) as molecular marker. This was left to run for 30 minutes at 100 volts. Pictures for K13 and K15, as well as the vector bands prior to ligation were taken using a gel document programme in the Autochemi system (UVP Bioimaging Ltd, Kent, UK).

2.5.1 Isolation of DNA from Agarose gels and DNA Purification

The DNA bands in the gel were visualized using a long UV light autochemiluminescence UVP Bioimaging system. Bands were excised from the gel using a scalpel, placed into an Eppendorf tube, and weighed. The Minelute gel extraction kit protocol (Qiagen Ltd, Crawley, UK) was followed and DNA was stored at -20°C until required.

2.5.2 Ligation of Insert to Vector

After the DNA was isolated from agarose gel and purified, the vector (Topo TA or pEGFP-N3B) was ligated to insert (K13 or K15 promoters) using the quick ligation kit (Invitrogen) and a ratio of 2:1 insert to vector was used. The ligation reaction was set up as in Table 2.2 and 2.3.

Table 2.3: Ligation of K13 or K15 promoter (Insert) into TOPO TA vector

Ligation components	K13/K15
TOPO® vector	1µl (1ng)
PCR product (Insert)	2µl (2ng)
Salt Solution	4µl
2X quick ligation buffer	3µl
T4 DNA ligase (1 unit/µl)	1 unit
Sterile dH ₂ O	4µl
Total	15µl

Reaction was vortexed and incubated for 5 minutes at room temperature and stored at 20°C until required.

Table 2.4: Ligation of K13 or K15 promoter (Insert) into pEGFP-N3B vector

Ligation components	K13/K15
pEGFP-N3B vector	1µl (1ng)
PCR product (Insert)	2µl (2ng)
2X quick ligation buffer	4 µl
T4 DNA ligase (1 unit/µl)	1 unit
Sterile dH ₂ O	4µl
Total	12µl

Reaction was vortexed and incubated for 5 minutes at room temperature and stored at 20°C until required.

2.5.3 Bacterial Strains used for Transformation in this Study

- One shot *E.coli* competent cells (Invitrogen Ltd , Paisley, UK).
- XLI0-Gold ultra competent cells (Stratagene Inc, La Jolla, USA)
- XLI0-Blue ultra competent cells (Stratagene Inc, La Jolla, USA)
- NovaBlue competent cells (Novagen Ltd, Beeston, UK)

2.5.4 Plasmid Transformation using Competent Bacterial Cells

50µl of a competent bacterial cell suspension were thawed on ice and 0.1µg of ligation mix or 1ng of plasmid was added, mixed and left on ice for 30 mins. The bacterial cells were then heat shocked at 42⁰C for 30 seconds and transferred onto ice for 2mins. 250µl of SOC medium (nutrient rich medium used for recovery of competent cells) was pipetted into bijoux tubes, into which the transformation reaction was pipetted and left on the shaker at 37⁰C for 1 hour at a speed of 250 rpm. 100µl was spread onto plates containing agar and 50mg/ml of ampicillin and these were incubated overnight at 37⁰C. Single colonies were picked with a sterile loop to inoculate in L-broth media.

2.5.5 Restriction Digestion

Miniprep DNA (2ng) was digested with 1µl of restriction enzyme (BstZ17I) in the presence of the appropriate reaction buffer supplied with endonuclease (1µl of 10X buffer) in a total volume of 10µl reaction mixture. The mixture was incubated for 1 hour at 37⁰C or overnight depending on the endonuclease and then 4µl of DNA

loading dye was pipetted into the digested DNA prior to electrophoresis on a 1% w/v agarose gel.

2.6 Purification of Plasmid DNA from 3-10ml of Bacterial Culture

For the initial analysis to confirm whether the insert had successfully been cloned into the vector, only a small amount of DNA was required and this was generated using a mini plasmid purification Qiagen kit and Beckman centrifuge tubes (40ml). 1ml of an overnight bacterial culture was pipetted into a 1.5ml Eppendorf tube and then centrifuged at 15,000 rpm at 4°C for 15 minutes. The supernatant was then discarded and the DNA was extracted from pellet using the Qiagen kit protocol for mini preparation of DNA (Qiagen Ltd, Crawley, UK), except for an alteration in the last step in which instead of using elution buffer provided with the kit, DNA was eluted off the column with 10mM Tris at pH 8.5.

2.6.1 Purification of Plasmid DNA from 100-500ml of Bacterial Culture (Maxiprep) using Qiagen Kit

A maxi plasmid purification kit (Qiagen Ltd, Crawley, UK) and a larger (250 ml) centrifuge tube (Beckman Instruments, UK) were used to prepare large amounts of DNA. A 500ml overnight bacterial culture was poured into two 250ml Beckman tubes and centrifuged at 6,000 rpm at 4°C for 15 minutes. The supernatant was then discarded and DNA was extracted from pellet using the Qiagen kit protocol.

2.6.2 DNA Precipitation

One tenth of 3M Sodium acetate at pH5.2 was added to the DNA solution in a 1.5ml eppendorf tube. This was then vortexed and 3X the volume of 100% ethanol was added. The solution was left at -70°C for 20 minutes and then microcentrifuged for 15 minutes at 15,000 rpm. The supernatant was discarded and the pellet formed was washed with 500µl of 70% v/v alcohol. The solution was re-centrifuged for 2 minutes in a microcentrifuge and the supernatant was discarded. Using a DNA concentrator vacuum, the DNA was spun at a speed of 13,000 rpm for 2 minutes and the supernatant discarded, leaving the pellet to dry. The DNA was resuspended in an appropriate volume of 10mM Tris HCl pH 8.5.

2.7 Spectrophotometer

The concentration and purity of DNA were determined by measuring absorbance at 260nm wavelength using a spectrophotometer. The concentration of DNA was calculated using the formula: $\text{Conc}^n = \text{Abs}_{260} \times \text{dilution factor} \times 50$ [A solution containing 50 $\mu\text{g}/\text{ml}$ of double stranded DNA has an absorbance of 1 at 260nm wavelength, assuming that the mass of a nucleotide pair in DNA is 0.66kDa]. 1:100 dilution of the DNA was made in a quartz cuvette and placed in the spectrophotometer. Another cuvette containing 100 μl of 10mM Tris HCL pH8.0 alone was used as the blank

2.8 Cell Culture Media and Types of Cell

Cancer Research UK (CRUK) central stores supplied Ham's F12 and E4 media (1:1 v/v) as 400ml aliquots which were then supplemented with RM+ reagent mix (Appendix: Table 7.8) and 10% foetal calf serum (Invitrogen Ltd, Paisley, UK), was added to the media. The RM+ supplemented media was used to maintain certain types of keratinocyte derived cell lines (Table 2.5). DMEM media was also supplemented with 10% foetal calf serum and 1% penicillin and 1% streptomycin (Invitrogen Ltd, Paisley, UK).

Table 2.5: The names of cell lines used in this study and their derivation

Name of cell line	Information of origin	Site	Reference	Where it was obtained from
SCC25	Squamous cell carcinoma of the tongue of 70 year old male	ventral tongue	(Rheinwald and Beckett 1980)	obtained from cancer research UK
RTS3b	Human Papillomavirus negative skin derived keratinocyte cell	Skin of the ear	(Purdie, et al. 1993)	Obtained from cancer research UK
HeLa	Adenocarcinoma of the cervix	Cervix	(Macville, et al. 1999)	Clinical diagnostic and oral sciences departmental archive
HFF	Human foreskin fibroblast	Human foreskin fibroblast	-	Obtained from cancer research UK
HaCaT	Epidermal keratinocytes	Adult Skin	(Boukamp et al, 1988)	Clinical diagnostic and oral sciences departmental archive
NHEK	Normal human epidermal keratinocytes	Foetal epidermal skin	-	Clinical diagnostic and oral sciences departmental archive
A431	A431 cell line was derived from an 85-year-old female with epidermal carcinoma	Human vulval carcinoma cell line	(Waseem et al, 1998)	Clinical diagnostic and oral sciences departmental archive
H357	human oral squamous cell carcinomas	ventral tongue	(Prime et al, 1990)	Clinical diagnostic and oral sciences departmental archive

2.8.1 Cell Seeding and Counting using a Haemocytometer

The media in the flasks containing adherent cells were aspirated using a glass pipette. Cells were washed with 10ml of PBS by swirling the flask from side to side. The PBS was aspirated, the cells were trypsinized with 5ml pre-thawed trypsin (Invitrogen Ltd, Paisley, UK), and spun using a microcentrifuge for 5 mins at 1, 800 rpm. The supernatant was aspirated and cells were resuspended with appropriate fresh medium, which was then vortexed. To count the number of cells in the

medium, 10 μ l of resuspended cells were pipetted onto the haemocytometer under the cover slip (Chance, Propper, Warley, UK). The number of cells in four grids consisting of 16 square boxes was counted and the average number of cells/ml was determined, using the following formula.

Average number of cells in four grids of 16 squares $\times 10^4 =$ number of cells in 1 ml

2.9 DNA Transient transfection into adherent cell lines using Fugene 6

Fugene-6 (Roche, Diagnostic, Mannheim, Germany) is a lipid based reagent, which works by forming a complex with DNA, which is then taken up by the cell via endocytosis. Cell lines (Table 2.5) were grown in separate flasks until 90% confluent, seeded into six well plates at a cell density of 80-200 $\times 10^3$ cells per well with 2ml of appropriate growth medium, and left for 24 hours in a 5% CO₂ incubator at 37⁰C prior to transfection. The medium was aspirated 8 hours before transfection and replaced with 1ml of fresh medium. The transfection master mix was made up in sterile Eppendorf tubes with PBS, to which Fugene 6 was added and the tube was vortexed for few seconds followed by the addition of DNA and further vortexing for few seconds, and then left at room temperature for 15 minutes. The transfection master mix was then pipetted dropwise into each well with swirling; 1ml of appropriate fresh media was used to top up each well, followed by incubation at 37⁰C in 5% CO₂ for 48-72 hours.

To match the same number of molecules to the promoterless pEGFP-N3B negative control plasmid, (Appendix; Table 7.3), different concentrations of the following constructs were used: K13 full length promoter, K13 promoter deletion fragments (R1 to R6) and pEGFP-N3B positive control vector were transiently transfected into each cell line (Table 2.5).

Table 2.6: Master Mix for Transfection

3:1: ratio of Fugene 6 to plasmid DNA.	
PBS	15µl
Fugene 6	7.5µl
Plasmid DNA (K13 full length promoter, K13 promoter deletion fragments, promoterless pEGFP-N3B or pEGFP-N3B positive control vectors.	xµg
Non-specific pUC 18 plasmid	made up to 2µg with pUC 18 plasmid
0.5µg pDsRed1-N1 plasmid.	0.5µg
Total	25µl.

2.9.1 DNA Transient Transfection into Adherent Cell Lines using Lipofectamine

The day before transfection, cells were seeded in media without antibiotic in a 6 well plate, so that they were 50-80% confluent on the day of transfection. The DNA was pre-complexed with the Plus reagent by diluting 1.2µg of either K13, K15 promoter constructs, pEGFP-N3B or promoterless pEGFP-N3B construct plus 0.4µg pDsRed1-N1 (internal control) DNA into 100µl of DMEM medium without serum. The Plus reagent was vortexed prior to use, then 16µl Plus reagent was added to the diluted DNA, vortexed and incubated at room temperature for 15 minutes. Lipofectamine (Invitrogen Ltd, Paisley, UK) reagent was then diluted (4µl into 100µl dilution medium without serum) in a second tube, and vortexed for a few seconds. The pre-complexed DNA was combined with diluted lipofectamine reagent, then vortexed and incubated at room temperature for 15 minutes. While the complexes were forming, the medium on the cells was replaced with 0.8ml of fresh medium without serum. The DNA-Plus lipofectamine reagent complexes were added drop wise into each well. Complexes were gently mixed into the medium by swirling the plates, and then the plates were incubated at 37°C in 5% CO₂ for 3 hours. After 3 hours incubation the medium was replaced with 2ml of fresh media containing 10% foetal calf serum (FCS).

2.10 Fluorescence Activated Cell-Sorting (FACS) Analysis

Over the past 30 years, fluorescence activated cell sorting (FACS) machines have evolved to become powerful equipment for analyzing and isolating single cells at very high rates. The properties of recombinant DNA can be expressed as fluorescent

tags in carrier cells. Modern FACS machines are capable of quantifying multicolour fluorescent signals and making sort decisions at the rates of up to 50,000 cells per second. As a result, cell sorting is an extremely efficient tool for screening large DNA libraries and reporter cell populations (Choe et al, 2005). FACS was used to measure the intensity and percentage of K15, K13 and CMV promoter driven GFP positive cells.

2.10.1 Visualization of EGFP and DsRed Labelled Promoters

The transfected cell lines expressing GFP and/or PDsRed1-N1 labelled promoters were visualized as live cells using a Nikon ECLIPSE TE2000-S biomedical microscope equipped with an epifluorescence attachment, a high speed filter wheel (Lambda 10-3) and photographed using an integrated digital camera. All images were obtained using Metamorph software, using a magnification of 10x or 20x. Reproduction and editing were completed using Adobe® Photoshop and Corel® Graphics Suite 11. All cell lines were transfected in triplicate with GFP and/or PDsRed1-N1 labelled promoters. The number of cells in suspension selected for analysis by the BD LSR II (Becton Dickinson Ltd, Plymouth UK) analyzer was constant (20,000 cells/s). Forward scatter (FS) and side scatter (SC) were collected through separate filters. The EGFP and DsRed signals were collected in separate channels through 530/30nm and 575/26nm band pass filters respectively. The smaller numbers in the band pass filter represent the width of the filter while the larger numbers represent the fluorescence emission. A light scatter gate was drawn in the FITC-A (EGFP) versus PerCP-cy5-5-A (DsRed) plot to exclude cell debris and include the viable transfected cells. The fractions of the various cell types were quantified using quadrant statistics in BD FACS Diva software version 4.12 (Beckton-Dickinson), while the formula below and student t-test were used to compare the significance of the data generated.

2.10.2 Flow Cytometry Data Analysis

To calculate the expression of K13 promoter, K15 promoter, promoterless constructs and CMV positive control in pEGFP-N3B vector transfection into different cell lines either transiently or stably, the following formulas were used:

1) % of positive cells expressing GFP (pEGFP-N3B) or DsRED MFI (median fluorescence intensity) for stable transfection experiments.

2) % of positive cells expressing GFP (pEGFP-N3B)* GFP MFI (median fluorescence intensity) for stable transfection experiments.

3) % of positive cells expressing GFP (pEGFP-N3B)* GFP MFI (median fluorescence intensity)
=GFP fluorescence intensity

% of positive cells expressing DsRED (pDsRed1-N1)*DsRED MFI (median fluorescence intensity)
= DsRED fluorescence intensity

$$\text{GFP expression} = \frac{\text{GFP fluorescence intensity}}{\text{DsRED fluorescence intensity}}$$

for transient transfection experiments.

The formula above was also used by (Soboleski et al, 2005), when green fluorescence was used as a quantitative reporter gene in individual eukaryotic cells. However, they used the mean to calculate the GFP fluorescence intensity, while in this thesis the median value was used to calculate the GFP fluorescence intensity, since the mean only measures normal distributed data but not skewed data. In addition, with GFP FACS data, a skewed data set is normally obtained and thus since median value is a measure of 500 events on either side of the data mean a more accurate measure was obtained using this parameter. Thus the median value is a measure of both normal and skewed distributed data, while the mean only measures the peak of the histogram data obtained.

2.10.3 Flow Cytometry

Post transfection, the medium was aspirated from cells in six well plates and the cells washed with phosphate buffer saline (PBS). The cells were trypsinized and the suspensions was collected into prelabelled 5ml Falcon FACS tubes, centrifuged at 1,000 rpm for 5 minutes, and the supernatant removed. Cells were washed with PBS and centrifuged at 1,000 rpm for 5 minutes, the supernatant was aspirated and the cells resuspended in an appropriate volume of PBS containing 2mM EDTA and 1% foetal calf serum. The resuspended cells were vortexed and transfered onto ice, ready for fluorescent activated cell sorting.

2.11 Addition of Pharmacological Agents to K13 and K15 Promoter Constructs

Transient transfection was carried out as in Section 2.9, except from 24 to 72 hours post transfection the cell medium was changed and replaced with 2ml of the appropriate fresh media containing the following pharmacological agents: 100nM

TPA, 4- α -PMA, 3 μ M Trichostatin A, 2mM Sodium Butyrate, 50 μ M of PD98059 or 25 μ M LY294002 into each of the six well plates. This was then swirled and incubated at 37°C in 5% CO₂ from 6 to 48 hours depending on the drug used.

2.12 DNA Sequencing

DNA sequencing (kindly done by Dr Ahmad Waseem) was performed to confirm the assembled constructs, since using PCR can introduce mutations into the amplified DNA (Jiang and Blumenberg, 1991). DNA templates were sequenced with the ABI PRISM[®] BigDye[™] v2 (Applied Biosystems) which is based on the dideoxy chain termination Sanger method (Sanger et al, 1977). The DNA sequence obtained from the K13 promoter construct 5' end deletion series, generating 6 fragments (R1 to R6), was put together and blasted against the entire genome using a BLAST database from NCBI (National Centre for Biotechnology Information) from the following website <http://www.ncbi.nlm.nih.gov/BLAST/>. The search located a homology sequence in chromosome 17 where all type I keratins genes are found in or the K13 sequence (Chapter 4 Figure 4.8). The K15 3.018kb upstream (promoter) and downstream (exon 1 and intron 1) nucleotide sequence was also placed in the appendix (Figure 7.7).

2.13 Transcription Factor Database

Using the following web address (<http://genome.ucsc.edu/cgi-bin/hgGateway>), roughly 2000 to 3400bp of the keratin 5'-end upstream region (promoter) was selected. Then the keratin promoter sequence was selected and subsequently pasted onto the following website (<http://www.cbrc.jp/htbin/nph-tfsearch>) in an attempt to find novel binding sites in basal and suprabasal keratin genes. A threshold score of 90% was selected in the database; this means that only transcription factors which have a binding site in keratin promoter sequences that have 90% or above homology sequence predicted by the database should be returned. This was to ensure that transcription factors with high homological sequence were returned. Information about transcription factors that bind the keratin promoter DNA sequence was grouped according to their site of expression in the human body. The basal keratins are expressed universally in all stratified epithelia. Each graphical representation of a transcription factor which binds to a keratin promoter was presented as basal versus suprabasal keratin markers at different sites (Chapter 3: Table 3.2).

2.14 Isolating and Truncating the Human K13 Promoter Construct

Once the K13 promoter was isolated from human genomic DNA using PCR, it was cloned into pCR-TOPO and then sub-cloned into pEGFP-N3B vector (Figure 2.5 A). Then a 5'-end deletion series of the full length parental pEGFP-N3BK13-3018bp (Figure 2.6 B and C) DNA to yield the following constructs: pEGFP-N3BK13-2540bp, pEGFP-N3BK13-1953bp, pEGFP-N3BK13-1512bp, pEGFP-N3BK13-1017bp, pEGFP-N3BK13-670bp and pEGFP-N3BK13-289bp. This was done using full length parental pEGFP-N3BK13-3018bp DNA as a template for PCR and forward primers located at -2540bp, -1953bp, -1512bp, -1017bp, -670bp and -289bp upstream of the K13 exon 1 (Figure 2.6 B). A BstZ17I restriction sequence was incorporated into the designed primers at the following sites -289, -670bp, -1017bp, -1512bp, -1953bp and 2540bp using PCR against the full length parental pEGFP-N3BK13-3018bp DNA insert as a template (Figure 2.6 H-N). To introduce these PCR based deletion mutations into the full length parental pEGFP-N3BK13-3018bp fragment in order to generate R1-R6 of (Figure 2.6 H-N) K13 promoter fragments a Quick change multi site directed mutagenesis kit (Stratagene) was used. Once the full length K13 promoter fragment (3.018kb) was 5'-end deleted to generate six K13 promoter fragments which were ligated to the 4.117kb pEGFP-N3B vector (Figure 2.6 H1-N1), these plasmid constructs were transformed with *E.coli* (Section 2.5.4). Once plasmids were transformed, the bacterial colony was selected in an appropriate antibiotic containing agar plate. Then the bacterial colonies formed for each of the six (R1-R6) K13 promoter fragment plasmids were miniprepared (Section 2.6). The resulting six (R1-R6) K13 promoter fragment plasmids DNA was analysed by restriction digest with BstZ17I and KpnI enzymes used to confirm the expected size and then the digested DNA plasmids was separated on 1% agarose gel at 100 volts for 2 hours. Once the six (R1-R6) K13 promoter fragment plasmids were confirmed, a maxipreparation (Section 2.6.1) of K13 truncated promoter constructs was made.

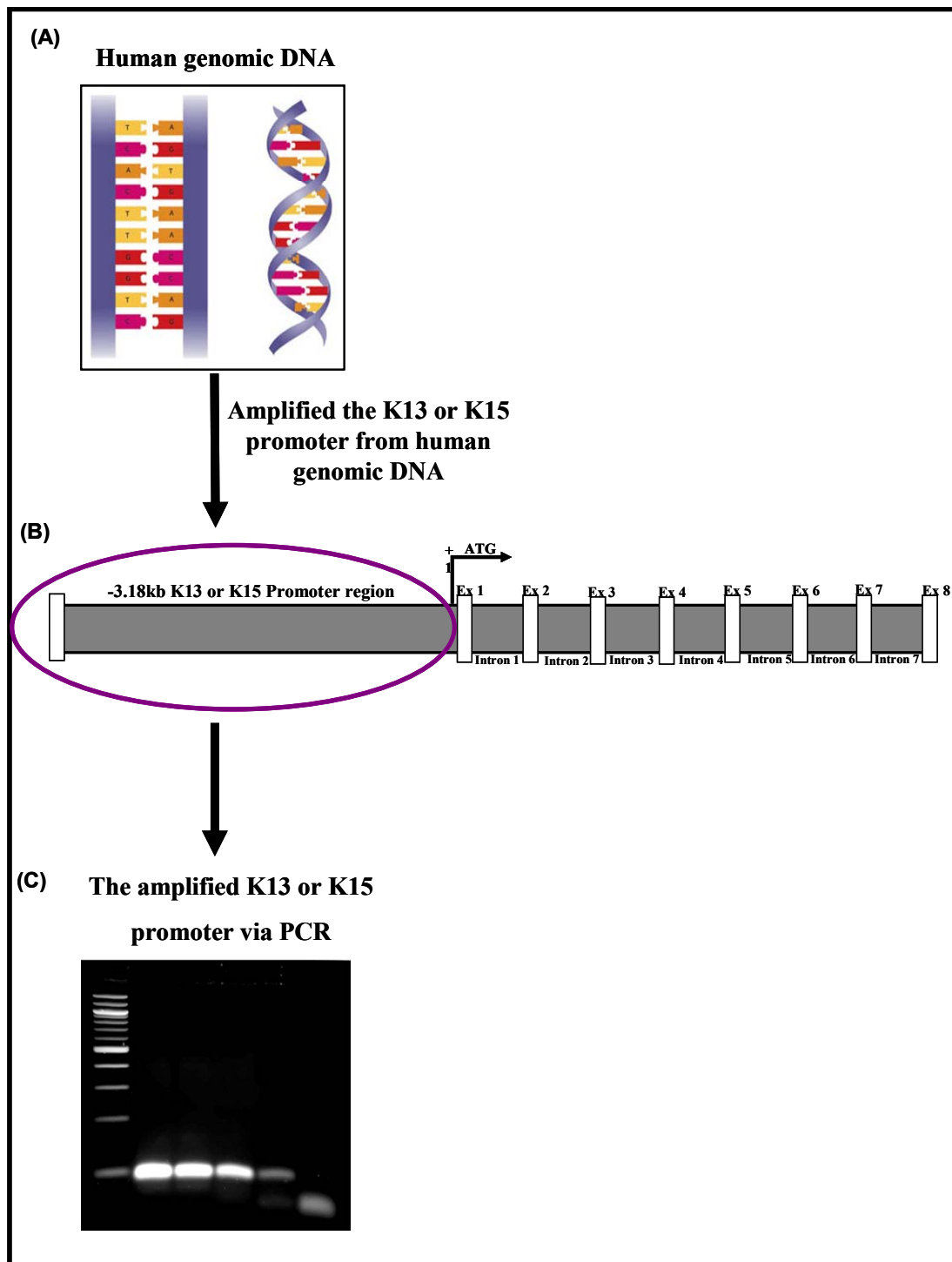


Figure 2.6 A-C: Diagram illustrating the steps involved in the cloning K13 or K15 promoter: The K13 and K15 promoter (B) were amplified from human genomic DNA (A) using PCR (C), then the PCR product was cloned into pCR TOPO vector, the K13 and K15 promoter fragments were sub-cloned into the pEGFP-N3 expression vector (picture A and C were adapted from website number 16 and 17 in the reference section and the two vectors from Invitrogen website (TOPO) Clontech (pEGFP-N3) website).

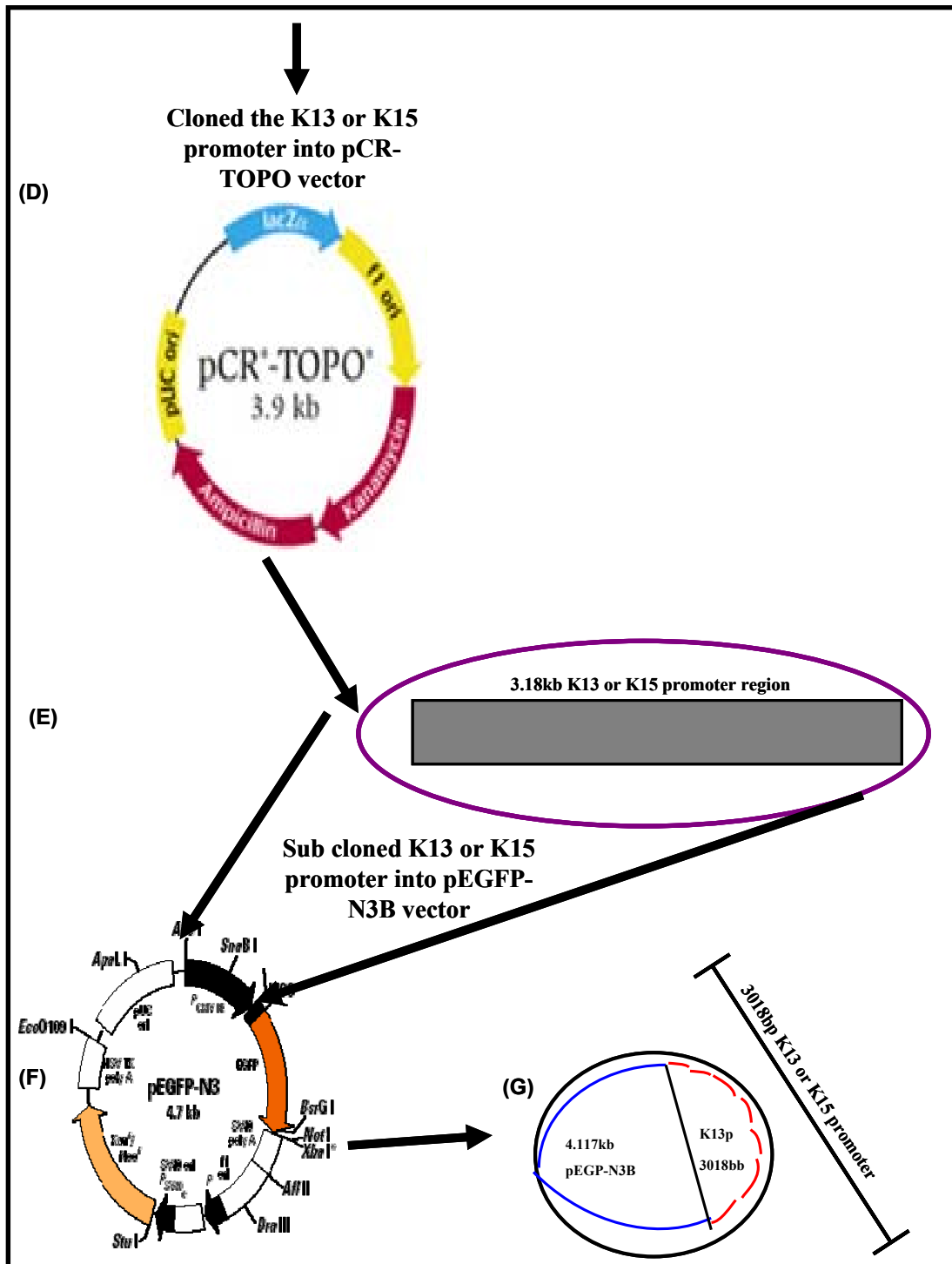


Figure 2.6 D-G: Diagram illustrating the steps involved in the cloning K13 or K15 promoter: The K13 and K15 promoter PCR product were cloned into pCR TOPO vector (D). Then the K13 or K15 promoter fragment (E) was sub-cloned into the pEGFP-N3B expression vector (F). Once the K13 but not the K15 promoter fragment was successfully sub-cloned into pEGFP-N3B vector (G), to make K13 promoter deletion series PCR was used against the K13 full length (K13 3018bp) promoter fragment insert (picture A and F were adapted from the Invitrogen and Clontech website).

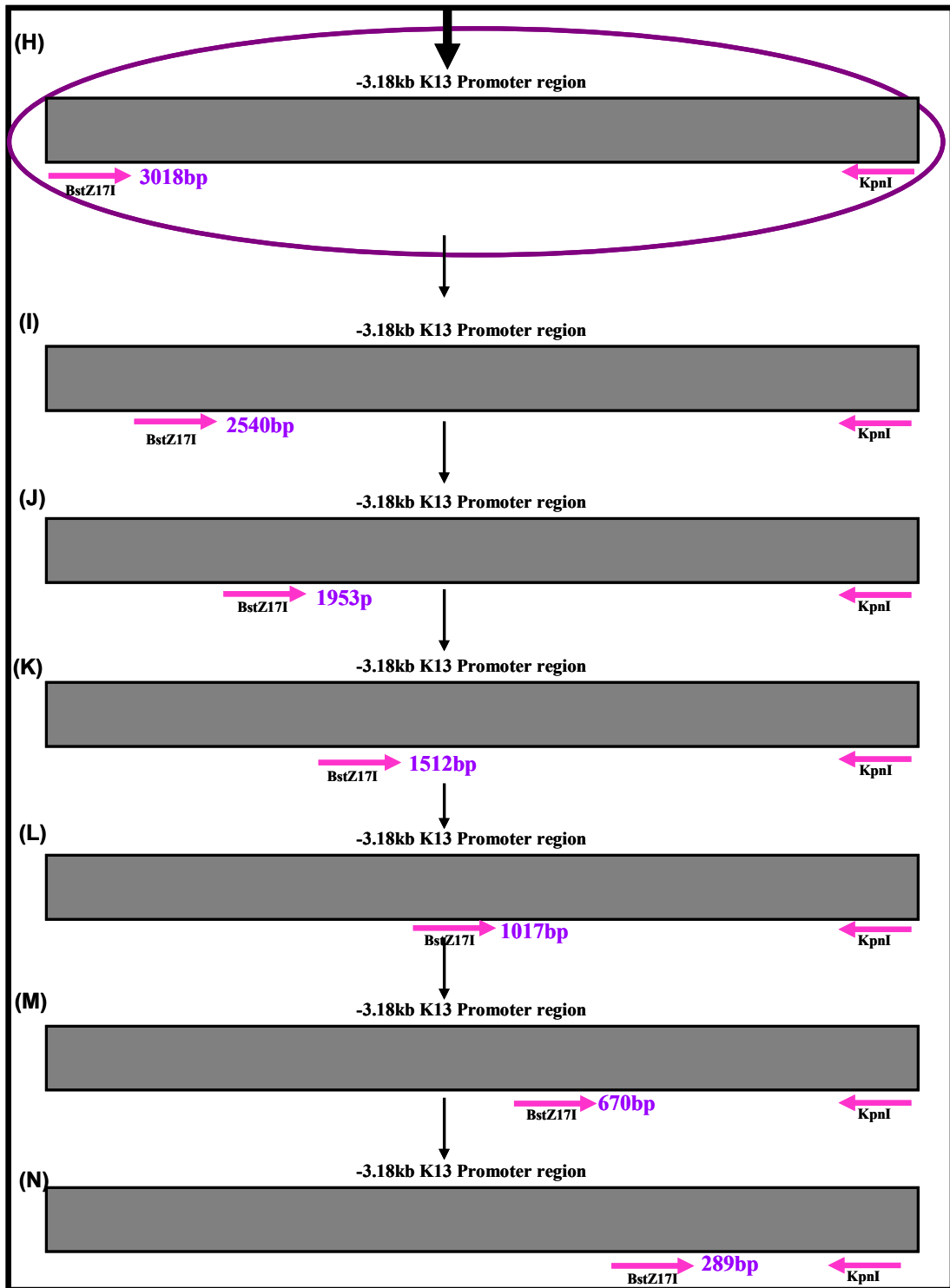


Figure 2.6 H-N: PCR against the K13 full length (3018bp) promoter in 4.117Kb pEGFP-N3B vector: Using the K13 full length promoter (3018bp) in 4.117Kb pEGFP-N3B vector as a DNA template (H) for PCR, a 5'-end deletion series using specific designed primers (pink arrows), generated six fragments (purple numbers) of K13 promoter. The six fragments generated from the full length K13 promoter are -2540bp (I), -1953bp (J) -1512bp (K) -1017bp (L) -670bp (M) and -289bp (N).

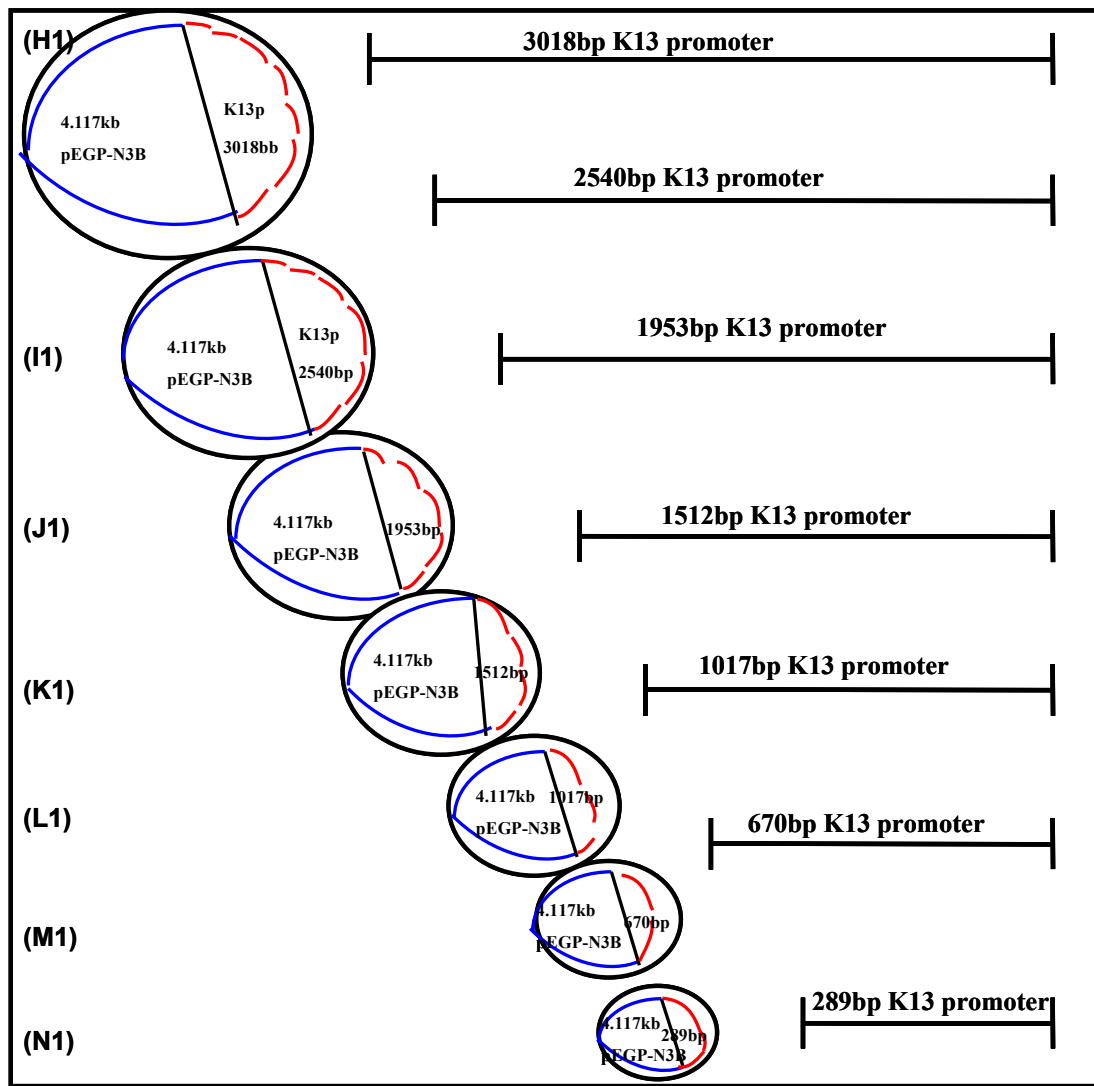


Figure 2.6 H1-N1: Various length of the truncated K13 promoter in 4.117kb pEGFP-N3B vector: Using the K13 full length promoter (H1) in 4.117kb pEGFP-N3B vector (blue half circle) as a DNA template (H) for PCR, a 5'-end deletion series using specific introduced BstZ171 site to generate six fragments (red half circle) of K13 promoter. The six fragments generated from the full length K13 promoter are -2540bp (I), -1953bp (J) -1512bp (K) -1017bp (L) -670bp (M) and -289bp (N).

2.14.1 Designing Primers for Site-directed mutagenesis of pEGFP-N3BK13Pro-7.117kb.

A BstZ171 restriction site (GTATAC) was introduced into the full length parental pEGFP-N3BK13-3018bp promoter sequence at positions K13-2540bp K13-1953bp, K13-1512bp, K13-1017bp, K13-670bp, and K13-289bp upstream from exon 1 sequence. The above positions were selected because they correspond to specific sequences which required minimal change to the BstZ171 site (GTATAC) in the original 3.018kb K13 promoter (Figure 2.7 A) sequence (Figure 2.7 B). Then once the positions were established for BstZ171 sequence a 20 nucleotides sequence up

and downstream from the BstZ171 site were selected. A complementary sequence (forward primer) was manually designed to this region. Then the reverse of this complementary sequence was deduced (reverse primer), and both forward and reverse primers were made (Appendix: Table 3).

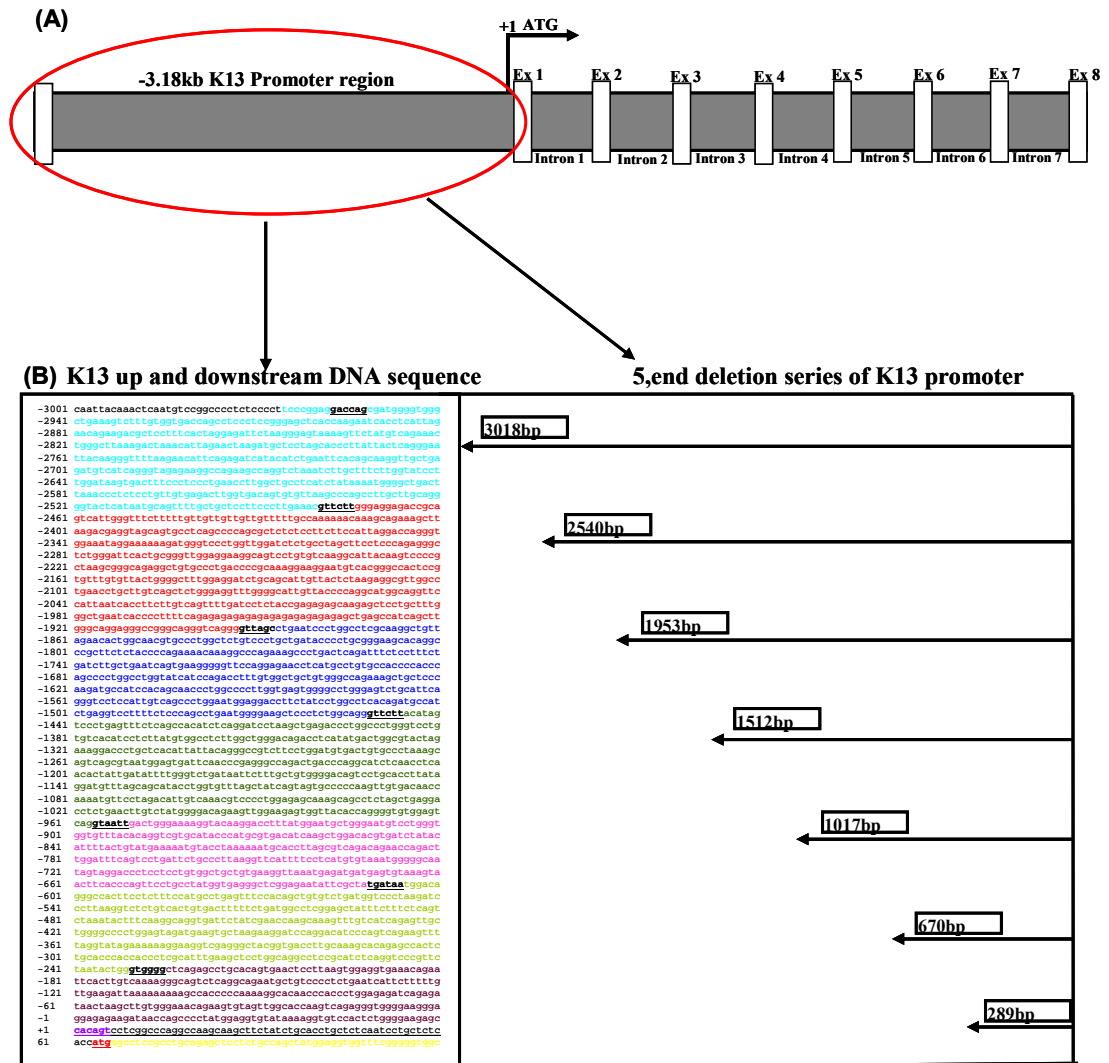


Figure 2.7: (A) Diagrammatic representation of K13 gene (with 3.018kb promoter, 8 exons and 7 introns). (B) illustrates the K13 upstream and downstream sequence from exon 1 position, the different coloured sequences correspond to various different length of the full length K13 promoter (-3018bp, turquoise), and the six (R1-R6) fragments generated from full length K13, R1 (-2540bp, red), R2 (-1953bp, navy blue), R3 (-1512bp, green), R4 (-1017bp, pink), R5 (-670bp lime green) and R6 (-289bp,). The purple underlined 6 nucleotides sequence correspond to the site where KpnI was designed. The original K13 promoter sequence (6 nucleotides, underlined in black) does not differ much from the BstZ171 site (GTATAC), so this sequence corresponds to the site where BstZ171 primer was designed, in attempt to retain or minimise change to the BstZ171 sequence. The red 3 nucleotides sequence corresponds to the ATG and the yellow highlighted sequence corresponds to the start of coding region.

2.14.2 Designing Primers for Sequencing of pEGFP-N3BK13Pro Deletion

Series

Using the sequence for pEGFP-N3B vector at the AseI enzyme site (which was changed to BstZ171) within 60-80 nucleotides to the left of the AseI enzyme site, a 21 nucleotide forward sequence was designed making sure the GC content was 40% or above. The designed primer was in the region between 4658 and 4678bp of pEGFP-N3B vector, the forward primer sequence (GCT GGC CTT TTG CTC ACA TGT T) was then synthesised (Appendix: Table 7. 4).

2.14.3 Site-Directed Mutagenesis Kit

Site-directed mutagenesis (SDM), is an *in-vitro* technique used for studying gene and protein structure-function relationship, this technique is also used for modifying vectors sequences to make cloning and expression more easier (Stratagene SDM kit booklet). Several approaches for SDM have been published, but these methods generally require the use of single stranded DNA template and normally permit a single point mutation at only one site per round; these methods are also technically difficult to carry out and labour intensive (Stratagene SDM kit booklet). However, the use of Stratagene's quick change site-directed mutagenesis kit has the advantages: that there is no need for sub-cloning into M13-based bacteriophage vector (normally used for cloning a large insert), since any plasmid of up to 8kb can be used. This techniques is also very is simple to carry out using the kit, allows oligo-mediated introduction of specific mutations in any double stranded plasmid and permits mutation at three different sites simultaneously (Stratagene SDM kit booklet). The principle behind SDM, as outlined in Figure 2.8, briefly involves 3 step procedures. In step one, after having set up 6 PCR reactions (Table 2.7), the K13 R1 to R6 DNA is denatured, then the mutagenic primers are able to anneal and the primers are extended and nicks are ligated with the quickchange multi-enzyme blend. Then in step two of the procedure the resulting mutant (synthetic) and original parental DNA template (methylated by bacteria during transformation stage) used for PCR are separated by digestion of template with DpnI enzyme (methylation sensitive). In the final step of the three stage procedure, the mutated R1-R6 K13 promoter fragments are transformed (Section 2.5.4).

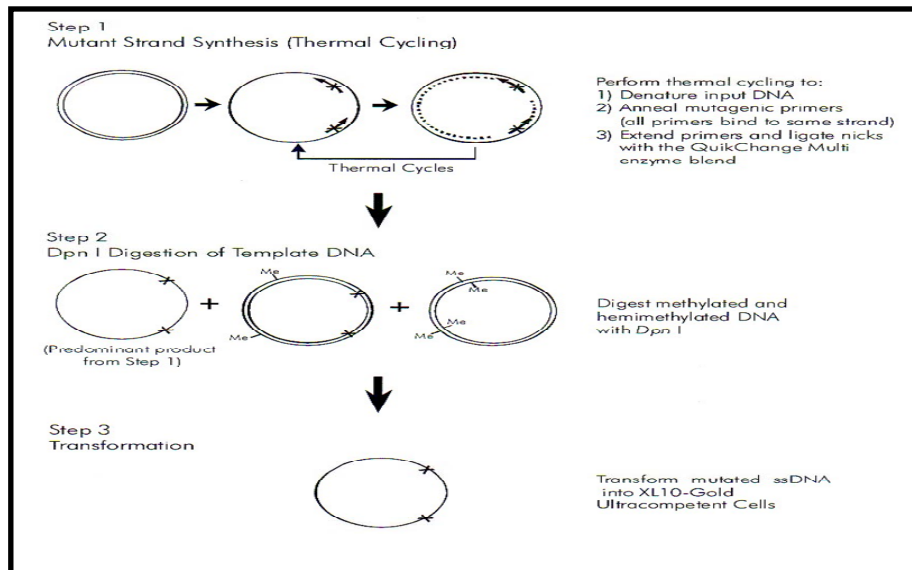


Figure 2.8: Overview of the Quick-change multi site directed mutagenesis method (Stratagene SDM kit booklet)

2.14.4 Quick-change Multi-site Directed Mutagenesis Kit (Stratagene)

The mutant strand synthesis reaction for thermal cycling was prepared as in Table 2.12 and depending on the plasmid size, the reaction components differed according to the Stratagene Quick-change multi-site directed mutagenesis kit, for a plasmid of exactly 5kb or more. Also according to the Stratagene kit protocol, depending on the number of mutagenesis primers used (1 to 3 primers =100ng) or (3 to 4 primers =50ng), the concentration of primers would differ; for this experiment, however, only single reverse primer sets were used. The cycling parameters used for both mutagenic and control reaction consisted of an initial cycle of denaturing at 95⁰C for 1 minute, then 20 cycles of denaturing at 95⁰C for 1 minute, then annealing of mutagenic primers to DNA at 55⁰C for 1 minute, then a final extension at 65⁰C for 2 mins per kilobase pair of plasmid length. Although normally an extension temperature of 70⁰C is used, with the Stratagene kit an extension temperature of 65⁰C was used because this is the optimal temperature recommended by the manufactures for the quick change multi blend enzyme used. Having followed the temperature cycling above, both mutagenic and control reaction PCR products were placed on ice for two minutes to cool the reaction to $\leq 37^{\circ}\text{C}$. The Quick-change multi site directed mutagenesis Stratagene kit manufacture protocol was then used except for an alteration in the Dpn I enzyme digestion of the amplified PCR products step in which the mutated PCR products obtained were subjected to sequential double digestion with Dpn I enzyme instead of the one time only as recommended in the

Stratagene protocol; this was done to ensure complete digestion of mutated PCR products.

Table 2.7: Mutagenesis Reactions

10x Quick-change Multi reaction buffer	2.5 μ l
Double distilled H ₂ O	18 μ l
QuickSolution	0.75 μ l
ds-DNA templates	1 μ l (100ng)
Mutagenic Primers (1-3)	1 μ l (100ng)
100mM dNTP mix	1 μ l
Quick-Change Multi Enzyme blend	1 μ l (1 unit)
Total	25μl

A control reaction was set up as in Table 2.8 and ran along with the site directed mutagenesis reaction.

Table 2.8: Control Reactions

10x Quick-change Multi reaction buffer	2.5 μ l
Double distilled H ₂ O	18 μ l
Quick-Change Multi control template	0.75 μ l (50ng/ μ l)
Quick-change multi control primer mix	1 μ l(100ng/ μ l)
Quick Solution	0.75 μ l
100mM dNTP mix	1 μ l
Quick-Change Multi Enzyme blend	1 μ l (1 unit)
Total	25μl

Table 2.9: The primary antibody used in the study

Primary antibody	Dilution used	Manufacturer	Catalogue number
Mouse monoclonal (IC7) to cytokeratin 13	1:10 for immunocytochemistry 1:50 for Western	Abcam	Ab22685
Mouse monoclonal (AE8) antibody	1:1000	Abcam	A166112
Anti-actin	1:10,000	Sigma	A2066
Mouse IgG2a Kappa monoclonal Mg2a-53 isotype control	1:10	Abcam	Ab18414
Cytokeratin 15 antibody (LHK15)	1:100	Abcam	Ab2414
Mouse monoclonal C8/144B clone	1:100	Dako	M7103

Table 2.10: The secondary antibody used in the study

Secondary antibody	Dilution used	Manufacturer	Catalogue number
Alexa fluorochrome 488 goat antimouse IgG	1:100	Invitrogen	A11029
Horseradish Peroxidase-Conjugated Goat Anti-Mouse IgG	1:4000	chemical	A11000
Horseradish Peroxidase-Conjugated Rabbit Anti-Mouse IgG	1:1000	Santa Cruz	C3006

2.15 Immunocytochemistry

Cells were seeded at 1×10^5 onto sterile cover slips (Chance, Propper, Warley, UK) in 24 well plates containing 1ml of appropriate medium for the cell type used and cells were then incubated at 37°C in 5% CO_2 for 24 hours. Cells were fixed with 1ml of ice-cold methanol/acetone (1:1) for 20 mins at -20°C . The fixative was aspirated and the cells washed with PBS three times. Using a 6 by 6 inch glass plate sealed with parafilm, 15 μl of 10% goat serum (Invitrogen Ltd, Paisley, UK) was dropped onto the parafilm to block non-specific binding of the primary antibody. The cover slips were flipped (ensuring that the cells were facing down) onto the drop of goat serum

and left for 20 minutes. After blocking, the cells were flipped onto a 15 μ l drop of primary K13 mouse monoclonal (Abcam Plc, Cambridge, UK) antibody (1:10 dilution of 500 μ g/ml stock concentration) made up in 10% goat serum and incubated for 1 hour at R/T. The cells were washed with 1ml of 0.2% tween in PBS for 3 minutes; this was repeated twice. Then, the goat anti-mouse secondary antibody Alexa fluorochrome 488 (Invitrogen Ltd, Paisley, UK) conjugated (1:100) was prepared in 10% goat serum and left on the cells for 1 hour at R/T in the dark. The cells were washed with 1ml of 0.2% Tween in PBS for 3 minutes and this step was repeated twice. The cells were then finally flipped onto 15 μ l of DAPI (Chroma Technology Corp Inc, Rockingham, USA) diluted with PBS 1:1000 in the dark for 1 min. The cells were washed with PBS containing 0.2% Tween once and then dipped into distilled water. The cover slip was flipped onto a slide with a drop of immunomount (Thermo electron corporation Ltd, Cheshire, UK), and then gently pressed down to get rid of bubbles. After a few minutes of air drying the edges of the cover slip were sealed with clear nail varnish.

2.16 MTT Assay

MTT is an assay (Mosmann 1983) based on the ability of viable cells to release mitochondrial dehydrogenase enzyme to cleave the tetrazolium rings of the pale yellow MTT to produce dark blue formazan crystals. These formazan are impermeable to cell membranes, which results in their accumulation within living cells. Solubilisation of the formazan crystals in the cells occurs when an appropriate solvent such as DMSO is added, which liberates the crystals into solution. The number of surviving cells is directly proportional to the level of the formazan product created. To assess the effectiveness of any pharmacological agent's ability to cause cell death, the amount of purple formazan produced by treated cells is normally compared to the amount of formazan produced by untreated control cells, usually through the production of a dose response curve. The quantification of colour is carried out using a simple colorimetric assay. One of the main advantages of the MTT assay is speed and accuracy and for this reason it was used to analyse the effect of Trichostatin A, Sodium butyrate, 4- α -PMA and TPA, MEK 1/2 inhibitor (PD98059) and PI3K/Akt pathway (LY294002) inhibitors (EMD Chemicals Inc, Darmstadt, Germany) on cell proliferation.

2.16.1 MTT Assay procedure

Depending on the cell line, cells were seeded between 5×10^3 and 12×10^3 per well of a 96 well plate and incubated overnight in a 5% CO₂ at 37⁰C. Each cell line (SCC25, RTS3b and HeLa) was treated for different time points and with a different dose range. The following pharmacological agents were used: TPA and 4- α -PMA (10nM, 20nM, 30nM, 40nM, 50nM, 100nM, 150nM, 200nM) for 6 hours, Trichostatin (0.5 μ M, 1 μ M, 2 μ M, 3 μ M, 4 μ M, 5 μ M and 6 μ M) for 14 hours, Sodium butyrate (0.5mM 1mM, 1.5mM, 2mM, 4mM, 6mM, 8mM and 10mM) for 24 hours. In addition, the other pharmacological agents used to treat the cells included: LY294002 (5 μ M, 10 μ M, 20 μ M, 25 μ M, 50 μ M, 75 μ M and 100 μ M) for 48 hours and PD98059 (10 μ M, 20 μ M, 40 μ M, 50 μ M, 75 μ M, 100 μ M and 110 μ M) for 48 hours. Appropriate media alone for the cell line used and equal volume of DMSO were used as normal and vehicle controls. Then 200 μ l of Thiazolyl Blue Tetrazolium Bromide solution (0.5mg/ml made in 20ml of appropriate media for the cell type been used was wrapped and stored at 4⁰C) was left at R/T for 10 minutes, then pipetted into each well of the 96 cell plate and incubated for 1 hour in a 5% CO₂ incubator at 37⁰C. The media containing MTT were carefully removed using a fine tip attached to the aspirator. The purple formazan dye was dissolved by adding 200 μ l of DMSO in each well and left until purple colour was formed. This was read at 570nm Optical Density using Fluostar OPTIMA BMG LABTECH plate reader. Epithelial monolayer cell line and primary cell viability was expressed as a percentage of the control cultures as:

$$\text{Viability} = \text{OD}_{(570\text{nm})} \text{ of Treated} / \text{OD}_{(570\text{nm})} \text{ of Untreated (Control)} * 100$$

2.17 Western Blot

2.17.1 Sample Collection

1×10^6 of each cell type was plated into a 6cm Petri dish and incubated (5% CO₂ at 37⁰C) until 70-90% confluence was reached. The cells were then treated with various drugs and their vehicle control (DMSO) for a given period of time, after which they were washed with an appropriate of volume of ice cold PBS twice. Then an appropriate volume (depending on cell density) of 2x Laemmli buffer was used to lyse cells, by pipeting Laemmli buffer onto the cells and leaving it for 2-3 minutes.

Cell scraper was used to remove the lysed cells, and the lysates were pipetted into a prelabelled Eppendorf tube and immediately placed onto a heating block, preset at 95⁰C, for 5mins.

2.17.2 SDS PAGE

A pre-cast Nupage 4-12% Acrylamide Bis tris gel 1.5mm thick with either 10 or 15 wells was used which was placed into an Xcell (Invitrogen Ltd, Paisley, UK) sure-lock gel tank. Appropriate volumes (such that roughly same band density would be obtainable for loading control β -actin) of sample lysates were loaded into the gel with 3 μ l of magic marker (MW range of 20-220kDa, Invitrogen Ltd, Paisley, UK). The tank was then filled with 1x NuPage (Invitrogen Ltd, Paisley, UK) buffer and sample in gel was run at 100volts until the samples had migrated a third of the length of the gel. The voltage was then increased to 140 volts.

2.17.3 Protein Transfer Membrane using Semi-dry Method

Once the gel was run to completion, the cassette was removed from the gel unit and taken apart. The gel was removed and placed in transfer buffer for 5 minutes. Four square filter paper sheets (Whatman International Ltd, Kent, UK) were cut to size (8x8cm) and left to soak in transfer buffer. A square of nitrocellulose transfer membrane (8x8cm) was left to soak in transfer buffer for 5 minutes. The filter paper, membrane and gel were taken out of the transfer buffer and placed on top of each other in the following sequence: 2 sheets of Whatman filter paper, nitrocellulose transfer membrane, gel and 2 sheets of Whatman filter paper. This was then placed into the Invitrogen protein transfer tank unit and the cathode plate cover was placed on top and the proteins were transferred at 32 volts for 1 hour.

2.17.4 Membrane Staining

The nitrocellulose membrane was stained with Ponceau-S staining solution for 1 minute while shaking gently. The Ponceau-S solution was poured into its container, and the excess dye was washed off with distilled running water, shaking and pouring off (repeated several times).

2.17.5 Blocking Membrane

10ml of 5% w/v milk powder (Marvel Ltd, Bristol, UK) solution was made up in PBS containing 1% Tween 20 (PBSMT) and membrane was immediately incubated with PBSMT solution and left on the shaker at 40 rpm for 1 hour.

2.17.6 Antibody Binding

The membrane was incubated in solution containing 10ml of PBSMT solution with primary mouse monoclonal AE8 anti-K13 (Abcam Plc, Cambridge, UK) at 1:1000 dilutions and left on the shaker at 10 rpm in a cold room overnight. The membrane was then washed with PBST three times for 5 minutes and then incubated with secondary goat anti-mouse IgG conjugated horseradish peroxidase (EMD Chemicals Inc, Darmstadt, Germany) at a dilution of 1:1000 in 10ml of PBSMT; the membrane was then left on the shaker at 40 rpm for 1 hour. The membrane was washed with PBST solution three times for 5 minutes. The loading control mouse anti-human β -actin antibody was made in 10ml of PBSMT solution at a dilution of 1:10,000 and this was then incubated with the membrane on the shaker at 40 rpm for 1 hour. The membrane was washed with PBST solution three times for 5 minutes. The secondary rabbit anti-mouse IgG conjugated horseradish peroxidase was made in 10ml PBSMT at a dilution of 1:4,000 and this was incubated with the membrane and left on the shaker at 40 rpm for 1 hour. The membrane was washed with PBST solution three times for 5 minutes.

2.17.7 ECL Detection

Enhanced Chemiluminescence Plus reagents (GE Healthcare, Bucks, UK) were made by mixing 1ml of solution 1 and 50 μ l of solution 2 and pipetting the mixture onto the membrane, then covering the membrane and leaving it for 1min. The excess ECL substrate was drained onto a tissue by holding the side of the membrane with forceps, and then the membrane was wrapped in a cling film inside the cassette and quickly closed. In a dark room the film (GE Healthcare, Bucks, UK) was placed on top of the membrane and the cassette was closed for 30 seconds to 5 minutes. The film was developed using a Hyperfilm processor (GE Healthcare, Bucks, UK).

2.17.8 Densitometry

The band density measurements were carried out using the densitometry programme of an Autochemi system (UVP Bioimaging) and each experiment was repeated three times using different lysate samples. The student t-test was used to assess significant differences between treated and untreated lysate samples for the expression of K13 protein.

2.18 Stable Transfection

The H357, SCC25 oral mucosa or vulval carcinoma A431 cells lines were transfected with the K13 or K15 promoter linked GFP constructs alone. Post-transfected cells were selected for 2 weeks using 0.5-1mg/ml G418 antibiotic, to create stable cell lines. Then the stably transfected K13 or K15 promoter linked GFP constructs cells were either 1) selected for over several more weeks in a T75 flask, 2) split and seeded onto a four 20mm coverslips placed in a 10cm Petri dish, or 3) FACS sorted according to four distinct populations (negative expressing, low expressing, medium expressing and high expressing GFP populations).

2.18.1 K13 or K15 Promoter linked GFP Expression in Oral SCC25 Cells

K13 or K15 promoter linked GFP constructs transfected into oral SCC25 were selected for several weeks in T75 flasks until selected cells formed many heterogeneous colonies corresponding to holoclone, meroclone and paraclones. The expression of the K13 or K15 promoter-linked GFP construct in holoclones or paraclones formed by oral SCC25 in T75 flasks was quantified by grading them from no expression to high GFP expression in 10 holoclone and in 10 paraclone colonies.

2.18.2 Analysis of K13 and K15 Promoter linked GFP Construct expression by FACS

Oral SCC25 cells stably transfected with K13 or K15 promoter linked GFP constructs were trypsinized and seeded at a clonal cell density of 2000/ml onto four 20mm cover slips pre-placed in a 10cm Petri dish. The cells were left to grow until holoclone, meroclone and paraclone colonies were formed. Colonies were scraped off using a fine needle under the microscope, such that two cover slips had only holoclone colonies and the other two cover slips only had paraclone colonies. The

expression of K13 or K15 promoter linked GFP constructs in holoclone and paraclone of oral SCC25 cells was then quantified by FACS.

2.18.3 Analysis of K13 or K15 Promoter linked GFP Construct Expression using Colony Forming Assay

Oral SCC25 cells stably transfected with K13 or K15 promoter-linked GFP constructs were trypsinized and sorted into four distinct GFP populations (negative expressing, low expressing, medium expressing and high expressing) using FACS. Once sorted, the cells were seeded at a clonal cell density of 600 cells/ml onto 6 well plates. Cells were fixed with 4% paraformaldehyde for 20 mins at 4°C, washed with PBS and then 1ml of 2% rhodamine blue was added to each of the 6 well plates and left on a shaker at a speed of 10 rpm overnight. Cells were then washed with distilled water and left to dry. The number of colonies formed was counted by taking pictures of the 6 well using a Nikon ECLIPSE TE2000-S biomedical microscope equipped with an epifluorescence attachment, a high speed filter wheel (Lambda 10-3) and photographed using an integrated digital camera. All images were obtained using Metamorph software, reproduction and editing was completed using Adobe Photoshop and Corel Graphics Suite 11.

Chapter 3

Comparative

Bioinformatics Analysis

of Keratin Promoters

3.1 Introduction

A gene can be expressed either at a specific time point or in a specific tissue in response to environmental changes, developmental signals and differentiation processes (Song et al, 2005). The rate at which a gene is transcribed, and hence expressed, is largely dictated by transcription factors which bind and alter the affinity of the RNA polymerase for the promoter (Song et al, 2005). Transcription factors are proteins which bind to the upstream regions of a gene and then either increase or decrease the expression of that particular gene and regulate gene expression (Tompa et al, 2005). Understanding the mechanism by which a gene is regulated has been a great hurdle, and a vital step towards understanding the mechanisms of gene regulation, is to identify the binding sites for transcription factors (also known as transcriptional elements or regulatory elements) (Tompa et al, 2005). Moreover, what makes the identification of transcription factor binding sites so essential is that it enables a better understanding of the regulatory network which controls cellular processes such as cell proliferation and differentiation (Euskirchen et al, 2007).

3.2 Computational Approach to Identifying Transcription Factor Binding Sites

The computational prediction programme for transcription factor binding sites is based on pattern matching or pattern detection. The pattern matching detection pathway is based on knowledge of previously characterised sequences after input into a transcription factor search database and matching to defined sequences of interest. The pattern detection pathway relies on the programme to detect these patterns on a genome-wide scale to identify putative transcription factor binding sites which might be present in the entered DNA sequence (Elnitski et al, 2006). The prediction of a transcription factor binding site (known as a motif) was initially a problem since binding sites were traditionally characterised by experimental methods which are labour intensive and costly (Song et al, 2005). However, this problem was later resolved by computational biologists who developed methods for predicting the transcription factor binding sites in the promoter DNA sequence of a gene (Tompa, et al. 2005). Furthermore, in mammalian cells many transcription factors work synergeristically, which enables the cells to respond to different types of environmental and developmental stimuli (Zhu et al, 2005). The functional interaction of transcription factors working in concert requires that they must be in close proximity to each other (Zhu et al, 2005). Thus, when the user of the

computational database provides a specific region of the DNA sequence of interest, which is believed to be co-regulated by combinatorial transcription, the database identifies a very small motif sequence which is statistically over represented in the regulatory regions (Tompa et al, 2005). According to the literature, prediction databases cannot accurately identify all transcription factor binding sites (motifs), for the following reasons:

- The motifs are very short DNA sequences (about 10bp long), which are in the centre of a much larger DNA sequence (usually about 1kb long) entered into the database by the user and hence in the midst of statistical noise
- The DNA sequence of the binding sites for different transcription factors varies (Tompa et al, 2005).

Another disadvantage of using the transcription factor search database is that the promoter DNA sequence being analysed is in a linear form (one-dimensional) but the transcription factor binding *in-vivo* is in a 3-dimensional form, thereby entering the promoter DNA sequence into the database is not expected to simulate fully the *in-vivo* environment. Transcription factors can bind to the promoter sequence in either orientation, but the database only predicts the binding sites of transcription factors in a linear form.

However, in this thesis, the difficulty of accurate identification of motifs was partially addressed by increasing the default setting on the database from 85% to 90% or above (their motif binding sites predicted to be 90% or above that which corresponds to any given transcription factor should be identified); this was done in attempt to reduce the number of false positive prediction binding sites for the database used.

3.2.2 Technical Approach used to Identify Regulatory Elements

Although the computational approach for finding potential binding sites for transcription factors (Figure 3.2) is used after the promoter has been truncated, there are other experimental methods which are used to validate the computational prediction databases. These methods include:

- The formaldehyde based ChIP (chromatin immunoprecipitation assay).
- Placing the promoter sequence into a reporter plasmid and co-expressing the transcription factor and the reporter construct and measuring the activity of the reporter gene in the presence and absence of the transcription factor to see whether it activates, represses or has no effect on the reporter construct.
- Using RNAi (RNA interference) to knock down the mRNA expression of the transcription factor in question (Oberley et al, 2006).
- *DNaseI hypersensitivity*: this method is used to observe whether the expression of a particular gene is switched off because of DNA methylation and histone acetylation and thus detects altered chromatin structure (Elnitski et al, 2006).

However, although these technical approaches are vital for identifying the interaction between DNA and its cognate binding protein, the disadvantage is that they do not address the interaction of both the DNA and the transcription factors, which bind to them at the endogenous loci. Furthermore, transcription factors normally work synergistically to bring about regulation of gene expression, and using a co-transfection of the DNA regulatory region in question and the transcription factor which is thought to regulate the region, a false negative result may be obtained from imbalances due over expression of a specific transcription factor (Oberley et al, 2006).

In summary, although both computational and technical validation (Figure 3.1) methods are equally important, bearing in mind that both approaches have their advantages and disadvantages, the inter-dependence of the two approaches when used together by far outweighs the use of only one approach (Elnitski et al, 2006).

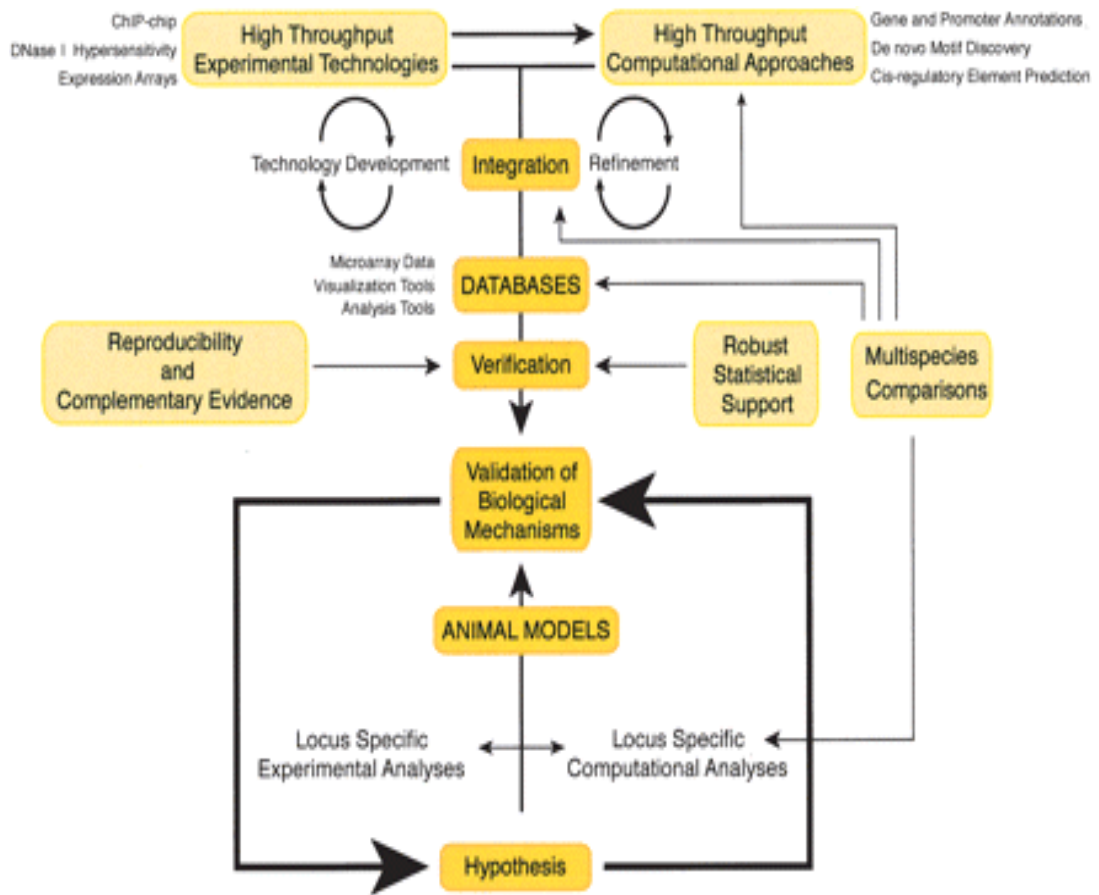


Figure 3.1: Diagrammatic illustration of the inter-dependence of both computational and experimental approaches for identifying the binding of transcription factors and its functional relevance (adapted from Elnitski et al, 2006).

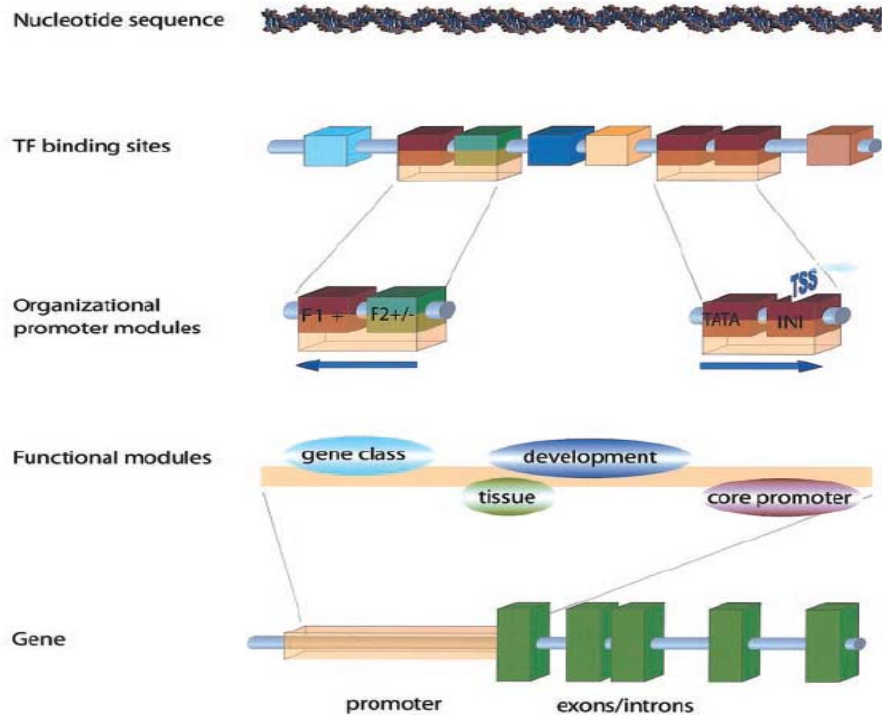


Figure 3.2: Simplified diagram (adapted from Werner et al, 2003), illustrating the basic principle behind any of the widely used transcription factor database searches available on the internet, from the moment the user inputs the DNA sequence into the database, through to how the sequence is pattern matched and pattern detected from prior knowledge of previous DNA sequences inputted into the database or genome wide based search (Elnitski et al, 2006).

3.2.3 Computational Databases used to Identify Tissue-Specific Keratin and their Transcription Factors

The control of gene expression occurs at numerous levels including:

- regulation of the rate at which mRNA is made
- the stability of the mRNA product
- the rate at which mRNA is translated into protein
- the stability of the protein product (Eckert et al, 1997).

Although the regulation of keratin expression is on occasion reported to be regulated at both translational and post-translational stages (McBride et al, 1999), most of the studies carried out from as early as Lersch et al, (1989), through to Jiang et al, (1990); Leask et al, (1991); Eckert et al, (1997); Wang et al, (2002); Popa et al, (2004) have shown that keratin gene expression is regulated at the post-transcriptional level. Moreover, a given single transcription factor alone does not govern keratin gene expression, but rather several transcription factors act synergistically to bring about tissue specific expression. To account for the tissue-

specific expression of keratin genes, two mechanisms have been suggested of which the most observable is 1) a positive regulatory element, which specifically activates keratin genes in epithelial tissue only, or 2) a negative regulatory element which either decreases the expression of keratin genes in non-epithelial tissue or an epithelial tissue which does not express the endogenous keratin gene (Jiang et al, 1990). Furthermore, in order to find these positive or negative regulatory elements many studies have utilized both experimental technologies and computational approaches to map the transcription factors binding sites in keratin gene promoters (Dale et al, 1990; Eckert et al, 1997; Casatorres et al, 1994; Tomic-Canic et al, 1998). Comparing transcription factors which bind basal and suprabasal keratin gene promoters, would give a better understanding of how basal and suprabasal cell specific keratin gene promoter expression is controlled by transcription factors in different environments (Casatorres et al, 1994).

In chapter 4, we showed that suppressor elements, which reside within the K13 full-length promoter construct, appear to confer K13 mucosal tissue-specific expression. Using the TFsearch database, GATA-1, Oct-1 and HSF transcription factors were identified. Also, in chapter 5, expression of basal K15 and suprabasal K13 markers of oral mucosa, correlation with sub-populations present in oral cell lines (differentiation) was investigated. This chapter links with chapter 4 and 5, in that in order to understand basal and suprabasal keratin gene regulation, the key is to map transcription factor binding sites and detect an emerging pattern of transcription factors. Therefore, this chapter aims to use bioinformatics to map transcription factors which govern keratin specific differentiation and the sequential basal to suprabasal keratin specific expression.

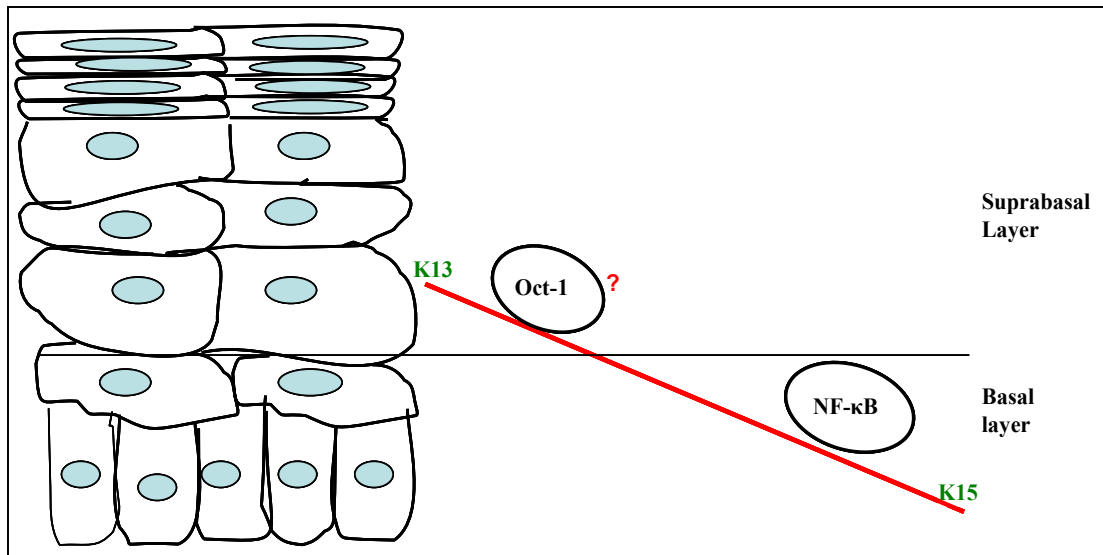


Figure 3.3: Diagram showing basal K15 and suprabasal K13 keratin genes expression and transcription factors though to be important for conferring their sequential basal to suprabasal specific expression. NF- κ B which has been shown to suppress the expression of K15 gene promoter (Radoja et al, 2004) and Oct-1 transcription factor might be important (found in this study but not confirmed) for suppressing the expression of K13 promoter in all non-permissive cell lines.

3.3 Aims

- 1) Use NCBI database to obtain approximately 2-3kb (Section 3.5.1) upstream sequence of 3 basal and 17 suprabasal keratin promoters.
- 2) To compare the transcription factor binding sites in basal and suprabasal keratin promoters.

3.4 Materials and Methods

Chapter 2 section 2.13 contains a detailed protocol of how the promoter sequence of each of the K1-K20 was searched. Once the keratin promoter sequence was obtained, then TF search database was used to find potential transcription factor binding sites in keratin gene promoters and several criteria was used to select specific transcription factors.

3.5 Results

3.5.1 5'-upstream region of Keratin Genes

Genes are normally organized in a linear form in the chromosome and keratins genes are organized in type-specific clusters in the chromosome (Bowden, 2005). To assess the maximum 5'-upstream region of keratin genes, the intergene distance is required. An intergenic region is a stretch of DNA sequence located between clusters of genes (Figure 3.4), which contains a few or no genes (Reference: website 18). Although, the exact role of the intergenic regions is not known, they are thought to act to control genes close to them (Reference: website 18). The intergenic region sequences in humans, comprise a large percentage of the genome (Reference: website 18). The 5'-upstream region of keratin genes lies in between the ATG site of the specific gene of interest and the poly A tail of the gene before it in the chromosome location. The maximum 5'-upstream region of K13 and K15 was determined to be 8kb for K13 and 4.6kb for K15 using the NCBI website (Appendix: Figure 7.6). Although in this chapter the size of the 5'-upstream region analyzed for all 20 epithelial keratins is 2-3kb, it should be noted that the 5'-upstream region of some keratin genes could be quite large. The importance of analyzing the maximum 5'-upstream region of keratin genes for correct regulation *in-vivo* is exemplified by human keratin 1 (HK1). By using a larger HK1 fragment, generated from transgenic mice, containing the coding region, 13Kb of upstream sequence and 3.4Kb of downstream sequence was shown to impart the correct regulation with regards to tissue and developmental specific expression of K1 gene and not the 12kb HKI fragment that was originally used (Blomhoff, 1994). It should be noted that the sizes chosen for analysis of 20 epithelial keratin 5'-upstream regions in study is incomplete especially for larger keratins such as K1.



Figure 3.4: Diagram illustrating the intergenic DNA region (red line), which is in between two sets of gene (blue line) clusters (adapted from website number 18 in the Reference section)

Table 3.1: The number of nucleotides in the 5'-end upstream promoter region of keratin genes analysed by TFsearch database.

Name of Keratin	The size of 5'-end - Upstream region of the keratin promoter (bp) analysed	Keratin Type
Basal keratin gene promoters		
K5	2465	Type II
K14	2061	Type I
K15	3050	Type I
Suprabasal keratin gene promoters		
K1	2557	Type II
K76 (K2p oral mucosa)	2658	Type II
K3	2456	Type II
K4	2619	Type II
K6a	2627	Type II
K7	2265	Type II
K8	2341	Type II
K9	2449	Type I
K10	2458	Type I
K12	2457	Type I
K13	3050	Type I
K16	2254	Type I
K17	2251	Type I
K18	2108	Type I
K19	2225	Type I
K20	2518	Type I

Table 3.1 above shows the length of each of the keratin promoter sequences selected for analysis. Of the 20 keratin promoters analyzed in this study, three were basal keratin promoters and 17 were suprabasal keratin promoters. -2000 to +100bp of basal and suprabasal keratin promoter sequence was obtained.

1	CAGCCGAAG	GATTTTAGTG	CTAGGACAGA	GTCCAGACA	GCAGTGCCAC	entry	score
51	AGTGATGGCG	AGGGAGAGGA	GTAGCAGGGG	AGCGGTGAGG	GGCACTTTCT	entry	score
						<----	M00028 HSF 100.0
						<----	M00029 HSF 96.0
					----->		M00154 STRE 92.5
						-	M00048 ADR1 92.3
							M00075 GATA-1 91.4
							M00048 ADR1 90.8
101	GGAGGAGGGT	ATAGGGCAAA	AACTGGGAGG	AGAAGAGGGA	CAAGGTTCAA	entry	score
						----->	M00028 HSF 95.3
						----->	M00029 HSF 93.7
							M00048 ADR1 92.3
151	TAGCGGAGTG	CAATGGAGAG	GACCGACACA	GCCAGCCCGA	TTCAGAGCCA	entry	score
						----->	M00048 ADR1 92.3
201	CAGAGTAATG	GGACCAGATG	ATCTTCACAG	ACTCCCTTTC	TCCCATAGAT	entry	score
						<-----	M00028 HSF 100.0
						<-----	M00029 HSF 96.0
						<-----	M00033 p300 90.1

Figure 3.5: An example of results obtained when the keratin promoter sequence was entered into the TF search database. The dark black arrows with the corresponding numbers below them illustrate the following: the sequence number (1), the actual K1 promoter sequence (2). The exact site within the sequence where the transcription factor binds to (3), the entry number given to that transcription factor (4), the name of the transcription factor (5), and score expressed as percentage of the likely similarities between the site and the transcription factors which binds that part of the sequence (6).

3.5.2 Data Organisation and Analysis

Table 3.2 shows an example of the transcription factors which bind the basal keratin 5 promoter. The table was organized such that it contains the name of the relevant transcription factor, the Reference number allocated to the particular transcription factor, and the motif sequence within the promoter to which the transcription factor is predicted to bind. The similarity of the transcription endogenous binding motif to the binding motif present in each of the 20 keratin promoters and the position within each of the promoters was also noted. Many transcription factors were selected for each of the 20 keratin promoters but only 9 transcription factors are analysed and presented in this chapter. Tables 3.2 and 3.3 show examples of transcription factors which bind to the basal K5 and suprabasal K76 promoter of the oral mucosa.

Table 3.2: An example of information on the selected transcription factor binding sites within basal K5 promoter sequence

Transcription Factor	Reference in database	Motif sequence	Similarity To K5 promoter sequence	Position within K5 promoter sequence
NF- κ B	M00054	GGGGCTTCCC	92.5	-1
YY1 Yin and Yang 1	M00059	ATGTGAA AATGGTGAGC	92.1	-201
GATA-2	M00076	AAGCCATCCCC TGGGATAGCT	92.9 96.0	-551 -1451



A threshold of 90% and above was selected for the similarity of the transcription factor endogenous binding motif to the binding motif present in each of the 20 keratin promoters.

Table 3.3: An example of information on the selected transcription factor binding sites within suprabasal K76 promoter sequence

Transcription factor	Reference in database	Motif sequence	Similarity to K2p promoter sequence	Position within K2p promoter sequence
HNF-3b	M00131 M00131	TTTAT CTTGTTT ACTTGTTTGCTC	90.2 90.2 96.0	-51 -101 -1301
GATA-2	M00076	GTGGATAGTG CCCTATCCCT	90.9 93.3	- 201 -1951
GATA-1	M00128 M00075 M00075	CGC GTGGATAGTG CACGAT GGGAA TCCGGATCACC CCCTATCCCT GGTGA TGGTC	90.9 98.6 90.6 90.6 90.2 90.2 94.3	- 201 - 201 -951 -1001 -1651 -1951 -2051
NF-kap	M00051 M00051	GGGGATCCCC GGGGATCCCC	98.1 98.1	-1051 -1051
STATx	M00223	TTCCCTGAA TTCCAGGAAT TTCCAGGAAT	92.3 94.2 91.3	-1701 -2051 -2051
HSF2	M00147	AGATGATTC TCAACT	92.9 92.9	-1851 -1901



A threshold of 90% and above was selected for the similarity of the transcription factor endogenous binding motif to the binding motif present in each of the 20 keratin promoters

Table 3.4: The keratins grouped according to their endogenous site of expression in normal and diseased states.

Site of Keratins expression in the body	Name of keratin (s)
Basal keratins expressed in basal layer of all stratified epithelia	K5, K14, and K15
Suprabasal keratins expressed in the skin	K1 and K10
Suprabasal keratins expressed in palm and sole epidermis	K7, K6, K16, K9 and K1
Suprabasal keratins expressed in the cornea	K3 and K12
Suprabasal keratins expressed in the oral mucosa	K2p, K4, and K13
Suprabasal keratins expressed in the simple epithelia.	K7, K17, K8, K18 and K19 and K20
Suprabasal keratins expressed in pathological conditions	K6, K16, and K17


3.5.3 Transcription Factor Selection

Prior to any analysis of the preselected 9 transcription factors and their putative binding sites in the 20 keratin promoters, keratin gene promoters were grouped according their site of expression in normal and abnormal (disease) states. Then the number of binding sites for each of the specific 9 transcription factors in all of the 20 keratin promoters was counted. Table 3.5 shows the raw data for a number of binding sites for 9 preselected transcription factors within each of the 20 keratin promoters, whilst Table 3.6 shows the presence or absence of the each of the 9 preselected transcription factors.


Table 3.5: Basal versus suprabasal keratin gene promoters: preselected transcription factors (n=9), putative number of binding sites found in each of the 20 keratin promoters.


Transcription factor	C/EBP	SP1	USF	GATA-1 2 3	Oct-1	AP-1	NF-κB	STATx	C-rel
Basal keratins	2	2	0	7	2	2	1	1	2
Suprabasal keratins of the skin	2	0	0	6	2	0	0	0	1
Transcription factor	C/EBP	SP1	USF	GATA-1 2 3	Oct-1	AP-1	NF-κB	STATx	C-rel
Basal keratins	2	2	0	7	2	2	1	1	2
Suprabasal keratins of the Cornea	1	0	0	4	2	1	1	1	1
Transcription factor	C/EBP	SP1	USF	GATA-1 2 3	Oct-1	AP-1	NF-κB	STATx	C-rel
Basal keratins	2	2	0	7	2	2	1	1	2
Suprabasal keratins of the oral mucosa	2	1	2	9	2	1	2	2	1
Transcription factor	C/EBP	SP1	USF	GATA-1 2 3	Oct-1	AP-1	NF-κB	STATx	C-rel
Basal keratins	2	2	0	7	2	2	1	1	2
Suprabasal keratins of the Palm and sole	8	0	1	34	3	02	1	1	0
Transcription factor	C/EBP	SP1	USF	GATA-1 2 3	Oct-1	AP-1	NF-κB	STATx	C-rel
Basal keratins	2	2	0	7	2	2	1	1	2
Suprabasal keratins of the pathological conditions	2	2	1	6	0	2	1	1	0
Transcription factor	C/EBP	SP1	USF	GATA-1 2 3	Oct-1	AP-1	NF-κB	STATx	C-rel
simple epithelia	4	4	1	13	3	6	1	0	1

Key

 The number of each of the 9 selected transcription factor binding site within each of the 20 keratin promoters.

 Body sites where a group of suprabasal keratin gene promoters are expressed.

 The name of the 9 transcription factors.

 The stratified basal group of keratin gene promoters.

Results in Figure 3.5 to 3.10 are all based on the results from Table 3.5.

Table 3.6: A summary of the 20 keratin promoters grouped according to the site of expression and whether the promoters contain a binding site for the 9 transcription factors.

Name of Keratin	Transcription elements								
	C/EBP	SP1	USF	GATA-1 2 3	Oct-1	AP-1	STATx	C-rel	NF-KB
K5 K14 K15	X	X		XX	X	X		X	X
				XXX					
		X		XX	X	X	X	X	
Suprabasal keratin gene partners	C/EBP	SP1	USF	GATA-1 2 3	Oct-1	AP-1	STATx	C-rel	NF-KB
	K1 K10	X		XXX	X			X	
	K3 K12	X		XXX	X	X			
K2p K4 K13				XXX			X		X
	X		X	XXX	X			X	
	X	X	X	XXX	X	X	X		X
K6 K16 K9	X		X	XX			X		
		X		XX		X			
				XXX					
K7 K17 K8 K18	X		X	XXX	X	X			
	X	X		XX		X			X
		X		XXX		X			
				X	X	X			
K19	X	X		XX		X		X	
K20	X	X		X X	X	X			

X= represents whether each of the 9 (C/EBP, Sp1, GATA 1, 2, 3, Oct-1, AP-1, STATx, C-rel, and NF-κB) transcription factor have a potential binding site in the 20 keratin promoter sequence. Abbreviations for the transcription factors are as follows: C/EBP=caat box enhancing binding protein, Sp1=stimulating protein 1, GATA 1, 2, 3, Oct-1, AP-1=activating protein 1, STATx=signal transducers and activator of transcription proteins, c-Rel, and NF-κB=nuclear factor kappa-light-chain-enhancer of activated B cell

Table 3.7: The function of C/EBP, Sp1, USF and GATA 1, 2, 3 transcription factors

Factors	Function of transcription factors	Reference
C/EBP	Has role in differentiation in many tissues including the epidermis and also suppression of adipocyte differentiation	<u>(Smith, et al. 2004)</u> <u>(Tong, et al. 2005)</u>
Sp1	Positively regulates epidermal differentiation markers.	<u>(Presland and Dale 2000)</u>
USF	Regulates various target genes and has a key role in hereditary haemochromatosis and familial combined hyperlipidaemia. Also regulates the transcription of genes in lung, prostate, colorectal and breast tumours.	<u>(Ocejo-Garcia, et al. 2005)</u>
GATA-1, 2, 3	GATA-2 and 3 have a role in the suppression of adipocyte differentiation.	<u>(Tong, et al. 2005)</u>
Oct-1	Oct-1 is a transcription factor which regulates the expression of common house keeping genes like histone H2B and small nuclear RNA. In addition, it is also expressed in normal epidermis and it is a candidate for cell determining transcription factor in the skin.	<u>(Hsu and Chen-Kiang 1993)</u> <u>(Andersen, et al. 1997)</u>

Table 3.8: The function of AP-1, STATx, c-Rel and NF-κB transcription factors

Factors	Function of transcription factors	Reference
AP-1	AP-1 in the epidermis regulates cell growth, differentiation and cellular transformation	(Rao, et al. 2003)
STATx	STAT-1 has been shown to be activated by gamma interferon and, as result of this activation, STAT induces K17 expression.	(Radoja, et al. 2004)
c-Rel	The intracellular Rel/NF-κB signalling pathway regulates skin development.	(Gugasyan, et al. 2004)
NF-κB	NF-κB, particularly the p65 isoform in the epidermis, regulates the transcriptional activation of keratin specific markers like K6a. NF-κB also has an anti-proliferative role in the skin.	(Rao, et al. 2003) (Radoja, et al. 2004)

Tables 3.7 and 3.8 summarise the reported function of each of the 9 transcription factors in the literature, all reported functions of the transcription factors were not listed but merely some functions related to each transcription factor were summarized.

3.5.4 Transcription Factor Binding Sites in Basal Keratin Promoters and Skin Suprabasal Keratins Promoters

Figure 3.6 shows that basal and suprabasal keratin promoters contain the same number of binding sites for C/EBP. This family has been reported to have a role in the regulation of suprabasal keratinocytes, both C/EBP α and C/EBP β are expressed in suprabasal keratinocytes of both mouse and human epidermis. Their expression is also up-regulated by calcium induced differentiation in primary keratinocytes which is accompanied by increased expression of K1 and K10, differentiation markers in the epidermis (Oh and Smart 1998). In addition, Sp-1, AP-1, STAT-1, NF-κB and the subunit of NF-κB c-Rel have more binding sites in basal (K5, K14 and K15) keratin promoters in comparison to suprabasal skin keratin (K1 and K10) promoters. It has been shown that Sp1 gene knock-down causes severe developmental defects,

which suggests that this transcription factor is important for maintaining differentiated phenotypes in many cells (Tomic-Canic et al, 1998). However, Tomic-Canic et al, (1998) have reported that the basal keratins contain Sp1 binding sites in their promoters, but not the suprabasal keratin differentiation markers. The AP-1 transcription factor is involved in regulation of many biological processes such cell proliferation, differentiation and cell transformation. The expression of AP-1 proteins, such as c-FOS has been reported to be present in the basal layer of the epidermis, while other reports have shown that c-FOS is not expressed in the basal layer, which correlates with a lack of phenotype in c-FOS knock-down mice. However, these conflicting results might be due to different epitopes recognised by the the antibodies used (Tomic-Canic et al, 1998). Later studies have shown that different protein components of the AP-1 family are expressed in different layers, for example the junB, junD and c-FOS are found in the granular layer, while Fra-1 and Fra-2 are found in basal cells. The expression of C/EBP, AP-1, STAT and NF-B have also been shown to regulate the expression of both basal (K5 and K14) and suprabasal (K6a and K17) epidermal keratin genes (Radoja et al, 2004).

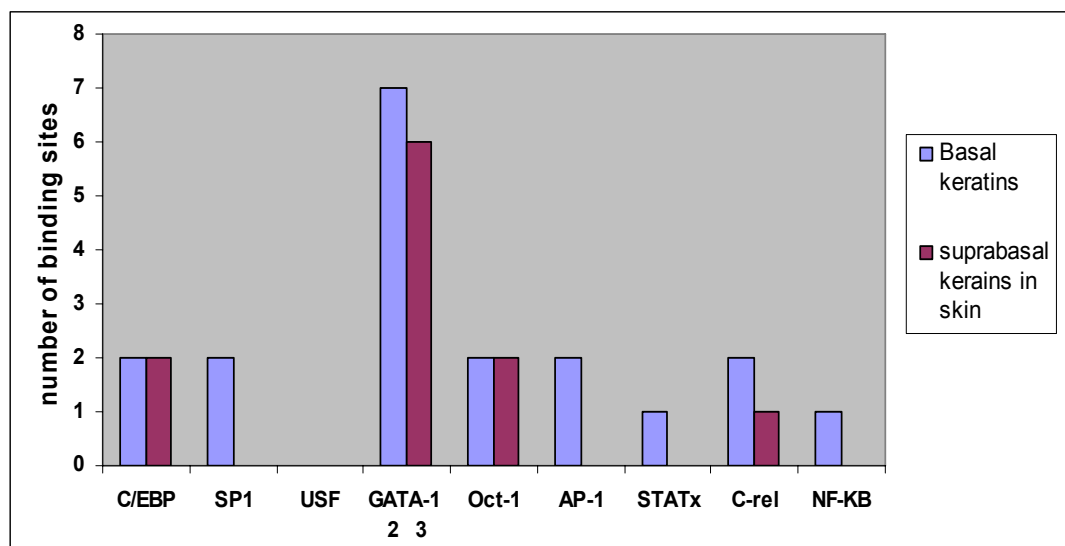


Figure 3.6: Comparison of C/EBP, Sp1, USF, GATA 1 2 3, Oct-1, AP-1, STATx, C-rel and NF-κB transcription factor binding sites in basal (K5, K14 and K15) and skin suprabasal K1 and K10 promoters.

3.5.5 Transcription Factor binding sites in Basal Keratin Promoters and Pathological Suprabasal Keratins Promoters

K6a, K16 and K17 expression is induced under conditions which are associated with hyper-proliferation and abnormal differentiation, such as viral infection, inflammation, psoriasis, after acute injury to various stratified epithelia and carcinoma (McGowan and Coulombe, 1998). The basal (K5, K14 and K15) and suprabasal keratin markers (K6a, K16, K17) have same number of binding sites for C/EBP, Sp1, AP-1, STATx and NF-κB (Figure 5.7). However, these transcription factors, with the exception of Sp1, have been reported to regulate epidermal K5, K6a, K14 and K17, which indicates the importance of C/EBP, AP-1, STATx and NF-κB in the regulation of both basal and suprabasal keratin promoters (Tomic-Canic et al, 1998).

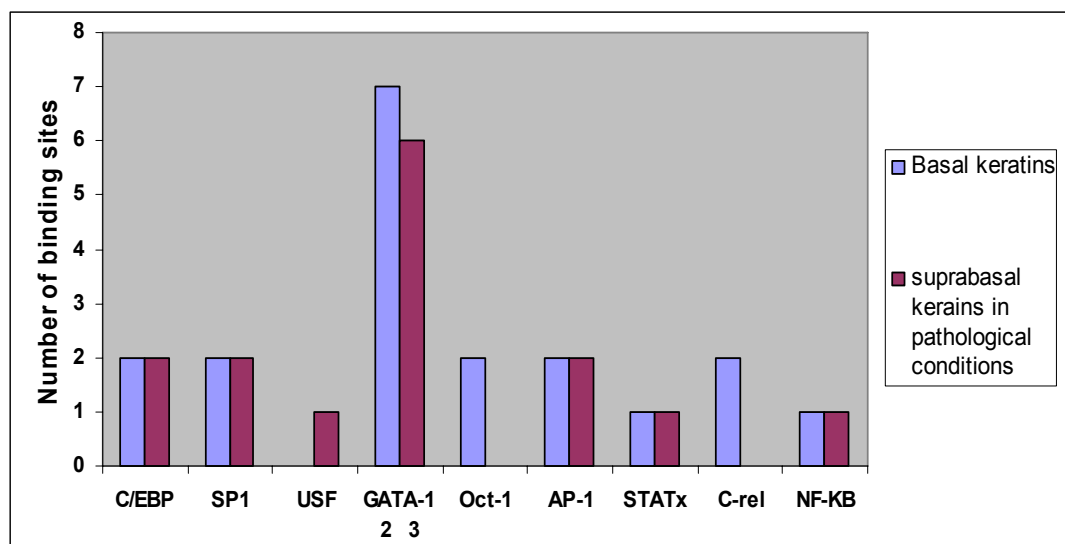


Figure 3.7: Comparison of number of C/EBP, Sp1, USF, GATA 1 2 3, Oct-1, AP-1, STATx, C-rel and NF-κB transcription factor binding sites in basal K5, K14 and K15 and pathological suprabasal K6a, K16 and K17 promoters.

3.5.6 Transcription Factor binding sites in Basal Keratin Promoters and Palm and Sole Suprabasal Keratin Promoters

Amongst the epidermal skin, only glabrous skin of the foreskin, sole and palm are unique in their structure (Compton, et al. 1998). They can be defined histologically as very thick, with a compact defined stratum corneum, a wide granulosum, long deep rete ridges and a stratum lucidum, where terminal differentiation occurs with formation of a cornified envelope (Compton, et al. 1998). Out of the selected K1, K6a, K9 and K16 promoters for palm and sole group, K9 is the only gene specifically expressed in palm and sole epidermis. Therefore although there are more C/EBP, USF, GATA -1,2,3, Oct-1 transcription factors binding sites of palm and sole suprabasal K1, K6a, K16, K1 K9 promoters in comparison to basal K5, K14 and K15 promoters (Figure 3.8), this is not an indication that these factors confer suprabasal palm and sole keratin specific expression.

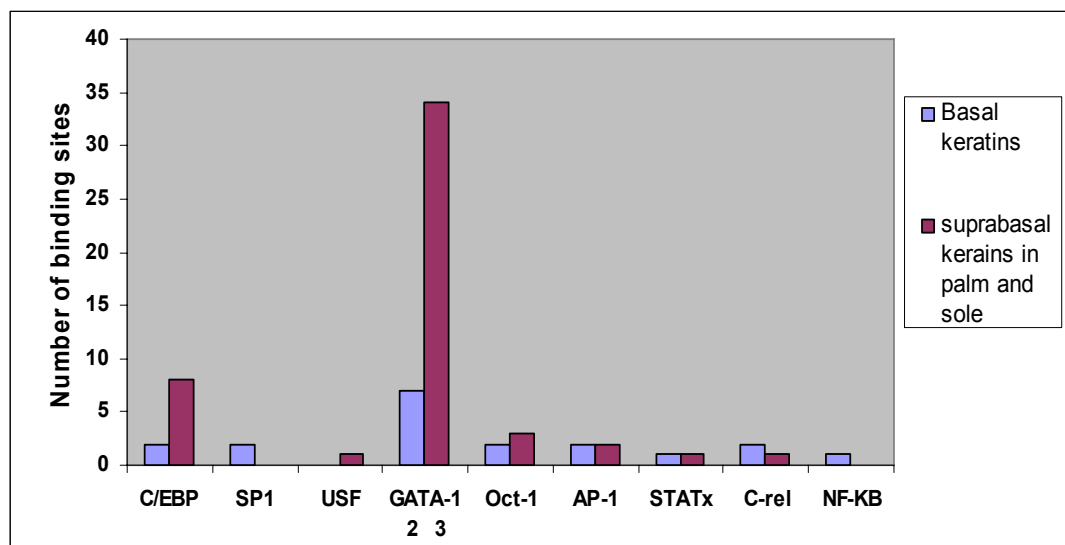


Figure 3.8: Comparison of C/EBP, Sp1, USF, GATA 1 2 3, Oct-1, AP-1, STATx, C-rel and NF-κB transcription factor binding sites in palm and sole basal K5, K14 and K15 and suprabasal K6a, K16, K9 and K1 promoters.

3.5.7 Transcription Factor binding sites in Basal Keratin Promoters and Oral Mucosa Suprabasal Keratins Promoters

There are more USF, GATA -1,2,3, STATx and NF-κB transcription factors binding sites in the oral mucosa suprabasal K76, K4 and K13 promoters (Figure 3.9) in comparison to basal K5, K14 and K15 promoters.

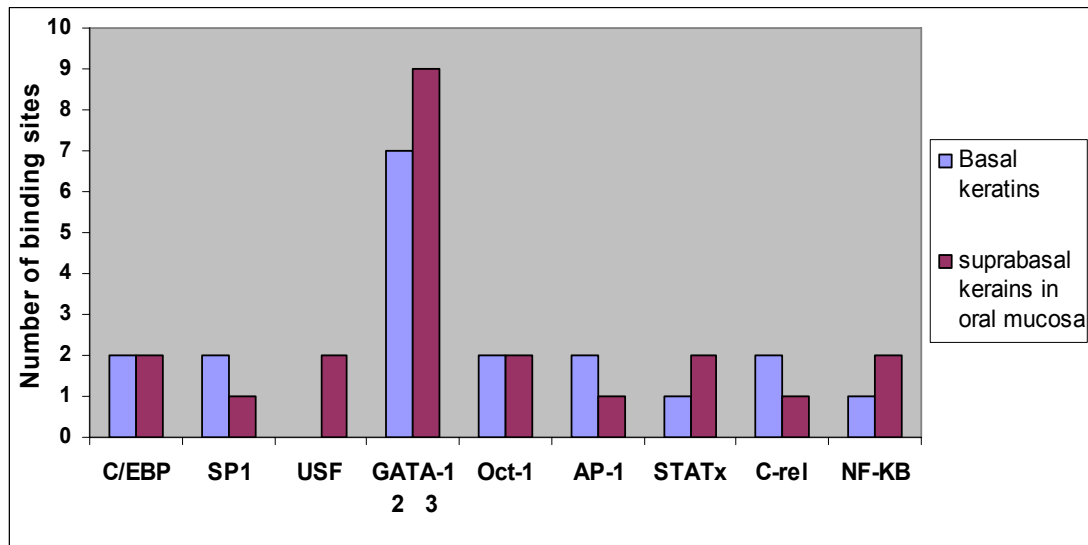


Figure 3.9: Comparison of C/EBP, Sp1, USF, GATA 1 2 3, Oct-1, AP-1, STATx, C-rel and NF-κB transcription factor binding sites in basal K5, K14 and K15 and oral mucosa suprabasal K76, K4 and K13 promoters.

3.5.8 Transcription Factor binding sites of Basal Keratin Promoters versus Cornea Suprabasal Keratins Promoters

There are more C/EBP, SP-1, GATA -1,2,3, AP-1 and C-rel binding sites in basal (K5, K14 and K15) than corneal suprabasal K3 and K12 promoters. While, Oct-1, STATx and NF-κB transcription factors have the same number of binding sites in both basal and cornea suprabasal K3 and K13 promoters (Figure 3.10). Both Sp1 and AP-2 family members have been shown to play an important role in regulation of basal keratin markers in general and specifically K14 (Waseem et al, 1998 and Ohkura et al, 2005).

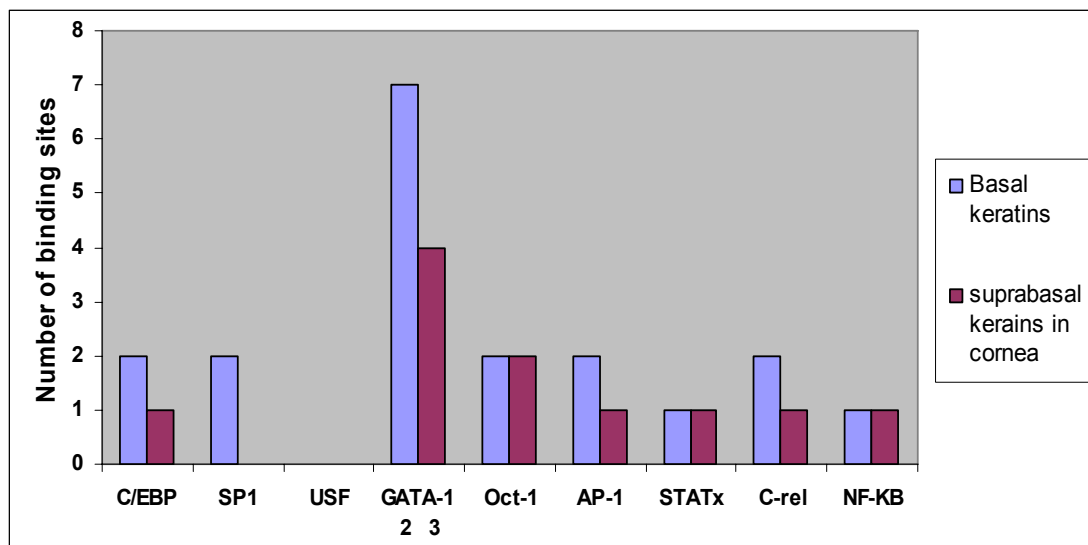


Figure 3.10: Comparison of C/EBP, Sp1, USF, GATA 1 2 3, Oct-1, AP-1, STATx, C-rel and NF-κB transcription factor binding sites in cornea basal K5, K14, K15 and suprabasal K3 and K12 promoters.

3.5.9 Transcription Factor binding site of Basal Keratin Promoters versus Simple epithelia Suprabasal Keratin Promoters

As simple epithelia do not express basal K5, K14, K15 keratin promoters, unlike stratified epithelia, thus these keratins were not included for the purpose of comparison to simple epithelia derived K7, K17, K8, K18, K19, K20 promoters. There are more C/EBP, Sp1, GATA-1,2,3, Oct-1 and AP-1 transcription factor binding sites than USF, STATx, C-rel and NF-κB in simple epithelia suprabasal K7, K17, K8, K18, K19 and K20 promoters (Figure 3.11).

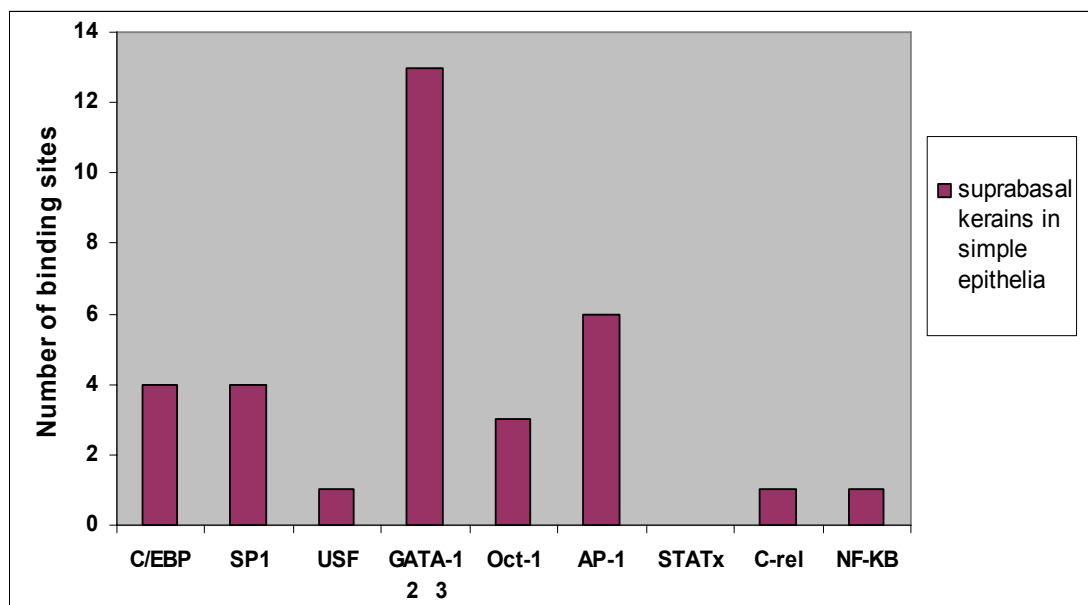


Figure 3.11: The number of C/EBP, Sp1, USF, GATA 1 2 3, Oct-1, AP-1, STATx, C-rel and NF-κB transcription factor binding sites in simple epithelia suprabasal K7, K17, K8, K18, K19 and K20 promoters.

3.5.10 Comparison of Transcription Factor binding sites of Basal and Suprabasal Keratin Promoters.

A summary of analysis from the database of a transcription factor search in both basal and suprabasal keratin promoters (Table 3.9 and Figure 3.12) has shown that in basal keratin promoters there are Sp1 and C-rel transcription binding sites, while in suprabasal keratin promoters there are more CEBP, USF, GATA-1,2,3, Oct-1 and AP-1 transcription factor binding sites (Figure 5.13).

Table 3.9: The comparison of the number of transcription factor binding sites in basal keratin versus suprabasal layers of skin, pathological conditions, palm and sole, oral mucosa, simple epithelia and cornea.

Basal keratin gene promoters							Suprabasal keratin gene promoters						
Name of Transcription element	S	PC	PS	OM	C	Total	S	PC	PS	OM	SE	C	Total
C/EBP	2	2	2	2	2	<u>10</u>	2	1	2	8	2	4	<u>19</u>
Sp1	2	2	2	2	2	<u>10</u>	0	0	1	0	2	4	<u>7</u>
USF	0	0	0	0	0	<u>0</u>	0	0	2	1	1	1	<u>5</u>
GATA-1,2,3	7	7	7	7	7	<u>35</u>	6	4	9	34	6	13	<u>72</u>
Oct-1	2	2	2	2	2	<u>10</u>	2	2	2	3	0	3	<u>12</u>
AP-1	2	2	2	2	2	<u>10</u>	0	1	1	2	2	6	<u>12</u>
STATx	1	1	1	1	1	<u>5</u>	0	1	2	1	1	0	<u>5</u>
c-rel	2	2	2	2	2	<u>10</u>	1	1	1	1	0	1	<u>5</u>
NF-κB	1	1	1	1	1	<u>5</u>	0	1	2	0	1	1	<u>5</u>

S=skin, PC=pathological condition, PS=palm and sole, OM=oral mucosa, SE=simple epithelia C=cornea.

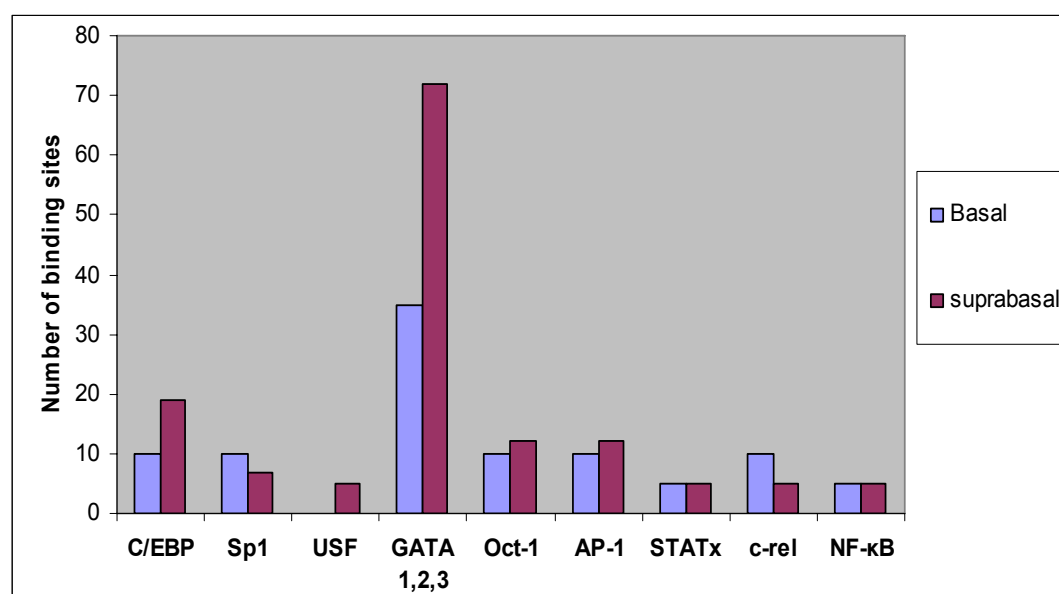


Figure 3.12: Comparison of C/EBP, Sp1, USF, GATA 1 2 3, Oct-1, AP-1, STATx, C-rel and NF-κB transcription factor binding sites in basal K5, K14 and K15 and suprabasal keratin promoters of skin, pathological conditions, palm and sole, oral mucosa, simple epithelia and cornea.

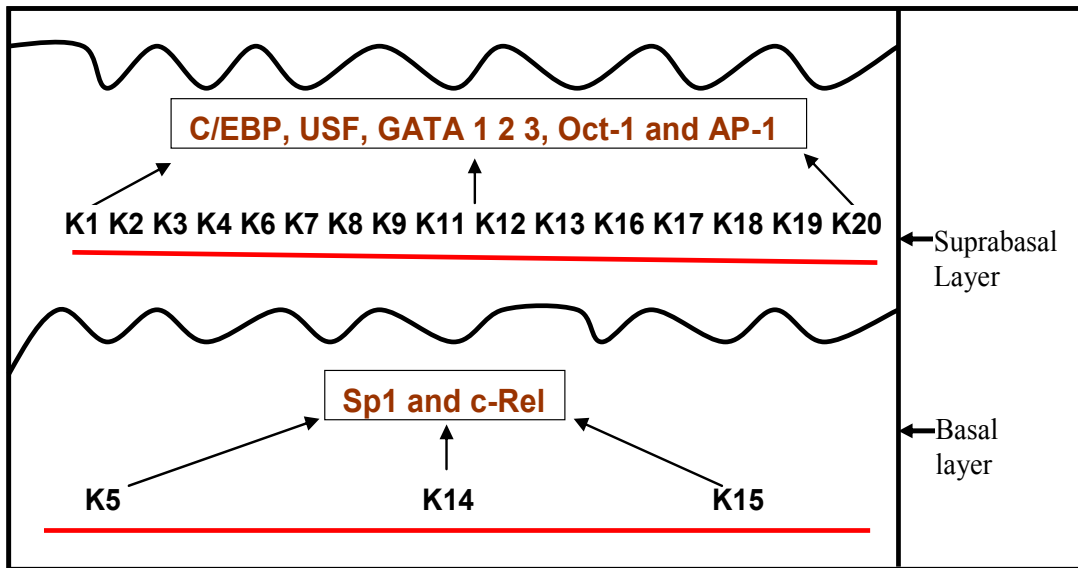


Figure 3.13: Diagram showing a summary of common transcription factor binding sites in basal (Sp1 and C-rel) and those transcription factors which have more binding sites in suprabasal (C/EBP, GATA-1,2,3 and USF) keratin promoters.

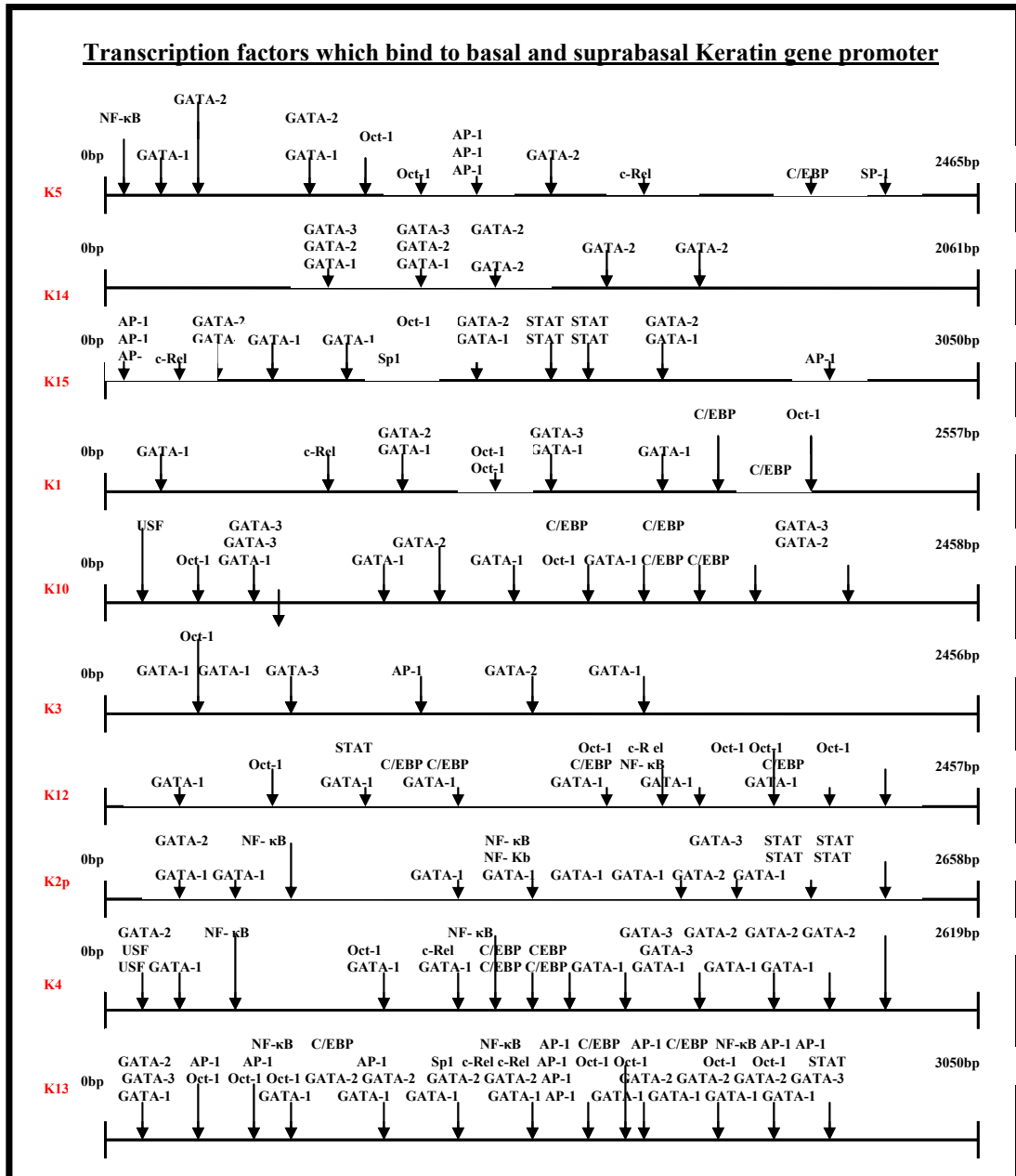


Figure 3.14: Computer analysis of transcription factors which bind to basal (K5, K14 and K15) and suprabasal (K1, K10, K3, K12, K76, K4 and K13) keratin promoter sequences.

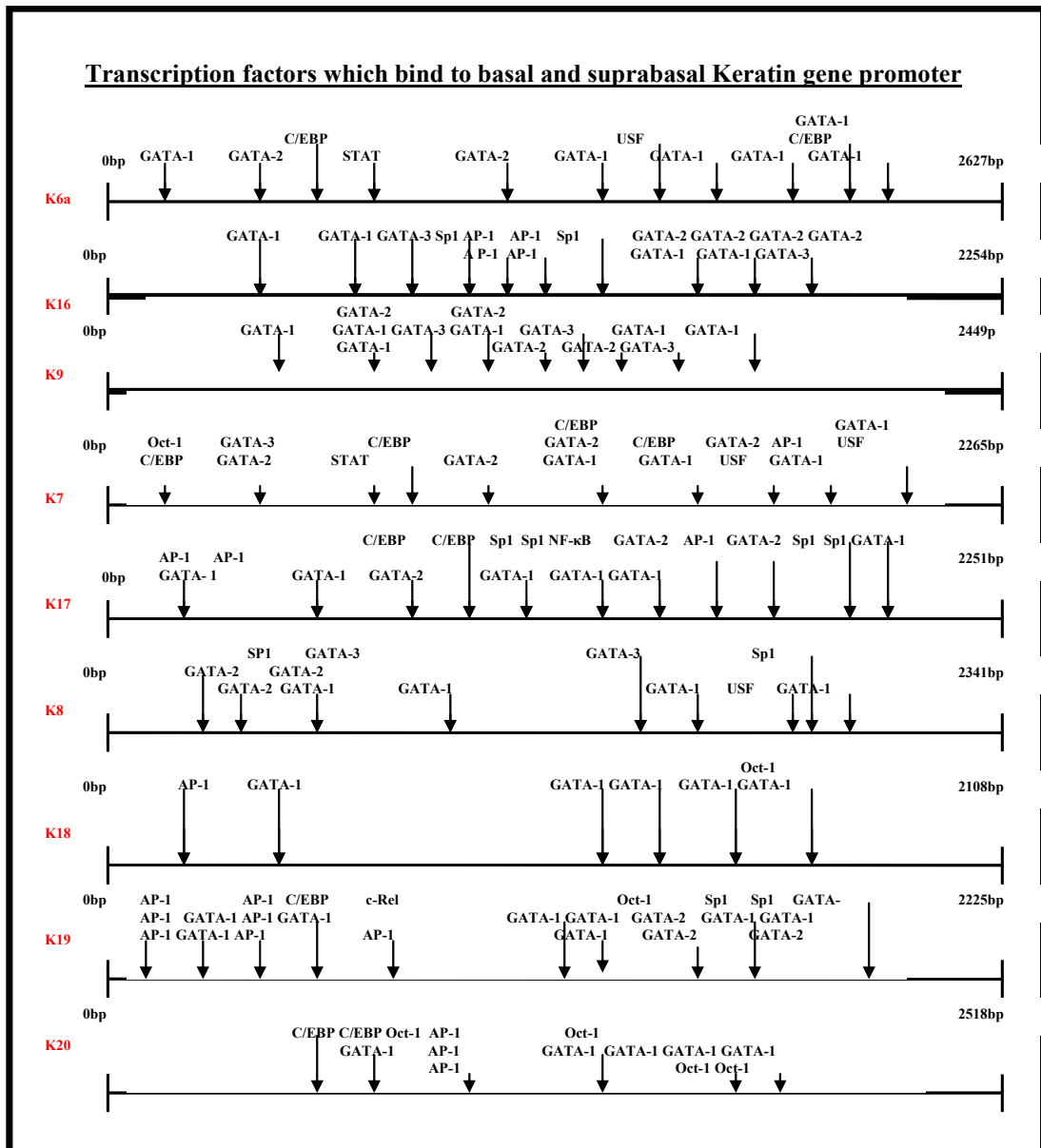


Figure 3.15: Computer analysis of transcription factors which bind to suprabasal (K6a, K16, K9, K7, K17, K8, K18, K19 and K20) keratin promoter sequences.

3.6 Discussion

The aim of this chapter was to compare the transcription factors which bind basal and suprabasal keratin gene promoters, in an attempt to distinguish the pattern of transcription factors which regulates them. Analysis of the database search for transcription factors in both basal and suprabasal keratin promoters (Table 4.9 and Figure 3.12) has shown that in basal keratin promoters there are Sp1 and C-rel, while in suprabasal keratin promoters there are more CEBP, GATA-1,2,3 and USF transcription factor binding sites. It is interesting to note that Sp1 is a common transcription factor that is reported to regulate basal keratin expression and the transcription factor database has identified more Sp1 binding sites in basal keratin gene promoters. Furthermore, Sp1 transcription factor has a binding site in some of the suprabasal differentiation markers such as those keratins which are expressed in the oral mucosa (K76, K4 and K13), in those keratins (K6a, K16, K17) which are expressed under pathological conditions such as psoriasis and also in simple epithelia keratin markers (K7, K17, K8 and K18). Despite the fact that the Sp1 transcription factor appears to confer differentiation specific expression and therefore should have more binding sites in suprabasal keratin gene promoters rather than in basal keratin gene promoters (Tomic-Canic et al, 1998), this study did not support this notion.

USF, GATA-1,2,3 and C/EBP transcription factors have more binding sites in suprabasal keratin promoters. C/EBP (Caat box enhanced binding protein) is a tissue specific transcription factor which is also expressed in the lung. The C/EBP transcription factor contains a binding site in almost all suprabasal keratin promoters of the skin, cornea, oral mucosa, pathological conditions and simple epithelial tissues apart from the suprabasal keratin gene promoters of palm and sole epidermis. C/EBP transcription factors normally interact with AP-1 and NF- κ B and as result of this interaction C/EBP transcription is able to regulate the expression of wide variety of genes in many cell types. This would explain the presence of C/EBP transcription factor binding site along with AP-1 and NF- κ B in most suprabasal keratin gene promoters (Tomic-Canic et al, 1998). The GATA family of proteins consists of a small, but enlarging, family of transcription factors with individual members represented in humans, mice, chicken, *Drosophila melanogaster* and fungi. GATA-1, the founding member of the family, was initially identified as an erythrocyte specific DNA-binding activity with presumptive target sites in the promoters or enhancers of

humans and chicken globin genes (Merika and Orkin, 1993). The GATA-1 transcription factor is essential for cell maturation and differentiation of red blood cells and its function depends upon its ability to bind to both DNA and protein partners. Disruption of either of these functions causes severe hematopoietic dysfunction and results in blood disorders such as anaemia (Lowry and Mackay 2006). Since the GATA-1 transcription factor is essential for cell maturation and differentiation of red blood cells, it could be possible that GATA-1 is involved in the maturation and differentiation of suprabasal keratinocytes and hence GATA-1 transcription factor having more binding sites in suprabasal keratin promoters.

It is well known that the regulation of keratin genes is not by a single transcription factor but rather several transcription factors which act together to bring about basal and suprabasal differentiation specific expression of keratin genes. However, it is unknown to date what initiates the up or down regulation of certain keratin genes. Although similar studies have been performed previously (Dale et al, 1990; Eckert et al, 1997; Tomic-Canic et al, 1998), in the present study we provide novel information derived from comparison of the transcription factors which regulate basal versus suprabasal keratin gene promoters. Therefore, our findings contribute to a better understanding of how basal and suprabasal cell specific keratin gene promoter expression are controlled by transcription factors in different environments (Casatorres et al, 1994).

In conclusion, although the approach of using transcription factor database is not fully accurate, given that it is a prediction database, it does act as a guide to assist experimental methods to identify putative binding sites in uncharacterized biological sequences. In addition, the use of a transcription factor database eliminates the labour intensiveness and high cost of the experimental approach, and for this reason an *in silico* (which means preformed on computer), approach for searching putative transcription binding sites was used.

Chapter 4

K13 Promoter Isolation

and Tissue Specific

Expression

4.1 Introduction

Developmental and tissue specific gene expression are usually conferred by enhancer or silencer DNA sequences (Strachan and Read, 2004). In addition, there are also other cis-acting sequences such as insulators and promoter; which are recognised by tissue specific transcription factors (Strachan and Read, 2004). Tissue specific silencer elements confer developmental site-specific expression of a gene by blocking the specific expression of the gene in all but the required tissue (Strachan and Read, 2004).

Keratin gene expression shows tissue and developmental-specific differentiation patterns (Lu et al, 2000). This is exemplified by K19, which has a unique expression pattern with expression in simple epithelia, basal cells of non-keratinized stratified squamous epithelia and in epidermal cells of embryos, but not in adult epidermis (Lu et al, 2000). In an attempt to understand the temporal and spatial sequential specific expression of K19 in cultured epidermal keratinocytes, two stage human keratinocyte culture was used (Lu et al, 2000). In addition, immunoblot and immunohistochemistry were used to quantify K19 expression and the results have shown that K19 is not expressed in cultured epidermal keratinocytes grown in basal (proliferation) media with supplements but was later expressed after three days, when the culture medium was changed to the differentiation medium basal DMEM with 10% foetal calf serum (Lu et al, 2000). However, when the epidermal keratinocytes were cultured in inserted culture dishes, K19 was expressed in all keratinocyte layers fed by medium in both the inner and the outer chamber. Taken together these results indicate that there are differences in the down-regulated expression pattern of K19 in the two culture system used and these differences might be related to signal transduction mechanisms induced by calcium and other factors in the medium (Lu et al, 2000).

It was reported that a 12kb DNA fragment of the human K8 locus containing 1.1kb of the 5'-flanking sequence, 7.7kb of the corresponding body of the gene and 3.2kb of the 3'-flanking sequence was required for the tissue specific and efficient expression of the human simple epithelial K8 gene in transgenic mice (Casanova et al, 1995). The expression pattern of the K8 transgene in simple epithelial cell types of the trachea, lung, liver and the kidney of the mice was identical to the expression

of the endogenous human K8 gene (Casanova et al, 1995). However, when the intron and exon sequence in the 7.7kb of the corresponding body of the K8 gene was replaced with *Escherichia Coli lacZ* gene, the resulting construct showed negligible expression in transgenic mice (Casanova et al, 1995). This result show the importance of intragenic sequences for conferring tissue specific expression of the K8 gene (Casanova et al, 1995).

Immunoblotting and immunofluorecence of tissue section have been used to investigate differentiation-dependent expression of the keratins in human oral epithelia in comparison to epidermis (Clausen et al, 1986). The results have shown that keratin expression patterns in the hard palate and epidermis, which are both examples of keratinized stratified epithelia, are similar since both express K10 and K1 (Clausen et al, 1986). This differs from the expression pattern of non-keratinized stratified buccal epithelia which expresses K13 and K4 (Clausen et al, 1986). The aim of this work is to understand the mechanism that regulates such differentiation-related specific expression with focus on K13 which is expressed in non-keratinized stratified buccal epithelia but not in keratinized stratified epidermal epithelia. Very little is known about the pathways that are important for the expression of K13 in oral mucosa. Thus, to provide insight into the pathways that govern K13 expression in general, as well as mucosal tissue specific expression, the 5'-upstream region of the *KRT13* gene was linked to a GFP reporter gene.

4.2 Aims

- 1) To isolate the 5'-upstream sequences of the human K13 gene in order to determine whether then it could confer oral mucosal tissue specific expression. This was done by transiently transfecting the K13 full length (FL) promoter construct into epithelial and non-epithelial cell lines.
- 2) To establish which regions of the K13 promoter are important for oral mucosal expression using deletion constructs.
- 3) To identify the DNA-protein interactions important for the K13 gene promoter using a transcription factor database (bioinformatics).
- 4) To investigate the influence of modulating individual transcription factor activities by pharmacological agents such as TPA and 4- α PMA, MEK 1/ 2 and PI3K/Akt inhibitor.
- 5) To investigate whether chromatin alteration, by use of a histone deacetylase inhibitor on non-permissive HeLa cells, can induce K13 expression.

4.3 Materials and Methods

As outlined in Chapter 2 section 2.2, the 3.018kb K13 promoter was isolated from genomic DNA and amplified using PCR (Chapter 2 Figure 2.6 A-C). This K13 PCR product was cloned into a pCR2.1-TOPO vector and then sub-cloned into a pEGFP-N3B expression vector (Chapter 2 Figure 2.6 D-G and Figure 4.1). The K13 FL promoter linked EGFP reporter gene expression in various epithelial and non-epithelial cell lines was investigated. The strength of the K13 FL promoter linked GFP expression was determined by measuring GFP median fluorescence intensity (MFI) using FACS (Chapter 2 section 2.10.1 and Figure 2.1). The MFI of the K13 FL promoter linked EGFP reporter gene was measured for each cell line to indicate whether K13 FL promoter was able to confer mucosal tissue-specific expression. The pathways that are important for the expression of K13 were also investigated using the K13 FL promoter construct. This was achieved by using various pharmacological inhibitors known to be important for the regulation of other keratin gene expression patterns (Chapter 2 section 2.11). The expression of K13 linked GFP reporter gene was assayed in the presence or absence of pharmacological agents using Western blot and FACS (Chapter 2 Figure 2.1).

4.4 Results

4.4.1 Restriction Analysis of K13 and K15 Full Length (FL) Promoter Constructs in pEGFP-N3B Vector

The K13 and K15 promoter reporter genes were constructed and verified in order to ascertain that they contained the correct K13 and K15 promoter sequences. The K13 and K15 promoter sequences were both approximately 3.018kb long. The pEGFP-N3B vector containing K13 or K15 promoters was subjected to endonuclease restriction digestion at certain sites contained either within the promoter or vector DNA sequence. Figure 4.2 shows endonuclease digestion of both K13 and K15 assembled promoter constructs. The K13 or K15 promoter was digested with BstZ17I/KpnI or BstZ17I/EcoRI respectively to release the 3.018kb FL inserts (Figure 4.2 lane 3 and Figure 4.3) within a 4117bp vector. Then the pEGFP-N3B vector containing the K13 or K15 promoter was digested with BstZ17I and NotI (Figure 4.2) enzymes to release a 4416bp (3018bp insert plus 1398bp vector) fragment of K13 or K15 insert plus vector (Figure 4.2 lane 4). The pEGFP-N3B vector containing the K13 or K15 promoter (7135bp) was then double digested with FspI, which is present within the pEGFP-N3B vector (Figure 4.2). Once the pEGFP-N3B constructs were digested with FspI enzyme, a fragment of 4416bp (BstZ17I and NotI sites in insert and vector) was released. In addition, a 1458bp (NotI and FspI sites in vector) fragment and a final vector fragment of 1261bp (vector=4117-FspI site of 2856=1261bp vector DNA) were released for K13 and K15 FL promoter DNA sequence. Moreover, once the K13 FL promoter in pEGFP-N3B vector (Figure 4.2) and K13 promoter deletion constructs were confirmed to contain the correct size fragments (Figures 4.4 to 4.6), the assembled constructs were sequenced (Figure 4.8) and subsequently used for transfecting different cell lines.

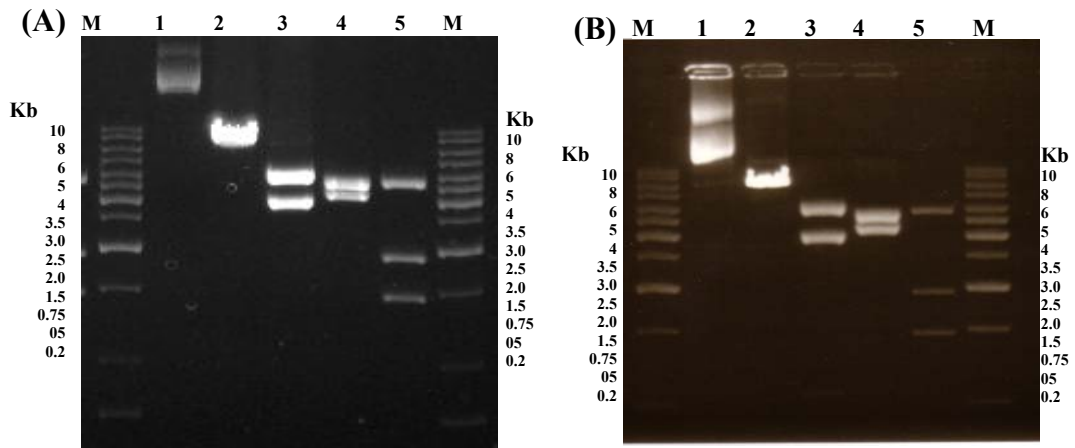


Figure 4.2: Restriction analysis of 7.135kb Keratin 13 (A) and 15 (B) promoter in pEGFP-N3B vector construct. Various enzyme digests of maxipreparation of K13 (A) and K15 (B) promoter in pEGFP-N3B vector. M=1Kb DNA ladder, 1=K13 or K15 uncut plasmid, 2= cut with BstZ17I to linearise, 3 = cut with BstZ17I and KpnI to release 3.018kb K13 promoter fragment and K15 cut with BstZ17I and EcoRI to release 3.018kb promoter fragment. 4= K13 promoter construct cut with BstZ17I and NotI and K15 promoter construct cut with BstZ17I and NotI 5= and then both K13 and K15 promoter constructs double digested with FspI. Markers (M), 1 Kb DNA ladder was run on both edges of the gel. The 1.2% agarose gel was run for one hour and half at 80 volts and stained with Ethidium bromide.

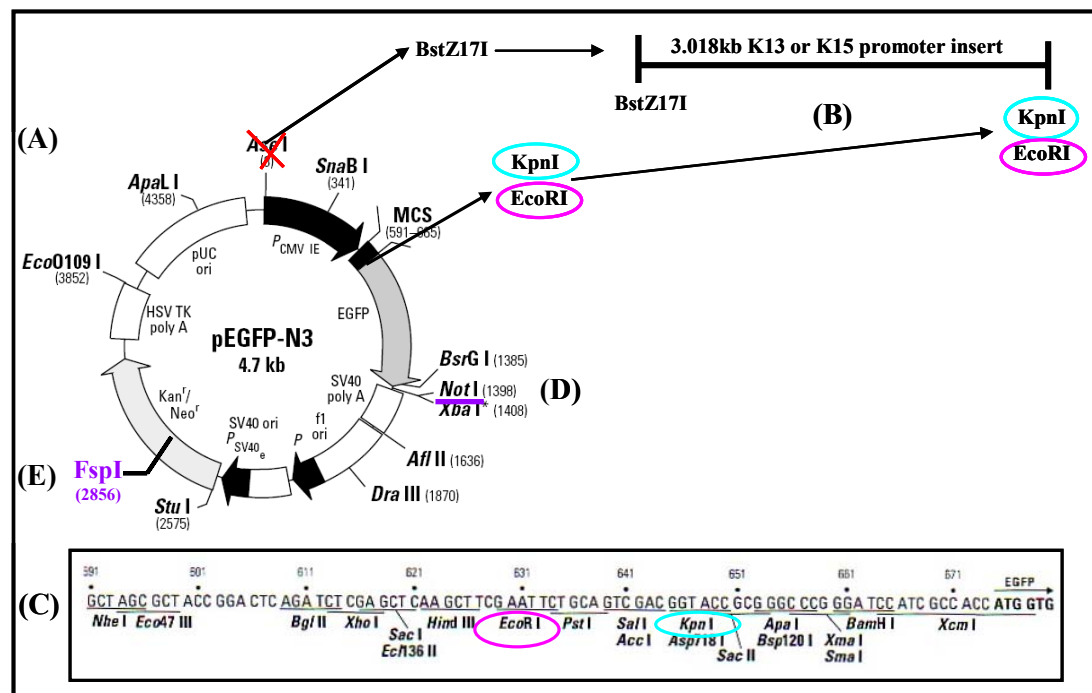


Figure 4.3: Restriction map of pEGFP-N3B vector. A: shows replacement of *AseI* restriction site with *BstZ17I* site. B: shows the 3.018kb K13 or K15 promoter insert with appropriate restriction enzymes on either side of the insert in pEGFP-N3B vector. C: shows sequence and position of various restriction enzymes within the multiple cloning sites and the *EcoRI* (pink) and *KpnI* (turquoise) are highlighted. D: shows the *NotI* restriction enzyme site within the pEGFP-N3B vector map and E: shows the *FspI* restriction enzyme site within the pEGFP-N3B vector map.

4.4.2 Restriction Digestion Analysis of K13 Promoter Deletion Fragments

A deletion clone is a copy of the parental DNA with a deletion mutation. Mutation can be defined as a change in the DNA sequence of a gene or chromosome of an organism, which results in a novel trait not found in the parental DNA. There are three main types of mutation which can be created in a DNA sequence and these include deletion, insertion and substitution. In this study the deletion mutation strategy was utilized to generate several truncated fragment deletion mutants of the K13 FL promoter. This was done in an attempt to determine which region of the K13 promoter is important for conferring the tissue specific expression of the K13 promoter. The 3.018kb K13 FL promoter in pEGFP-N3B was truncated using PCR based site directed mutagenesis (Chapter 2 section 2.14 and Figure 2.6 H-N). Several deletion fragments were constructed using the K13 FL promoter as a template (Chapter 2 Figure 2.6 H-N). The constructs (Chapter 2 Figure 2.6 H1-N1 and 4.4) generated are referred to as K13Pro-2540bp (R1), K13Pro-1953bp (R2), K13Pro-1512bp (R3), K13Pro-1017bp (R4), K13Pro-670bp (R5) and K13Pro-289bp (R6). In Figure 4.6, the exact positions in which the BstZ17I site was introduced in the K13 FL promoter DNA sequence to generate the six R1-R6 K13 promoter deletion fragments are marked in the sequence.

Figure 4.4 shows restriction analysis of DNA from positive selected clones of K13 R1 to R6 deletion fragments and the K13 FL promoter. This restriction analysis was carried out with BstZ17I and KpnI for the K13 FL promoter insert, while for the K13 promoter deletion fragments R1 to R6 BstZ17I and KpnI sites in either end of the fragments were used. The result in Figure 4.4 show the 7135bp pEGFP-N3B K13 promoter constructs releasing various sizes of K13 promoter fragments. These fragments released from the 7135bp pEGFP-N3B K13 promoter constructs include: 479bp to yield the K13-2540bp plus 4117bp pEGFP-N3B construct, 1079bp to yield the K13-1953bp plus 4117bp pEGFP-N3B construct, 1499bp to yield the K13-1512bp plus 4117bp pEGFP-N3B construct: in addition, 2039bp to yield the K13-1017bp plus 4117bp pEGFP-N3B construct 2399bp to yield the K13-670bp and 4117bp pEGFP-N3B construct and 2759bp to yield the K13-289bp plus 4117bp pEGFP-N3B construct.

Once the K13 FL promoter was deleted and confirmed via restriction analysis, the fragments generated were then ligated (Figure 4.5) back to 4117bp pEGFP-N3B vector, such that several deletion clones were created from parental K13 FL promoter. The deletion constructs generated from K13 FL promoter insert in pEGFP-N3B construct (7135bp) were as follows: K13 R1 deletion promoter fragment 6657bp pEGFP-N3B construct, K13 R2 deletion promoter fragment 6070bp pEGFP-N3B construct, K13 R3 deletion promoter fragment 5629bp pEGFP-N3B construct, K13 R4 deletion promoter fragment 5134bp pEGFP-N3B construct, K13 R5 deletion promoter fragment 4787bp pEGFP-N3B construct, K13 R6 deletion promoter fragment 4406bp pEGFP-N3B construct. Furthermore, Figure 4.5 appears to show very little difference between these different K13 promoter fragments, although approximately 400-500bp difference exists between the K13 FL promoter, R1, R2, R3, R4, R5 and R6 K13 deletion fragments. This might be because the constructs of interest lie in the upper spectrum of the DNA ladder and using a different percentage gel or allowing the gel to over-run might have resolved the various close K13 deletion fragment sizes.

To ensure that the K13 promoter fragments have been successfully ligated to 4117bp pEGFP-N3B vector and contained the expected size of the K13 promoter fragments, the constructs were digested with BstZ171 and KpnI (Figure 4.6). This led to the release of a 3018bp K13 FL promoter from the 7135bp pEGFP-N3B vector construct using BstZ171 and KpnI. The 2540bp, 1953bp, 1512bp, 1017bp, 670bp and 289bp K13 deletion R1 to R6 fragments are released from the 7135bp pEGFP-N3B vector construct using BstZ171 and KpnI on either side of the fragment.

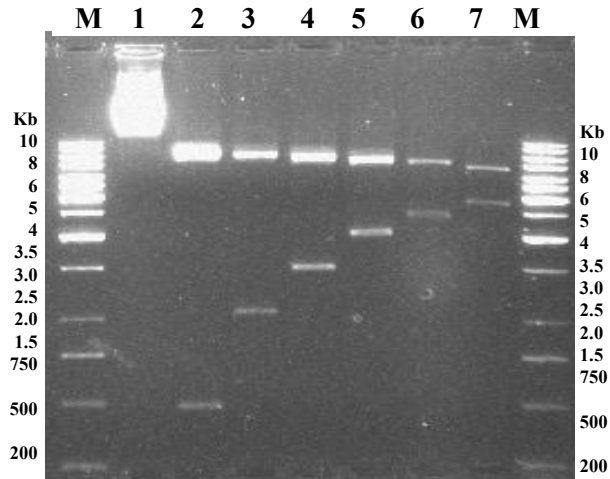


Figure 4.4: Restriction analysis of DNA from positive clones of the K13 promoter deletion series using BstZ17I and KpnI enzyme. The pEGFP-N3B vector gives a band at 7135bp and inserts of various sizes are released. Lane 1, uncut 3.018kb FL K13 promoter DNA; lane 2, 479bp; lane 3, 1079bp; lane 4, 1499bp; lane 5, 2039bp; lane 6, 2399bp and lane 7, 2759bp. Markers (M), 1 Kb DNA ladder was run on both edges of the gel . The 1.2% agarose gel was run for one hour and half at 80 volts and stained with Ethidium bromide.

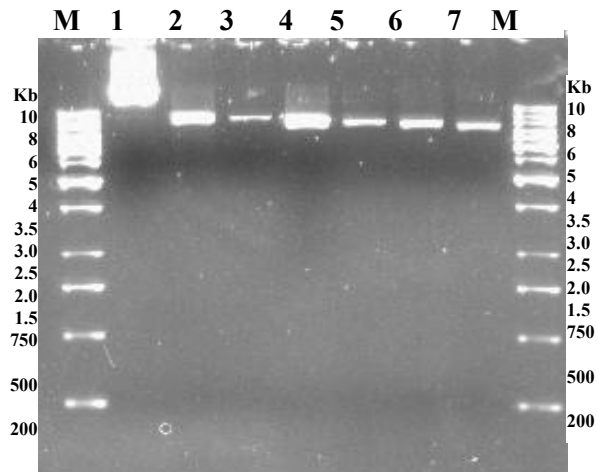


Figure 4.5: Analysis of DNA from positive clones of the K13 promoter deletion series re-ligated back to the pEGFP-N3B vector. The pEGFP-N3B vector plus various insert sizes of K13 promoter fragment religated back to the pEGFP-N3B vector constructs is shown. Lane 1 shows a religated construct consisting of the 3018bp K13 FL promoter insert plus the 4117bp pEGFP-N3B vector. Lane 2 shows construct consisting of the 2540bp K13 promoter deletion fragment R1 plus the 4117bp pEGFP-N3B vector. Lane 3 shows construct consisting of the 1953bp K13 promoter deletion fragment R2 plus the 4117bp pEGFP-N3B vector. Lane 4 shows construct consisting of the 1512bp K13 promoter deletion fragment R3 plus the 4117bp pEGFP-N3B vector. Lane 5 shows construct consisting of the 1017bp K13 promoter deletion fragment R4 plus the 4117bp pEGFP-N3B vector. Lane 6 shows construct consisting of the 670bp K13 promoter deletion fragment R5 plus the 4117bp pEGFP-N3B vector. Lane 7 shows construct consisting of the 289bp K13 promoter deletion fragment R6 plus the 4117bp pEGFP-N3B vector. Markers (M), 1 Kb DNA ladder was run on both edges of the gel. The 1.2% agarose gel was run for one hour and half at 80 volts and stained with Ethidium bromide.

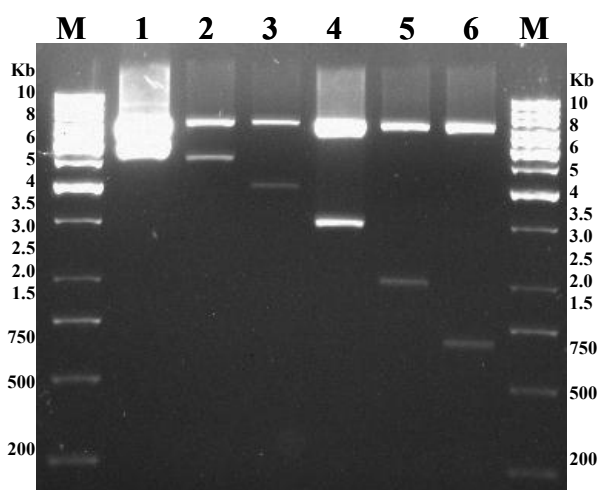


Figure 4.6: Restriction analysis of DNA from positive clones of the K13 promoter deletion series using BstZ17I and KpnI enzyme. The pEGFP-N3B vector construct gives a band at 7.135kb and inserts of various sizes are released. Lane 1, the 3.018kb FL K13 promoter DNA released from 7135bp pEGFP-N3B vector construct using BstZ17I and KpnI on either side of the fragment. Lane 2, the 2540bp K13 deletion R1 fragment is released from the 7135bp pEGFP-N3B vector construct using BstZ17I on either side of the fragment. Lane 3, the 1921bp K13 deletion R2 fragment is released from the 7117bp pEGFP-N3B vector construct. Lane 4, the 1512bp K13 deletion R3 fragment is released from the 7135bp pEGFP-N3B vector construct using BstZ17I and KpnI on either side of the fragment. Lane 5, the 1017bp K13 deletion R4 fragment is released from the 7135bp pEGFP-N3B vector construct using BstZ17I and KpnI on either side of the fragment. Lane 6, the 670bp K13 deletion R5 fragment is released from the 7135bp pEGFP-N3B vector construct using BstZ17I and KpnI on either side of the fragment. Markers (M), 1 Kb DNA ladder was run on both edges of the gel. The 1.2% agarose gel was run for one hour and half at 80 volts and stained with Ethidium bromide.

4.4.3 K13 FL Promoter DNA Sequence and Transcription Factor Database

The K13 FL upstream and downstream sequence was obtained using the NCBI database (www.pubmed.org) as shown in Figure 4.7. Entrez Pubmed NCBI database. Transcription factor search (TFSearch) database was used to identify putative transcription factor (Table 4.1) binding sites in each of the colour coded upstream K13 promoter DNA sequences (Figure 4.7). This was done in an attempt to unravel novel transcription factor binding sites in the uncharacterised K13 promoter deletion DNA sequence. A summary of transcription factors identified to bind to the K13 promoter deletion fragment DNA sequence is shown in Table 4.1. In addition in Figure 4.7 the K13 upstream coloured (turquoise to brown) sequence corresponds to K13 FL, R1, R2, R3, R4, R5 and R6 deletion fragments. Thus it should be noted that the same colours are used in the transcription identified and its corresponding

sequence (Figure 4.7 and Table 4.1) in which it was identified. This was done to show that each set of transcription factors was identified to bind each of the truncated K13 promoter fragments DNA sequence (Table 4.1 and Figure 4.2). Furthermore, each deletion fragment of the K13 FL promoter DNA sequence was analysed individually using the TFSearch database. When searching for transcription factor binding sites, 90% stringency at the sequence level was selected: this was done in an attempt to eliminate false positive transcription factor binding sites in the DNA sequence. Also in Figure 4.7, the three red nucleotides highlighted in the sequence correspond to the ATG and the yellow highlighted sequence corresponds to the start of the coding region (exon 1), while the light blue highlighted sequence corresponds to the K13 intron 1 sequence (Figure 4.7).



Figure 4.7: (A) Diagrammatic representation of K13 gene (with 3kb promoter, 8 exons and 7 introns). (B) illustrates the K13 upstream and downstream sequence from exon 1 upstream, the different coloured sequences correspond to various different length of the full length K13 promoter (-3018bp, turquoise), and the six (R1-R6) fragments generated from full length K13 promoter, R1 (-2540bp, red), R2 (-1953bp, navy blue), R3 (-1512bp, green), R4 (-1017bp, pink), R5 (-670bp, lime green) and R6 (-289bp, purple). The purple underlined 6 nucleotides sequence correspond to the site where KpnI was designed. The original K13 promoter sequence (6 nucleotides, underlined in black) does not differ much from the BstZ17I site (GTATACT), so this sequence corresponds to the site where BstZ17I primer was designed, in attempt to retain or minimise change to the BstZ17I sequence. The red 3 nucleotides sequence corresponds to the ATG and the yellow (+683-541) highlighted sequence corresponds to the start of coding region (exon 1). The light blue (+541-1861) highlighted sequence corresponds to K13 intron 1.

Table 4.1: Transcription factor binding sites in K13 FL promoter and K13 deletionR1-R6 fragments

K13 fragment name	K13 FL	K13 DFR1	K13 DFR2	K13 DFR3	K13 DFR4	K13 DFR5	K13 DFR6
Size of K13 constructs	-3018bp	-2540bp	-1953bp	-1512bp	-1017bp	-670bp	-289bp
Size of K13 fragment	466bp	587bp	443bp	493bp	345bp	381bp	374bp
Transcription Factors which bind K13 fragments	GATA-1 Oct-1 HSF 2 HSF 1 HSF 2 TATA TATA	C/EBPa NF-E2 GATA-1 RREB-1 E2F AP-1 GATA-1 AP-1 GATA-1 GATA-2	Sp1 GATA-2 GATA-1 c-Ets c-Ets AP-1 AP-1 AP-1 AP-1 AP-1 NF-E2 C/EBPa AP-1 Sp1 GATA-2 SREBP- GATA-2 GATA-2 GATA-2	Oct-1 Oct-1 AP-1 GATA-1 HSF2 GATA-X HNF-3b GATA-1 HSF2 GATA-X HNF-3b GATA-2 GATA-1	USF USF USF USF USF SREBP- c-Myc/ Max Max N-Myc CRE-BP CRE-BP CREB CREB CRE-BP GATA-1 GATA-1 GATA-1 CRE-BP	HSF2 HSF1 HSF2 HSF1 Oct-1 GATA-3 C/EBP GATA-1 AP-4 AP-1 GATA-2 GATA-1 USF USF USF GATA-1 HSF2 GATA-2	AP-1 C/EBP AP-1 STATx TATA TATA GATA-1 Evi-1 GATA-2 GATA-1 Sp1 GATA-1 GATA-2 GATA-3 GATA-1 GATA-1 GATA-1

4.4.4 Sequencing the K13 Full Length 3.018kb Promoter and Deletion Constructs (R1-R6)

To ensure no error was introduced during PCR or incorporated by the bacteria during the bacterial transformation stage of cloning the K13 promoter deletion constructs was sequenced (Chapter 2 section 2.12). Figure 4.8 shows the DNA sequencing result obtained for the K13 FL and some of the deletion constructs of K13 promoter DNA sequence put together. The K13 FL and deletion constructs of K13 promoter DNA sequence was obtained using both forward and reverse primers for K13-R1 to K13-R6 constructs. However, the K13 FL, R2 and R4 deletion constructs were not amplifiable with the reverse primers. It should be noted that the letter N, in the DNA sequencing result means that the computer was unable to recognise that specific nucleotide and thus it allocates the letter N (pink) for not recognised. The entire

sequence in Figure 4.8 was then blasted against the human genome using the NCBI database (Chapter 2 section 2.12) and the search located sequence in chromosome 17 where all type I keratin genes are found in or the K13 sequence. The taxonomy blast result (Figure 4.9) shows a 99% homology of the sequence obtained to that of K13 DNA sequence in the human genome database.

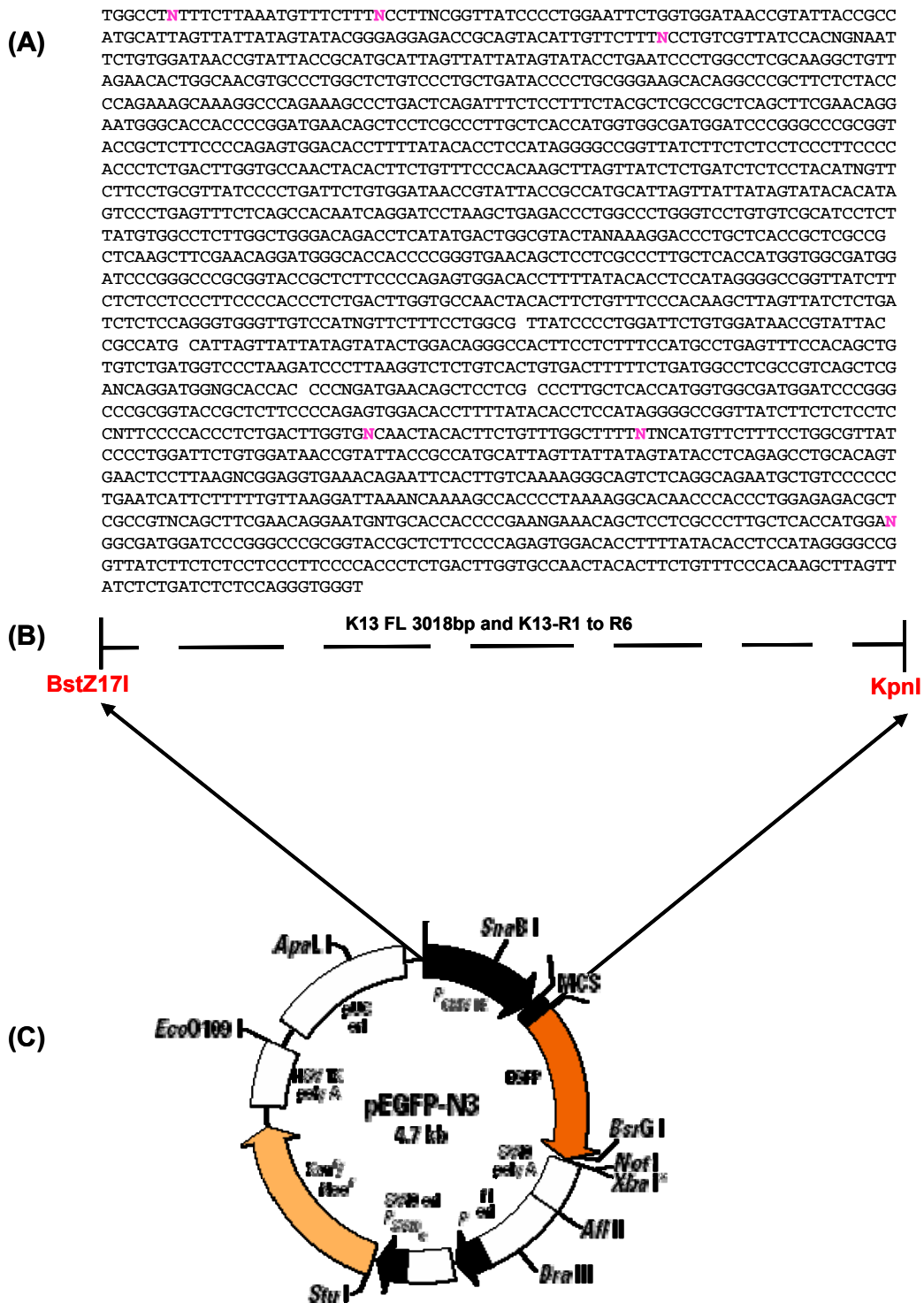


Figure 4.8: DNA sequencing Result of K13 FL and deletion fragments in pEGFP-N3B vector: (A) Shows the K13 R1 to R6 constructs of K13 promoter DNA sequence result using forward and reverse primers, the pink highlighted N means that the computer was unable to recognise that specific nucleotide and thus it allocates the letter N for not recognised. (B) Shows the insert enzyme sites (BstZ17I and KpnI) used to digest the K13 FL fragment and K13 R1 to R6 promoter constructs. (C) Shows 4.7kb pEGFP-N3B vector and the site where the K13 FL and subsequent deletion series fragments was cloned into using BstZ17I and KpnI enzymes sites by removing CMV promoter.

```

Tax BLAST Report
Features flanking this part of subject sequence:
64 bp at 5' side: keratin 13

Score = 265 bits (143), Expect = 2e-67
Identities = 145/146 (99%), Gaps = 0/146 (0%)
Strand=Plus/Plus

Query 895      GCTCTTCCCCAGAGTGGACACCTTTTATACACCTCCATAGGGGCCGTTATCTTCTCTCC
                |||
Sbjct 3386162 GCTCTTCCCCAGAGTGGACACCTTTTATACACCTCCATAGGGGCTGGTTATCTTCTCTCC

```

Figure 4.9: Taxonomy Blast result of short piece of sequence at the 3`end of the K13-R6 promoter fragment, which happens to be the reverse complement of the K13 promoter sequence.

4.4.5 GFP Expression can be used to Quantify K13 Promoter Activity using FACS

To assess whether using GFP as a reporter gene provides good quantification of CMV, K13 and K15 promoter levels, increasing concentrations of promoter plasmid DNA versus GFP expression were investigated using FACS. An initial optimization of the project was done before any subsequent experiments were carried out with the constructs. Figure 4.10 shows representative images of GFP expression using 3.2µg of CMV, K13 and K15 gene reporter constructs, as well as the internal control (DsRed) and promoterless pEGFP-N3B vector transfected into an oral SCC25 cell line. A DNA concentration of 2.5µg of CMV, K13 and K15 promoter driven GFP constructs, which falls in the linear part of the graph (Figure 4.11), was used for subsequent transient transfection experiments. These initial experiments do not quantify the CMV, K13 and K15 promoters as such, but rather demonstrate a linear relationship between the promoters used and the EGFP signal. This EGFP signal was measured using a FACS (Beckton Dickinson) with separate channels for EGFP and DsRed (Figure 4.10) with different band pass filters for different coloured fluorescent proteins. In addition, the units of GFP expression used throughout the thesis will be arbitrary units; this is because the fluorescence data is measured on a logarithmic scale and GFP units are noted as arbitrary units in previous reports which use GFP reporter gene. It should also be noted that the data presented in Figure 4.11 are the raw data for EGFP median fluorescence intensity and the data obtained for the internal controls (pDesRed-N1) were not used. This was done in an attempt to observe the EGFP median fluorescence intensity only as the aim of this particular experiment was to observe whether there is a linear relationship between EGFP signal and increasing CMV, K13 and K15 promoter plasmid DNA concentrations

(Figure 4.11). Hence the data values in Figure 4.11 are smaller than all other data presented in the thesis. The data in Figure 4.11 also shows that CMV produces the largest MFI signal in comparison to K13 and K15. The percentage of oral SCC25 cells that have taken up CMV promoter linked EGFP is about 10-20% while in the K13 and K15 promoter-linked EGFP expressions in oral SCC25 cells this was 3-10%. The EGFP expression of CMV, K13 and K15 constructs transfected cells was not counter stained with DAPI. The data in Figure 4.11 also shows that the CMV, K13 and K15 promoter levels can be quantified and this quantitation of promoter activity can be used to deduce that the GFP reporter gene assay can be used as quantitative marker of keratin promoter activity.

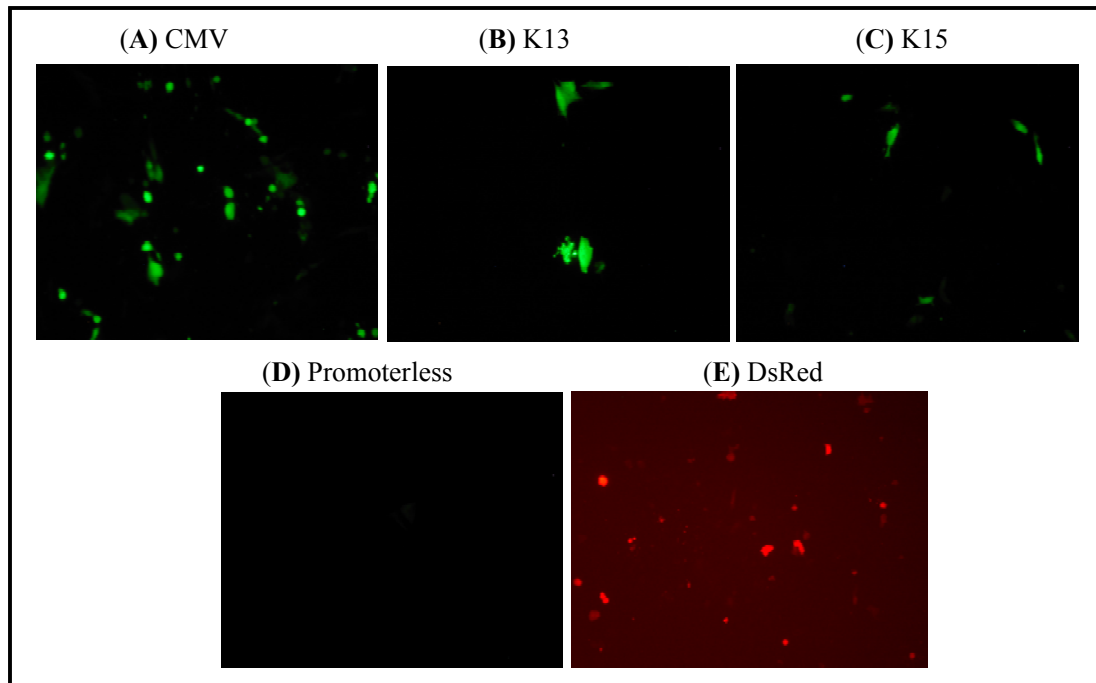


Figure 4.10: Representative images of human oral SCC25 cell line transfected with pEGFP-N3B, PL pEGFP-N3B and pDsRed-N1 vectors. A: shows oral SCC25 cells transfected with CMV promoter in pEGFP-N3B vector DNA (3.2 μ g) used as positive control. B: shows oral SCC25 cells transfected with K13 promoter in pEGFP-N3B vector DNA (3.2 μ g). C: shows oral SCC25 cells transfected with K15 promoter in pEGFP-N3B vector DNA (3.2 μ g). D: shows oral SCC25 cells transfected with promoterless (PL) pEGFP-N3B vector DNA (3.2 μ g) used as negative control. D: shows oral SCC25 cells transfected with CMV promoter in pDsRed-N1 vector DNA (3.2 μ g) used as internal control. The cell populations were photographed using a fluorescent microscope and the picture magnification is 100x.

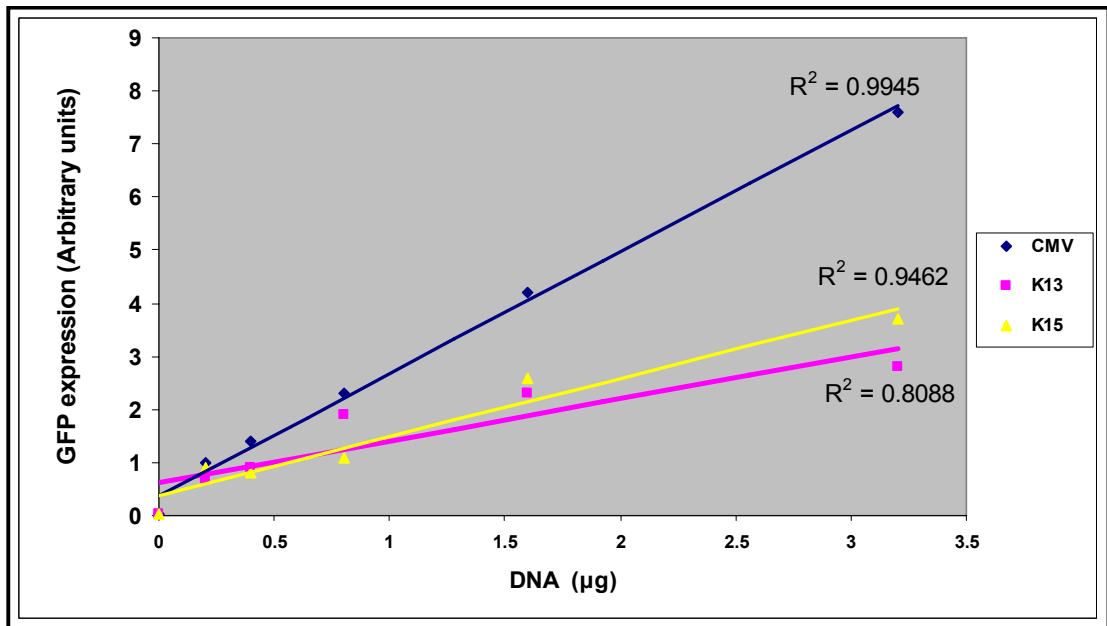


Figure 4.11: Shows the effect of varying concentration of promoter driven GFP plasmid expression in SCC25 cell line. GFP reporter gene can be used to quantify CMV and keratin promoter level since there was a linear relationship between GFP expression (arbitrary units) and increasing DNA concentration of CMV (navy blue), K13 (pink), and K15 (yellow) promoter constructs. Each point in graph represents the mean of four different experimental values for each construct.

4.4.6 Qualitative data of K13 promoter linked GFP expression shows epithelial specific expression

The K13 FL promoter-linked GFP construct was transiently transfected into various epithelial and non-epithelial cell lines (Figure 4.12 to 4.15). Comparison of K13 promoter driven GFP expression in oral SCC25, RTS3b, HeLa and HFF cell lines shows the K13 promoter signal is the strongest in HeLa, then in oral SCC25, followed by RTS3b cells, while the K13 promoter expression in HFF cells is negligible. In Figure 4.14 the co-expression of K13 promoter linked GFP and the DsRed internal control plasmid expression is shown by merging the same field view of GFP and DsRed fluorescent proteins. This type of qualitative data as shown in Figure 4.12 to 4.15 is one of the advantages that the use of GFP has over other reporter genes.

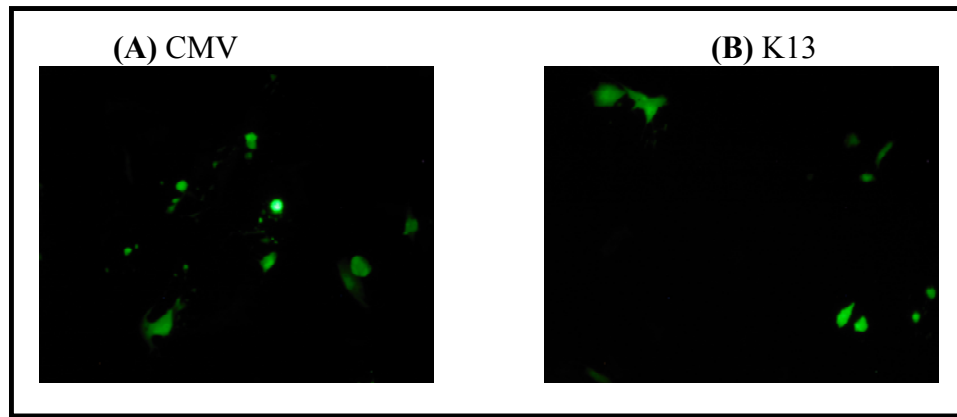


Figure 4.12: Representative images of human oral SCC25 cell line transfected with CMV or K13 promoter in pEGFP-N3B vector. A: shows oral SCC25 cells transfected with CMV promoter in pEGFP-N3B vector DNA used as a positive control. B: shows oral SCC25 cells transfected with K13 promoter in pEGFP-N3B vector DNA. The cell populations were photographed using a fluorescent microscope and the picture magnification is 100x.

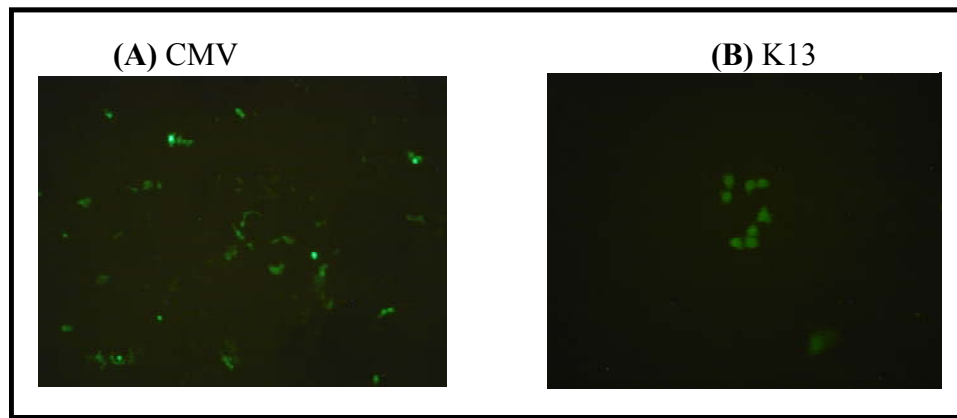


Figure 4.13: Representative images of human epidermal derived RTS3b cell line transfected with CMV or K13 promoter in pEGFP-N3B vector. A: shows RTS3b cells transfected with CMV promoter in pEGFP-N3B vector DNA used as a positive control. B: shows RTS3b cells transfected with K13 promoter in pEGFP-N3B vector DNA. The cell populations were photographed using a fluorescent microscope and the picture magnification is 100x.

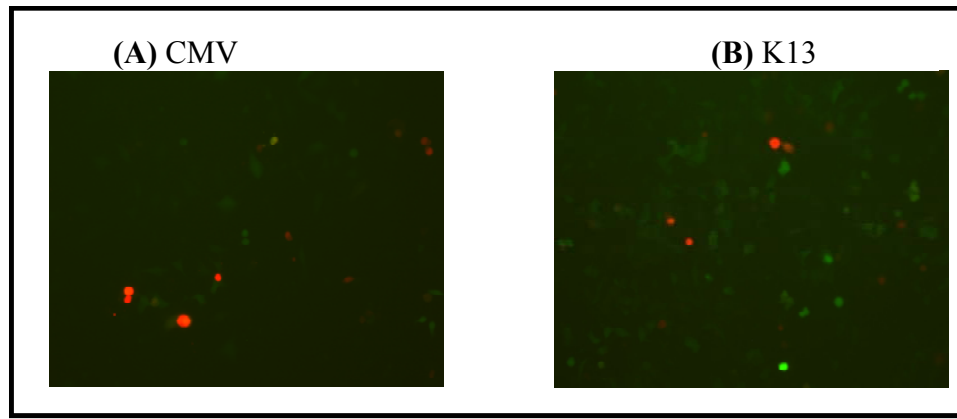


Figure 4.14: Representative image of HeLa cell line transfected with CMV or K13 promoter in pEGFP-N3B vector. A: shows HeLa cells transfected with CMV promoter in pEGFP-N3B vector DNA used as a positive control. B: shows HeLa cells transfected with K13 promoter in pEGFP-N3B vector DNA. The cell populations were photographed using a fluorescent microscope and the picture magnification is 100x.



Figure 4.15: Representative images of human foreskin fibroblast derived HFF cell line transfected with CMV or K13 promoter in pEGFP-N3B vector. A: shows HFF cells transfected with CMV promoter in pEGFP-N3B vector DNA used as a positive control. B: shows HFF cells transfected with K13 promoter in pEGFP-N3B vector DNA. The cell populations were photographed using a fluorescent microscope and the picture magnification is 100x.

4.4.7 FACS analysis of K13 Promoter linked GFP to examine Oral Mucosal Tissue Specific Expression

To examine the mucosal tissue specific expression of the K13 promoter construct, the K13 promoter construct was transiently transfected into various epithelial and non-epithelial cell lines. Although expression of the K13 promoter was highest in the oral SCC25 cell line (Figure 4.16) in comparison to RTS3b, HeLa and HFF cell lines, the increased level of expression was not significant ($P=0.354, 0.249, 0.189$). The CMV promoter-driven GFP in pEGFP-N3B vector, which was used as a positive

control transiently transfected into SCC25, RTS3b, HeLa and HFF cell lines (Figure 4.17), shows relatively similar expression levels in all cell lines tested. This result was as expected given that the CMV promoter was used as a positive control and thus should not show variation in its expression in different cell lines (Figure 4.17). The data presented in Figure 4.16 and 4.17 are in the same arbitrary units, the expression of K13 promoter in comparison to CMV promoter differs by a factor of 1000. This might be due to the fact that CMV is a very active constitutive viral promoter, which causes GFP to be expressed strongly at all times. The data in Figure 4.16 and 4.17 were not presented together because any variation of K13 expression in different cell lines could not be observed as easily if data were combined. In Figure 4.16 and 4.17 the standard deviation is high and this might be because of inconsistency in the transfection efficiency. Moreover, Table 4.2 shows the MFI of K13 promoter linked GFP expressing cells which was quantified using FACS and Figure 4.16 result is based on Table 4.2 raw data.

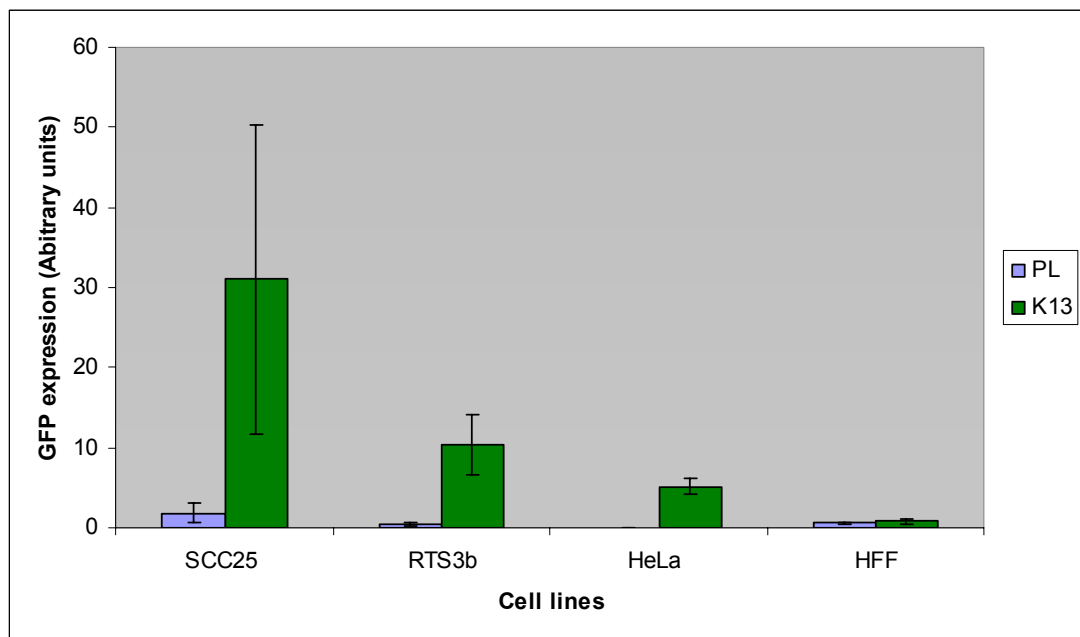


Figure 4.16: The expression of K13 promoter and promoterless (PL) pEGFP-N3B vector in epithelial and non-epithelial cell lines. PL (blue) is the promoterless pEGFP-N3B construct expression in SCC25, RTS3b, HeLa and HFF cell lines, the PL construct was used as a negative control for transfection. The figure also shows the K13 promoter driven GFP construct expression in SCC25, RTS3b, and HeLa and HFF cell lines. There was no significant difference between K13 FL promoter construct expression in oral SCC25 cells in comparison to RTS3b ($P=0.354$), and HeLa ($P=0.249$), and HFF ($P=0.189$) cell lines. The results are expressed as the mean \pm the standard deviation (SD) of three experiments.

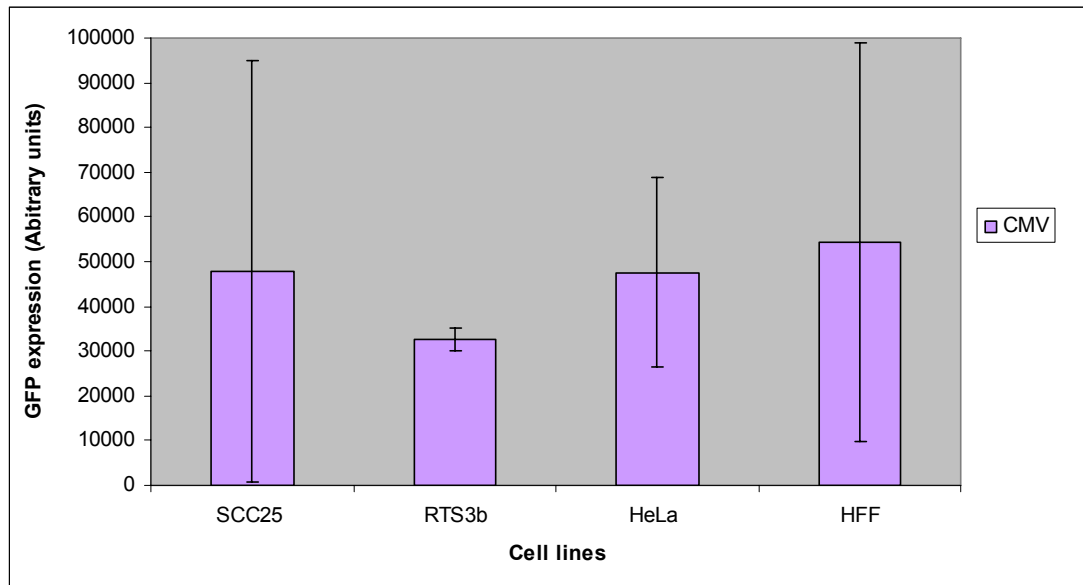


Figure 4.17: The expression of CMV promoter driven GFP expression in epithelial cell lines oral SCC25, RTS3b, HeLa and non-epithelial HFF cell line. The expression of CMV promoter expression in oral SCC25 in comparison to RTS3b, HeLa and HFF cell lines was not significant ($P=0.242, 0.122, 0.085$).

Table 4.2: The K13 promoter linked GFP expression in epithelial and non-epithelial cell lines

Cell types	Origin	Expression of K13	MFI of GFP over DsRed expressing cells
Oral mucosa SCC25 cells	Ventral tongue carcinoma	Yes	31
skin derived RTS3b cells	Epidermoid carcinoma	Yes	10
Simple epithelia derived HeLa cells	Cervical carcinoma	No	5
Human foreskin fibroblast derived HFF cells	Foreskin fibroblast	No	0.8

MFI= median fluorescence intensity

4.4.8 K13 protein shows mucosal epithelial tissue-specific expression using Western Blot

To confirm the results of the K13 FL promoter construct (Figure 4.16) showing tissue specific expression at protein level, Western blotting was used. This technique is sensitive, quantitative and specific for detecting target proteins (Figure 4.18). The disadvantages of using Western blotting include results are subject to interpretation, although the intensity of the bands can be addressed by the use of densitometry (Reference: website 19). The A431 cell line was used as a positive control for K13 protein expression, since this cell line has been shown to have very high expression of K13 protein (Waseem, et al. 1998). The expression of K13 protein is the second highest in the oral SCC25 cell line after A431 positive control cell line, and in the skin derived RTS3b cell line K13 protein expression is moderate (Figure 4.19). Although in the literature both K13 and K19 are not normally expressed in the epidermis skin, K13 protein was detected by Western blot in RTS3b cells (Figure 4.18). Western blot quantification of K13 protein band density is shown to be greatest in the oral SCC25 cell line (green) in comparison to RTS3b (purple, $P=0.340$), HeLa (pink, $P=0.003$) and HFF (black, $P=0.05$) cell lines (Figure 4.19). In summary, the western blot data for K13 showed greater protein expression in oral SCC25 cells is consistent with the K13 promoter construct expression pattern, which indicates that K13 shows epithelial cell specific expression.

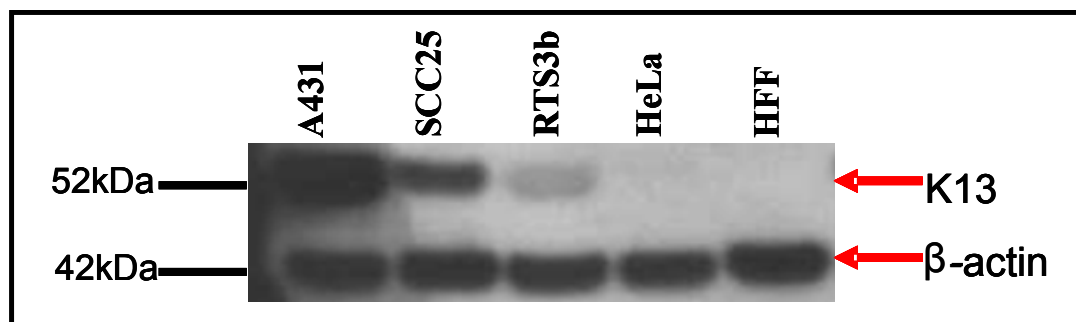


Figure 4.18: Expression of K13 protein in various epithelial and human foreskin fibroblast derived cell lines. The K13 protein is strongly expressed in A431 cell line, then in SCC25 and RTS3b cells show negligible K13 protein expression, while both HeLa and HFF cell lines show no K13 protein expression. A431, SCC25, RTS3b, HeLa and HFF cells were grown until 80% confluent and lysed in Laemmli buffer before analysing by SDS-PAGE. Proteins were transferred onto nitrocellulose and probed for K13 expression using AE8 antibody as described in Chapter 2 section 2.17.

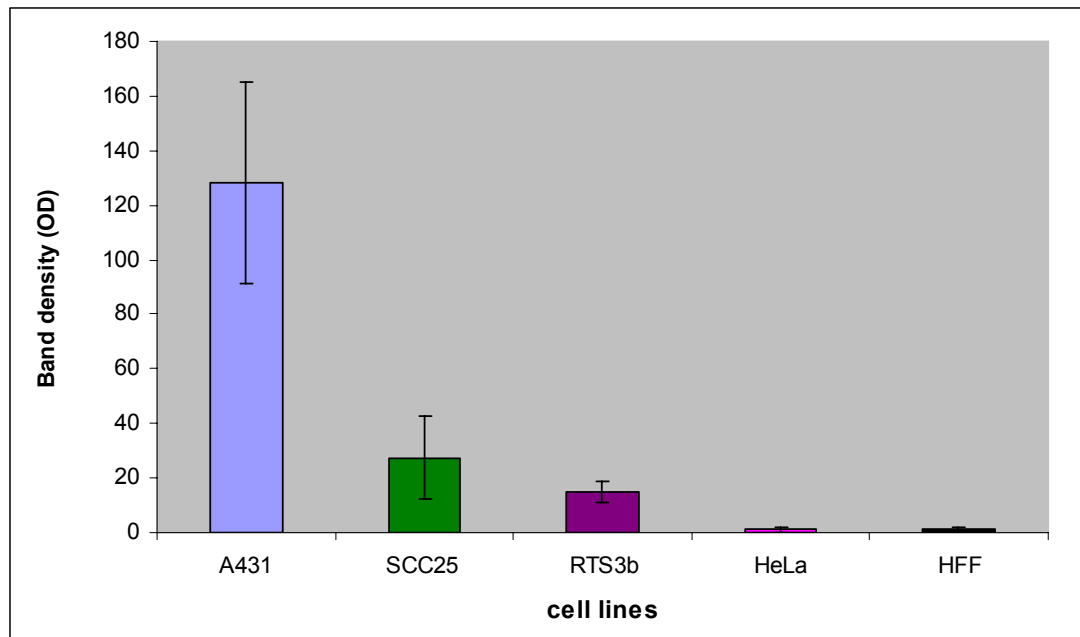


Figure 4.19: Quantification of band density derived from western blot data in Figure 4.18 using densitometry to quantify K13 protein expression in epithelial and non-epithelial cell lines. The expression of K13 protein in epithelial A431 (blue), SCC25 (green), RTS3b (purple), HeLa (pink) cell lines and in non-epithelial HFF (black) cell line are shown. The results are expressed as the mean \pm the standard deviation (SD) of five experiments. Each K13 band has been normalised to β -actin band density (loading control). The expression of K13 protein is increased in oral SCC25 cell in comparison to RTS3b (purple, $P=0.340$), HeLa (pink, $P=0.003$) and HFF (black, $P=0.05$) cell lines. A431 cell was used as positive control for western blot technique given that this cell line shows abundant K13 protein expression.

4.4.9 FACS Data

A representative plot of typical FACS data for both positive control pEGFPN-3B and promoterless (PL) pEGFPN-3B vector are shown in Figure 4.20 A and B. The lower left quadrant shows the percentage of non-transfected oral SCC25 cells, while in the upper left quadrant shows the percentage of SCC25 cells transfected with CMV linked GFP pEGFP-N3B vector (positive control) or PL. However, in the lower right quadrant the percentage of oral SCC25 cells transfected with CMV promoter linked DsRed (internal control) is shown. In the upper right quadrant the percentage of oral SCC25 cells which have taken up the co-transfected CMV promoter linked DsRed and CMV promoter linked GFP plasmids are shown.

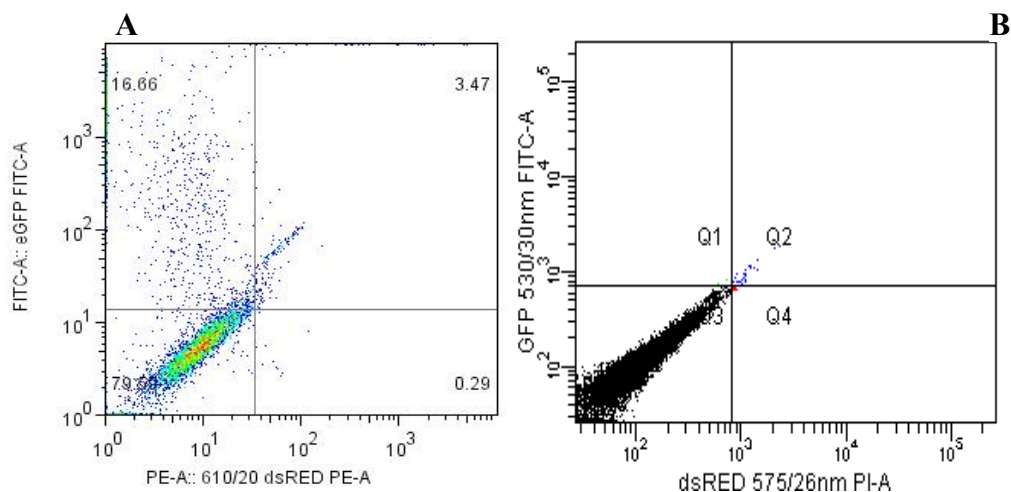


Figure 4.20: An example of FACS plot data obtained with CMV driven pEGFP-N3B vector (positive control) and PL plasmid transfected in oral SCC25 cells. The upper left quadrant shows the percentage of GFP positive SCC25 cells for pEGFP-N3B (A) and PL (B). The upper right quadrant shows the percentage of pEGFP-N3B or PL and pDsRed1-N1 (PE-A or PI-A fluorescence) positive cells. The lower left quadrant shows percentage of non-fluorescing cells and lower right quadrant shows percentage of positive cells expressing pDsRed1-N1 plasmid (PE-A fluorescence) alone. This FACS plot figure was included to clarify that all data obtained looks similar but the percentage of cells, which have taken GFP (the upper left quadrant) changes depending on the construct used.

4.4.10 FACS Analysis of K13 FL promoter and Truncated K13 Promoter R1 and R2 Deletion Fragments

Representative FACS data of FL (red), R1 (green) and R2 (blue) K13 promoter fragments transfected into oral SCC25 (Figure 4.22), RTS3b (Figure 4.23), HeLa (Figure 4.24) and HFF (Figure 4.25) cells are shown. The ability of each fragment (FL-R2) to drive GFP is measured by FACS. The FACS data are circled (red, green and blue) for each of the 4 cell lines used, to indicate that there is an emerging trend in the pattern of K13pro-3018bp (FL), K13pro-2540bp (R1), K13pro-1953bp (R2) expression in SCC25, RTS3b, HeLa and HFF cells. The pattern (Figure 4.21) of expression for the three constructs in oral SCC25 cells (Figure 4.22) shows a basal expression of K13 FL promoter then with K13-R1 fragment the expression increases; this is then followed by a rapid decrease in GFP expression with K13-R2 fragment compared to R2. In RTS3b cells (Figure 4.23 and 4.21) the K13 FL promoter shows the basal expression, then the K13 promoter expression increases with the R1 fragment, which is followed by a decrease in GFP expression with the K13-R2 fragment compared to fragment R2. Also the same pattern is observed for HeLa and HFF cells (Figure 4.25) in that the pattern of expression of FL K13 promoter shows

the basal expression, then the K13 promoter expression increases with R1; this rapid increase is followed by a decrease with the K13-R2 fragment compared to fragment R2. This data taken together indicate the presence of important suppressor regulatory elements which reside between the K13-FL and K13-R1 deletion fragments.

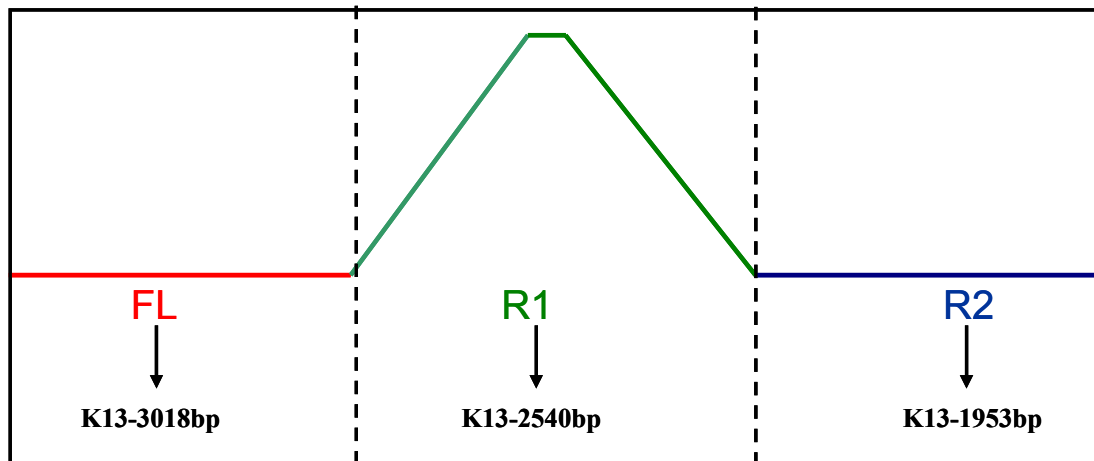


Figure 4.21: Diagrammatic representation of K13 full length promoter (FL), R1 and R2 fragment expression trend observed from FACS data. The diagram shows the K13 FL (red) promoter as a starting point for the full length promoter expression, the diagram then shows that with R1 (green) fragment the expression of K13 promoter increases, this indicates that a repressor element which resides in the K13 FL has been removed. The K13 expression level goes back down to K13-FL level with R2 (blue) fragment. The dashed lines in the diagram are used as a divider between the expression of FL, R1 and R2 K13 promoter constructs. This figure was included to simplify the overall expression of K13-FL, R1 and R2 fragments as shown in figure 4.22 to 4.25.

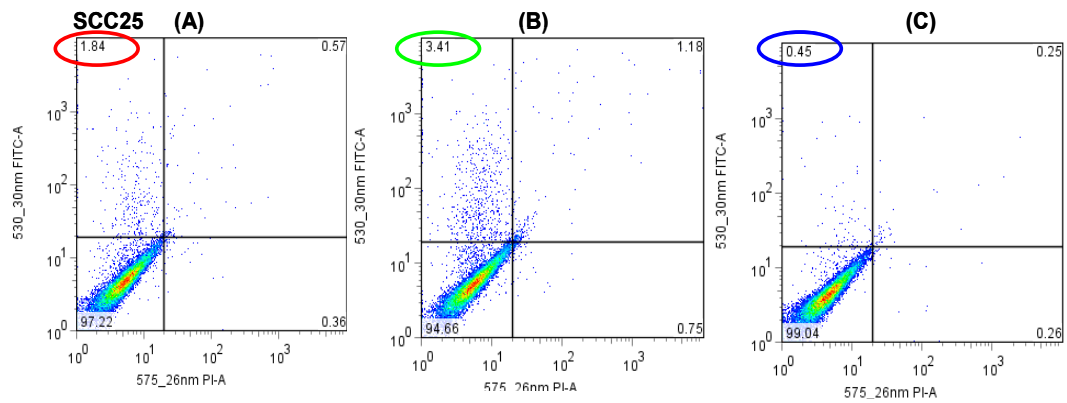


Figure 4.22: Represents FACS plot data for full length (FL) K13 promoter and various lengths (R1 and R2) of K13 promoter in oral SCC25 cells. A= shows FACS plot data for the full length K13 promoter, the red circle highlights the percentage of GFP positive oral SCC25 cells transfected with FL K13 promoter linked GFP construct. B= shows plot data for R1 K13 promoter fragment, the green circle in the data highlights the percentage of GFP positive oral SCC25 cells transfected with R1 K13 promoter linked GFP construct. C= shows FACS plot data for R2 K13 promoter fragment, the blue circle in the FACS data highlights the percentage of GFP positive oral SCC25 cells transfected with R2 K13 promoter linked GFP construct. The pattern emerging with FL, R1 and R2 K13 promoter fragments in oral SCC25 cells seems to increase with R1 fragment followed by a decrease in K13 promoter expression as indicated by decrease in percentage of GFP positive SCC25 cells which have up taken the K13pro-R2 construct.

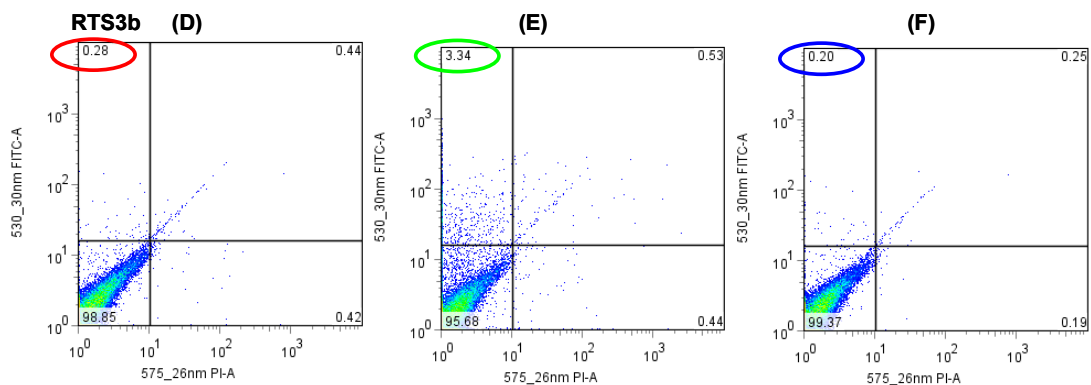


Figure 4.23: Shows FACS plot data for full length (FL) K13 promoter and various lengths (R1 and R2) of K13 promoter in RTS3b cells. D= shows plot data for the full length K13 promoter, the red circle in the data highlights the percentage of GFP positive RTS3b cells transfected with FL K13 promoter linked GFP construct. E= shows plot data for R1 K13 promoter fragment, the green circle in the data highlights the percentage of GFP positive RTS3b cells transfected with R1 K13 promoter linked GFP construct. F= shows FACS data for R2 K13 promoter fragment, the blue circle in the FACS data highlights the percentage of GFP positive RTS3b cells transfected with R2 K13 promoter linked GFP construct. The pattern emerging with FL, R1 and R2 K13 promoter fragments in RTS3b cells seems to increase with R1 fragment followed by a decrease back down to the level of K13-FL promoter expression as indicated by decrease in percentage of GFP positive RTS3b cells which have up taken the K13pro-R2 fragment construct.

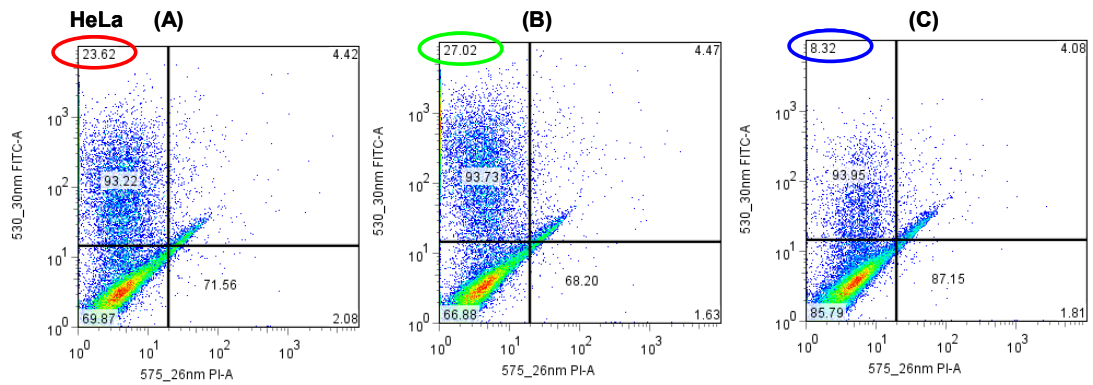


Figure 4.24: Representing FACS plot data for full length (FL) K13 promoter and various lengths (R1 and R2) of K13 promoter in HeLa cells. A= shows FACS data for the full length K13 promoter, the red circle in the highlights the percentage of GFP positive HeLa cells transfected with FL K13 promoter linked GFP construct. B= shows plot data for R1 K13 promoter fragment, the green circle in the FACS data was used to highlight the percentage of GFP positive HeLa cells transfected with R1 K13 promoter linked GFP construct. C= shows FACS plot data for R2 K13 promoter fragment, the blue circle in the data highlights the percentage of GFP positive HeLa cells transfected with R2 K13 promoter linked GFP construct. The pattern emerging with FL, R1 and R2 K13 promoter fragments in HeLa cells seems to increase with R1 fragment followed by a decrease, compared to R1, in K13 promoter expression as indicated by decrease in percentage of GFP positive HeLa cells which have up taken the K13pro-R2 fragment construct.

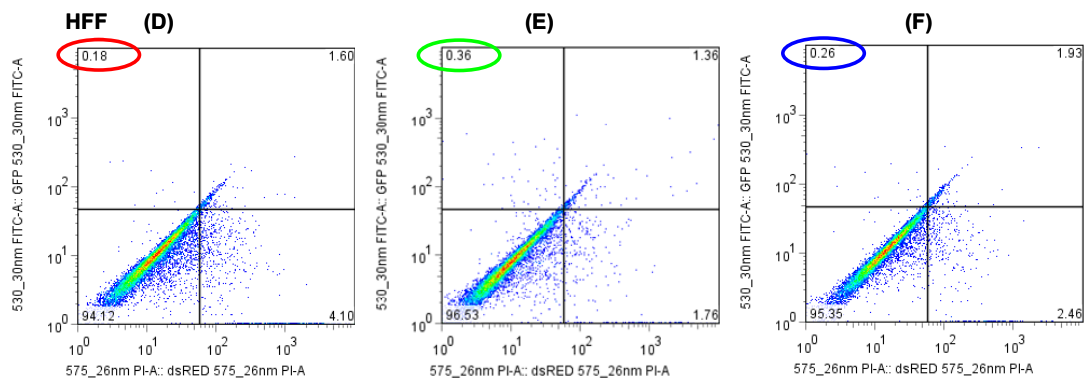


Figure 4.25: Shows FACS plot data for full length (FL) K13 promoter and various lengths (R1 and R2) of K13 promoter in HFF cells. D= shows FACS data for the full length K13 promoter, the red circle in the FACS data highlights the percentage of GFP positive HFF cells transfected with FL K13 promoter linked GFP construct. E= shows FACS data for R1 K13 promoter fragment, the green circle in the plot data highlights the percentage of GFP positive HFF cells transfected with R1 K13 promoter linked GFP construct. F= shows FACS plot data for R2 K13 promoter fragment, the blue circle in the data highlights the percentage of GFP positive HFF cells transfected with R2 K13 promoter linked GFP construct. The pattern emerging with FL, R1 and R2 K13 promoter fragments in HFF cells seems to increase with R1 fragment followed by a decrease, compared to R1, in K13 promoter expression as indicated by decrease in percentage of GFP positive HFF cells which have up taken the K13pro-R2 fragment construct.

4.4.11 The 3.018kb K13 FL Promoter and K13 Truncated Promoter R1 to R6 Deletion Fragments Transfected into Epithelial and non-Epithelial Cell Lines

The K13 FL promoter and the R1 to R6 K13 promoter fragments were transiently transfected into oral SCC25, RTS3b, HeLa and HFF cell lines (Figure 4.26). The results indicate that there is a trend in the pattern of the K13 FL (K13-3018bp) and K13 R1 (K13-2540bp) to R2 (K13-1953bp) expression in SCC25, RTS3b, HeLa and HFF cell lines. As shown in Figure 4.26, after almost 500bp is removed from the K13 FL promoter the expression of R1 fragment goes up significantly in SCC25 ($P=0.003$), RTS3b ($P=0.01$), HeLa ($P=0.002$) and HFF ($P=0.01$) cells relative to FL K13 promoter. This is then followed by a significant decrease in the K13 promoter driven GFP expression with the R2 fragment compared to K13 FL in HeLa ($P=0.0003$) and HFF ($P=0.02$) cell lines. The expression pattern of the FL K13 promoter, R1 and R2 K13 promoter fragments is consistent in oral SCC25, RTS3b, HeLa and HFF cells. However the expression of the K13 promoter deletion fragment R3 (K13-1512bp), R4 (K13-1017bp), R5 (K13-670bp) and R6 (K13-289bp) differ depending on the cell line being tested. The expression of the K13 promoter fragment R3 increases in SCC25, RTS3b and HFF (Figure 4.26 A, B and C) relative to FL K13 promoter, while in HeLa cells (Figure 4.26 D) there is a slight decrease in R3 fragment expression relative to the FL K13 promoter. The expression of K13 promoter fragment R4 increases in SCC25 ($P=0.05$), RTS3b and HFF ($P=0.004$) (Figure 4.26 A, B and D) relative to FL K13 promoter, while in HeLa cells (Figure 4.25 C) there is a significant ($P=0.001$) decrease in R4 fragment relative to the FL K13 promoter. In addition, the expression of K13-R5 promoter fragment increases in SCC25 and HFF (Figure 4.26 A and D) relative to FL K13 promoter. While in RTS3b cells (Figure 4.26 B) the expression remains the same and with HeLa cells (Figure 4.26 C) there is decrease in R5 fragment relative to the FL K13 promoter. Finally the expression of K13-R6 promoter fragment increases in SCC25, RTS3b and HFF ($P=0.004$) (Figure 4.26 A, B and D) relative to FL K13 promoter. While in HeLa cells (Figure 4.26 C) there is a significant ($P=0.0003$) decrease in R6 fragment relative to the FL K13 promoter.

Figure 4.26 results are based on Table 4.3 and they represent the average of FACS for three different transient transfection experiments of promoterless (PL) pEGFP-N3B, K13 FL promoter and K13 promoter deletion fragments R1 to R6 into SCC25,

RTS3b, HeLa and HFF cell lines. The FACS data were normalized to the pDsRed1-N1 internal control for PL, FL K13 promoter and K13 deletion R1 to R6 fragments. In addition, Table 4.3 shows the fold induction of PL, K13 FL and R1 to R6 K13 promoter fragment expression in SCC25 cells in comparison to HeLa cells. This comparison was done to highlight the fact that, although K13 is not normally expressed in HeLa cells, they show greater expression of PL, K13 FL and R1 to R6 K13 promoter fragment expression in comparison to SCC25 cells, which endogenously express K13. Possible reasons for abnormal expression K13 in HeLa cells are discussed in section 4.5.

In summary the results for K13 FL promoter, K13-R1 and K13-R2 deletion fragment expression indicates that there similar expression pattern of all three constructs in SCC25, RTS3b, HeLa and HFF cell lines, with an increase in K13-R1 fragment expression in comparison to FL K13 promoter. This is then followed by a decrease in K13 R2 fragment expression in comparison to FL K13 promoter in HeLa and HFF cell lines. While the expression pattern of K13 promoter deletion fragments K13-R3 to K13-R6 promoter driven GFP expression pattern differs depending on the cell line being tested.

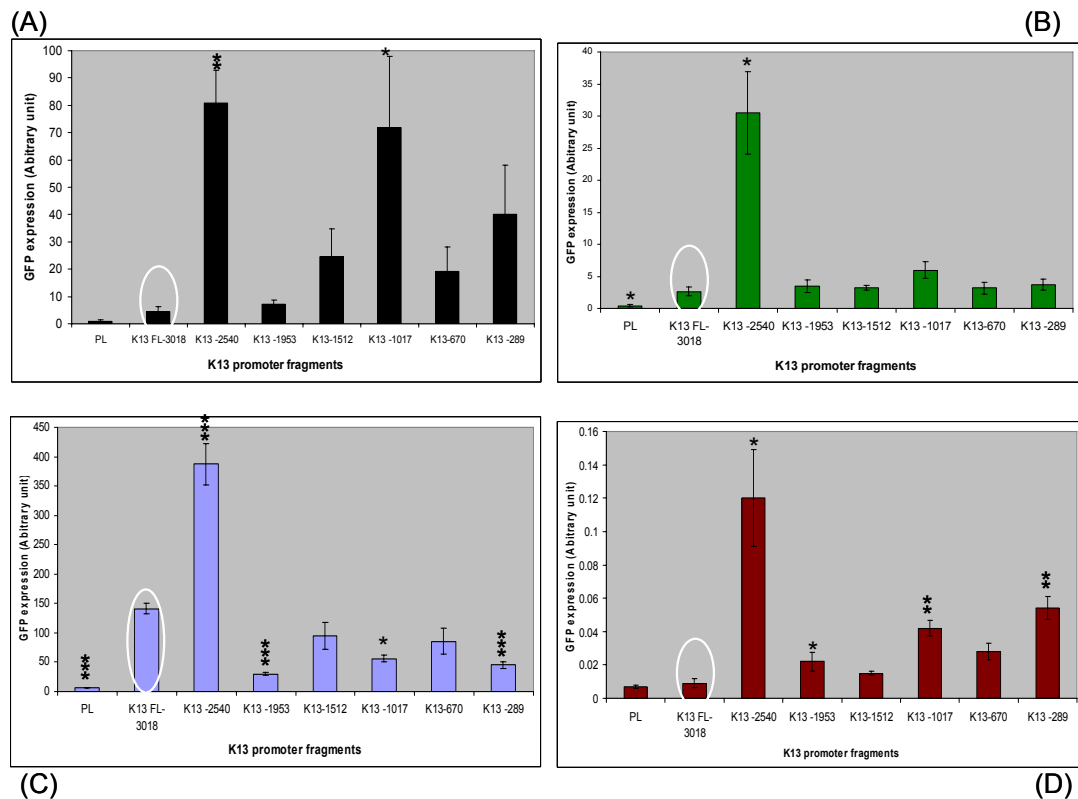


Figure 4.26: The GFP expression of promoterless (PL) pEGFP-N3B vector, FL K13 promoter and K13 R1 to R6 deletion fragments in SCC25 (A), RTS3b (B), HeLa (C) and HFF (D) cell lines. The K13 promoter-linked GFP expression is the highest in HeLa, SCC25, RTS3b and then in HFF cell line. HFF cell line was used as a negative control for transfection experiment since fibroblasts don't express keratins hence the negligible K13 fragment expression in HFF cells. The number of asterisks in each figure represents the significance of PL and K13 R1 to R6 (K13-2540 to K13-289bp) deletion fragments relative to the FL K13 promoter (K13-3018bp). The white circle in each figure highlights the GFP expression of the FL K13 promoter in pEGFP-N3B vector relative to R1 to R6 K13 promoter fragments.

Table 4.3: Average FACS data obtained for truncated K13 promoter fragment constructs transiently transfected into epithelial and non-epithelial cell lines.

K13 promoter construct name	PL	K13 FL-3018	K13 -2540	K13 -1953	K13-1512	K13 -1017	K13-670	K13 -289
SCC25	1	4	81	7	25	72	19	40
RTS3b	0	3	30	3	3	6	3	4
HeLa	6	141	387	30	95	56	86	45
HFF	0.01	0.01	0.12	0.02	0.01	0.04	0.03	0.05
K13 promoter fold up regulation expression in HeLa in comparison to oral SCC25 cell line	6	32	5	4	4	1	4	1

4.4.12 Pathways involved in the Induction of K13 Expression

The exact mechanism of transcriptional regulation of many mammalian genes which are required for maintaining normal cellular proliferation and differentiation is unknown. However, abnormal tissue growths and developmental disorders have been reported to result directly from abnormal expression of a single transcription factor, which eventually leads to deregulation of numerous target genes (Weinmann et al, 2002). Furthermore, it could also be that aberrant gene expression might be an indirect result of a transcription factor altering signal transduction pathways (Weinmann et al, 2002). Therefore, by utilizing pharmacological agents such as TPA, PD98059 (MEK 1/2 inhibitor), and LY294002 (PI3K inhibitor), Trichostatin A and sodium butyrate, pathways important for K13 expression were investigated. These pathways has been investigated in an attempt to obtain information on the important signalling events related to K13 expression. MEK 1/2 and PI3K are the two major kinase pathways activated by growth stimulatory signals such as epidermal growth factor (Yano et al, 2004). The MEK 1/2 pathway has also been reported to be important for expression of other differentiation markers like K10.

4.4.13 Cytotoxicity of Pharmacological Inhibitors on Oral SCC25, RTS3b and HeLa cells using 3-(4,5-Dimethylthiazol-2-yl)-2,5-diphenyltetrazolium bromide, a tetrazole (MTT) assay.

Prior to their use an MTT assay was performed to examine the effect of each pharmacological agent on cell toxicity (Figure 4.35). The LD₅₀, is an index of drug toxicity and a measure of the lethal dose of any given substance required to kill 50% of the test experimental cell population. The MTT assay showed the following drug concentrations 100nM 4- α -PMA, 100nM TPA, 50 μ M PD98059 were not toxic to oral SCC25 cells ($P=0.88$, 0.40, 0.60) in comparison to control. In addition, the treatment of RTS3b and HeLa cells ($P=0.06$, $P=0.81$) with 3 μ M Trichostatin A drug concentration which showed no cell toxicity in comparison to control. However, the MTT assay did show significant ($P=0.001$) difference between the untreated (control) and treated oral SCC25 cells with 25 μ M LY294002 (test). Moreover, the LY294002 compound only killed 32% of oral SCC25 cells and 68% of the cells were viable (Figure 4.27). Thus, if the LD₅₀ is used as an index of LY294002 compound toxicity, it can be inferred that the decrease in K13 promoter construct and protein

expression in oral SCC25 cells is probably not due to LY294002 induced cell toxicity, but rather a true reflection of the importance of this pathway for K13 expression.

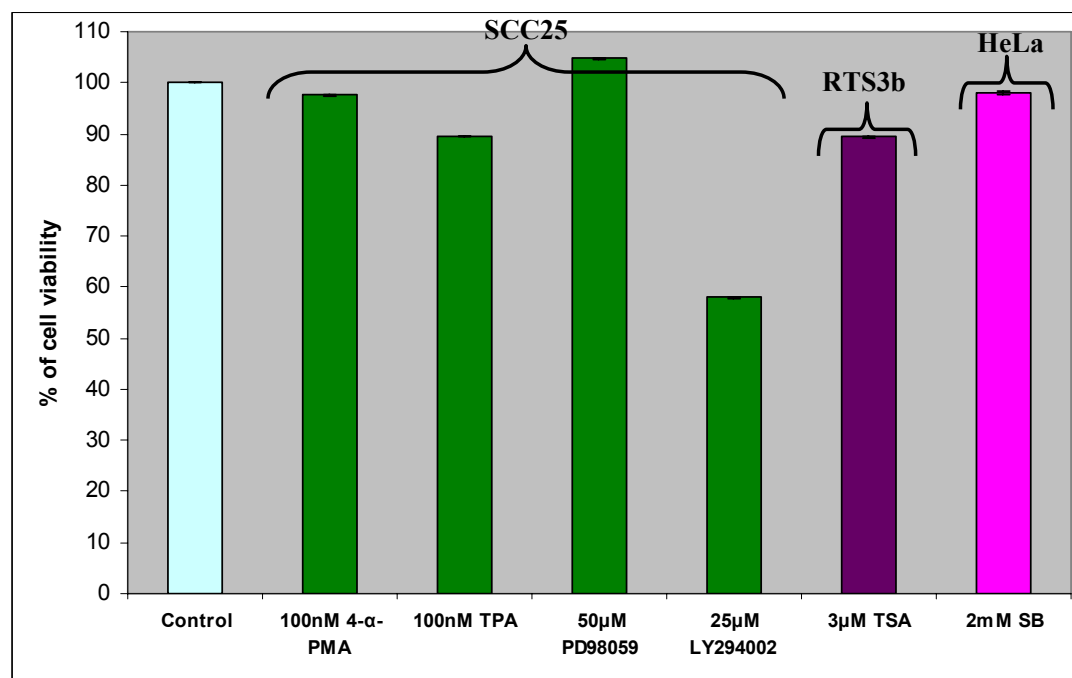


Figure 4.27: Cytotoxicity of various pharmacological agents on oral SCC25, RTS3b and HeLa cell viability. Depending of the cell type being tested, 5×10^3 to 12×10^3 were plated per well into 96 well plate, in the presence or absence of 4- α -PMA (green), TPA (green), PD98059 (green), LY294002 (green), TSA (purple) and sodium butyrate (pink) and incubated overnight in a 5% CO₂ incubator at 37°C for various times. Cytotoxicity was measured with the MTT assay (as in the method and materials section 2.16.1). The net absorbance taken from the wells with cells from cultured media was taken as a 100% viability value (control). The percentage viability of the treated cells was calculated from the net absorbance of the sample divide by the net absorbance of the control x 100. Each data point represents the mean \pm SD from three individual wells.

4.4.14 Induction of K13 Expression by TPA through the Activation of Protein Kinase C Pathway

Protein kinase C (PKC) is essential for the expression of certain differentiation related genes and TPA activates the PKC pathway, therefore one of the aims of the study was to address whether markers for epithelial differentiation such as K13 can be induced by TPA. While TPA is an activator of PKC, 4- α -PMA was used as a negative control for the experiment, since 4- α -PMA is an inactive analogue of TPA. Thus if K13 expression is higher in the presence of TPA in comparison to 4- α -PMA,

it indicates that K13 expression can be activated via the PKC pathway. However, if the activity of K13 is the same or lower in the presence of TPA in comparison to 4- α -PMA, then K13 expression is not induced by TPA through the PKC pathway. The results show that both K13 FL promoter construct and protein expression were not significantly increased ($P=0.414$ and $P=0.89$) in presence of TPA in comparison to 4- α -PMA (Figures 4.28 and 4.31). This indicates that the K13 expression is not induced through the PKC pathway. In addition, there was no significant ($P=0.978$) difference between the K13 promoter deletion R2 fragment in the presence of TPA or 4- α -PMA, which again indicates that K13-1953bp R2 fragment expression is not induced through the protein kinase C pathway. Moreover Figure 4.29 shows that the effect of TPA or 4- α -PMA on the CMV promoter was not significant ($P=0.316$), given that there was no difference between CMV promoter expression in presence of TPA or 4- α -PMA. This indicates the CMV promoter expression is not induced through the protein kinase C pathway. These results taken together show that K13 FL, K13-1953bp R2 fragment and CMV promoter expression are not induced through the PKC pathway, since there was no significant difference between the expressions of these constructs in the presence of TPA compared to 4- α -PMA.

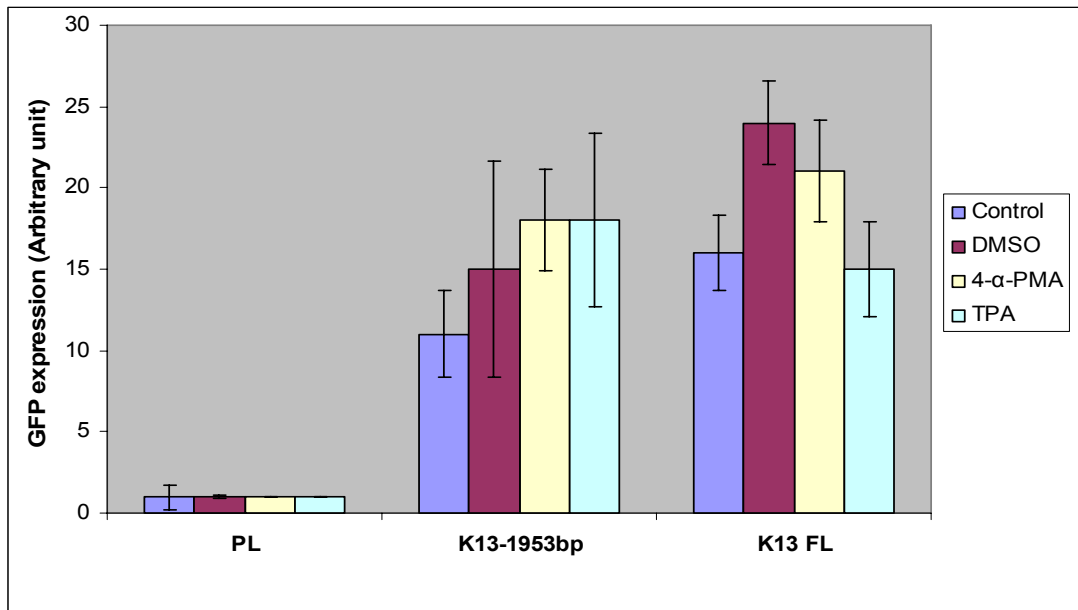


Figure 4.28: The effect of 100nM 4- α -PMA and TPA on EGFP expression transfected in oral SCC25 cells containing promoterless (PL), truncated K13 promoter (K13-1953bp) or the K13 full length promoter (K13-FL) construct expression. The promoter constructs alone form the cell control (blue), while the addition of DMSO forms the vehicle control (mauve). The effects of the addition of either 100nM 4- α -PMA or TPA are shown in yellow and turquoise respectively. K13 FL promoter and K13-1953bp deletion fragment activity in response to 100nM 4- α -PMA versus TPA showed no significant difference ($P=0.414$ and 0.978). The results are expressed as the mean \pm SD from three experiments.

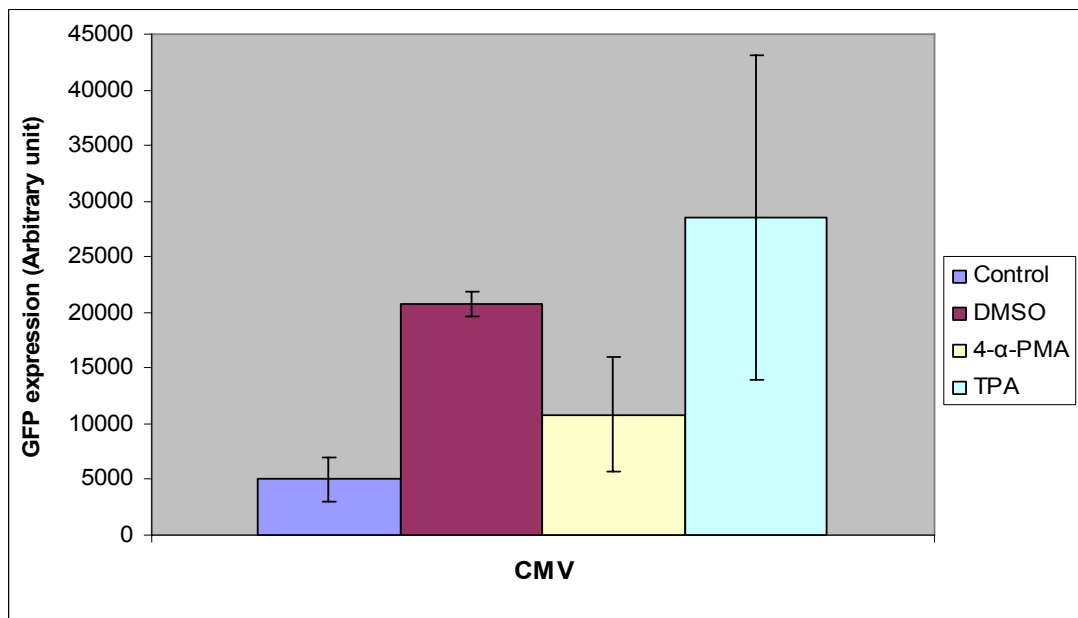


Figure 4.29: The effect of 100nM 4- α -PMA and TPA on EGFP expression transfected in oral SCC25 cells containing CMV promoter (pEGFP-N3B). The CMV promoter alone form the cell control (blue), while the addition of DMSO forms the vehicle control (mauve). The effects of the addition of either 100nM 4- α -PMA or TPA are shown in yellow and turquoise respectively. CMV promoter activity in response 100nM 4- α -PMA versus TPA showed no significant difference ($P=0.316$). The results are expressed as the mean \pm SD from three experiments.

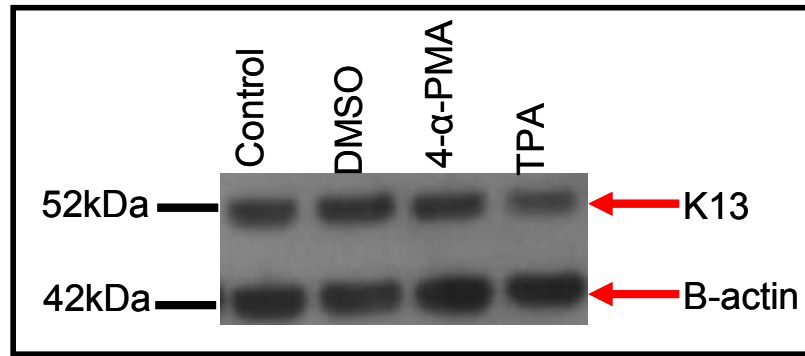


Figure 4.30: Effect of TPA and 4- α -PMA on K13 protein expression in oral SCC25 cells. K13 protein expression appears slightly decreased in the presence of TPA compared to control. Cells were exposed to 100nM TPA and 4- α -PMA for 6 hours and then lysed in Laemmli buffer before SDS PAGE analysis. Protein was transferred onto nitrocellulose and probed for K13 using AE8 antibody as described in Chapter 2 section 2.17.

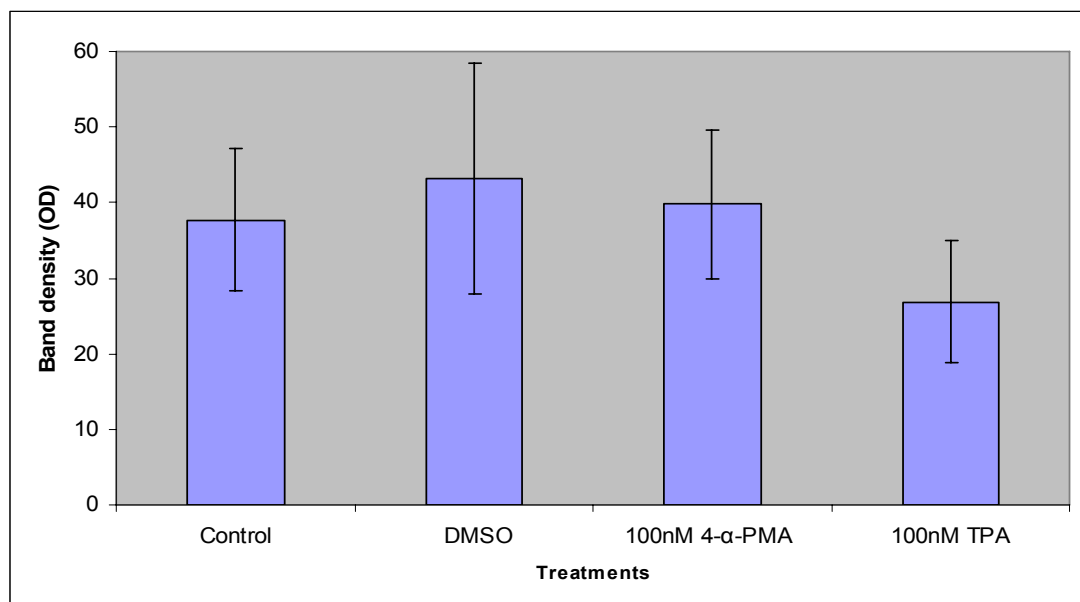


Figure 4.31: Quantification of band density derived from western blot data in figure 4.30 using densitometry to show alterations in K13 protein expression after treatment of SCC25 cells with DMSO (control vehicle), 4- α -PMA (100nM) and TPA (100nM) for 6 hours. The results are expressed as the mean \pm SD from three experiments. Each K13 band has been normalised to β -actin band density (loading control). There is no significant difference between K13 protein expression in the presence of 4- α -PMA and TPA.

4.4.15 MEK 1/ 2 and PI3K/Akt pathways

MEK 1/2 and PI3K/Akt, are the two major kinase pathways which are activated by growth stimulatory signals such as epidermal growth factor (Yano et al, 2004) and the effect of inhibition of these pathways on K13 was investigated using specific

inhibitors. These pathways were examined to show whether altered differentiation in the oral mucosa reflects specific changes in either pathways.

4.4.16 Inhibition of MEK 1/ 2 Pathway on the Induction of K13 FL Promoter Construct and Protein Expression

Inhibition of MEK 1/2 pathway with 50 μ M PD98059 significantly decreased ($P=0.030$, Figure 4.32) the K13 FL promoter construct expression and insignificantly increased ($P=0.162$ Figure 4.34) the expression of K13 protein in comparison to the control. In Figure 4.33, the CMV promoter expression in the presence of 50 μ M PD98059, MEK1/2 pathway, inhibitor has shown significant decrease in GFP expression in comparison to control ($P=0.01$ Figure 4.33). Furthermore, although the data presented in Figure 4.32 and 4.33 are in the same arbitrary units, the expression of K13 FL promoter in comparison to CMV promoter differs by 10 fold. This might be because CMV is a very active constitutive viral promoter, which causes GFP to be expressed strongly at all times, therefore, greater CMV expression (Figure 4.33) in comparison to K13 promoter expression (Figure 4.32) is observed. The result for CMV promoter (Figure 4.33) was not as expected given that CMV promoter was used as positive control and thus should not be affected by a pharmacological agent. This highlights some of the flaws associated with the use of GFP reporter genes. Also the decrease in CMV promoter seems to be non-specific given that DMSO, which normally causes induction of cell differentiation, appears to be causing this decrease, rather than the PD98059 MEK 1/2 inhibitor (Figure 4.33), while the decrease in K13-FL promoter seems to be specifically caused by PD98059 MEK 1/2 inhibitor, given that K13-FL promoter in the presence of DMSO is not decreased. This shows that inhibition of MEK 1/2 by PD98059 is specific for K13-FL promoter, but not for the CMV promoter. Moreover, inhibition of the MEK 1/2 pathway with 50 μ M PD98059 did not significantly ($P=0.162$) increase the K13 protein expression in comparison to control (Figure 4.35). This contradictory result for both K13-FL promoter and K13 protein expression in the presence of PD98059 could mean that different mechanisms might exist for the inhibition of K13-FL promoter activity, which has nothing to do with K13 protein. In summary, the inhibition of MEK 1/2 pathway with PD98059 significantly decreased the K13 FL promoter construct and the expression of CMV promoter, while the inhibition of this pathway insignificantly increased the K13 protein expression in comparison to control.

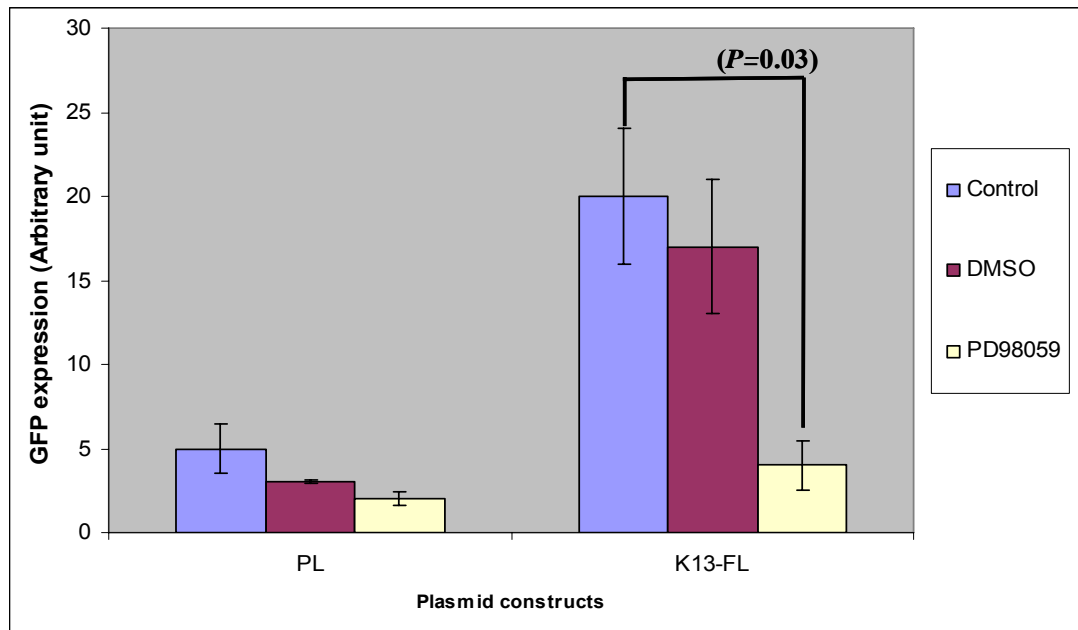


Figure 4.32: The effect of MEK 1/ 2 pathway inhibitor PD98059 on EGFP expression in oral SCC25 cells containing promoterless (PL) or the K13 full length promoter (K13-FL) construct expression. The promoter constructs alone form the cell control (blue), while the addition of DMSO forms the vehicle control (mauve). The effects of the addition of PD98059 are shown in yellow. K13 FL promoter activity in response to 50 μ M PD98059 versus control caused a significant ($P=0.03$) decrease in K13-FL promoter. The results are expressed as the mean \pm SD from three experiments.

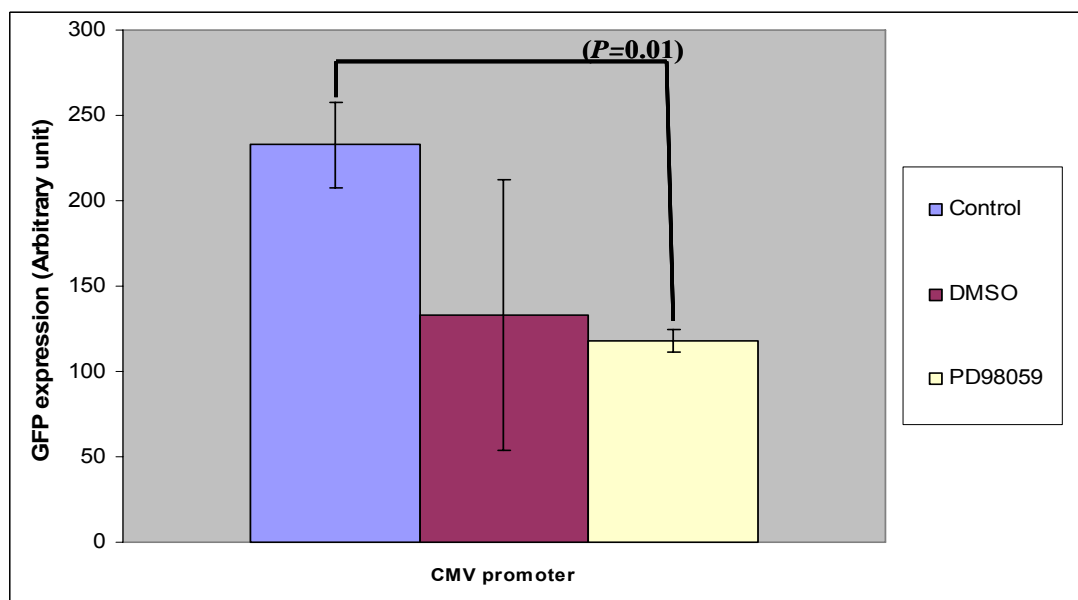


Figure 4.33: The effect of MEK 1/ 2 pathway inhibitor PD98059 on EGFP expression in oral SCC25 cells containing CMV promoter in pEGFP-N3B vector (positive control). The CMV promoter in pEGFP-N3B vector alone form the cell control (blue), while the addition of DMSO forms the vehicle control (mauve). The effects of the addition of PD98059 are shown in yellow. CMV promoter in response to 50 μ M PD98059 versus control caused a significant ($P=0.01$) decrease in CMV promoter. The results are expressed as the mean \pm SD from three experiments.

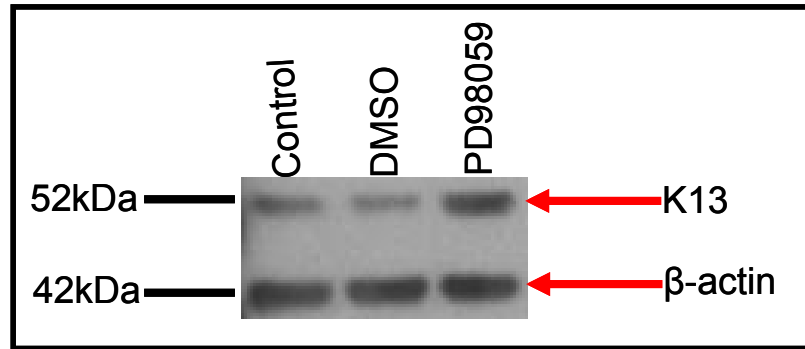


Figure 4.34: Effect of MEK 1/ 2 inhibitor PD98059 on K13 protein expression in an oral mucosa SCC25 cell line. K13 protein expression appears slightly increased in the presence of PD98059 compared to control Cells were grown in 50 μ M PD98059 for 48 hours and lysed in Laemmli buffer before analysing on SDS gels. The gels were transferred on nitrocellulose and probed for K13 expression using AE8 antibody as described in Chapter 2 section 2.17.

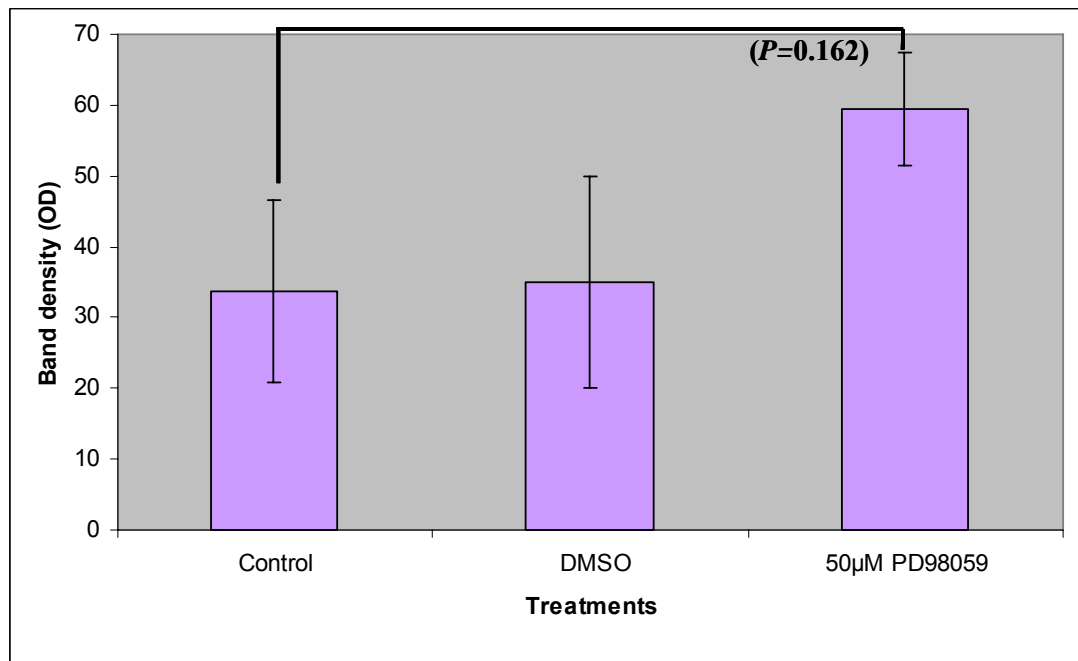


Figure 4.35: Quantification of band density derived from western blot data in Figure 4.34 using densitometry to show the alteration in K13 protein expression after treatment of SCC25 cells, in absence and presence of DMSO (control vehicle) and MEK 1/ 2 pathway inhibitor PD98059 (50 μ M), for 48 hours. The results are expressed as the mean \pm SD from three experiments. Each K13 band has been normalised to β -actin band density (loading control). There is no significant ($P=0.162$) difference between K13 protein expression in the presence of PD98059 in comparison to control.

4.4.17 Effect of inhibition of PI3K/Akt Pathway and Expression of K13 FL Promoter Construct and K13 Protein

Inhibition of the PI3K/Akt pathway with 25 μ M LY294002 significantly decreased ($P=0.01$, Figure 4.36) the K13 FL promoter construct and K13 protein ($P=0.003$, Figure 4.38) expression in comparison to the control. In Figure 4.37, the CMV promoter expression in the presence of 25 μ M LY294002, a PI3K/Akt pathway inhibitor, shows a decrease in GFP expression in comparison to control. Furthermore, although the data presented in Figure 4.36 and 4.37 are in the same arbitrary units, the expression of K13 FL promoter in comparison to CMV promoter differs by 20 fold. This might be because CMV is a very active constitutive viral promoter, which causes GFP to be expressed strongly at all times. The CMV promoter appears to be affected by LY294002 compound (Figure 4.37). Inhibition of the PI3K/Akt pathway with 25 μ M LY294002, significantly ($P=0.003$) decreased K13 protein in comparison to control (Figure 4.38 and 4.39). In summary, the inhibition of the PI3K/Akt pathway with LY294002 compound significantly decreased the K13 FL promoter construct, K13 protein expression and insignificantly decreased the expression of CMV promoter in comparison to control. This consistent decrease in K13 promoter construct and protein expression caused by the LY294002 compound might reflect the importance of this pathway for K13 expression in the oral mucosa.

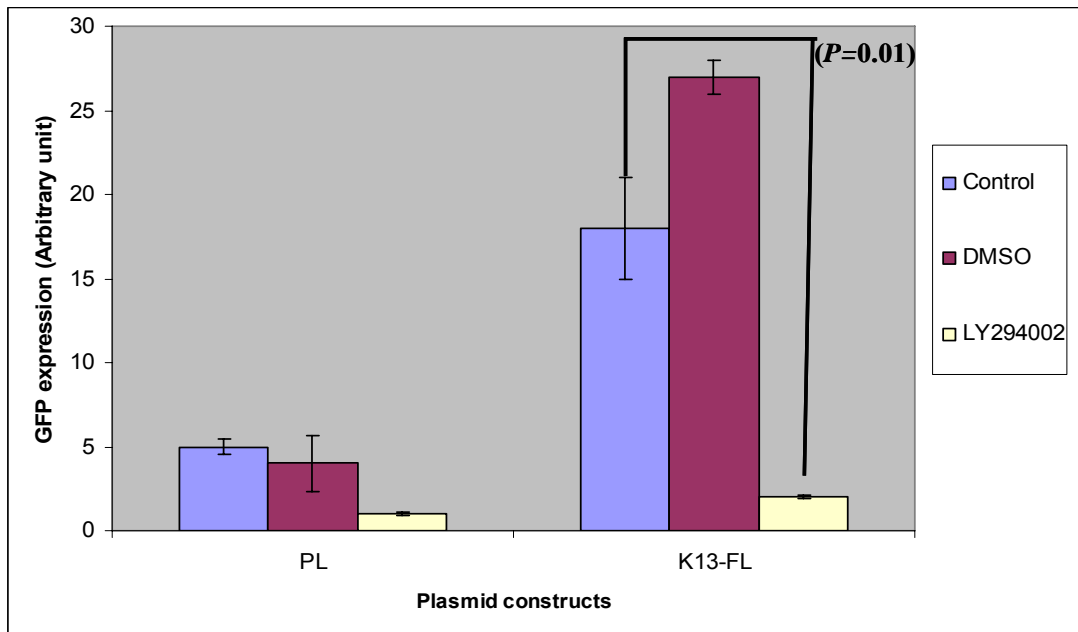


Figure 4.36: The effect of PI3K/Akt pathway inhibitor LY294002 on EGFP expression transfected in oral SCC25 cells containing promoterless (PL) or the K13 full length promoter (K13-FL) construct expression. The promoter constructs alone form the cell control (blue), while the addition of DMSO forms the vehicle control (mauve). The effects of the addition of LY294002 are shown in yellow. K13 FL promoter activity in response to 25 μ M LY294002 versus control caused a significant ($P=0.01$) decrease in K13-FL promoter. The results are expressed as the mean \pm SD from three experiments.

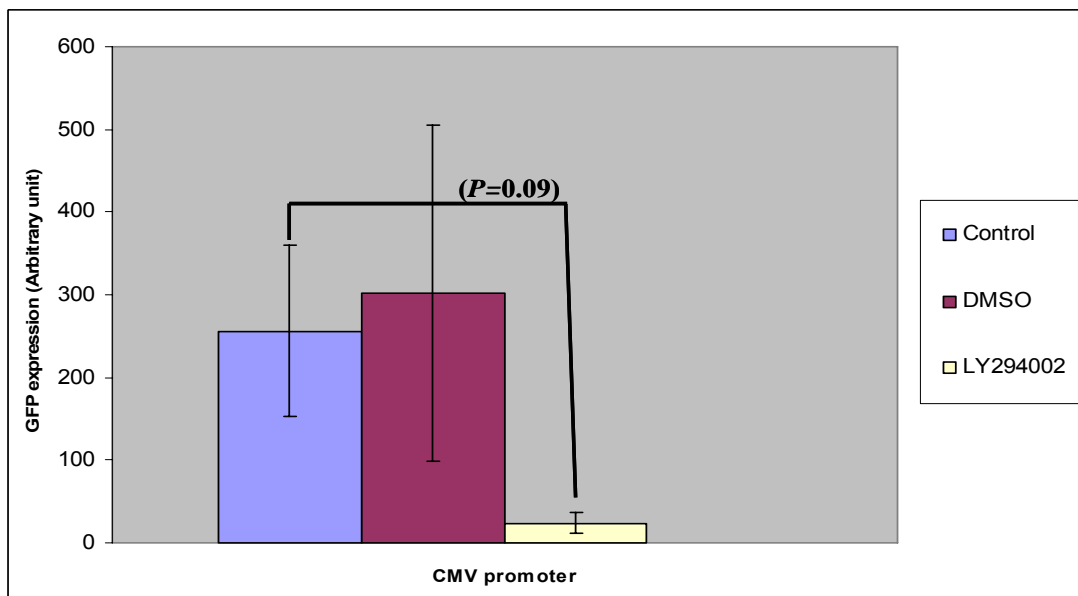


Figure 4.37: The effect of PI3K/Akt pathway inhibitor LY294002 on EGFP expression transfected in oral SCC25 cells containing CMV promoter in pEGFP-N3B vector (positive control). The CMV promoter in pEGFP-N3B vector alone form the cell control (blue), while the addition of DMSO forms the vehicle control (mauve). The effects of the addition of LY294002 are shown in yellow. CMV promoter in response to 25 μ M LY294002 versus control caused insignificant ($P=0.09$) decrease in CMV promoter. The results are expressed as the mean \pm SD from three experiments.

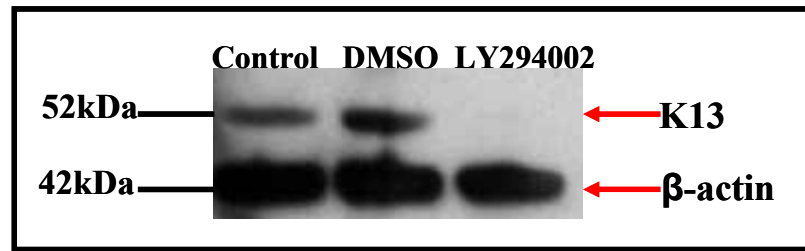


Figure 4.38: Effect of PI3K/Akt pathway inhibitor LY294002 on K13 protein expression in oral SCC25 cells. K13 protein expression is absent in the presence of LY294002 compound compared to control. Cells were grown in 25 μ M LY294002 for 48 hour and lysed in Laemmli buffer before analysing on SDS gels. The gels were transferred on nitrocellulose and probed for K13 expression using AE8 antibody as described in Chapter 2 section 2.17.

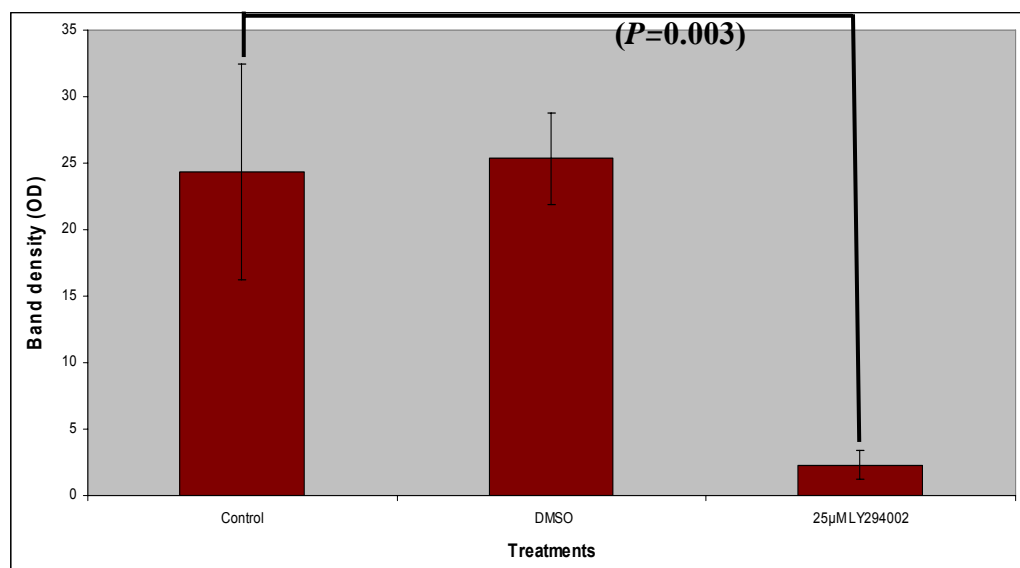


Figure 4.39: Quantification of band density derived from western blot data in Figure 4.38 using densitometry to show the alteration in K13 protein expression after treatment of SCC25 cells, in absence and presence of DMSO (control vehicle) and PI3K/Akt pathway inhibitor LY294002 (25 μ M), for 48 hours. The results are expressed as the mean \pm SD from three experiments. Each K13 band has been normalised to β -actin band density (loading control). There was a significant ($P=0.003$) difference between K13 protein expression in the presence of LY294002 in comparison to control.

4.4.18 Post-transcriptional Regulation of K13 Gene Expression

Regulation of gene expression includes many processes that cells use to convert the information in genes into gene products (Strachan and Read, 2004). Gene regulation is essential for eukaryotes as this leads to increased adaptability of the organism by allowing the cell to express protein when needed (Strachan and Read, 2004). Histone post-translational covalent modification is associated with regulating gene expression (Oberley et al, 2006). Histone is the major protein component of chromatin that acts

as beads around which DNA winds. Histone acetylation involves the addition of an acetyl group to histone protein by acetylase and de-acetylation involves the removal of an acetyl group by the deacetylase enzyme known as HDACS. Trichostatin A is a selective inhibitor of histone deacetylase and sodium butyrate, a normal dietary constituent found in butter, an inhibitor of proliferation, inducer of differentiation and non-selective inhibitor of histone deacetylase (Gillenwater et al, 2000). Trichostatin A and sodium butyrate either directly or indirectly prevent removal of acetyl groups from the core histone proteins by inhibiting histone deacetylase. Addition of an acetyl group to histones is associated with active transcription of a gene, while removal of an acetyl group is associated with the repression of transcription of certain genes (Markova et al, 2007). Addition of both Trichostatin A and sodium butyrate causes increased gene transcription by inhibiting HDAC and thus allowing increased binding of acetyl groups to histones either through direct or indirect pathways respectively.

Eukaryotic chromatin is usually present in two distinct forms: heterochromatin, condensed and transcriptionally silent regions of the genome or euchromatin, the transcriptional permissive state and less condensed form (Markova et al, 2007). The cell environment in which genes are expressed can be either permissive or non-permissive. In a non-permissive environment chromatin is usually present in the heterochromatin state and here the DNA region of interest within the chromatin is in a condensed and transcriptionally silent region. Thus the transcription factor is unable to access that region; this is due the action of the deacetylase enzyme removing acetyl group from histone and causing a subsequent repression of transcription of certain genes (Markova et al, 2007). In a permissive environment, chromatin is usually present in the euchromatin form, where the region corresponding to the selected gene in the DNA region of interest of the chromatin is in a transcriptional permissive state and less condensed form (Markova et al, 2007). Thus the transcription factor can access that region, due to the action of acetylase enzyme adding an acetyl group to the N-terminal of histone proteins, and transcription of certain genes can occur (Markova et al, 2007).

The question that is been asked in this thesis is why do some subset of genes present in the cell get expressed and translated into protein, while others genes do not get

expressed. Therefore, the aim of this section was to investigate whether chromatin structures in epidermal RTS3b cells are in a non-permissive environment and this causes lack of K13 protein expression. This was addressed by using Trichostatin A and sodium butyrate. Trichostatin A and sodium butyrate might increase the *KRT13* transcription, which might lead to increased K13 protein expression.

4.4.19 K13 Protein Expression in Permissive and Non-permissive Epithelial Cell Lines

An initial experiment was performed to assess the relative abundance of K13 protein expression in A431 (positive control), HeLa (negative control), HaCaT (test), RTS3b (test) and NHEK (test) cells. HaCaT, RTS3b, and NHEK (Chapter 2 Table 2.5) are epidermal keratinocytes that express K13 protein (Figures 4.40 and 4.41). This was done in an attempt to see if the expression of K13 protein can be induced or increased by Trichostatin A or sodium butyrate in cell lines which show low or negligible K13 protein expression. The result has shown that K13 expression was lowest in the RTS3b and HeLa cells, therefore subsequent experiments of the effect of Trichostatin A and sodium butyrate on K13 expression in RTS3b and HeLa cell lines was assessed. Although K13 protein is already expressed at basal line level in RST3b cells, the question that was addressed in this study was: can Trichostatin A and sodium butyrate increase K13 protein expression. The results have shown that Trichostatin A did not increase ($P=0.283$) K13 protein expression in comparison to control, while sodium butyrate significantly ($P=0.0027$) increased K13 protein expression compared to control (Figures 4.42 and 4.43). This suggests that in derived RTS3b cells, K13 protein expression might be diminished because of the chromatin structure in skin cells being in a condensed and transcriptionally silent region in the genome (heterochromatin), which can be overcome by non-specific histone deacetylase inhibitor sodium butyrate.

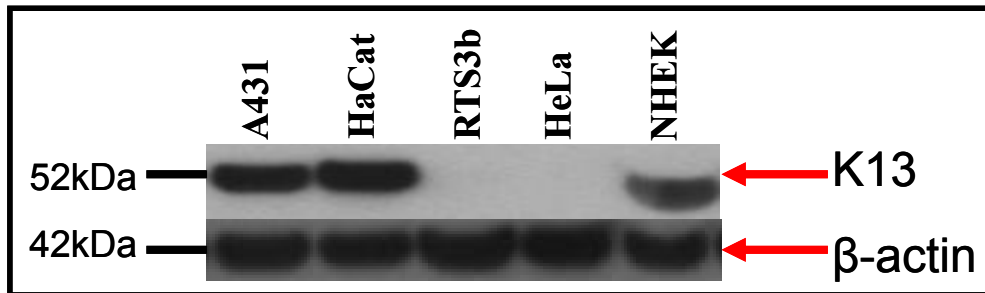


Figure 4.40: K13 protein expression in various epithelial cell lines. The K13 protein is strongly expressed in A431 and HaCat cells , then in NHEK cells, while the K13 expression is absent in both RTS3b and HeLa cell lines. The expression of K13 protein expression was initially assessed in 80% confluent A431, HaCaT, RTS3b, HeLa and NHEK cells and lysed in Laemmli buffer before analysing on SDS PAGE gels. The gels were transferred onto nitrocellulose and probed for K13 expression using AE8 antibody as described in Chapter 2 section 2.17. This experiment was done once only.

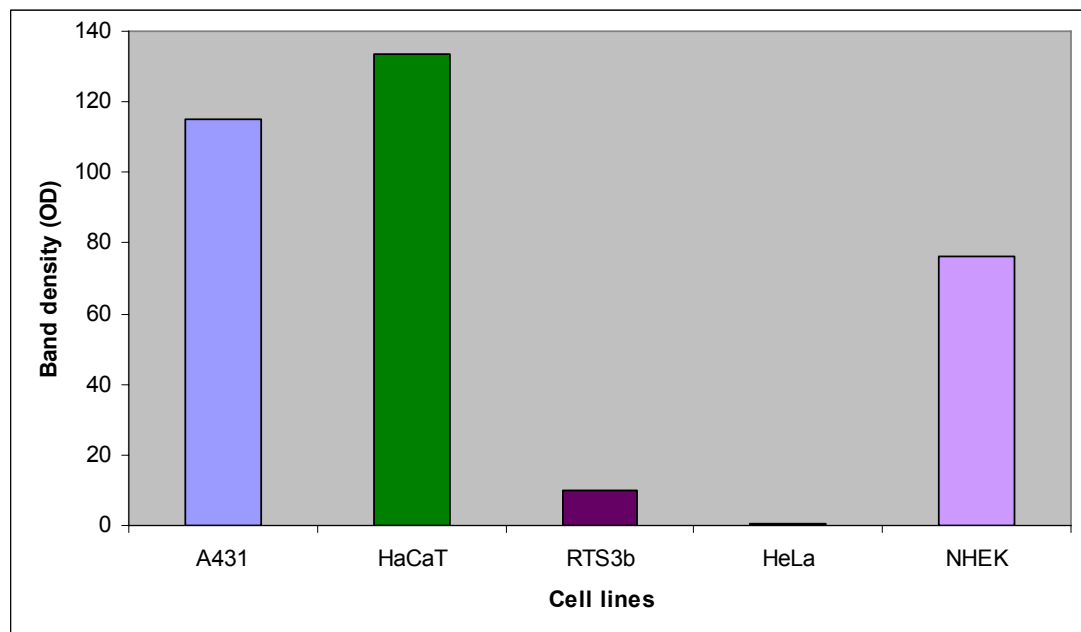


Figure 4.41: Quantification of band density derived from western blot data in Figure 4.40 using densitometry to quantify K13 protein expression in permissive and non-permissive epithelial cell lines. The expression of K13 protein in epithelial A431 (blue), HaCaT (green), RTS3b (purple), HeLa (pink) and NHEK (lilac) cells are shown. Each K13 band has been normalised to β -actin band density (loading control). A431 cell was used as positive control for western blot technique given that this cell line shows abundant K13 protein expression. Error bars are not present in this figure because n=1 experiment.

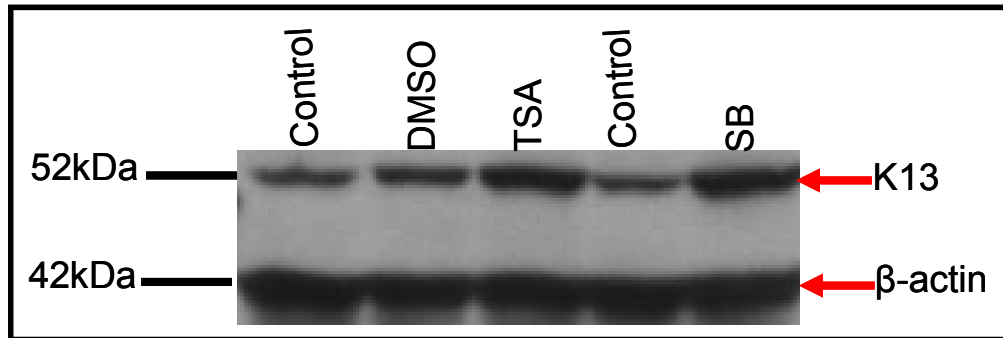


Figure 4.42: Effect of Trichostatin A and sodium butyrate on K13 protein expression in skin derived RTS3b cell line. K13 protein expression appears to be increased in the presence of TSA and Sodium butyrate compared to control. Cells were grown in the presence of 3 μ M Trichostatin A and 2mM sodium butyrate for 14 and 24 hours respectively and lysed in Laemmli buffer before analysing on SDS gels. The gels were transferred on nitrocellulose and probed for K13 expression using AE8 antibody as described in Chapter 2 section 2.17.

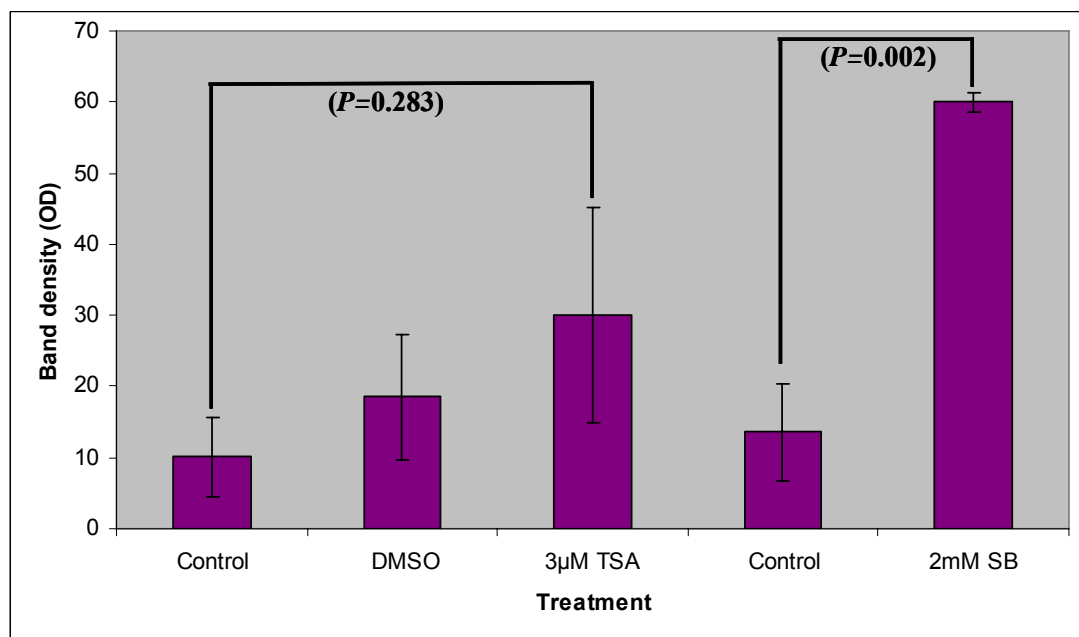


Figure 4.43: Quantification of band density derived from western blot data in Figure 4.42 using densitometry to quantify the effect of 3 μ M Trichostatin A and 2mM sodium butyrate on K13 protein expression in epidermal derived RTS3b cells. There was no difference in the K13 protein expression in presence of Trichostatin A in comparison to control ($P=0.283$), while there was a significant increase in K13 protein expression ($P=0.002$) in presence of sodium butyrate in comparison to control in RTS3b cells (purple). Each K13 band has been normalised to β -actin band density (loading control). The results are expressed as the mean \pm SD from three experiments. RTS3b cells were chosen because initially they showed the lowest K13 protein expression (Figure 4.41).

4.4.20 The effect of Trichostatin A and Sodium butyrate on Post-transcriptional Regulation of K13 Expression in HeLa Cell Line.

After assessing the abundance and relative expression of K13 protein in various cells (Figure 4.44 and 4.45), the results showed that K13 protein expression was negligible in HeLa cells, as previously reported (Waseem et al. 1998). For this reason HeLa cells served as a negative control for the Western blot. Trichostatin A and sodium butyrate should have increased the expression of K13 protein expression if K13 expression was switched off by a heterochromatin state in a non-permissive environment such as HeLa cells. However, the result has shown that both Trichostatin A and Sodium butyrate did not increase ($P=0.4$ and 0.8) K13 protein expression in HeLa cells (Figure 4.44 and 4.45). The value shown in the control in Figure 4.45 does not correlate with K13 protein but rather reflects the sensitivity of the densitometry detection, which picks up even non-specific background faint bands (Figure 4.44). In summary, Trichostatin A and sodium butyrate did not increase K13 protein expression in HeLa cells.

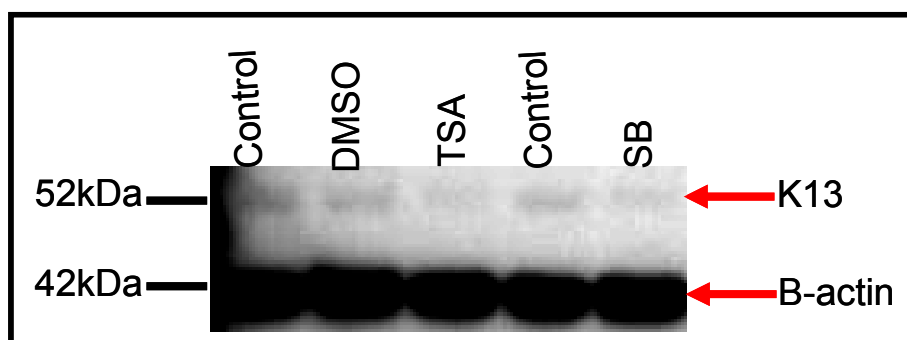


Figure 4.44: Effect of Trichostatin A and sodium butyrate on K13 protein expression in simple epithelial cervical carcinoma derived HeLa cells. Cells were grown in the presence of $3\mu\text{M}$ Trichostatin A and 2mM sodium butyrate for 14 and 24 hours respectively and lysed in Laemmli buffer before analysing on SDS gels. The gels were transferred on nitrocellulose and probed for K13 expression using AE8 antibody as described in Chapter 2 section 2.17.

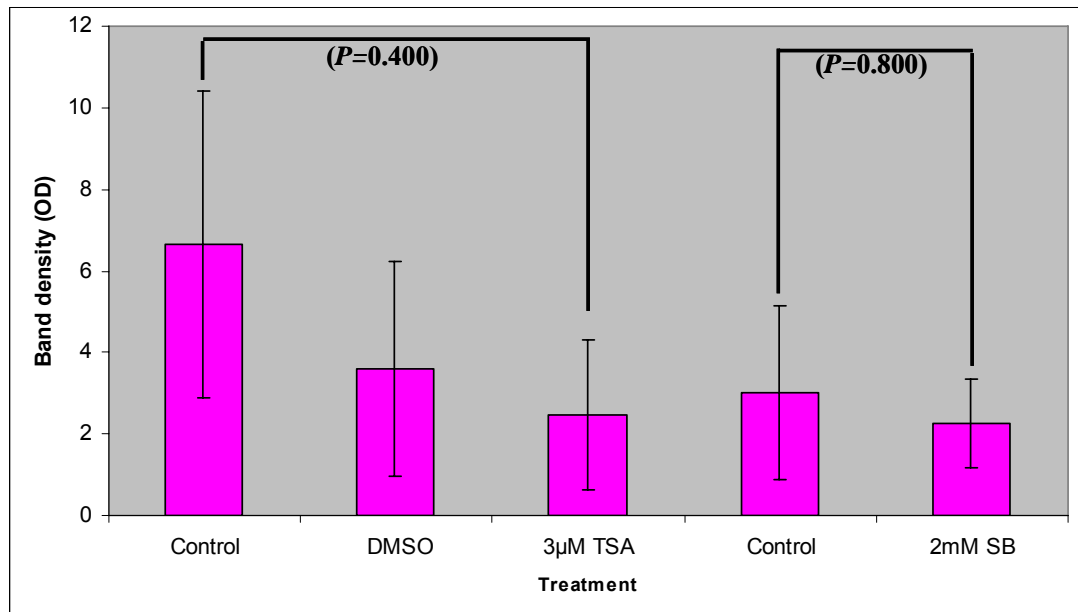


Figure 4.45: Quantification of band density derived from western blot data in Figure 4.44 using densitometry to quantify the effect of 3µM Trichostatin A and 2mM sodium butyrate on K13 protein expression in simple epithelial cervical carcinoma derived HeLa cells. There was no significant difference in the K13 protein expression in presence of Trichostatin A and sodium butyrate in comparison to control ($P=0.4$ and $P=0.8$) in HeLa cells (pink). Each K13 band has been normalised to β -actin band density (loading control). The results are expressed as the mean \pm SD from three experiments. HeLa cells were chosen because initially they showed the lowest K13 protein expression after RTS3b cells (Figure 4.41).

4.5 Discussion

The K13 FL promoter and deletion constructs showed expression in both permissive (SCC25) and non-permissive (RTS3b, HeLa and HFF) cell lines. This may be due to the chromatin structure playing an important role in the differential control of gene expression in eukaryotes. This is exemplified when tissue-specific genes are transcribed following transfection into cells which do not express their endogenous chromosomal counterparts, and are also transcribed *in-vitro* as purified DNA when added to extracts from non-expressing cells (Workman et al, 1990).

The quantitative FACS data of K13 FL promoter expression were not significantly increased in oral SCC25 cells in comparison to non-permissive epithelial RTS3b, HeLa and non-epithelial HFF cell lines. At the protein level, K13 expression was greater in oral SCC25 cells in comparison to non-permissive epithelial RTS3b, HeLa and non-epithelial HFF cell lines. The K13 FL promoter and protein expression shows epithelial specificity, since its expression is negligible in HFF, which do not normally express keratins. This finding is also consistent with the literature (Blessing et al, 1989 and Jiang et al, 1990) in which an enhancer in the upstream region of the bovine keratin 6 gene conferred epithelial specific expression and a 300bp upstream sequence of keratin 14 driven CAT reporter gene was shown to confer epithelial specificity.

Although K13 protein is not normally expressed in the epidermis, K13 protein was expressed in cultured epidermal-derived RTS3b cells; this K13 expression has also been reported in earlier studies in which K13 protein is expressed in cultured epidermal cells (Kopan et al, 1987). Thus although K13 expression is absent in the normal epidermis, its up-regulated in squamous cell carcinoma of the skin (Kopan et al, 1987). Furthermore, since the RTS3b cell line is transformed with HPV-16 and passaged many times, it could have acquired genetic instability and hence abnormal expression of keratins. This inherent flaw associated with the use of transformed cells is one of the disadvantages in using cell culture models and must be considered at the initial stage when choosing models. Also several factors have been reported to influence keratinocyte differentiation, namely the age of the epithelium donor from which the monolayer was derived, the serum, retinoic acid and calcium concentration in the growth medium (Gasparoni et al, 2004). The serum in the media contains

retinoic acid, which has been shown to influence the expression of K13 expression in skin (Kopan et al, 1987). The medium used to culture or grow RTS3b cells was E4/F12 medium with RM⁺ supplement which contains a calcium concentration of 1.5-1.8mM, as well as extra growth hormones, as opposed to other types of medium such as E4/F12 media alone without the RM⁺ supplement which contains 1.2-1.5mM calcium.

The K13 truncated promoter fragments revealed that the K13 FL promoter 3018bp could drive GFP expression in all the epithelial cells but not in the HFF cells (non-epithelial). Secondly a suppressor element that confers K13 promoter tissue specific expression in oral SCC25 cell lines resides in the K13 FL (between -3018bp to -2540bp) promoter construct (Figure 4.46). The K13 FL promoter construct and deletion fragments (R1-R6) promoter appear to show increased expression in HeLa cell line in comparison with SCC25 cells that endogenously expresses K13. Many factors could shed light in these findings, such as: 1) the endogenous K13 gene might be permanently shut off in HeLa cells by DNA methylation at the time the HeLa cell type embarks on simple epithelial as opposed to a stratified, differentiation pathway (Jiang et al, 1990). This however, is unlikely, as one report (Waseem et al, 1998) suggests that human K13 gene, unlike its mouse counterpart, is not regulated by DNA methylation. Alternatively, 2) the 3018bp 5'-upstream K13 promoter sequence may contain all the necessary regulatory motifs but lack specific structural constraints imposed by the local chromosomal structure (Wu et al, 1993), which normally switches off K13 expression in the epidermis and simple epithelial tissues. Also, 3) it could be that the 3018bp K13 upstream promoter region might contain all the necessary information for conferring epithelial specificity but not all the necessary information for oral tissue specific expression (Wu et al, 1993). Lastly, HeLa was derived from an adenocarcinoma of the cervix in 1952 and was the first human epithelial cancer cell line established for long-term culture manipulation and as result it has become genetically unstable. Karyotyping has revealed 20 abnormal chromosomes in HeLa cells including chromosome 17 where K13 is expressed (Macville et al, 1999), and this might cause increased K13 expression.

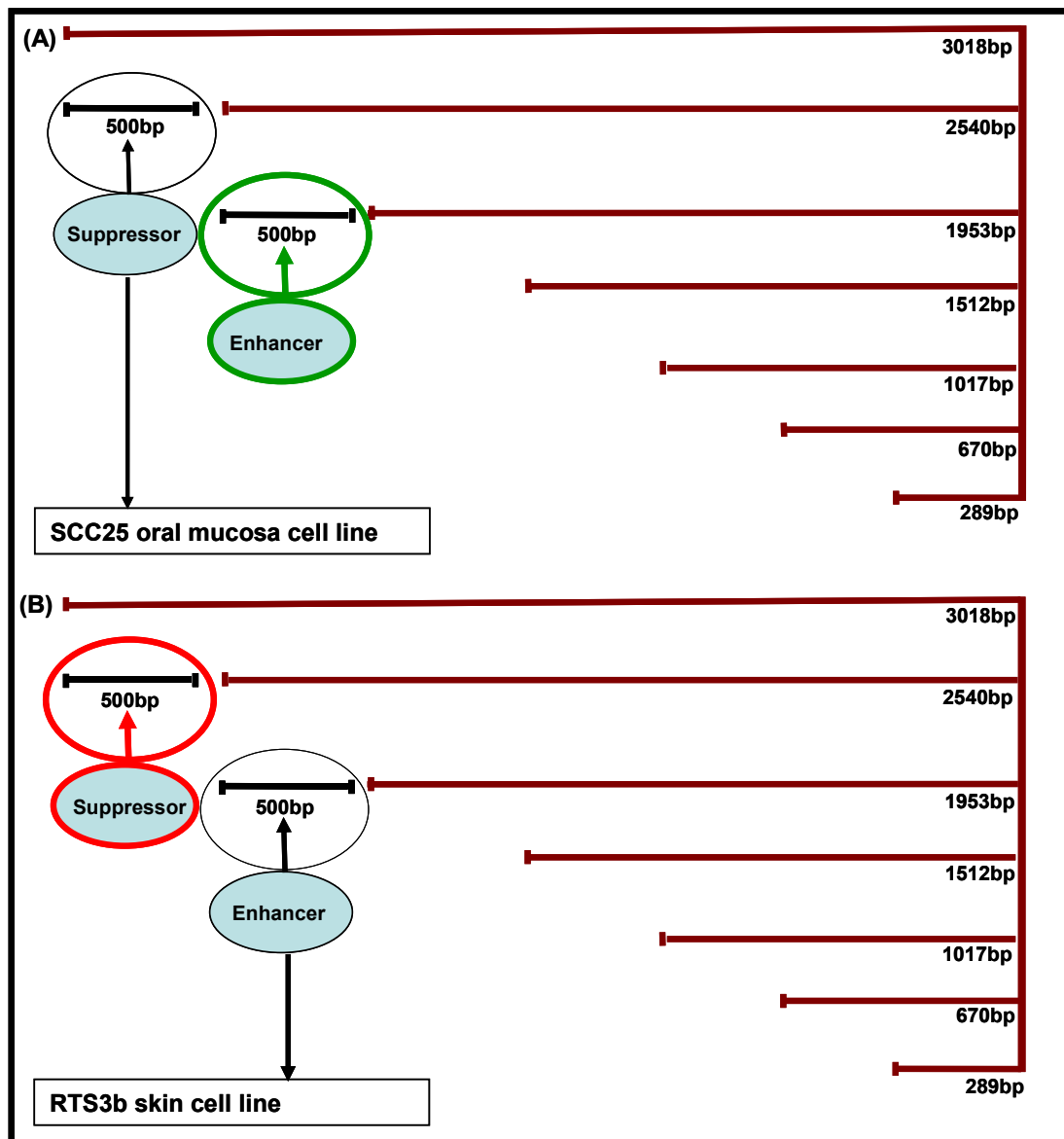


Figure 4.46: Diagram showing regions important for the regulation of K13 promoter expression in oral SCC25 and skin RTS3b cell lines. Diagram A shows a positive regulatory element (green) which binds fragment 2540bp when 1000bp has been removed from the full length K13-3018bp promoter fragment in permissive oral mucosa SCC25 cell line, which might be causing increased K13 promoter driven GFP expression in oral SCC25 cell line. Diagram B shows a negative regulatory element (red) which binds fragment 2540bp when 500bp has been removed from the FL K13-3018bp promoter fragment in epidermal derived RTS3b cell line, which might be causing decreased K13 promoter driven GFP expression in RTS3b cells. This indicates that the K13 promoter driven GFP expression in non-permissive epidermal RTS3b cells might be regulated by suppressor elements.

Furthermore, it is worth mentioning that although the diagram shown in Figure 4.46 only shows regulatory elements which seem important for the expression of K13 FL promoter construct in oral SCC25 cells versus epidermal RTS3b cells, there could

equally be other important regulatory elements which could have been tested if a larger K13 upstream sequence had been analysed.

Protein kinase C is known to be essential for the expression of differentiation and proliferation related genes in keratinocytes (Yuspa et al, 1991) and tumour-promoting TPA causes the release of *in-vitro* Ca²⁺ activated phospholipid-dependent protein kinase C (Castagna et al, 1982). This leads to activation of PKC by diacylglycerol and TPA activates PKC by mimicking the action of diacylglycerol, which is a natural ligand and activator of PKC (Castagna et al, 1982). TPA increases morphological differentiation, a change that is accompanied by an increase in the expression of keratinocyte-specific differentiation markers (Efimova et al, 1998). Given that K13 is a suprabasal keratinocyte-specific differentiation marker, it was thought that TPA might increase the activity of K13 protein expression. However, the results have shown that K13 expression is not induced through the protein kinase C pathway, since TPA did not increase the expression of K13 promoter construct or K13 protein. In addition, TPA had no effect on the K13-1953bp deletion fragment. The K13-1953bp deletion fragment was included in the TPA experiment for the following reason; TPA had no effect on FL K13-3018bp promoter and it could be argued that the suppressor elements in the K13-3018bp FL promoter construct could be opposing TPA overall effects on K13 expression. This might be overcome by directly adding TPA to the K13-1953bp deletion fragment of the K13 FL promoter; also the K13-1953bp deletion promoter fragment contains a cluster of AP-1 binding sites (Table 4.1). Furthermore, protein kinase C has been reported to be implicated in the regulation of several transcription factors such as AP-1 and NF-Kb (Richard et al, 1999). Given that AP-1 and NF-Kb have been reported to regulate the expression of K5, K6, K14 and K17 (Ma et al, 1997) and the K13-1953bp deletion fragment contains a cluster of AP-1 binding sites it would seem logical to investigate the effect of TPA on this fragment.

The results obtained for the effect of MEK 1/2 and PI3K/Akt pathway inhibition on K13 expression are similar to the results obtained previously (Dackour et al, 2005). In the Dackour study, an oesophageal carcinoma derived cell line was used, while in this study an oral SCC25 cell line was used, so the anatomical location under which K13 is expressed and the functional manifestations as a result of K13 aberrant

expression in oesophageal and oral cancer may differ. Thus, the pathways through which K13 aberrant expression is induced might or might not be the same in both oesophageal and oral cancer, therefore to address the importance of these pathways, known inhibitors affecting K13 expression were used.

The finding that the inhibition of the MEK 1/2 pathway not increasing K13 protein expression in oral SCC25 cells is parallel to others reports for epidermal specific K1 differentiation marker in mouse skin (Dackour et al, 2005). Also, mechanical stretching of human epidermal keratinocyte cell layers for 24 hours was concomitant with suppression of K10 which was further reduced in expression by U0126 (MEK 1/2 inhibitor). This indicates that keratinocyte mechanical stretching (which occurs at times during pregnancy and wound healing) suppresses keratinocyte differentiation, as evident by further reduction in K10 expression (Yano et al, 2004). These results imply that although the MEK 1/2 pathways regulate the expression of differentiation markers of human oral mucosa (K13) and skin (K1) in the same manner, it may affect the expression of K1 compared to its partner K10 differently (which could be explained by the fact that both studies utilized different species; mouse and human). LY249002 (PI3K/Akt pathway inhibitor) caused a significant decrease in the expression of the K13 promoter construct and protein expression in oral SCC25 cells, which implies the importance of the PI3K/Akt pathway in altered differentiation of oral mucosa. Furthermore, recent reports have shown that the inhibition of the PI3K/Akt pathway and transducing cells with the dominant negative form of PI3K increased the expression of K1/ K10 in normal human skin keratinocytes (Sayama et al, 2002). Thus, the same pathways which regulate the expression of suprabasal keratin genes might have different effects on the induction of keratin expression.

Sodium butyrate caused an increase in K13 protein expression in skin derived RTS3b cells, which suggests that in non-permissive skin derived RTS3b cells, K13 protein expression might be decreased in comparison to permissive oral mucosa SCC25 cells, because the chromatin structure in skin is in a heterochromatin state. These experiments were repeated on three separate occasions and on three different lysate samples. Sodium butyrate is a non-selective histone deacetylase inhibitor, thus it is arguable that it might be causing increased K13 gene transcription and subsequently protein expression through other unknown indirect pathways rather than influencing

the acetylation state of nuclear core histone gene expression. Nevertheless, the importance of sodium butyrate in increased K13 gene transcription, and hence K13 protein expression, is a step towards understanding why K13 protein is not expressed in normal epidermis.

In conclusion, this study has shown that the K13 promoter is expressed in an epithelial specific manner, and a suppressor element which confers this epithelial specific expression resides in the full length K13-3018bp promoter. K13 protein expression is induced by sodium butyrate which might or might not be through an alteration of chromatin structure in non-permissive skin derived RTS3b cells. The MEK 1/ 2 pathway seems not to be necessary for the expression of K13, but the PI3K pathway is important for expression of K13 in oral mucosa.

Chapter 5

The Correlation of K15

and K13 Expression

with Oral Cell Line

Maturation

5.1 Introduction

Differentiation is process whereby cells undergo a change to become a specialized cell type within a tissue (Alberts et al, 1994). In the previous chapter, differentiation related K13 expression in both oral mucosa and skin was discussed. This chapter will focus on the maturation related K15 and K13 expression pattern in oral cell lines. In both maturation (Figure 5.2) and differentiation (Figure 5.1), keratin expression varies in different epithelia of the body and also within specific regions of the body such as the oral mucosa which shows regional variation (Clausen et al, 1986). K15 and K13, represent basal and suprabasal markers of the oral mucosa and exemplify regional maturation in this tissue.

Barrandon and Green (1985) showed that cultured keratinocytes isolated from epidermis form different types of colonies according to cell size. For example, cells of smaller size range (in a range of 11-20 μ m), produced small rapidly growing colonies in culture, while cells of diameter larger than 20 μ m did not divide and became committed to terminal differentiation. This indicates that cell size could be used to determine the clonal ability of human keratinocytes. When keratinocytes form colonies in culture, three different types can be distinguished. The small keratinocytes give rise to cells which have a high proliferative rate, termed holoclones, which are classified as the origin. Larger keratinocytes give rise to two other types of colonies: termed meroclones and paraclones. Meroclones contain a mixture of both growing and terminally differentiating cells, while paraclones give rise to cells with limited growth potential resulting in large and sparse colonies (Barrandon and Green, 1987). These three types of colonies are thought to be derived from stem cells, early and late amplifying cells (Mackenzie, 2006).

When cells are plated *in-vitro*, an earlier degree of maturation is associated with a different morphology. The unidirectional growth of the three types of colony, with holoclones being the founding colony type, followed by the sequential formation of meroclones and paraclones, shows that a paraclone colony cannot become a holoclone. Also when keratinocytes are passaged and plated *in-vitro* there is a regeneration of clonal heterogeneity in keratinocytes (Mackenzie, 2005). Suggesting that the generation of stem and amplifying cells is an inherent characteristic of

keratinocytes whether they are plated *in-vitro* or whether the keratinocytes are present within the *in-vivo* natural epithelium (Mackenzie, 2005).

In the previous chapter, the data presented suggested that subpopulations of oral SCC25 and skin derived RTS3b cells either express or not express K13; therefore, there is heterogeneity, and If this is the case there maybe be molecules expressed by colonies, that identify holoclones or paraclones.

Maturation in the oral mucosa epithelia involves sequential synthesis of specific basal and suprabasal keratin genes. This chapter aims to address whether keratin expression can be correlated with morphological heterogeneity typically found in oral malignant epithelial cell lines, by the use of K15, a marker of basal and K13, a marker of suprabasal buccal epithelial maturation or differentiation. Depending on the whether the result shows a positive correlation between increased K15 expression in holoclones in comparison to paraclones and increased K13 expression in paraclone in comparison to holoclones. It is anticipated that potential novel transcription factors associated with the maturation specific K15 and K13 expression in holoclones and paraclone cell population might be identified.

The K15 and K13 maturation specific expression will be studied by the use of stable transfection, FACS, colony forming assay and immunocytochemistry. There are several disadvantages of studying tumours *ex-vivo* and this includes the availability of tissue biopsies, constraint with conserving the tissue, heterogeneity that exists amongst tissues and the difficulty in isolating cellular components such as RNA from epithelial cells. For these reasons, the use of cell lines as an *in-vitro* model of the oral epithelium as opposed to using oral mucosa biopsies was adopted.

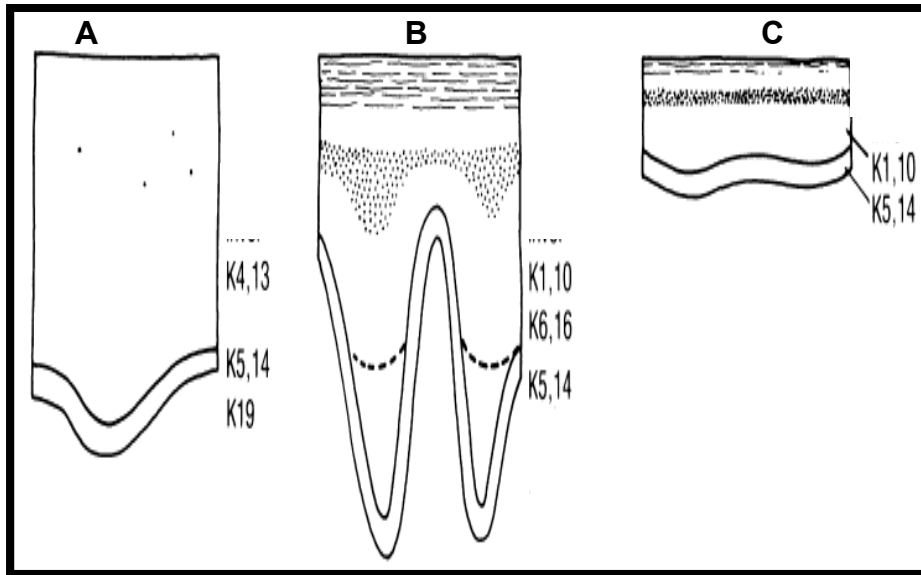


Figure 5.1: Differentiation of specific keratin expression in (A) buccal cells, which expresses K13/K4 in the suprabasal layer, while in the basal layer K5, K14 and K19 are expressed. In diagram (B) palate epithelia is shown, which expresses K1/K10 in suprabasal layer as well as K6/K16 and K5, K14 in the basal layer, while in diagram (C) a epidermal epithelia is shown, which expresses K1/K10 in the suprabasal layer and K5, K14 in the basal layer (Dale et al, 1990).

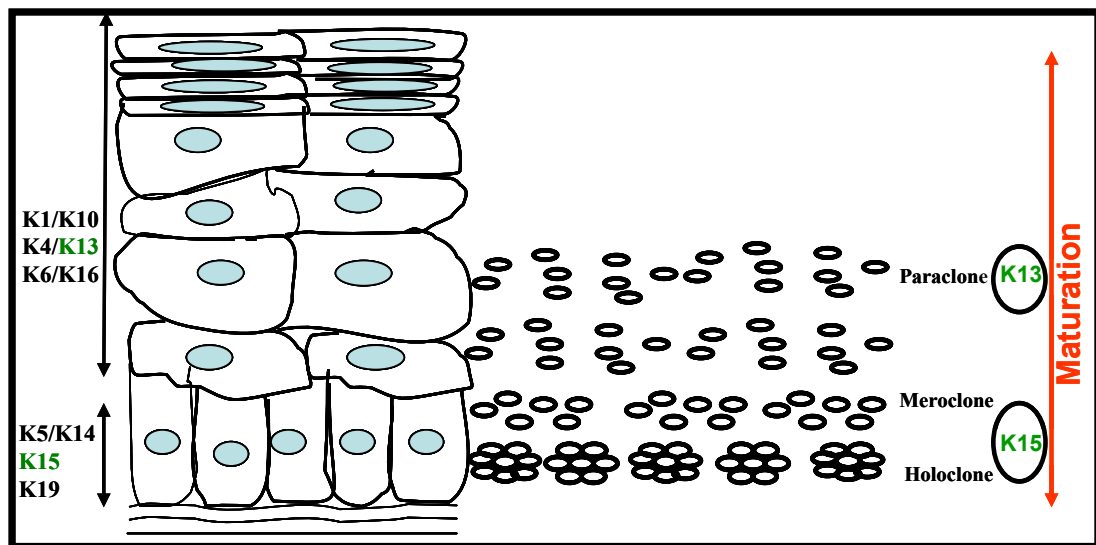


Figure 5.2: Schematic representation of maturation specific keratin expression in normal oral epithelium (on the left side of the diagram) as exemplified by K15, basal marker and K13, marker of buccal epithelial differentiation. While, on the right side of the diagram, the three distinct cell type populations known as holoclone, meroclone and paraclone are shown and in relation to where these different three subpopulation of cells are found relative to the *in-vivo* oral mucosa epithelia.

5.2 Aims

- 1) Stably transfect K13 and K15 promoter linked-GFP constructs into vulval epithelia carcinoma (A431) and oral mucosa (H357 and SCC25) derived cells lines, to see the level of K15 and K13 promoter linked-GFP expression.
- 2) To use the intensity score semi-quantitative method to determine whether K15 and K13 promoter linked-GFP expression can be correlated with a heterogeneous population within oral mucosal SCC25 cells, using FACS.
- 3) To use immunocytochemistry to investigate if endogenous K15 and K13 protein expression can be correlated with oral mucosa SCC25 cell differentiation, using A431 cell as positive control.
- 4) Use a colony forming assay to test if the pre-selected and FACS sorted oral mucosa SCC25 cells expressing K15 and K13 promoter linked-GFP positive cells can be correlated with the number of colonies formed.

5.2.1 Hypothesis

It is hypothesized that K15 and K13 expression is correlated with heterogeneous cell population present within the differentiating oral epithelial cell line.

5.2.2 Materials and Methods

For a detailed protocol of how the stable transfection, immunocytochemistry, colony forming assay and FACS was carried refer to Chapter 2 sections 2.10.3, 2.18 to 2.18.3.

5.3 Results

5.3.1 RNA extracts of K15 and K13 in Holoclones and Paraclones using Affymetrix HG-U133A Arrays.

Pilot experiments with RNA extracts of K15 and K13 from holoclones and paraclones using Affymetrix HG-U133A gene expression arrays in various head and neck tumour derived cell lines formed the preliminary data (Figure 5.3 and 5.4) which provided the hypothesis as to whether K13 and K15 promoter constructs expression can be correlated with oral mucosa cell line maturation. This data was kindly provided by Professor I. C. Mackenzie. Given that K15 is expressed in the basal layer and is a marker of proliferative potential and K13 is expressed in the suprabasal layer and is a marker of differentiation, it is thought that the expression of K15 should be high in holoclone and K13 high in paraclone colonies.

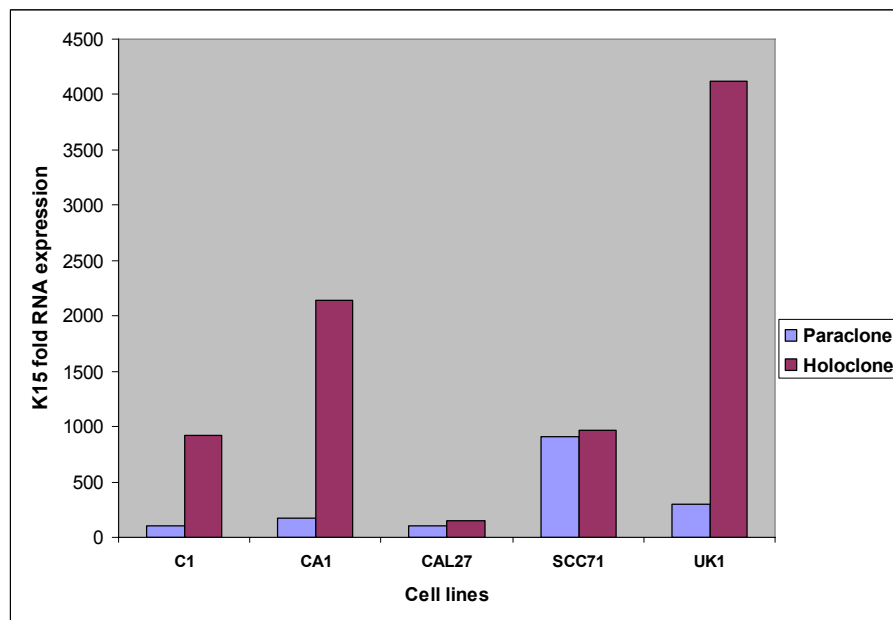


Figure 5.3: K15 RNA expression level in paraclones and holoclones of C1, CA1, CAL27, SCC71 and UK1 oral mucosal tumour derived cell lines.

K15 RNA expression was high in holoclone colonies formed by three cell lines (C1, CA1, and UK1). K13 RNA expression was low in paraclones and high in holoclone colonies formed by three cell lines (C1, CA1, CAL27 and SCC71). Although the increased K15 RNA expression in holoclone colonies is consistent with the *in-vivo* environment of the oral epithelium, but the increase in K13 expression in holoclone colonies was inconsistent with the role of K13 as a marker of differentiation in the oral mucosa. However, this experiment was only done once on pooled holoclone or

paraclone colonies, so the data may not be a true biological reflection of K13 expression, hence the reason why the work went further and few different methods was used to confirm this preliminary findings.

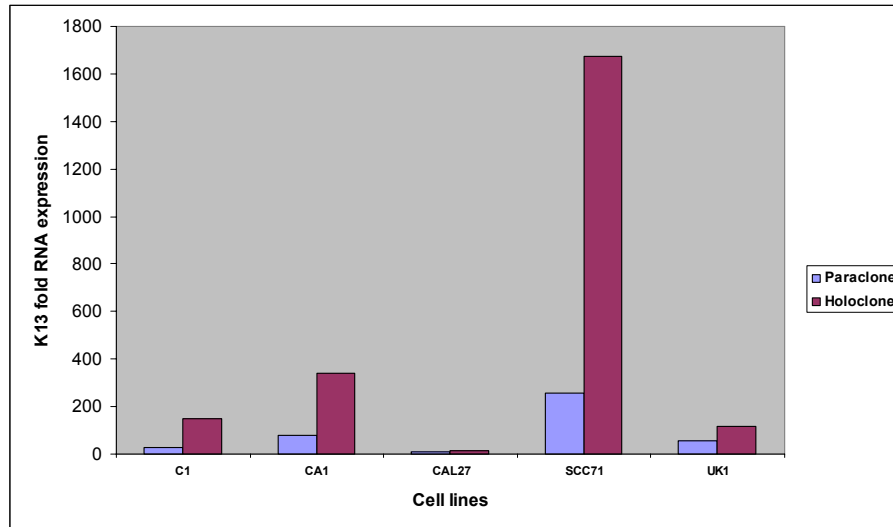


Figure 5.4: K13 RNA expression level in paraclone and holoclone of C1, CA1, CAL27, SCC71 and UK1 oral mucosal tumour derived cell lines.

5.3.2 K15 and K13 Promoter driven GFP Expression in Oral (SCC25, H357) and (A431) Vulval Carcinoma Cell Lines.

K15 and K13 promoter linked GFP reporter gene construct expression was initially assessed by stable transfection into oral (H357, SCC25) and vulval (A431) cell lines. A431 cells were used as a positive control, since these cells are known to express both K15 and K13 abundantly. However, the transfection efficiency of K15 and K13 promoter construct in H357 and A431 was very low (Figure 5.5 and 5.6). For this reason, all subsequent K15 and K13 promoter linked GFP reporter gene construct expression experiments were carried out in the oral SCC25 cell line, as this cell line shows high K15 and K13 promoter expression (Figure 5.7).

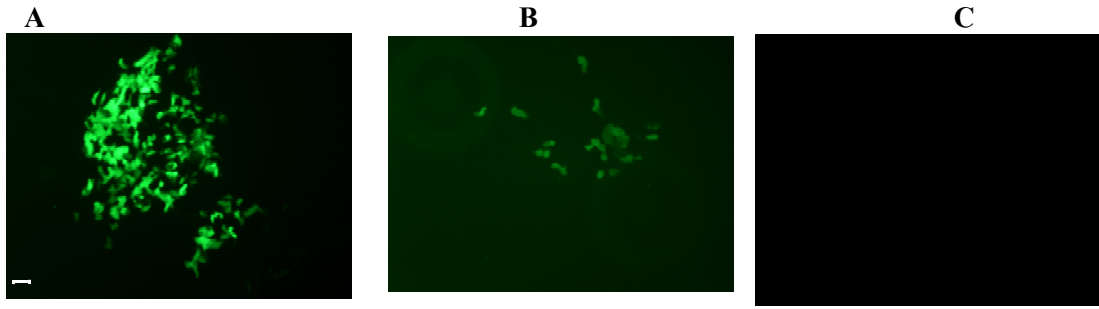


Figure 5.5: EGFP expression in A431 vulval carcinoma cell line stably transfected with CMV (A), K13 (B), and K15 (C) promoters in pEGFP-N3B vector. The cell population was photographed using a fluorescence microscope and the picture magnification is 100x. GFP expression was detected with blue light. Scale bar: 50 μ M, same for Figure 5.5 and 5.6). The EGFP expression of K13 (B) and K15 (B) promoter constructs are negligible in A431 cells.

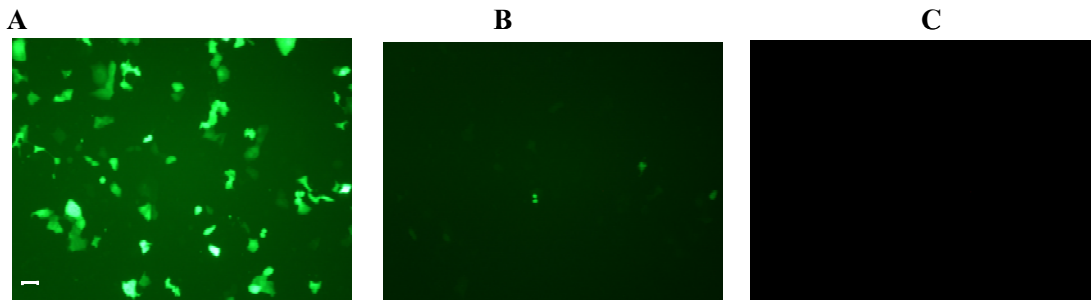


Figure 5.6: EGFP expression in H357 oral mucosa cell line stably transfected with CMV (A), K13 (B), and K15 (C) promoters in pEGFP-N3B vector. The cell population was photographed using a fluorescence microscope and the picture magnification is 100x. GFP expression was detected with blue light. The EGFP expression of K13 (B) and K15 (B) promoter constructs are negligible in H357 cells.

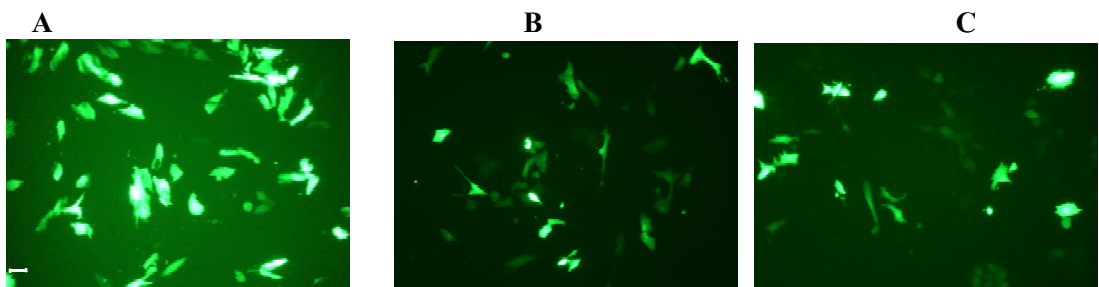


Figure 5.7: EGFP expression in SCC25 oral mucosa cell line stably transfected with CMV (A), K13 (B), and K15 (C) promoters in pEGFP-N3B vector. The cell population was photographed using a fluorescence microscope and the picture magnification is 100x. GFP expression was detected with blue light. The EGFP expression of K13 (B) and K15 (B) promoter constructs are very high in SCC25 cells.

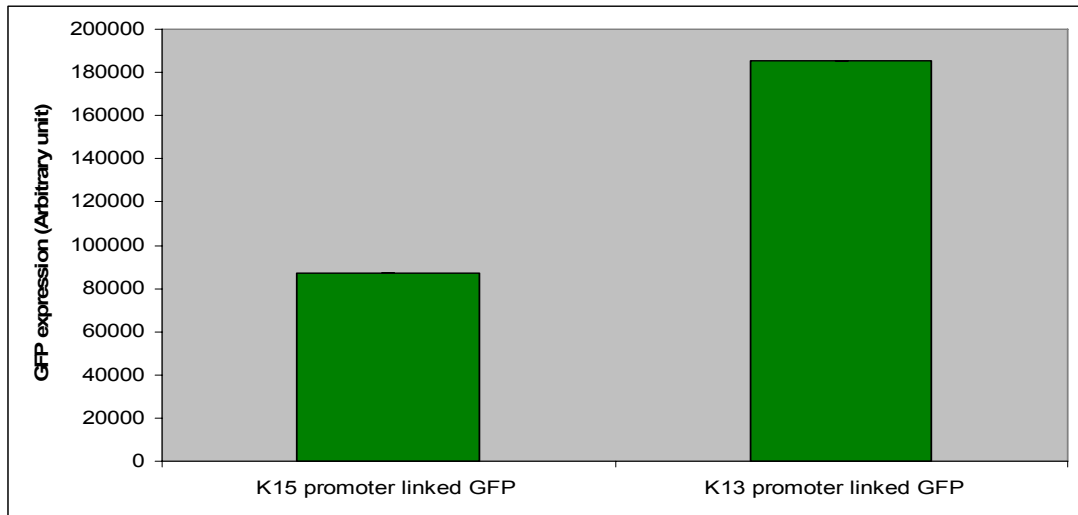


Figure 5.8: The expression of K15 and K13 promoter linked GFP construct expression in oral mucosa SCC25 cell line. This was done to determine the initial expression of both K15 and K13 promoter constructs in oral mucosa cell line (SCC25).

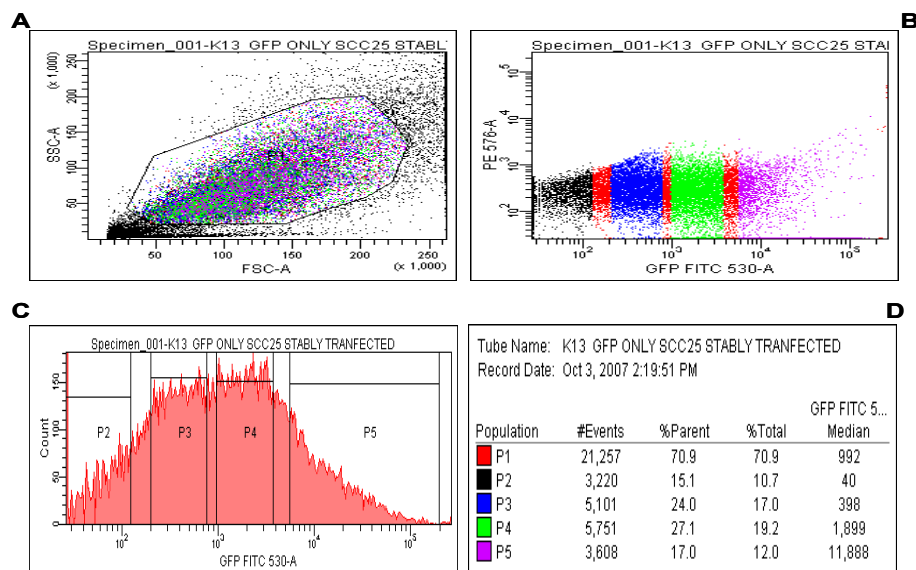


Figure 5.9: Representative plots of typical FACS data obtained for K13 promoter linked GFP construct expression in oral mucosa SCC25 cells after selecting for several weeks. Image A shows a scatter of the total cell population gated to exclude cell debris, Image B shows scatter plot based on image A, but divided into four (no expression, low, medium and high) distinct GFP expressing cell populations using FACS. Image C shows a histogram of the four distinct GFP expressing cell populations and image D shows the percentage of cells within each population expressing K13 promoter linked GFP construct and median fluorescence intensity of each of the four distinct GFP expressing cell populations. The colours used for the different four cell population are the same in image B and image D, black (P2) coloured cell population are those population which show no GFP expression, while the blue (P3) coloured cell population are those population which show low GFP expression. The green (P4) coloured cell population are those population which show medium GFP expression and the purple (P5) coloured cell population are those population which show high GFP expression. The red (P1) coloured cell population shown in image A, B, C and D are total gated cell population.

5.3.3 Stably Transfecting and Selecting the K15 and K13 Promoter Construct in Oral SCC25 Cell Lines.

After initially establishing the effectiveness of GFP expression of the K15 or K13 promoter constructs using FACS (Figure 5.8), the K15 and K13 promoter constructs were then stably transfected in oral SCC25 cells and selected for about a month. The oral SCC25 cells were then sorted according to the four distinct populations (Figure 5.10). In Figure 5.10, the FACS data of the EGFP expression of K15, K13 and CMV promoter in pEGFP-N3B vector are shown. In the negligible GFP expressing cell population, it can be seen that all three promoter constructs show the same level of GFP expression. This is also true for the low GFP expressing cell population, which shows low GFP expression (Figure 5.10). However, in the cell population, which shows medium and high GFP expression for K15, K13 and CMV promoter in pEGFP-N3B vector, the results are similar, in that the K15 promoter shows the lowest expression followed by CMV promoter and then the K13 promoter, which shows the greatest GFP expression. These results were unexpected, given the fact that CMV promoter was used as a positive control and should ideally show the highest GFP expression. The aim of this part of the study was to use the CMV promoter as a positive control for stable transfection, it might not be of value, it should be noted that in chapter 4, the expression of CMV promoter compared to K13 promoter was 10-30 fold higher. This might be explained by the fact that transient transfection was used in the experiments carried out in the previous chapter, while in this chapter stable transfection was used (Figure 5.10). It is possible that the transient versus stable transfection of plasmid constructs can cause a difference in the expression pattern of constitutive (K13) expressed gene versus the stronger viral (CMV) exogenous expressed gene. Furthermore, in Figure 5.11, phase contrast and GFP fluorescence of oral SCC25 cells are shown. These pictures were taken after selecting and FACS sorting the oral SCC25 cells for about a month to confirm that the sorted K15 and K13 promoter constructs stably transfected into SCC25 cells respectively contained negative and high GFP expressing cell populations. Figure 5.11 shows pictures of several paraclone and holoclone colonies formed by negative (Figure 5.11 E1 to H1) and high (Figure 5.11 A1 to D1) GFP expressing SCC25 sorted cells. The negative and high GFP expressing oral SCC25 cells contain K15 promoter linked GFP constructs (Figure 5.11). Although in Figure 5.11 F1 and G1, which are the GFP negative SCC25 sorted cells that contain the K15 promoter linked GFP construct,

they do however show K15 GFP positive cells. One possible explanation for this dubious result could be when the FACS machine was used to sort cells, there could have been contamination of some high expressing GFP positive cells sorted into GFP negative oral SCC25 cells.

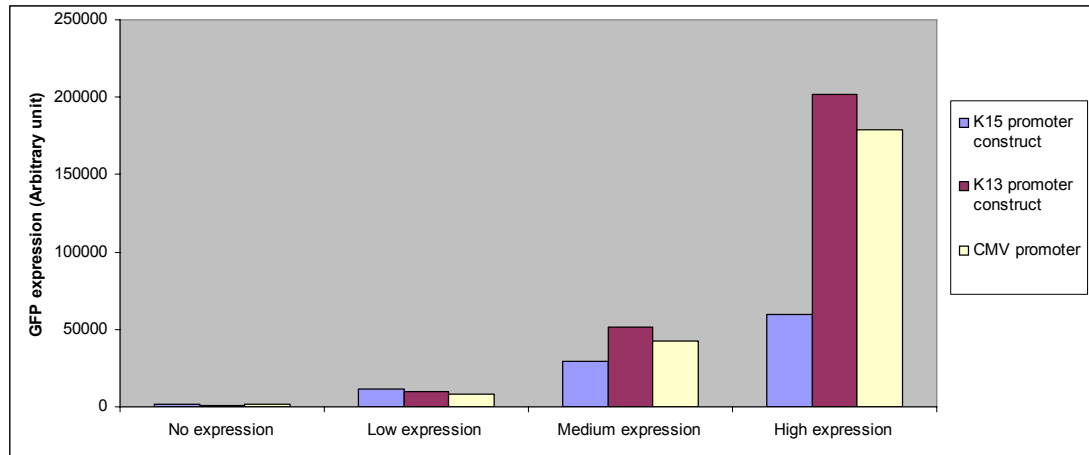


Figure 5.10: EGFP expression in oral SCC25 cells containing K15, K13 and CMV promoter in pEGFP-N3B vector. After stably transfecting the K15, K13 or CMV promoter driven GFP in pEGFP-N3B vector expression in oral mucosa SCC25 cells after have been sorted into four distinct cell population, using CMV promoter as a positive control for the transfection efficiency.

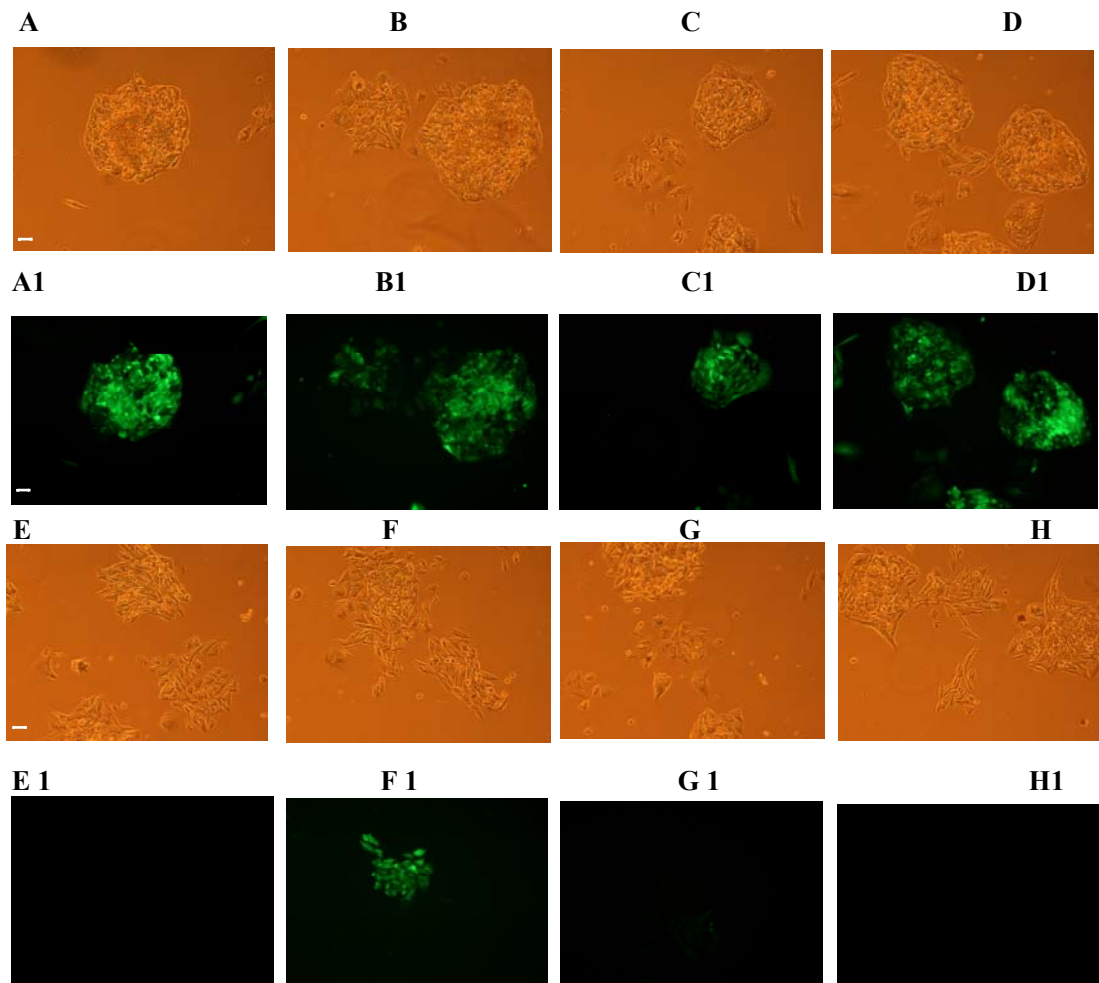


Figure 5.11: Brightfield and fluorescence pictures of holoclone and paraclone colonies formed by oral SCC25 cells stably transfected with K15 promoter in pEGFP-N3B vector. The images show the distinct populations of plated cells after G418 (1mg/ml) selection for a month, and FACS sorted into GFP negative and GFP high expressing cell populations. Images A to D are brightfield view of holoclone colonies formed by high GFP expressing SCC25 cells, while images A1 to D1 are the corresponding fluorescence images of brightfield view images (A to D). Images E to H are brightfield view of paraclone colonies formed by negative GFP expressing SCC25 cells, while images E1 to H1 are the corresponding fluorescence images of brightfield view images (E to H). An inverted Fluorescence microscope was used to take above images and the image magnifications are 100x the original size, the scale bar for each image is 50 μ M.

5.3.4: The Correlation of K15 and K13 Promoter driven GFP High and Negative Expressing Oral SCC25 Cells with the Colony Forming efficiency of Oral SCC25 cell line

The colony forming ability of both K15 and K13 promoter construct in negative and high GFP expressing oral SCC25 cells was assessed, and the results showed that there was is no significant difference between the expression of K15 and K13 promoter construct in negative and high GFP expressing oral SCC25 cells. However,

the K15 negative and high expressing cells had more colonies compared to K13 negative and high GFP expressing SCC25 cells (Figure 5.13). This indicates that K15 might be used as a potential marker of cell proliferation (Porter, et al. 2000), but the fact that there was no significant difference between K15 and K13 negative and high GFP expressing SCC25 cells shows that K15 and K13 promoters expression cannot be correlated with oral SCC25 cell maturation. In addition, Figure 5.12, shows a representative image of the colony forming assay, and each well was analysed for the number of SCC25 cells colonies formed which were respectively transfected with the K15 and K13 promoter constructs. The black lines (Figure 5.12) were created using Adobe Photoshop Image Software to facilitate counting the number of SCC25 colonies formed.

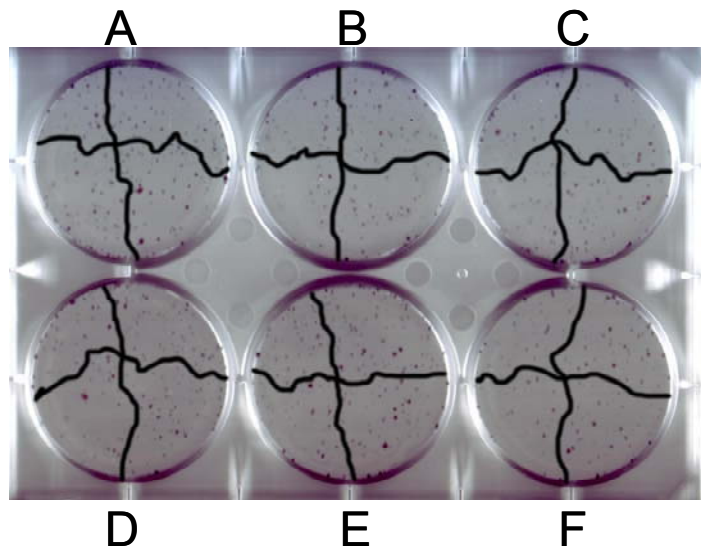


Figure 5.12: A representative image of the colony forming assay used for negative GFP expressing oral SCC25 cells, containing the K15 and K13 promoter construct, plated at clonal density and fixed with Rodamine B. Each experiment was performed in triplicate. Images A to C show colonies formed by selected SCC25 GFP negative cells containing K15 promoter construct, plated at colony density and selected with G418 (1mg/ml) for 2 weeks. While, images D to F show colonies formed by selected SCC25 GFP negative cells containing K13 promoter construct, plated at colony density and selected with G418 (1mg/ml) for 2 weeks. The numbers of colonies formed by K15 and K13 promoter linked GFP expressing SCC25 cells were analysed using image software and black lines in each well were used to facilitate counting colonies formed.

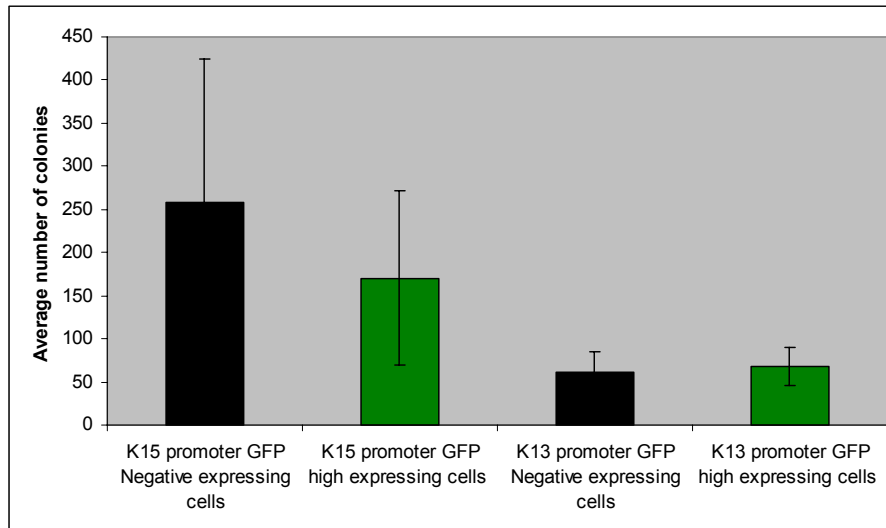


Figure 5.13: Number of colonies formed by negative and high expressing K15 and K13 promoter driven GFP expression in oral SCC25 cells. Results are expressed as the mean \pm SD from three experiments and each experiment was done in triplicate. There is no significant difference between negative and high GFP expressing SCC25 cells containing K15 promoter construct ($P=0.575$) or between colonies expressing GFP negative or GFP high SCC25 cells containing K13 promoter construct ($P=0.980$).

5.3.5: K15 and K13 Promoter Expression in Holoclone and Paraclone Cell populations formed by Oral Mucosa SCC25 Cells using the Promoter Intensity Scoring Method.

K15 and K13 promoter linked GFP reporter gene construct expression was initially assessed to detect whether promoter expression could be correlated with formation of the holoclone and paraclone colonies by oral SCC25 cells. The intensity of K15 and K13 promoter expression in holoclones and paraclones was assessed by observing the GFP intensity in each type of colony formed and allocating a number ranging from zero for negligible expression to three for strong expression (Table 5.1 and Figure 5.18). Based on this scoring, the results showed that the K15 promoter expression was twice as high in holoclone colonies as paraclone, while the K13 promoter expression was 4.5 times higher in paraclone colonies than holoclones (Figure 5.18). In addition, although these results seem interesting and blind scoring was used, it is however important to note that this type of GFP intensity measurement used is subjective and open to bias. However, FACS analysis was also utilized to confirm the data, given that this technique is quantitative and an accepted technique used for measuring GFP expression (Figure 5.20). In addition, holoclones in this experiment were defined morphologically as compact round colonies, while

paraclones were defined as colonies, which form loose irregular morphologies. However, it is arguable as to whether there is any difference in holoclone versus paraclone colony sizes and shape of images generated at 100x magnification in Figure 5.14 to 5.17. In retrospect, this might have been resolved by using a higher objective lens. In the images generated in Figure 5.14 to 5.17 the difference between low and background (no GFP expression) is undetectable at this magnification. This was why an initial FACS analysis was carried out to 1) sort the cells into four populations and 2) quantitate the GFP expression in the four populations (Figure 5.10 and 5.20). The results in Figure 5.10 clearly show a difference, although not significant, in negative and low GFP expressing SCC25 cell population. In summary, although the data generated with the GFP intensity scoring approach (Figure 5.18) as it stands does not appear convincing enough, it is however, a novel approach to quantify K15 and K13 promoter linked GFP expression in holoclone and paraclone colonies. The GFP intensity scoring approach could also benefit from stringent selection criteria for defining and choosing negative, low, medium and high GFP expressing SCC25 cells forming holoclone and paraclone colonies and this can be implemented in the future experiments.

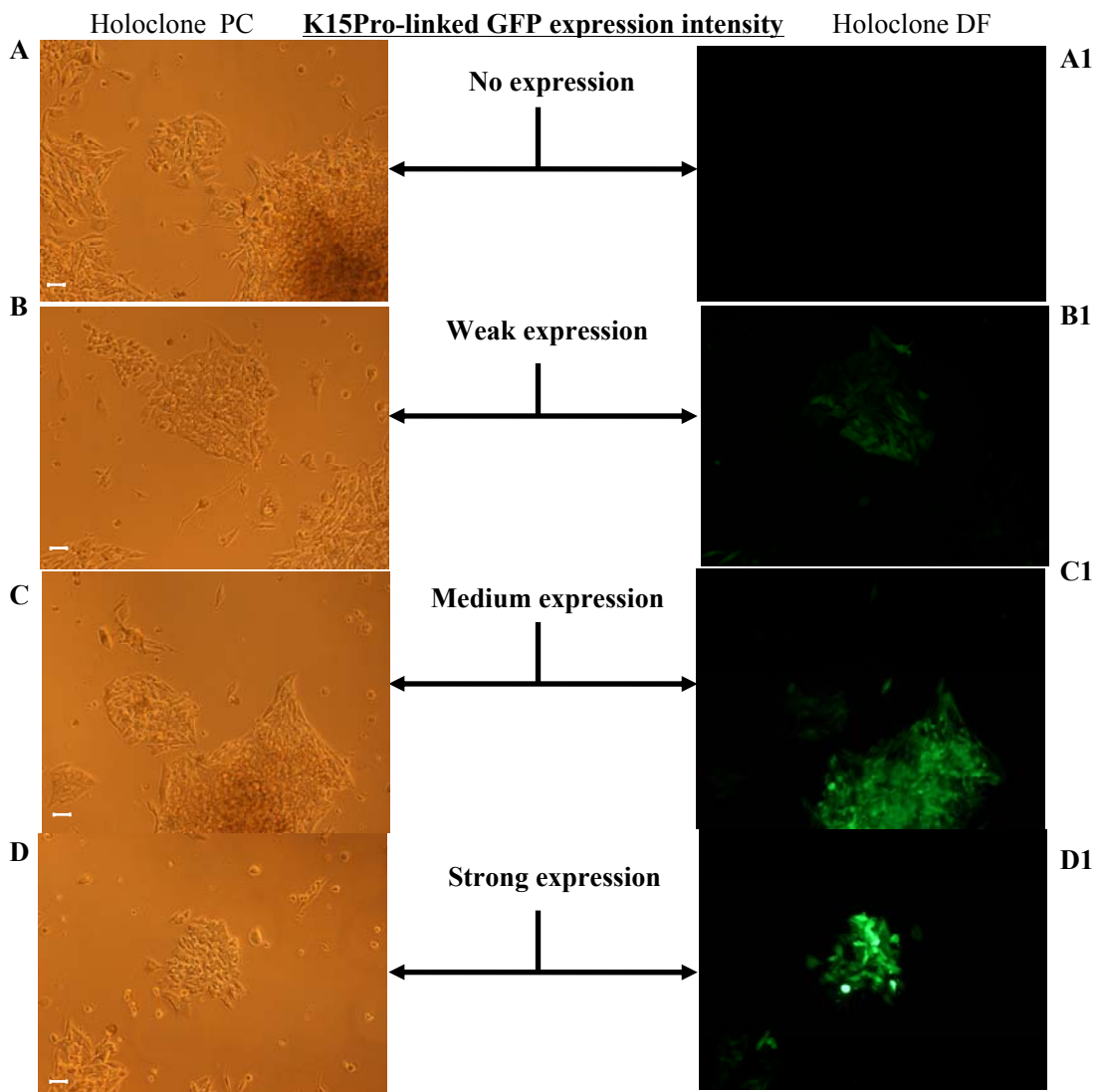


Figure 5.14: Brightfield and fluorescence images of holoclone colonies formed by oral SCC25 cells stably transfected with K15 promoter in pEGFP-N3B vector. The holoclone colonies formed by SCC25 cells were correlated with the intensity of K15 promoter construct. Image A and A1 show phase contrast (PC) and corresponding dark field (DF) view of holoclone colony showing negligible K15 GFP expression. Image B and B1 show phase contrast (PC) and corresponding dark field (DF) view of holoclone colony showing low K15 GFP expression. Image C and C1 show phase contrast (PC) and corresponding dark field (DF) view of holoclone colony showing medium K15 GFP expression. Image D and D1 show phase contrast (PC) and dark field (DF) view of holoclone colony showing high K15 GFP expression. Pictures were photographed using a fluorescence microscope and the image magnifications are 100x the original size, the scale bar on each image is 50 μ M.

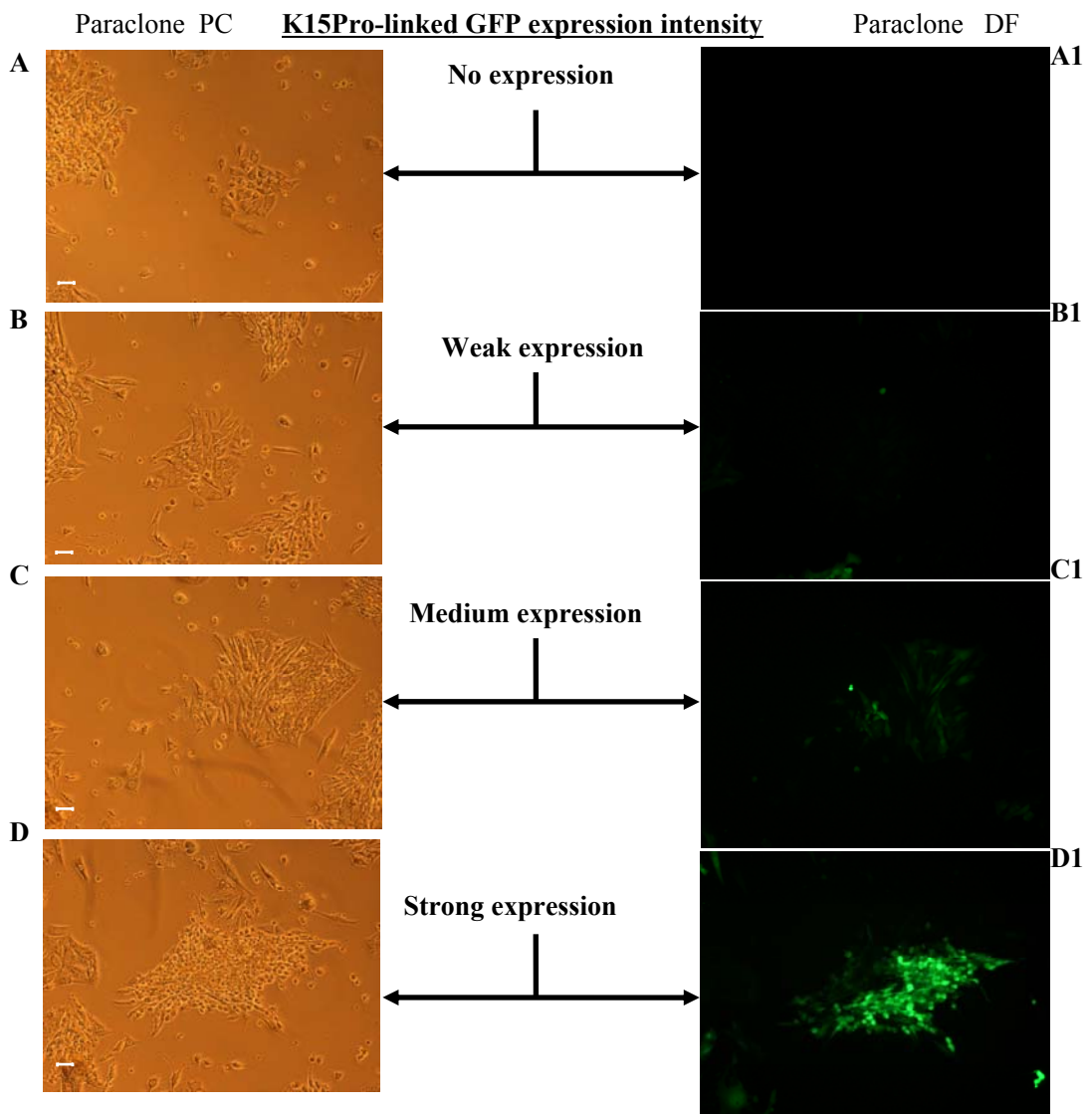


Figure 5.15: Brightfield and fluorescence images of paraclone colonies formed by oral SCC25 cells stably transfected with K15 promoter in pEGFP-N3B vector. The paraclone colonies formed by SCC25 cells were correlated with the intensity of K15 promoter construct. Image A and A1 show phase contrast (PC) and corresponding dark field (DF) view of paraclone colony showing negligible K15 GFP expression. Image B and B1 show phase contrast (PC) and corresponding dark field (DF) view of paraclone colony showing low K15 GFP expression. Image C and C1 show phase contrast (PC) and corresponding dark field (DF) view of paraclone colony showing medium K15 GFP expression. Image D and D1 show phase contrast (PC) and dark field (DF) view of paraclone colony showing high K15 GFP expression. Pictures were photographed using a fluorescence microscope and the image magnifications are 100x the original size, the scale bar on each image is 50 μ M.

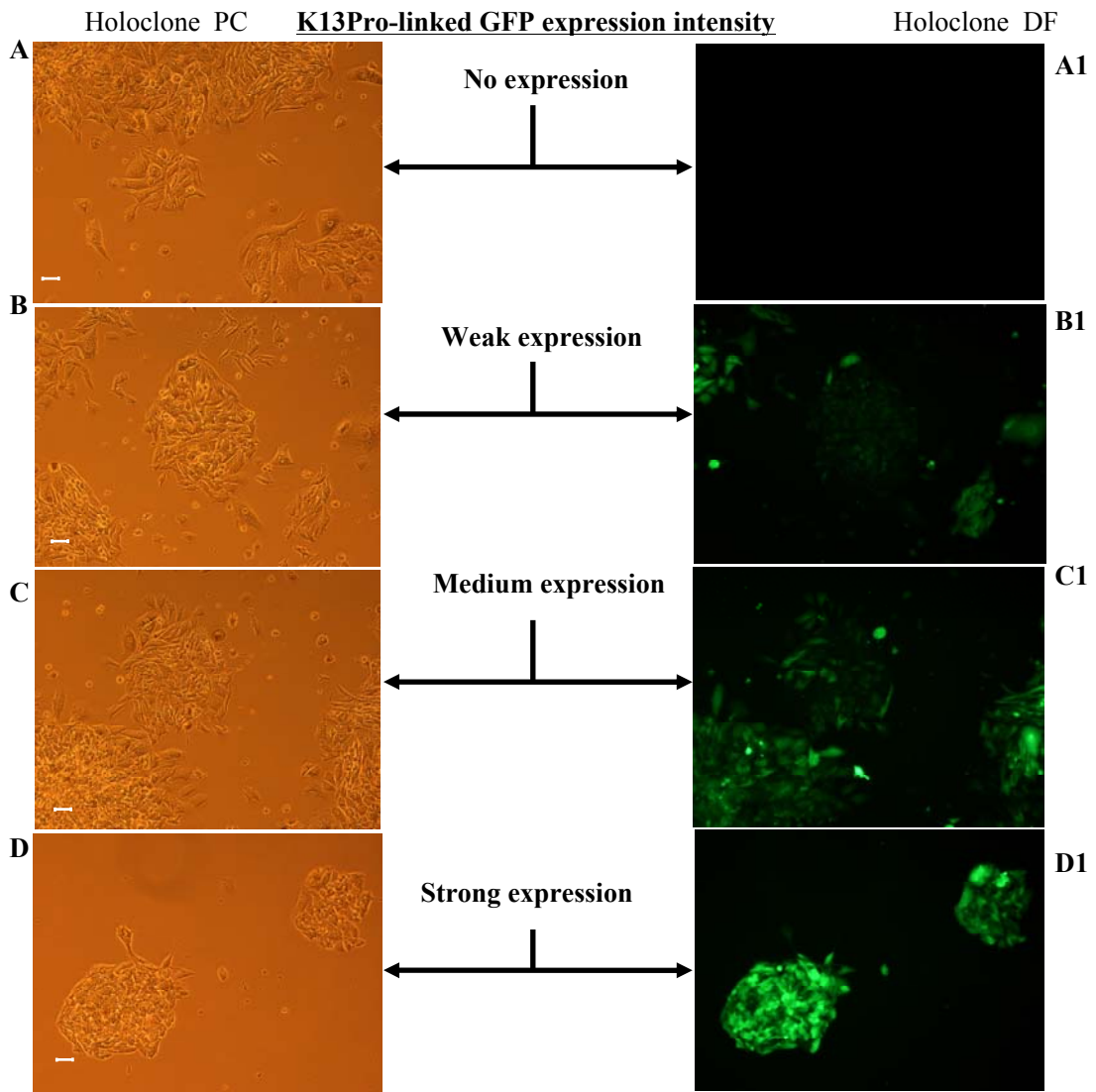


Figure 5.16: Brightfield and fluorescence images of holoclone colonies formed by oral SCC25 cells stably transfected with K13 promoter in pEGFP-N3B vector. The holoclone colonies formed by SCC25 cells were correlated with the intensity of K13 promoter construct. Image A and A1 show phase contrast (PC) and corresponding dark field (DF) view of holoclone colony showing negligible K13 GFP expression. Image B and B1 show phase contrast (PC) and corresponding dark field (DF) view of holoclone colony showing low K13 GFP expression. Image C and C1 show phase contrast (PC) and corresponding dark field (DF) view of holoclone colony showing medium K13 GFP expression. Image D and D1 show phase contrast (PC) and dark field (DF) view of holoclone colony showing high K13 GFP expression. Pictures were photographed using a fluorescence microscope and the image magnifications are 100x the original size, the scale bar on each image is 50 μ M.

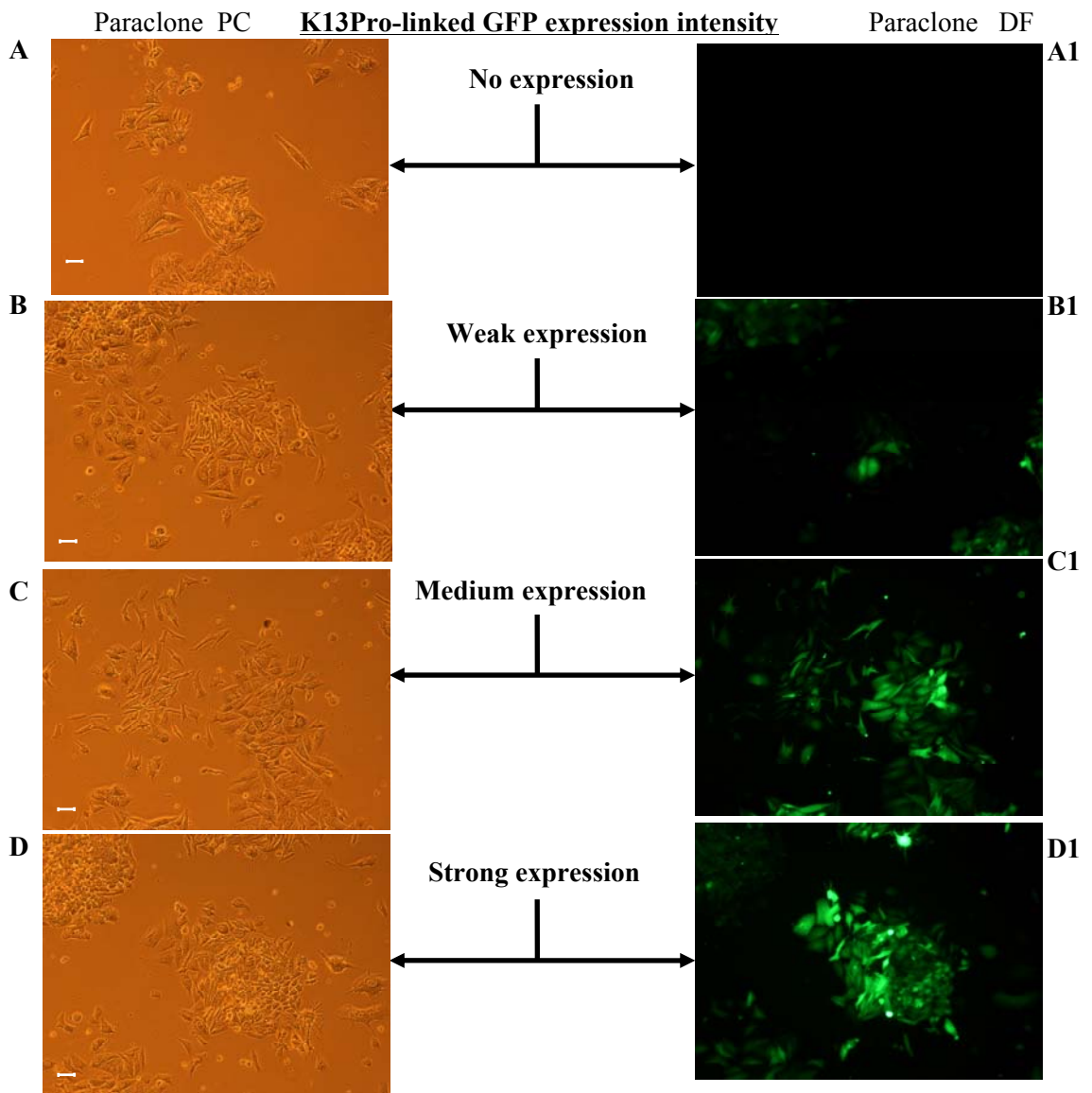


Figure 5.17: Brightfield and fluorescence images of paraclone colonies formed by oral SCC25 cells stably transfected with K13 promoter in pEGFP-N3B vector. The paraclone colonies formed by SCC25 cells were correlated with the intensity of K13 promoter construct. Image A and A1 show phase contrast (PC) and corresponding dark field (DF) view of paraclone colony showing negligible K13 GFP expression. Image B and B1 show phase contrast (PC) and corresponding dark field (DF) view of paraclone colony showing low K13 GFP expression. Image C and C1 show phase contrast (PC) and corresponding dark field (DF) view of paraclone colony showing medium K13 GFP expression. Image D and D1 show phase contrast (PC) and dark field (DF) view of paraclone colony showing high K13 GFP expression. Pictures were photographed using a fluorescence microscope and the image magnifications are 100x the original size, the scale bar on each image is 50 μ M.

Table 5.1: The name of different categories of K15 or K13 promoter linked GFP expression in SCC25 cell line and the score allocated to the different categories.

Name of different categories	Scoring number
No expression of K15 or K13 promoter linked GFP expression in SCC25 cell line	0
Weak expression of K15 or K13 promoter linked GFP expression in SCC25 cell line	1
Medium expression of K15 or K13 promoter linked GFP expression in SCC25 cell line	2
Strong expression of K15 or K13 promoter linked GFP expression in SCC25 cell line	3

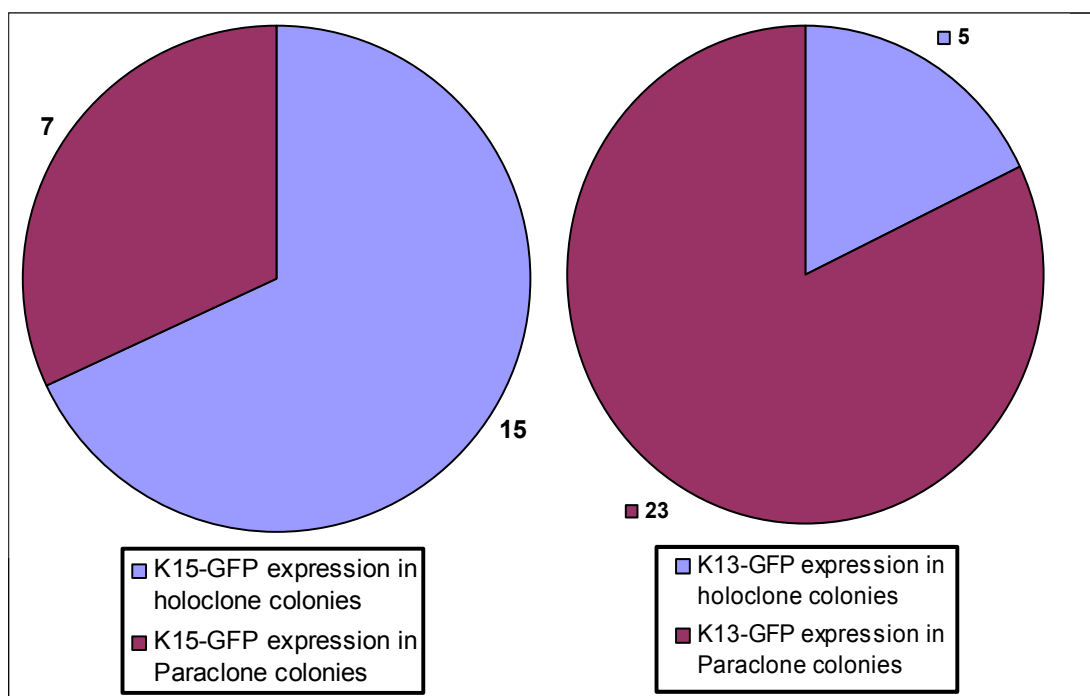


Figure 5.18: Pie chart showing the correlation of K15 and K13 promoter linked GFP plasmid intensity with the holoclone and paraclone formed by oral SCC25 cells plated at clonal density. The numbers in pie chart are measure of the intensity of GFP expression driven by K15 or K13 promoter in holoclone or paraclone colonies of SCC25 cells. The values in the pie chart are based on scoring number in table 5.1 allocated to GFP intensity of K15 and K13 promoter. SCC25 cells were selected for several weeks with 0.5-1mg of G418 antibiotic.

5.3.6: K15 and K13 Promoter Driven GFP Expression in Holoclone and Paraclone Cell populations formed by Oral Mucosa SCC25 Cells using FACS.

K15 or K13 promoter driven GFP expression in holoclone and paraclone colony formed by oral SCC25 cells (Figure 5.20) was determined using FACS in order to confirm the promoter intensity scoring results (Figure 5.18). However, there was inconsistency in the results obtained for both the promoter intensity scoring and FACS technique. The FACS results has shown that K15 or K13 promoter linked GFP expression in holoclone and paraclone colonies formed by SCC25 cells were very similar (Figure 5.20). This indicates that there is no correlation between K15 or K13 promoter driven GFP expression and SCC25 cell line maturation as marked by similar K15 or K13 promoter linked GFP expression in holoclone and paraclone colonies (Figure 5.20). One advantage of using FACS to quantify keratin gene expression as opposed to K15 and K13 promoter intensity scoring, is a quantitative and accurate approach, while scoring promoter intensity is more subjective. However, it could also be that stably transfected K15 or K13 promoter linked GFP gene reporters in holoclones and paraclones formed by SCC25 cells may not be a suitable approach to address the aims.

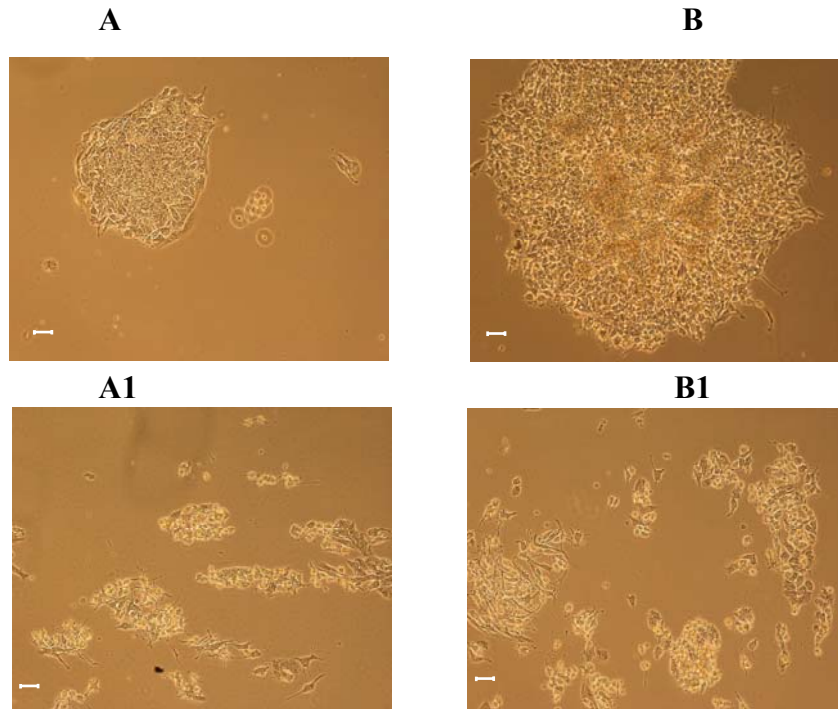


Figure 5.19: Phase contrast images of SCC25 cells stably transfected with K15 (A and A1) and K13 (B and B1) promoter constructs and plated at clonal density such that when holoclone and paraclone colonies formed on cover slips, they were subsequently scraped off such that each of the four cover-slips either contained holoclones (A or B) or paraclones (A1 or B1). The relative K15 or K13 promoter linked GFP expression in holoclone and paraclone colonies formed by SCC25 cells was measured using FACS. 10x objective was used for taking the above pictures. Scale bar: 50 μ M.

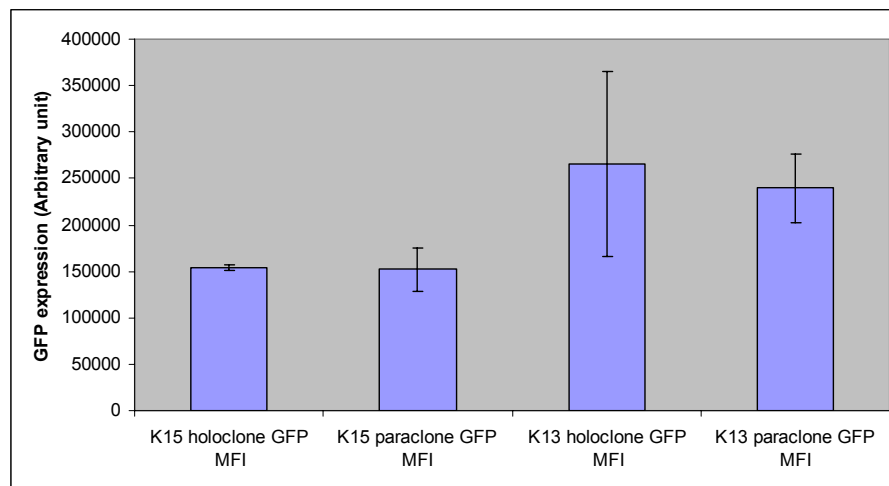


Figure 5.20: FACS plot data for K15 or K13 promoter driven GFP construct expression in holoclone and paraclone colonies formed by oral SCC25 cells. There is no significant ($P=0.595$ and 0.885) difference between K15 or K13 promoter linked GFP expression in holoclone and paraclone colonies formed by oral SCC25 cell. The results are expressed as the mean \pm SD from three experiments.

5.3.7: The Correlation of K15 and K13 Protein Expression with Differentiation in Oral Mucosa derived SCC25 and A431 Vulval Carcinoma Cell Lines

K15 protein expression has been investigated using monoclonal primary antibodies (Lyle et al, 1998) in Western blot and Immunohistochemistry assay. Using clone C8/144B and LHK15 monoclonal antibodies to detect K15 protein expression in holoclones and paraclones formed by A431 (positive control) and SCC25 cells, it was shown that both antibodies did not stain for K15 protein. In addition, there was no difference between the control (primary antibody omitted) and C8/144B, LHK15 stained K15 expression in A431 and SCC25 cells (Figure 5.21 and 5.22). K15 protein expression using clone C8/144B antibody has been investigated (Lyle et al, 1998) using in western blot and immunocytochemistry. Lyle et al, 1998 were unable to detect K15 protein by Western blot, but it was detected via Immunohistochemistry. Western blot results in denaturing of the protein such that the clone C8/144B antibody cannot detect the K15 protein in the denatured form, but can detect it when immunohistochemistry is used, as the protein is in its native form and the epitope for K15 antigen is exposed. Both Waseem et al, 1999 and Porter et al, 2000, used the LHK15 antibody to try to detect K15 protein via Western blots or immunohistochemistry on frozen section, and have successfully detected a 54kDa band corresponding to K15 protein in western blots. No other study has been reported so far using clone C8/144B and LHK15 monoclonal antibodies to detect K15 protein expression by immunocytochemistry, which prevents comparison of this study with other studies.

K13 protein immunostaining in holoclone and paraclone colonies formed by oral SCC25 cells using IC7 primary monoclonal antibody has shown that K13 protein staining is much stronger in paraclone (Figure 5.23B) than in holoclone and primary omitted control colonies (Figure 5.23A, 5.22C). The A431 cell line is known to have abundant K13 protein expression (Waseem et al, 1998) and results of K13 protein immunostaining using IC7 has shown that in the founding holoclone colony differentiating into a paraclone colony, the staining is stronger in paraclone than in the holoclone (Figure 5.24A). While in Figure 5.24B K13 protein staining in paraclone colony formed by A431 cells show strong K13 protein expression in comparison to the primary omitted control colony (Figure 5.24C). In summary, these data taken together show, the K15 staining with C8/144B and LHK15 and in

holoclone and paraclone colonies formed by SCC25 and A431 cells are negative. While on the contrary, K13 protein staining with IC7 has shown stronger staining of K13 in paraclone colonies in comparison to holoclone formed by SCC25 and A431 cells using primary antibody omitted as a control. The results taken together indicate that using immunocytochemistry to stain for K15 protein expression cannot be correlated with distinct heterogeneous population formed by epithelial SCC25 and A431 cells, while the opposite is true for K13 protein expression in correlating with oral SCC25 cell line maturation.

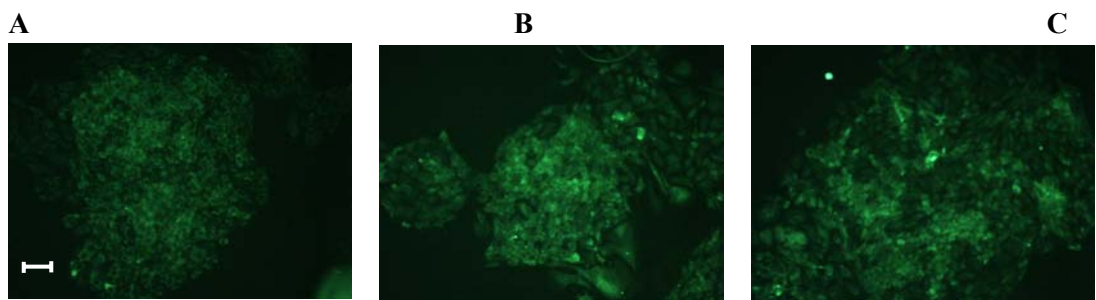


Figure 5.21: K15 protein expression in oral SCC25 cell line as detected with C8/144B and LKH15 antibodies: Image A shows K15 protein expression in holoclone colony formed by SCC25 cells as detected with C8/144B antibody using 1:100 dilution. Image B shows K15 protein expression in holoclone colony formed by SCC25 cells as detected with LHK15 antibody at 1:100 dilution. Image C shows K15 protein expression in holoclone colony formed by SCC25 cells as detected with primary antibody omitted (control). Magnification is x200, scale bar=100µM.

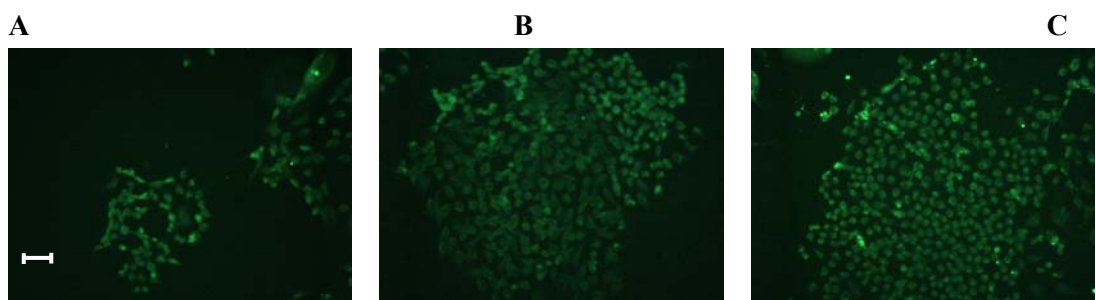


Figure 5.22: K15 protein expression in A431 cell line as detected with C8/144B and LKH15 antibodies: Image A shows K15 protein expression in holoclone colony formed by A431 cells as detected with C8/144B antibody using 1:100 dilution. Image B shows K15 protein expression in holoclone colony formed by A431 cells as detected with LHK15 antibody at 1:100 dilutions. Image C shows K15 protein expression in holoclone colony formed by A431 cells as detected with primary antibody omitted (control). Picture magnification is x200, scale bar=100µM.

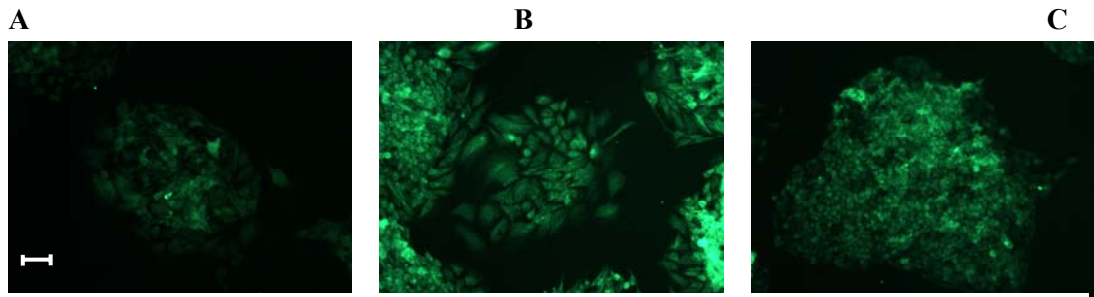


Figure 5.23: K13 protein expression in oral SCC25 cell line as detected with IC7 antibody: Image A shows K13 protein expression in holoclone colony formed by SCC25 cells as detected with IC7 antibody using 1:100 dilution. Image B shows K13 protein expression in paraclone colony formed by SCC25 cells as detected with IC7 antibody at 1:100 dilution. Image C shows control with primary IC7 antibody omitted in holoclone colony formed by SCC25 cells. Magnification is x200 and scale bar=100 μ M.

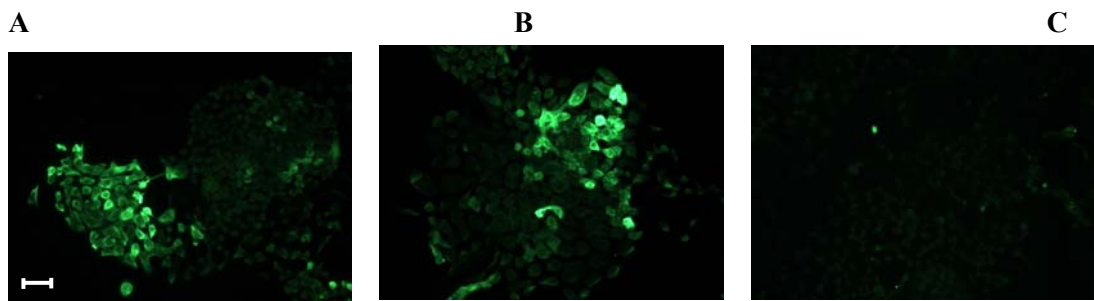


Figure 5.24: K13 protein expression in A431 cell line as detected with IC7 antibody: Image A shows K13 protein expression in holoclone colony formed by A431 cells as detected with IC7 antibody using 1:100 dilution. Image B shows K13 protein expression in paraclone colony formed by A431 cells as detected with IC7 antibody at 1:100 dilutions. Image C shows control with primary IC7 antibody omitted in holoclone colony formed by A431 cells. Picture magnification is x200, scale bar is=100 μ M.

5.4 Discussion

This chapter examined the hypothesis that if heterogeneity exists within a particular type of cell, then there may be molecules expressed by the subpopulation of cells, which identify which stage of maturation the cells have attained which is identified by colony morphologies, corresponding to holoclone, meroclone and paraclone. These three types of colonies are thought to be derived from stem, early and late amplifying cells (Mackenzie, 2006). Maturation in the oral mucosal epithelia involves sequential synthesis of specific basal and suprabasal keratin genes. K15 and K13 were chosen as representative of basal and suprabasal markers because of their *in-vivo* sequential specific expression.

The purpose of this study was to identify molecular differences between holoclone and paraclone cells within malignant oral cell lines, as this might provide a new opportunity for *in-vitro* monitoring of the effectiveness of methods developed to target the malignant oral stem cell population (Mackenzie 2005). Both K15 and K13, which are respectively expressed by holoclone and paraclones were used in this study and the association of K15 and K13 promoter and protein expression with oral SCC25 cell line maturation was assessed. This was done using the following experimental techniques: colony-forming assay, GFP reporter gene expression quantification, FACS, scoring method, gene array and immunocytochemistry.

From the Affymetrix data, K15 RNA expression (Figure 5.3) in holoclone versus paraclone in several oral cell lines has been shown to have several fold higher expression in holoclone colonies. However, K13 RNA expression (Figure 5.4) also shows a several fold increased expression in holoclone colonies compared to paraclone. This result is opposite to that expected, since K13 is a maturation marker in buccal oral mucosa (Bloor et al. 2000) and thus should be increased in expression in paraclone compared to holoclone.

The results of colony forming assay, FACS, scoring method, gene array and immunocytochemistry taken together indicate that the K15 and K13 promoter construct and protein expression does not correlate with maturation of oral SCC25 cells. As there was no significant difference between the K15 or K13 promoter linked GFP construct expression in holoclone and paraclone colonies formed by oral

SCC25 cells. There could be several reasons to explain why K15 and K13 expression could be not be correlated with oral SCC25 cell maturation. Firstly, it could be the fact that cancer cells lines are being used, which means cell maturation is altered which could account for the lack of correlation between K15 and K13 expression and SCC25 cell line maturation. Also although using cell lines is much easier and less laborious way to assess whether the expression of K15 and K13 can be correlated with cell maturation, this approach may not be suitable.

These experiments could have benefited from being done in primary normal oral keratinocytes (NOK). Although a limitation of this approach is that, the transfection efficiency is very low, especially in primary cells. This low transfection efficiency, could have been overcome by cloning the K15 and K13 promoter into retrovirus and transducing the oral cells with the K15 and K13 promoters. Transfection has the advantages that it is technically simple and fast to set up, safe and non-biologically hazardous compared to viral transduction. However, retroviral transduction is better than stable transfection, as some classes of virus can transduce both dividing and non-dividing cells. This approach was taken into consideration in the initial part of the project (Appendix: Figure 7.1, 7.2 and 7.3). However, cloning K15 and K13 promoter PCR into pRRL/m Cherry and pRRL/GFP respectively was unsuccessful, since the 3kb insert (K15 or K13 promoter) and transfer vector (10kb) into which it had been cloned were large. Due to time limitation, this approach could no longer be pursued, and stable transfection of K15 and K13 promoter into oral cell lines was adopted.

Quantitative-polymerase chain reaction (q-PCR) could have been used to quantify the K15 and K13 endogenous and exogenous (i.e. stably transfection of K15 and K13 promoters) expression in holoclone and paraclone colonies formed by SCC25 cells to follow up the Affymetrix gene array data as shown in Figure 5.3. This could be done using laser capture microdissection (LCM), a method used for isolating DNA, RNA or protein from specific microscopic region from colonies formed by cell lines or tissue section (Reference: website 20). Tissue sections or cell lines are either grown on a palm duplex petridish (P.A.L.M Microlaser Technologies AG, Inc, Munich, Germany) or slides made from specific material such that it is clear enough to be penetrated by the light beam and then the petridish or slides are placed under a

microscope (Reference: website 20). Once the specific required region are found in the center of the field of view within slide or petridish, the operator pushes a button, which activates a near IR laser diode integral with the microscope optics (Reference: website 20). This pulsated laser beam activates a precise spot on the transfer film, fusing the film with the underlying cells of choice, then this cells are catapulted into a small transfer film, which then placed into a tiny eppendorf tube in case of when cell lines are been used (Reference: website 20). The LCM method has the advantage of not altering, damaging the morphology or chemistry of the sample collected without disturbing surrounding cells (Reference: website 20). However, although an initial experiments with LCM is shown in Figure 7.4 and 7.5 in the appendices section was carried out, however due to time constraints this technique could not be carried out.

Chapter 6
General Discussion
and
Future Studies

6.1 General Overview

K15 and K13 are basal and suprabasal markers of differentiating oral epithelium and very little is known about the mechanism of transcriptional regulation which governs their sequential specific expression in the oral mucosa. Establishing the mechanism which confers tissue specific expression of K15 and K13 using a reporter gene assay and an *in silico* approach, were expected to give a better understanding about the mechanism of transcriptional regulation of the K15 and K13 genes. Therefore the aim of the study was to look at three important aspects of differentiation in oral mucosa. The first was to examine tissue specific expression of differentiation markers. The second aim involved using an *in silico* approach to find out whether there is a pattern of transcription factor binding sites in the basal keratin promoters and suprabasal keratin promoters. The third aim was to investigate whether the *in-vitro* expression of differentiation marker expression can be correlated with differentiating epithelial cell lines, using a keratin promoter linked GFP reporter gene assay as an *in-vitro* model.

6.2 Chapter 3 Discussion

The molecular mechanisms that govern keratin tissue specific expression are still unknown and investigations which have looked into keratin gene regulation and how this is linked to keratin differentiation specific expression have led to the identification of numerous transcription factors (Wanner et al, 1997). The discovery and analysis of these regulatory elements were facilitated by a database based bio-informatics approach. These databases, which include TFsearch and TRANSFAC, normally contain information on transcription name, their origins, the exact binding site within the sequence, and the function of the transcription factor (Hehl and Wingender, 2001). The search for transcription factor binding sites in uncharacterised biological sequences utilizing databases of keratin promoters was first carried out in oral mucosa in studies done by Dale et al, 1990. This study found that there was Sp1 transcription factor binding sites in the promoter of basally expressed K14 gene. Furthermore, the TRANSFAC database was used to scan the 5-flanking region of human K16 gene, with results showing that the identified regulatory elements in the K16 gene include AP1 and Sp1 (Wang and Chang, 2003). In addition, using the TRANSFAC transcription database to scan a 1.251kb sequence of the K15 promoter led to the identification of the following transcription factors:

AP-1, AP-2, C/EBP, GATA-1, GATA-3 and c-Myc (Radoja et al, 2004). The transcription factors, PAX6, AP-1 and CREB, were identified as conferring mouse K12 promoter specific expression in corneal epithelium (Liu et al, 1999). In Chapter 3, an in silico investigation using TFsearch for transcriptional binding sites in basal and suprabasal keratin promoters was adopted in an attempt to identify patterns emerging in transcription factor binding sites in keratin promoter DNA sequences. The results have revealed that basal keratin promoters contain more binding sites for Sp1 and C-rel than for CEBP, GATA-1, 2, 3 and USF transcription factor binding sites. This finding for basal keratin promoters is similar to other findings by Dale et al, 1990 and Liu et al, 2003. The mouse K15 promoter was used to target epithelial stem cell hair follicle bulge and analysis of promoter DNA sequences has revealed a number of regulatory elements including Sp1 (Liu et al, 2003).

6.2.1 TFsearch and Suprabasal Keratin Promoters

The results for suprabasal keratin promoters in this study has revealed that there are more C/EBP, GATA-1,2,3, USF, Oct-1 and AP-1 transcription factor binding sites in suprabasal keratin promoters than Sp1 and C-rel. Some of these transcription factors, such as AP-1, correlate with reports in the literature of suprabasal keratins promoters such as the K1 containing binding site for AP-1. Human epidermal differentiation specific calcium induced K1 expression is mediated by AP-1, which binds to a 5'-upstream element to mediate the calcium response element (Lu et al, 1994). AP-2 transcription factor has been shown to act in concert with Notch to orchestrate terminal differentiation in skin epidermis (Wang, et al. 2008). The parallel pathways of AP-2 and Notch signalling converge to govern C/EBP genes and coordinate the transition from basal proliferation to suprabasal differentiation. C/EBP transcription factor has also been shown to work concomitantly with AP-2 factors to orchestrate a complex program of gene expression which is vital for the formation of epidermal barrier (Wang, et al. 2008). Moreover, mouse epidermal K10 promoter analysis has revealed that differentiation specific expression requires both C/EBP and AP-2 transcription factors (Maytin et al, 1999). Given that differentiation signals lead to loss of the AP-2 transcription factor and this in turn causes depression of C/EBP α isoform promoter, which is specifically expressed in the upper layers of the epidermis, this then results in the activation of K10 expression as the keratinocytes migrate towards the surface (Maytin et al, 1999). However, C/EBP transcription

factors normally interact with AP-1 and NF- κ B and when this interaction occurs C/EBP transcription is able to regulate the expression of wide variety of genes in many cell types (Tomic-Canic et al, 1998). This prerequisite interaction of C/EBP with AP-1 and NF- κ B transcription factors would explain the presence of C/EBP along with AP-1 and NF- κ B in most of the analysed suprabasal keratin gene promoters. In summary, the results of chapter 3 show similar findings to other published literature and through the use of TFsearch database to scan basal versus suprabasal keratin promoter sequences have led to the identification of basal and suprabasal promoter specific transcription factors.

6.3 Chapter 4 Discussion

The aim of chapter 4 was to understand the mechanism of K13 transcriptional oral mucosal specific regulation, given that K13 is not normally expressed in the epidermis. The results have shown that there is increased K13 FL promoter expression in oral SCC25 cells in comparison to epidermal derived RTS3b, simple epithelial derived HeLa and human foreskin fibroblast HFF cell lines. However, when the K13 FL and deletion fragment (R1-R6) of the K13 FL promoter were transfected into SCC25, RTS3b, HeLa and HFF cell lines, the K13 FL and deletion fragment (R1-R6) expression was increased in HeLa (which does not express endogenous K13) cells in comparison to SCC25 cells (which does express the endogenous K13). These observations suggest that the K13 FL promoter and deletion fragments (R1-R6) show epithelial specific expression, given that the K13 promoter is expressed in all epithelial cell lines (SCC25, RTS3b and HeLa) and there is negligible K13 promoter expression in non-epithelial cells (HFF cell line). Furthermore, although the K13 deletion fragments (R1-R6) show epithelial expression, they do not however show oral mucosa tissue specific expression. Other studies by Jiang et al, 1990, have shown similar unusual expression for the 300bp K14 promoter which confers K14 epithelial specific expression. The K14 promoter showed negligible expression in fibroblast cell lines, it was however highly expressed in MCF-7 and HeLa cells derived from simple epithelial cell lines that do not express the endogenous K14 gene in comparison to SCC-12 cells (Jiang et al, 1990). Other studies which report similar findings to this study also include Wu et al, 1993, in which the 300bp upstream sequence of rabbit K13 promoter was able to confer keratinocyte specific expression but lacked corneal specificity. Although the

exact reason as to why there is abnormal expression of keratin promoter linked reporter gene is unknown, it could be that the K13 promoter lacks specific structural constraints imposed by local chromosomal structure which normally shut off K13 in all but the permissive environment (Wu et al, 1993). This also highlights the importance of using an *in-vivo* approach (i.e. transgenic mice), as this would eliminate some of the disadvantages encountered with using reporter gene assays and cell lines.

6.3.1 K13 FL Promoter and Deletion Fragments (R1-R6)

Important observations were noted concerning the trend of K13 promoter deletion fragment driven GFP expression in oral SCC25, RTS3b, HeLa, and HFF cells. From the pattern of K13 FL and deletion fragments (R1-R6) expression, there appears to be a suppressor element that confers K13 FL promoter oral SCC25 tissue specific expression in comparison to epidermal RTS3b cells. However, this study did not identify the specific transcription factors which confer K13 promoter specific oral expression. In line with these suppressor regulatory elements involved in the K13 promoter, other studies have found that SP-1 activates, while AP-2 suppresses, K3 gene in differentiating rabbit corneal epithelia (Chen et al, 1997).

6.3.2 Important Pathways Involved in K13 Induction in Oral SCC25 Cells

In this study, I have shown that the PI3K/Akt pathway appears to be important for K13 expression in oral mucosa. LY249002, a PI3K/Akt pathways inhibitor, caused a significant decrease in K13 promoter and protein expression in oral SCC25 cell lines, and this implies the importance of the PI3K/Akt pathway in altered differentiation of oral mucosa. This inhibitor killed 32% of SCC25 cells in comparison to the control (untreated) as measured by MTT assay. It could be argued that the reduction in K13 expression as measured by Western blot might be due to cell death rather than a reflection of the importance of the PI3K/Akt pathway for K13 expression in the oral SCC25 cells. However, this 32% death in oral SCC25 cells can in part be explained by the fact that active expression of Akt, a downstream effector of PI3K in keratinocytes, is involved in both growth arrest and differentiation. This means that pharmacological inhibition of the PI3K/Akt pathway not only leads to inhibition of differentiation but also causes cell death (Calautti et al, 2005). In addition, the normal activation of PI3K/Akt pathways in keratinocyte differentiation is dependent

on epidermal growth factor receptor, Src families of tyrosine kinase and E-cadherin-mediated adhesion activity (Calautti et al, 2005). PI3K increasingly associates with cadherin-catenin protein complex with their tyrosine phosphorylated YXXM motif (Calautti et al, 2005). Therefore the PI3K/Akt pathway is thought to regulate either epidermal differentiation or cell death as a reciprocal cross talk between tyrosine kinase and the cadherin-catenin protein complex (Calautti et al, 2005). A proposed mechanism of PI3K activation, subsequent signalling of downstream effectors, and their involvement in cell differentiation or cell death is shown in Figure 6.1.

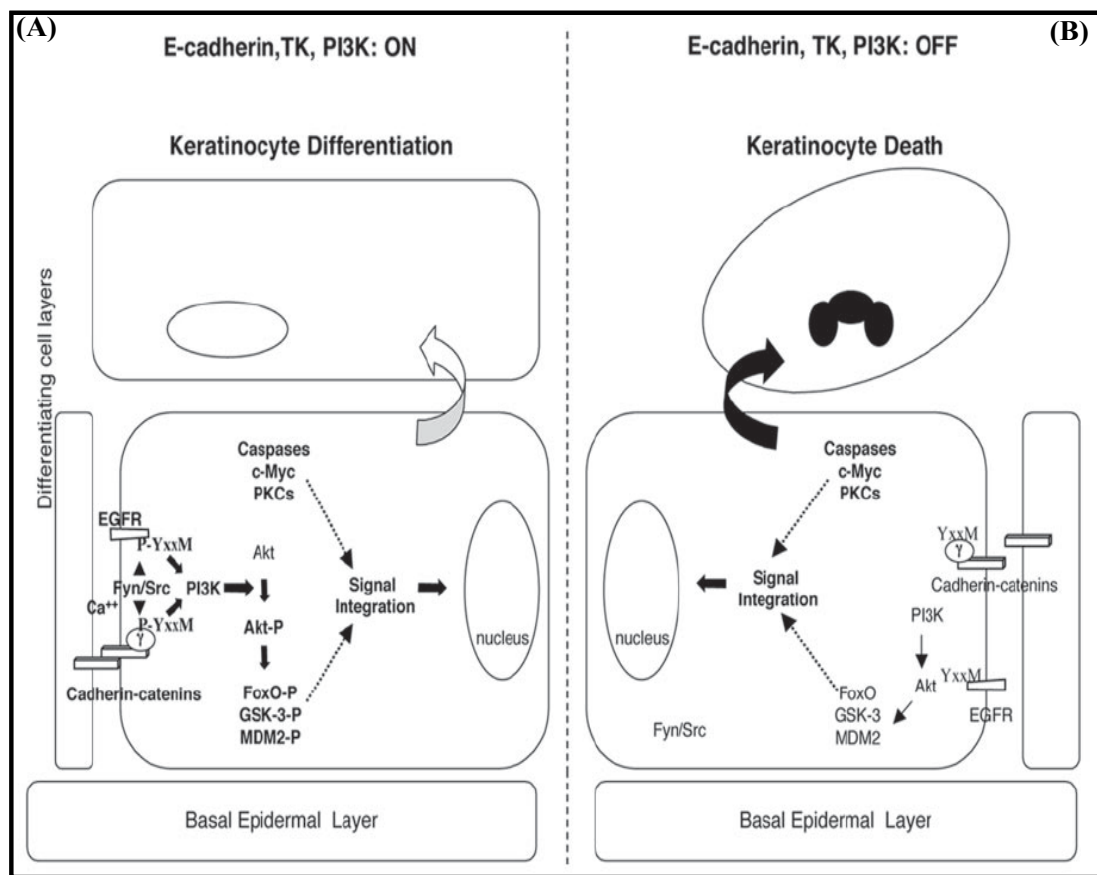


Figure 6.1: Diagrammatic representation of the proposed role of PI3K/Akt activation of its downstream effector E-cadherin and tyrosine kinases in differentiation and cell death. Diagram A shows when the EGFR and Cadherin-catenin activation leads to their tyrosine phosphorylated at YXXM motif by Fyn/Src, this results in the activation of PI3K and phosphorylation of Akt by PI3K, which in turn leads to phosphorylation of FoxO, GSK-3 and MDM2. Activation of these proteins taken together with activation of caspase, cMyc and PKCs lead to signal integration sent to the nucleus which in turn causes cell differentiation. While diagram B shows when the EGFR and Cadherin-catenin activation leads to their tyrosine phosphorylated at YXXM motif. This in turn leads to direct phosphorylation of Akt by PI3K, which in turn leads to phosphorylation of FoxO, GSK-3 and MDM2. Activation of these proteins taken together with activation of caspase, cMyc and PKCs lead to a signal integration sent to the nucleus which in turn causes cell death (adapted from Calautti et al, 2005).

6.3.3 K13 Expression in Simple and Stratified Epidermal Non-Permissive Environment Induced Sodium Butyrate

Sodium butyrate, a non specific histone deacetylase inhibitor, caused an increase in K13 protein expression in epidermal derived RTS3b cells. This suggests that in these cells K13 protein expression might be decreased in comparison with oral mucosa SCC25 cells, because the chromatin structure in skin is in the heterochromatin state. However, sodium butyrate is a non-selective histone deacetylase inhibitor, and its effects on K13 gene transcription might not be through histone core protein alteration. Findings similar to those for K13 protein have been reported for K23 mRNA expression which was highly induced by both specific and non specific histone deacetylase inhibitors, Trichostatin A (TSA) and sodium butyrate (SB) during pancreatic (AsPC-I cancer line) cell differentiation (Zhang et al, 2001). The mechanism of TSA and SB induced K23 expression in AsPC-I cells is thought to be through histone hyperacetylation, given that using antisense RNA to block expression of p21 WAF/CIPI (cell cycle regulator) caused K23 induction. It was thought that p21 WAF/CIPI might serve as a vital mediator of SB induced K23 expression (Zhang et al, 2001).

6.4 Chapter 5 Discussion

The aim of Chapter 5 was to investigate whether there is a correlation between K15 or K13 expression and differentiation of distinct heterogeneous populations in oral SCC25 cells. There was negative staining for K15 protein expression in holoclones or paraclones formed by oral SCC25 cells using immunocytochemistry, this appeared to be due to the un-availability of a specific K15 antibody for immunocytochemistry. However studies have found that immunohistochemical staining to identify molecules, which are differentially expressed by stem and differentiating cells, can be used to assess the position of stem cells (Mackenzie, 2006). These molecules, which include integrins $\alpha 6$ and $\beta 1$, p63, CD44, K19 and K15, whose higher expression levels have been reported in human progenitor and stem cells and are now used as a standard assessment to identify the anatomical location of stem cell zones in a given tissue (Mackenzie, 2006). This study shows that K15 can be used as a putative marker of stem cell zones and hence K15 expression should be increased in and correlated with its representative *in-vitro* holoclone colonies which contain stem cells in the *in-vivo* environment. K15 was used as a molecular marker to identify

stem cells in both normal oral mucosa and diseased (hyperkeratosis) buccal mucosa (Kose, et al. 2007). K15 staining has shown that its expressed in the basal layer in normal buccal and its expression is downregulated in oral lichen planus. This shows that stem cell phenotype as marked by K15, in pathology is altered in comparison to normal buccal mucosa (Kose, et al. 2007). Thus changes in responses to altered pathological signalling, as marked by decreased K15 expression, is important for the understanding of the role of adult stem cells in oral diseases which is characterised by abnormal keratinocyte proliferation and differentiation (Kose, et al. 2007).

There was a positive staining for K13 protein expression in paraclones compared to holoclone colonies formed by SCC25 cells. This finding is similar to other studies, whereby using immunocytochemical staining of K6 differentiation marker has shown that K6 was strongly expressed in paraclones but absent in holoclones formed by CaLH2 and CaLH3 cell lines derived from head and neck squamous cell carcinoma (Harper et al, 2007).

6.4.1 FACS Analysis and Colony Forming Assay of K15 or K13 Expressing SCC25 cells

Colony forming assay and FACS analysis results of K15 or K13 promoter linked GFP reporter gene expression have shown that there was no significant difference between K15 and K13 promoter expression in holoclone and paraclone colonies formed by SCC25 cells. However, contrary to this finding are the results of FACS analysis of cells previously stained for CD44, CD133 and CD29 cell surface markers, in the following cell lines; CA1, CaLH2, CaLH3 and H357 (Harper et al, 2007). The results of the FACS analysis have shown that a small population of cells within the cell lines tested showed high CD133 expression (Harper et al, 2007). These high expressing populations are thought to be the stem cell population within the heterogeneous cell population present within cancer cell lines, while FACS analysis of cells co-stained for CD44 and CD29 has shown a high expressing population of both CD44 and CD29 present within in CA1, CaLH2, CaLH3 and H357 cell lines (Harper et al, 2007).

6.4.2 Use of Q-PCR for K15 or K13 Expression in Oral SCC25 cells

An initial Q-PCR experiment, used to assess the expression of K15 and K13 in holoclone and paraclone colonies formed by oral SCC25 cells, was not completed due to time constraints. However other studies have utilized Q-PCR to assess the differences in gene expression between holoclones and paraclones formed by several oral cancer cell lines (Locke et al, 2005). Some of the molecules analysed include p16, hsp90 and Erb-B3 and their expression was upregulated in holoclone in comparison to paraclone colonies formed by C1, CA1, VB6, SCC71, CAL27 oral mucosa cell lines (Locke et al, 2005). It has also been reported that p16, hsp90 and Erb-B3 increased expression is associated with epithelial malignancy but their expression has not been related to stem cells as such and thus their expression in holoclones derived from malignant cells indicate that some markers are specifically expressed by stem cells in malignant tissue (Locke et al, 2005). Thus identifying molecules associated with stem cells in malignant tissue would hopefully lead to advances in therapy aimed at eliminating cancer stem cells (Locke et al, 2005)

In summary, the expression of K15 and K13 did not correlate with heterogeneous populations present in oral SCC25 cells. However, if there was a positive correlation, this would have been the first study to utilize K15 or K13 promoters and associate their specific expression in holoclone or paraclone colonies to specific transcription factors governing their holoclone and paraclone colony restricted expression. This might have led to a better understanding of the transcription factors which not only governs the differentiation specific expression of keratins genes, but also show transcription factors involved in sequential basal to suprabasal keratin specific maturation related expression in the oral mucosa.

6.5 Limitations of the study

Some of the limitations encountered in this study with the use of the CMV promoter plasmid as positive control, showed a substantial difference in its activity in different cell types, which has also been reported before (Qin and Gunning, 1997). This is a common problem with the use of viral promoter plasmid vectors. In an attempt to overcome this problem, Fugene 6 transfection reagent was used initially. However, the use of Fugene 6 transfection reagent for CMV promoter plasmid transfection into different cell lines did not result in similar transfection efficiency,

since there was a significant ($P=0.01-0.0012$) difference of CMV plasmid increased expression in SCC25 in comparison to other cell lines used in this study. Although the CMV promoter has been widely used in a variety of human cell lines and supports a sustained expression of a variety of foreign genes, the CMV promoter has been reported to be incapable of directing the expression of a rotavirus antigen (VP7) used to transform mouse fibroblast 3T3 and pig PF10 fibroblast cells (Qin and Gunning, 1997). It could be that in this present study viruses used to transform different cell types are driven or directed in their expression at different rates by CMV promoter plasmid. Therefore, in an attempt to resolve this problem, Lipofectamine another lipid based transfection reagent, was used, since this reagent gives very high transfection efficiency of positive controls (CMV) in fibroblast cell lines such as NIH3T3. However, out of all cell lines used in comparison to SCC25, only HeLa cell lines showed significant increase in CMV expression ($P=0.033$) in comparison to oral SCC25 cell line. Moreover, this shows that the use of Lipofectamine partially resolved the problem; which indicates that some transfection reagents such as Lipofectamine are better in their relative transfection efficiency of plasmids across a spectrum of cell types than other transfection reagents like Fugene 6. Another problem with CMV promoter plasmid is that some pharmacological agents, such as PD98059 and LY294002, an inhibitor MEK 1/2 and PI3K/Akt pathway, have also caused (Chapter 4; Figure 4.33 $P=0.01$ PD98059 and Figure 4.37 $P=0.09$ for LY294002) a reduction of CMV promoter expression. This appears to cast a doubt on whether MEK 1/2 and PI3K/Akt pathways have functional significance in the K13 full length promoter expression since the pharmacological agents also effect the expression of CMV promoter plasmid in a similar manner (Chapter 4; Figure 4.33 and 4.37). However, in order to gain more confidence in the validity of the results and address the limitation of the CMV promoter plasmid, western blot was also used (Chapter 4; Figure 4.35 and Figure 4.39). The K13-FL promoter linked GFP expression was specifically decreased in the presence of PD98059 and LY294002 inhibitors but not in the presence of the DMSO, the vehicle control (Chapter 4; Figure 4.32 and Figure 4.36). This indicates that PD98059 and LY294002 effects are specific for the K13-FL promoter but not the CMV promoter (Chapter 4; Figure 4.33 and Figure 4.37). There was also inconsistency in replicating transient transfection experiments, as exemplified by K13 FL promoter expression in the oral SCC25 cell line (Chapter 4; Figure 4.21) as the standard error of the mean

was very large. This inconsistency of the K13 FL promoter linked GFP expression was addressed by the use of pDsRedN-1 plasmid as an internal control to take into account the biological variation, which occurs from day to day, and the relative transfection efficiency of K13 promoter linked GFP expression in each well.

In summary, although the use of CMV promoter linked GFP reporter gene assay as a positive control has many advantages, the results however, highlight that no model is without flaws.

6.6 Future Studies

It is evident from the data obtained from this thesis in Chapter 4, that K13 contains suppressor elements, and so future studies could address the specific transcription factors involved in conferring the tissue specific expression of K13 in oral mucosa. This could be done by mutating specific transcription factor binding sites which were identified through the use of TFsearch database which corresponds to 500bp in the full length K13 promoter fragment, by using PCR introduced mutation and comparing the expression to wild type fragments using FACS.

Once transcription factors thought to be important in suppressing the K13 promoter expression have been established, then dominant negative forms of these transcription factors can be co-transfected with the wild type K13 full length promoter fragment. The GFP activity of the construct in the presence and absence of dominant negative transcription can be measured using FACS.

Also the 500bp suppressor elements conferring K13 tissue specific expression could be used to address whether this suppressor element is specific for K13 or could also be a suppressor for other keratins such as K15 promoter expression. This can be done through cloning the 500bp in front of the K15 promoter and comparing the activity of K15 original promoter and the altered one which contains 500bp fragment expression, using FACS.

Sodium butyrate has been shown to increase K13 protein expression in epidermal derived RTS3b cell lines. To ensure whether sodium butyrate is increasing K13 protein expression at posttranscriptional level, this experiment could be repeated

using northern blot or RT-PCR to see whether K13 mRNA is also increased in the presence of sodium butyrate. Other differentiation modulating pharmacological agents such as Bromodeoxyuridine which is known to increase K19 protein expression at posttranscriptional level (Meleady and Clynes, 2001) could also be used on K13, to detect if it is able to increase K13 protein expression. Both of these experiments could be done using primary cells rather than cell lines which show aberrant keratin expression.

In Chapter 5 it was established that there was no correlation between K15 and K13 promoter and protein expression with the limited differentiation that occurs *in-vitro*; these results have been performed in only one cell line (SCC25), and therefore the study could have benefited from using more oral cell lines. In addition, Western blots could have been used to detect K15 protein (LHK15 antibody) expression in both holoclone and paraclone colonies. Also Q-PCR could be used to quantify the K15 and K13 exogenous (i.e. stable transfection of K15 and K13 promoters) expression in holoclone and paraclone colonies formed by SCC25 and other oral cells to follow up the affymetrix data. Moreover, the K15 and K13 stable transfection experiment lacked proper known positive stem cell (basal) and transient amplifying (suprabasal) markers which should have been included, such as CD44.

All experiments should be done in primary oral cells, and poor transfection efficiency associated with primary cells would be overcome by cloning the K15 and K13 promoter into a lentivirus and transducing the oral cells with the K15 and K13 promoter. With a viral transduction approach, a more consistent and reliable result is obtainable than with transfection.

6.7 Conclusions

In conclusion, the K13 promoter shows both epithelial and mucosal tissue specific expression and this tissue specificity might be conferred by suppressor elements within the K13 full length promoter. K13 expression is increased by Sodium butyrate in non-permissive skin-derived RTS3b cells. The MEK 1/2 pathway seems unnecessary for the expression of K13, but the PI3K/Akt pathway is important for expression of K13 in oral mucosa. K15 and K13 expression can not be correlated with oral SCC25 cell differentiation *in-vitro*. The restricted expression of basal and

suprabasal keratin promoters might be co-ordinated by the synergistic action of Sp1 and c-rel in basal cells and GATA-1,2,3, C/EBP, Oct-1 and AP-1 transcription factors in suprabasal cells.

Reference

Alberts, B., Bray, D., Lewis, J., Raff, M., Roberts, K., and Watson, J. D. (1994). *Molecular Biology of the Cell*. 4th edition. New York and London: Garland Publishing, Inc.

Alonso, L. and E. Fuchs (2003). "Stem cells of the skin epithelium." Proc Natl Acad Sci U S A **100 Suppl 1**: 11830-5.

Alonso, L. and E. Fuchs (2003). "Stem cells in the skin: waste not, Wnt not." Genes Dev **17(10)**: 1189-200.

Alt, A., M. Gartsbein, M. Ohba, T. Kuroki and T. Tennenbaum (2004). "Differential regulation of alpha6beta4 integrin by PKC isoforms in murine skin keratinocytes." Biochem Biophys Res Commun **314(1)**: 17-23.

Andersen, B., Weinberg, W. C., Rennekampff, O., McEvilly, R. J., Bermingham, J. R., Jr., Hooshmand, F., Vasilyev, V., Hansbrough, J. F., Pittelkow, M. R., Yuspa, S. H., and Rosenfeld, M. G. (1997) "Functions of the POU domain genes Skn-1a/i and Tst-1/Oct-6/SCIP in epidermal differentiation". Genes Dev **11**:1873-84.

Barrandon, Y., and Green, H. (1985) "Cell size as a determinant of the clone-forming ability of human keratinocytes". Proc Natl Acad Sci U S A **82**:5390-4.

Barrandon, Y., and Green, H. (1987) "Three clonal types of keratinocyte with different capacities for multiplication". Proc Natl Acad Sci U S A **84**:2302-6.

Beachy, P. A., S. S. Karhadkar and D. M. Berman. (2004). "Mending and malignancy." *Nature* **431(7007)**: 402.

Beri, S., Tonna, N., Menozzi, G., Bonaglia, M. C., Sala, C., and Giorda, R. (2007) "DNA methylation regulates tissue-specific expression of Shank3". J Neurochem **101**:1380-91.

Berkovitz, B. K. B., Holland, G. R., Moxham, B. J. (2002). *Oral Anatomy, Histology and Embryology*. 3rd edition. Mosby.

Bikle, D. D. (2004) "Vitamin D regulated keratinocyte differentiation". J Cell Biochem **92**:436-44.

Bird, A. (2007). "Perceptions of epigenetics." Nature **447(7143)**: 396-8.

Blessing, M., Jorcano, J. L., and Franke, W. W. (1989) "Enhancer elements directing cell-type-specific expression of cytokeratin genes and changes of the epithelial cytoskeleton by transfections of hybrid cytokeratin genes". Embo J **8**:117-26.

Bloor, B. K., S. V. Seddon and P. R. Morgan (2000). "Gene expression of differentiation-specific keratins (K4, K13, K1 and K10) in oral non-dysplastic keratoses and lichen planus." J Oral Pathol Med **29**(8): 376-84.

Bloor, B. K., N. Tidman, et al. (2003). "Expression of keratin K2e in cutaneous and oral lesions: association with keratinocyte activation, proliferation, and keratinization." Am J Pathol **162**(3): 963-75.

Blomhoff, R. (1994). Vitamin A in Health and Disease: CRC Press.

Boisnic, S., J. P. Ouhayoun, M. C. Branchet, C. Frances, J. Y. Beranger, Y. Le Charpentier and H. Szpirglas (1995). "Alteration of cytokeratin expression in oral lichen planus." Oral Surg Oral Med Oral Pathol Oral Radiol Endod **79**(2): 207-15.

Boukamp, P., Petrussevska, R. T., Breitkreutz, D., Hornung, J., Markham, A., and Fusenig, N. E. (1988) "Normal keratinization in a spontaneously immortalized aneuploid human keratinocyte cell line". J Cell Biol **106**:761-71.

Bowden, P. E. (2005) "The human type II keratin gene cluster on chromosome 12q13.13: final count or hidden secrets?" J Invest Dermatol **124**:xv-xvii.

Bowden, P. E., Haley, J. L., Kansky, A., Rothnagel, J. A., Jones, D. O., and Turner, R. J. (1995) "Mutation of a type II keratin gene (K6a) in pachyonychia congenita". Nat Genet **10**:363-5.

Bowden, P. E., Quinlan, R. A., Breitkreutz, D., and Fusenig, N. E. (1984) "Proteolytic modification of acidic and basic keratins during terminal differentiation of mouse and human epidermis". Eur J Biochem **142**:29-36.

Bowden, P. E., Stark, H. J., Breitkreutz, D., and Fusenig, N. E. (1987) "Expression and modification of keratins during terminal differentiation of mammalian epidermis". Curr Top Dev Biol **22**:35-68.

Brembeck, F. H. and A. K. Rustgi (2000). "The tissue-dependent keratin 19 gene transcription is regulated by GKLf/KLf4 and Sp1." J Biol Chem **275**(36): 28230-9.
Brown, T.A. (1986). Gene Cloning: an introduction. Padstow, Cornwall.

Brembeck, F. H., Moffett, J., Wang, T. C., and Rustgi, A. K. (2001). "The keratin 19 promoter is potent for cell-specific targeting of genes in transgenic mice." Gastroenterology **120**(7): 1720-8.

Byrne, C., Hardman, M., and Nield, K. (2003) "Covering the limb--formation of the integument". J Anat **202**:113-23.

Brysk, M. M., I. Arany, H. Brysk, S. H. Chen, K. H. Calhoun and S. K. Tyring (1995). "Gene expression of markers associated with proliferation and differentiation in human keratinocytes cultured from epidermis and from buccal mucosa." Arch Oral Biol **40**(9): 855-62.

Burns, T., Breathnach, S., Cox, N., and Griffiths, C. (2004). *Rook's Text book of Dermatology*. 7th edition. pp.45-128. Blackwell Science.

- Calautti, E., Li, J., Saoncella, S., Brissette, J. L., and Goetinck, P. F. (2005)** "Phosphoinositide 3-kinase signaling to Akt promotes keratinocyte differentiation versus death". J Biol Chem **280**:32856-65.
- Casanova, L., Bravo, A., Were, F., Ramirez, A., Jorcano, J. J., and Vidal, M. (1995)** "Tissue-specific and efficient expression of the human simple epithelial keratin 8 gene in transgenic mice". J Cell Sci **108 (Pt 2)**:811-20.
- Casatorres, J., J. M. Navarro, M. Blessing and J. L. Jorcano (1994).** "Analysis of the control of expression and tissue specificity of the keratin 5 gene, characteristic of basal keratinocytes. Fundamental role of an AP-1 element." J Biol Chem **269(32)**: 20489-96.
- Castagna, M., Y. Takai, K. Kaibuchi, K. Sano, U. Kikkawa and Y. Nishizuka (1982).** "Direct activation of calcium-activated, phospholipid-dependent protein kinase by tumor-promoting phorbol esters." J Biol Chem **257(13)**: 7847-51.
- Chen, T. T., R. L. Wu, F. Castro-Munozledo and T. T. Sun (1997).** "Regulation of K3 keratin gene transcription by Sp1 and AP-2 in differentiating rabbit corneal epithelial cells." Mol Cell Biol **17(6)**: 3056-64.
- Choe, J., H. H. Guo and G. van den Engh (2005).** "A dual-fluorescence reporter system for high-throughput clone characterization and selection by cell sorting." Nucleic Acids Res **33(5)**: e49.
- Chu, P. G. and L. M. Weiss (2002).** "Keratin expression in human tissues and neoplasms." Histopathology **40(5)**: 403-39.
- Clausen, H., Vedtofte, P., Moe, D., Dabelsteen, E., Sun, T. T., and Dale, B. (1986)** "Differentiation-dependent expression of keratins in human oral epithelia". J Invest Dermatol **86**:249-54.
- Compton, C. C., Nadire, K. B., Regauer, S., Simon, M., Warland, G., O'Connor, N. E., Gallico, G. G., and Landry, D. B. (1998)** "Cultured human sole-derived keratinocyte grafts re-express site-specific differentiation after transplantation". Differentiation **64**:45-53.
- Costea, D. E., Loro, L. L., Dimba, E. A., Vintermyr, O. K., and Johannessen, A. C. (2003)** "Crucial effects of fibroblasts and keratinocyte growth factor on morphogenesis of reconstituted human oral epithelium". J Invest Dermatol **121**:1479-86.
- Coulombe, P. A. and M. B. Omary (2002).** "'Hard' and 'soft' principles defining the structure, function and regulation of keratin intermediate filaments." Curr Opin Cell Biol **14(1)**: 110-22.
- Cribier, B., Peltre, B., Langbein, L., Winter, H., Schweizer, J., and Grosshans, E. (2001)** "Expression of type I hair keratins in follicular tumours". Br J Dermatol **144**:977-82.

Csikos, M., Szalai, Z., Becker, K., Sebok, B., Schneider, I., Horvath, A., and Karpati, S. (2004) "Novel keratin 14 gene mutations in patients from Hungary with epidermolysis bullosa simplex". Exp Dermatol **13**:185-91.

Curradi, M., Izzo, A., Badaracco, G., and Landsberger, N. (2002) "Molecular mechanisms of gene silencing mediated by DNA methylation". Mol Cell Biol **22**:3157-73.

Dabelsteen, E. (1998). "Molecular biological aspects of acquired bullous diseases." Crit Rev Oral Biol Med **9**(2): 162-78.

Dackour, R., Carter, T., and Steinberg, B. M. (2005) "Phosphatidylinositol 3-kinase regulates early differentiation in human laryngeal keratinocytes". In Vitro Cell Dev Biol Anim **41**:111-7.

Dale, B. A., Salonen, J., and Jones, A. H. (1990) "New approaches and concepts in the study of differentiation of oral epithelia". Crit Rev Oral Biol Med **1**:167-90.

DePianto, D. and P. A. Coulombe (2004). "Intermediate filaments and tissue repair." Exp Cell Res **301**(1): 68-76.

Eckert, R. L., T. Efimova, S. R. Dashti, S. Balasubramanian, A. Deucher, J. F. Crish, M. Sturniolo and F. Bone (2002). "Keratinocyte survival, differentiation, and death: many roads lead to mitogen-activated protein kinase." J Investig Dermatol Symp Proc **7**(1): 36-40.

Eckert, R. L., Crish, J. F., Banks, E. B., and Welter, J. F. (1997) "The epidermis: genes on - genes off". J Invest Dermatol **109**:501-9.

Efimova, T., P. LaCelle, J. F. Welter and R. L. Eckert (1998). "Regulation of human involucrin promoter activity by a protein kinase C, Ras, MEKK1, MEK3, p38/RK, AP1 signal transduction pathway." J Biol Chem **273**(38): 24387-95.

Ellenberg, J., Lippincott-Schwartz, J., and Presley, J. F. (1999) "Dual-colour imaging with GFP variants". Trends Cell Biol **9**:52-6.

Elnitski, L., Jin, V. X., Farnham, P. J., and Jones, S. J. (2006) "Locating mammalian transcription factor binding sites: a survey of computational and experimental techniques". Genome Res **16**:1455-64.

Essenfelder, G. M., Larderet, G., Waksman, G., and Lamartine, J. (2005) "Gene structure and promoter analysis of the human GJB6 gene encoding connexin 30". Gene **350**:33-40.

Euskirchen, G. M., Rozowsky, J. S., Wei, C. L., Lee, W. H., Zhang, Z. D., Hartman, S., Emanuelsson, O., Stolc, V., Weissman, S., Gerstein, M. B., Ruan, Y., and Snyder, M. (2007) "Mapping of transcription factor binding regions in mammalian cells by ChIP: Comparison of array- and sequencing-based technologies". Genome Res **17**:898-909.

- Fillies, T., Werkmeister, R., Packeisen, J., Brandt, B., Morin, P., Weingart, D., Joos, U., and Buerger, H. (2006).** "Cytokeratin 8/18 expression indicates a poor prognosis in squamous cell carcinomas of the oral cavity." BMC Cancer **6**: 10.
- Fuchs, E. (1994).** "Intermediate filaments and disease: mutations that cripple cell strength." J Cell Biol **125**(3): 511-6.
- Fujimoto, W., Nakanishi, G., Arata, J., and Jetten, A. M. (1997)** "Differential expression of human cornifin alpha and beta in squamous differentiating epithelial tissues and several skin lesions". J Invest Dermatol **108**:200-4.
- Furtado, A. and R. Henry (2002).** "Measurement of green fluorescent protein concentration in single cells by image analysis." Anal Biochem **310**(1): 84-92.
- Gandarillas, A. (2000)** "Epidermal differentiation, apoptosis, and senescence: common pathways?" Exp Gerontol **35**:53-62.
- Gasparoni, A., Fonzi, L., Schneider, G. B., Wertz, P. W., Johnson, G. K., and Squier, C. A. (2004)** "Comparison of differentiation markers between normal and two squamous cell carcinoma cell lines in culture". Arch Oral Biol **49**:653-64.
- Gervasio, O. L., R. A. Dutra, S. M. Tartaglia, W. A. Vasconcellos, A. A. Barbosa and M. C. Aguiar (2001).** "Oral squamous cell carcinoma: a retrospective study of 740 cases in a Brazilian population." Braz Dent J **12**(1): 57-61.
- Gibbs, S. and M. Ponc (2000).** "Intrinsic regulation of differentiation markers in human epidermis, hard palate and buccal mucosa." Arch Oral Biol **45**(2): 149-58.
- Gillenwater, A., Zou, C. P., Zhong, M., and Lotan, R. (2000)** "Effects of sodium butyrate on growth, differentiation, and apoptosis in head and neck squamous carcinoma cell lines". Head Neck **22**:247-56.
- Goto, H., Tanabe, K., Manser, E., Lim, L., Yasui, Y., and Inagaki, M. (2002)** "Phosphorylation and reorganization of vimentin by p21-activated kinase (PAK)". Genes Cells **7**:91-7.
- Gu, L. H. and P. A. Coulombe (2007).** "Keratin function in skin epithelia: a broadening palette with surprising shades." Curr Opin Cell Biol **19**(1): 13-23.
- Gugasyan, R., Voss, A., Varigos, G., Thomas, T., Grumont, R. J., Kaur, P., Grigoriadis, G., and Gerondakis, S. (2004)** "The transcription factors c-rel and RelA control epidermal development and homeostasis in embryonic and adult skin via distinct mechanisms". Mol Cell Biol **24**:5733-45.
- Harper, L. J., Piper, K., Common, J., Fortune, F., and Mackenzie, I. C. (2007)** "Stem cell patterns in cell lines derived from head and neck squamous cell carcinoma". J Oral Pathol Med **36**:594-603.

Hatakeyama, S., Hayashi, S., Yoshida, Y., Otsubo, A., Yoshimoto, K., Oikawa, Y., and Satoh, M. (2004) "Retinoic acid disintegrated desmosomes and hemidesmosomes in stratified oral keratinocytes". J Oral Pathol Med **33**:622-8.

Heath, J. W., Young, B., and Livingstone, C. (2000). Wheater's Functional Histology: A Text and Colour Atlas. 4th edition. pp.20-128: Churchill Livingstone.

Hehl, R., and Wingender, E. (2001) "Database-assisted promoter analysis". Trends Plant Sci **6**:251-5.

Hesse, M., T. M. Magin and K. Weber (2001). "Genes for intermediate filament proteins and the draft sequence of the human genome: novel keratin genes and a surprisingly high number of pseudogenes related to keratin genes 8 and 18." J Cell Sci **114**(Pt 14): 2569-75.

Hesse, M., A. Zimek, K. Weber and T. M. Magin (2004). "Comprehensive analysis of keratin gene clusters in humans and rodents." Eur J Cell Biol **83**(1): 19-26.

Hsu, W., and Chen-Kiang, S. (1993) "Convergent regulation of NF-IL6 and Oct-1 synthesis by interleukin-6 and retinoic acid signaling in embryonal carcinoma cells". Mol Cell Biol **13**:2515-23.

Huff, C. A., S. H. Yuspa and D. Rosenthal (1993). "Identification of control elements 3' to the human keratin 1 gene that regulate cell type and differentiation-specific expression." J Biol Chem **268**(1): 377-84.

Janes, S. M., and Watt, F. M. (2006) "New roles for integrins in squamous-cell carcinoma". Nat Rev Cancer **6**:175-83.

Jiang, C. K., H. S. Epstein, M. Tomic, I. M. Freedberg and M. Blumenberg (1990). "Epithelial-specific keratin gene expression: identification of a 300 base-pair controlling segment." Nucleic Acids Res **18**(2): 247-53.

Jiang, C. K., H. S. Epstein, M. Tomic, I. M. Freedberg and M. Blumenberg (1991). "Functional comparison of the upstream regulatory DNA sequences of four human epidermal keratin genes." J Invest Dermatol **96**(2): 162-7.

Karatsaidis, A., Schreurs, O., Axell, T., Helgeland, K., and Schenck, K. (2003) "Inhibition of the transforming growth factor-beta/Smad signaling pathway in the epithelium of oral lichen". J Invest Dermatol **121**:1283-90.

Kashiwagi, M., Morgan, B. A., and Georgopoulos, K. (2007) "The chromatin remodeler Mi-2beta is required for establishment of the basal epidermis and normal differentiation of its progeny". Development **134**:1571-82.

Kautsky, M. B., P. Fleckman and B. A. Dale (1995). "Retinoic acid regulates oral epithelial differentiation by two mechanisms." J Invest Dermatol **104**(2): 224-30.

Kim, S. Y., D. Berger, S. O. Yim, P. G. Sacks and M. A. Tainsky (1996). "Coordinate control of growth and cytokeratin 13 expression by retinoic acid." Mol Carcinog **16**(1): 6-11.

King, I. A. and E. F. Hounsell (1989). "Cytokeratin 13 contains O-glycosidically linked N-acetylglucosamine residues." J Biol Chem **264**(24): 14022-8.

Kishi, M., Y. Emori, Y. Tsukamoto and K. Abe (2001). "Primary culture of rat taste bud cells that retain molecular markers for taste buds and permit functional expression of foreign genes." Neuroscience **106**(1): 217-25.

Kopan, R., Traska, G., and Fuchs, E. (1987) "Retinoids as important regulators of terminal differentiation: examining keratin expression in individual epidermal cells at various stages of keratinization". J Cell Biol **105**:427-40.

Kose, O., Lalli, A., Kutulola, A. O., Odell, E. W., and Waseem, A. (2007) "Changes in the expression of stem cell markers in oral lichen planus and hyperkeratotic lesions". J Oral Sci **49**:133-9.

Krauss, S. and W. W. Franke (1990). "Organization and sequence of the human gene encoding cytokeratin 8." Gene **86**(2): 241-9.

Ku, N. O., Liao, J., and Omary, M. B. (1998a) "Phosphorylation of human keratin 18 serine 33 regulates binding to 14-3-3 proteins". Embo J **17**:1892-906.

Ku, N. O., Michie, S. A., Soetikno, R. M., Resurreccion, E. Z., Broome, R. L., and Omary, M. B. (1998b) "Mutation of a major keratin phosphorylation site predisposes to hepatotoxic injury in transgenic mice". J Cell Biol **143**:2023-32.

Kuruc, N., R. E. Leube, I. Moll, B. L. Bader and W. W. Franke (1989). "Synthesis of cytokeratin 13, a component characteristic of internal stratified epithelia, is not induced in human epidermal tumors." Differentiation **42**(2): 111-23.

Lane, E. B., and McLean, W. H. (2004) "Keratins and skin disorders". J Pathol **204**:355-66.

Langbein, L., Rogers, M. A., Winter, H., Praetzel, S., and Schweizer, J. (2001) "The catalog of human hair keratins. II. Expression of the six type II members in the hair follicle and the combined catalog of human type I and II keratins". J Biol Chem **276**:35123-32.

Leask, A., C. Byrne and E. Fuchs (1991). "Transcription factor AP2 and its role in epidermal-specific gene expression." Proc Natl Acad Sci U S A **88**(18): 7948-52.

Leask, A., M. Rosenberg, R. Vassar and E. Fuchs (1990). "Regulation of a human epidermal keratin gene: sequences and nuclear factors involved in keratinocyte-specific transcription." Genes Dev **4**(11): 1985-98.

Lee, C. H., Ko, Y. C., Huang, H. L., Chao, Y. Y., Tsai, C. C., Shieh, T. Y., and Lin, L. M. (2003) "The precancer risk of betel quid chewing, tobacco use and alcohol consumption in oral leukoplakia and oral submucous fibrosis in southern Taiwan". Br J Cancer **88**:366-72.

Lersch, R., V. Stellmach, C. Stocks, G. Giudice and E. Fuchs (1989). "Isolation, sequence, and expression of a human keratin K5 gene: transcriptional regulation of keratins and insights into pairwise control." Mol Cell Biol **9**(9): 3685-97.

Liu, J. J., Kao, W. W., and Wilson, S. E. (1999) "Corneal epithelium-specific mouse keratin K12 promoter". Exp Eye Res **68**:295-301.

Liu, Y., S. Lyle, Z. Yang and G. Cotsarelis (2003). "Keratin 15 promoter targets putative epithelial stem cells in the hair follicle bulge." J Invest Dermatol **121**(5): 963-8.

Locke, M., Heywood, M., Fawell, S., and Mackenzie, I. C. (2005) "Retention of intrinsic stem cell hierarchies in carcinoma-derived cell lines". Cancer Res **65**:8944-50.

Lowry, J. A. and J. P. Mackay (2006). "GATA-1: One protein, many partners." Int J Biochem Cell Biol **38**(1): 6-11.

Lu, B., Rothnagel, J. A., Longley, M. A., Tsai, S. Y., and Roop, D. R. (1994) "Differentiation-specific expression of human keratin 1 is mediated by a composite AP-1/steroid hormone element". J Biol Chem **269**:7443-9.

Lu, H., A. Zimek, J. Chen, M. Hesse, H. Bussow, K. Weber and T. M. Magin (2006). "Keratin 5 knockout mice reveal plasticity of keratin expression in the corneal epithelium." Eur J Cell Biol.

Lu, M. H., Yang, P. C., Chang, L. T., and Chao, C. F. (2000) "Temporal and spatial sequence expression of cytokeratin K19 in cultured human keratinocyte". Proc Natl Sci Counc Repub China B **24**:169-77.

Lyle, S., Christofidou-Solomidou, M., Liu, Y., Elder, D. E., Albelda, S., and Cotsarelis, G. (1998) "The C8/144B monoclonal antibody recognizes cytokeratin 15 and defines the location of human hair follicle stem cells". J Cell Sci **111 (Pt 21)**:3179-88.

Ma, S., L. Rao, I. M. Freedberg and M. Blumenberg (1997). "Transcriptional control of K5, K6, K14, and K17 keratin genes by AP-1 and NF-kappaB family members." Gene Expr **6**(6): 361-70.

Macville, M., Schrock, E., Padilla-Nash, H., Keck, C., Ghadimi, B. M., Zimonjic, D., Popescu, N., and Ried, T. (1999) "Comprehensive and definitive molecular cytogenetic characterization of HeLa cells by spectral karyotyping". Cancer Res **59**:141-50.

Mackenzie, I. C. (2005). "Retention of stem cell patterns in malignant cell lines." Cell Prolif **38**(6): 347-55.

Mackenzie, I. C. (2006). "Stem cell properties and epithelial malignancies." Eur J Cancer **42**(9): 1204-12.

Markova, N. G., Karaman-Jurukovska, N., Pinkas-Sarafova, A., Marekov, L. N., and Simon, M. (2007) "Inhibition of histone deacetylation promotes abnormal epidermal differentiation and specifically suppresses the expression of the late differentiation marker profilaggrin". J Invest Dermatol **127**:1126-39.

Marshall, D., Hardman, M. J., Nield, K. M., and Byrne, C. (2001) "Differentially expressed late constituents of the epidermal cornified envelope". Proc Natl Acad Sci U S A **98**:13031-6.

Maytin, E. V., Lin, J. C., Krishnamurthy, R., Batchvarova, N., Ron, D., Mitchell, P. J., and Habener, J. F. (1999) "Keratin 10 gene expression during differentiation of mouse epidermis requires transcription factors C/EBP and AP-2". Dev Biol **216**:164-81.

Merika, M. and S. H. Orkin (1993). "DNA-binding specificity of GATA family transcription factors." Mol Cell Biol **13**(7): 3999-4010.

Meleady, P., and Clynes, M. (2001) "Bromodeoxyuridine increases keratin 19 protein expression at a posttranscriptional level in two human lung tumor cell lines". In Vitro Cell Dev Biol Anim **37**:536-42.

McBride, S., D. Walsh, P. Meleady, N. Daly and M. Clynes (1999). "Bromodeoxyuridine induces keratin protein synthesis at a posttranscriptional level in human lung tumour cell lines." Differentiation **64**(3): 185-93.

McGowan, K. M., and Coulombe, P. A. (1998) "Onset of keratin 17 expression coincides with the definition of major epithelial lineages during skin development". J Cell Biol **143**:469-86.

Milisavljevic, V., Freedberg, I. M., and Blumenberg, M. (1996) "Characterization of nuclear protein binding sites in the promoter of keratin K17 gene". DNA Cell Biol **15**:65-74.

Moll, R., Franke, W. W., Schiller, D. L., Geiger, B., and Krepler, R. (1982) "The catalog of human cytokeratins: patterns of expression in normal epithelia, tumors and cultured cells". Cell **31**:11-24.

Moll, R., Divo, M., and Langbein, L. (2008) "The human keratins: biology and pathology". Histochem Cell Biol **129**:705-33.

Mosmann, T. (1983) "Rapid colorimetric assay for cellular growth and survival: application to proliferation and cytotoxicity assays". J Immunol Methods **65**:55-63.

Nagler, R. M. (2002). "Molecular aspects of oral cancer." Anticancer Res **22**(5): 2977-80.

Nebert, D. W. (2002). "Transcription factors and cancer: an overview." Toxicology **181-182**: 131-41.

Nemes, Z., Marekov, L. N., and Steinert, P. M. (1999) "Involucrin cross-linking by transglutaminase 1. Binding to membranes directs residue specificity". J Biol Chem **274**:11013-21.

Nemes, Z., and Steinert, P. M. (1999) "Bricks and mortar of the epidermal barrier". Exp Mol Med **31**:5-19.

Oberley, M. O., Kirmizis, A., Schelman, W. R., and Farnham, P. J. (2006). Using RNA interference to validate target genes identified by coupling chromatin immunoprecipitation with CpG-island microarrays. In: Promoter and CpG Island Microarrays. Winegarden, N. A. and Takahashi, M. (eds.), pp. 89-104: DNA Press.

Ocejo-Garcia, M., Baokbah, T. A., Ashurst, H. L., Cowlshaw, D., Soomro, I., Coulson, J. M., and Woll, P. J. (2005) "Roles for USF-2 in lung cancer proliferation and bronchial carcinogenesis". J Pathol **206**:151-9.

Oh, H. S., and Smart, R. C. (1998) "Expression of CCAAT/enhancer binding proteins (C/EBP) is associated with squamous differentiation in epidermis and isolated primary keratinocytes and is altered in skin neoplasms". J Invest Dermatol **110**:939-45.

Ohkura, S., Kondoh, N., Hada, A., Arai, M., Yamazaki, Y., Sindoh, M., Takahashi, M., Matsumoto, I., and Yamamoto, M. (2005) "Complex formations involving both SP-1 and SP-3 at the transcriptional regulatory sequence correlate with the activation of the Keratin 14 gene in human oral squamous cell carcinoma cells". Oncol Rep **14**:1577-81.

Omary, M. B., Ku, N. O., Liao, J., and Price, D. (1998) "Keratin modifications and solubility properties in epithelial cells and in vitro". Subcell Biochem **31**:105-40.

Opitz, O. G., Jenkins, T. D., and Rustgi, A. K. (1998) "Transcriptional regulation of the differentiation-linked human K4 promoter is dependent upon esophageal-specific nuclear factors". J Biol Chem **273**:23912-21.

Opitz, O. G. and A. K. Rustgi (2000). "Interaction between Sp1 and cell cycle regulatory proteins is important in transactivation of a differentiation-related gene." Cancer Res **60**(11): 2825-30.

Owens, D. W. and E. B. Lane (2003). "The quest for the function of simple epithelial keratins." Bioessays **25**(8): 748-58.

Paramio, J. M. and J. L. Jorcano (2002). "Beyond structure: do intermediate filaments modulate cell signalling?" Bioessays **24**(9): 836-44.

Paramio, J. M., Segrelles, C., Casanova, M. L., and Jorcano, J. L. (2000) "Opposite functions for E2F1 and E2F4 in human epidermal keratinocyte differentiation". J Biol Chem **275**:41219-26.

Plachot, C. and S. A. Lelievre (2004). "DNA methylation control of tissue polarity and cellular differentiation in the mammary epithelium." Exp Cell Res **298**(1): 122-32.

Popa, C., Dahler, A. L., Serewko-Auret, M. M., Wong, C. F., Smith, L., Barnes, L. M., Strutton, G. M., and Saunders, N. A. (2004) "AP-2 transcription factor family member expression, activity, and regulation in human epidermal keratinocytes in vitro". Differentiation **72**:185-97.

Porter, R. M., D. P. Lunny, P. H. Ogden, S. M. Morley, W. H. McLean, A. Evans, D. L. Harrison, E. L. Rugg and E. B. Lane (2000). "K15 expression implies lateral differentiation within stratified epithelial basal cells." Lab Invest **80**(11): 1701-10.

Presland, R. B. and B. A. Dale (2000). "Epithelial structural proteins of the skin and oral cavity: function in health and disease." Crit Rev Oral Biol Med **11**(4): 383-408.

Presland, R. B. and R. J. Jurevic (2002). "Making sense of the epithelial barrier: what molecular biology and genetics tell us about the functions of oral mucosal and epidermal tissues." J Dent Educ **66**(4): 564-74.

Prime, S. S., Nixon, S. V., Crane, I. J., Stone, A., Matthews, J. B., Maitland, N. J., Remnant, L., Powell, S. K., Game, S. M., and Scully, C. (1990) "The behaviour of human oral squamous cell carcinoma in cell culture". J Pathol **160**:259-69.

Purdie, K. J., Sexton, C. J., Proby, C. M., Glover, M. T., Williams, A. T., Stables, J. N., and Leigh, I. M. (1993) "Malignant transformation of cutaneous lesions in renal allograft patients: a role for human papillomavirus". Cancer Res **53**:5328-33.

Purves, W. K., Orians, G. H., Heller, H. G., Sadava, D. (1998). *Life: The Science Of Biology*. 5th edition. Massachusetts. Sinauer associates, Inc and W.H.Freeman and company.

Qin, H. and P. Gunning (1997). "The 3'-end of the human beta-actin gene enhances activity of the beta-actin expression vector system: construction of improved vectors." J Biochem Biophys Methods **36**(1): 63-72.

Qiu, J. (2006). "Epigenetics: unfinished symphony." Nature **441**(7090): 143-5.

Radoja, N., O. Stojadinovic, A. Waseem, M. Tomic-Canic, V. Milisavljevic, S. Teebor and M. Blumenberg (2004). "Thyroid hormones and gamma interferon specifically increase K15 keratin gene transcription." Mol Cell Biol **24**(8): 3168-79.

Ramirez, A., M. Vidal, A. Bravo, F. Larcher and J. L. Jorcano (1995). "A 5'-upstream region of a bovine keratin 6 gene confers tissue-specific expression and

hyperproliferation-related induction in transgenic mice." Proc Natl Acad Sci U S A **92**(11): 4783-7.

Rao, L. S., Long, W. S., Kaneko, T., and, and Blumenberg, M. (2003) "Regulation of transcription factor activity by extracellular signals in epidermal keratinocytes". Acta Dermatoven APA **12**:3-14.

Raymond, K., Kreft, M., Janssen, H., Calafat, J., and Sonnenberg, A. (2005) "Keratinocytes display normal proliferation, survival and differentiation in conditional beta4-integrin knockout mice". J Cell Sci **118**:1045-60.

Reibel, J. (2003) "Prognosis of oral pre-malignant lesions: significance of clinical, histopathological, and molecular biological characteristics". Crit Rev Oral Biol Med **14**:47-62.

Reibel, J. (2003). "Tobacco and oral diseases. Update on the evidence, with recommendations." Med Princ Pract **12 Suppl 1**: 22-32.

Rheinwald, J. G. and M. A. Beckett (1980). "Defective terminal differentiation in culture as a consistent and selectable character of malignant human keratinocytes." Cell **22**(2 Pt 2): 629-32.

Richard, G., V. De Laurenzi, B. Didona, S. J. Bale and J. G. Compton (1995). "Keratin 13 point mutation underlies the hereditary mucosal epithelial disorder white sponge nevus." Nat Genet **11**(4): 453-5.

Rickard, K. L., Gibson, P. R., Young, G. P., and Phillips, W. A. (1999) "Activation of protein kinase C augments butyrate-induced differentiation and turnover in human colonic epithelial cells in vitro". Carcinogenesis **20**:977-84.

Romano, V., E. Raimondi, P. Bosco, S. Feo, C. Di Pietro, R. E. Leube, S. M. Troyanovsky and N. Ceratto (1992). "Chromosomal mapping of human cytokeratin 13 gene (KRT13)." Genomics **14**(2): 495-7.

Rothnagel, J. A., Seki, T., Ogo, M., Longley, M. A., Wojcik, S. M., Bundman, D. S., Bickenbach, J. R., and Roop, D. R. (1999) "The mouse keratin 6 isoforms are differentially expressed in the hair follicle, footpad, tongue and activated epidermis". Differentiation **65**:119-30.

Rosenthal, D. S., Steinert, P. M., Chung, S., Huff, C. A., Johnson, J., Yuspa, S. H., and Roop, D. R. (1991) "A human epidermal differentiation-specific keratin gene is regulated by calcium but not negative modulators of differentiation in transgenic mouse keratinocytes". Cell Growth Differ **2**:107-13.

Rugg, E. L., J. E. Common, A. Wilgoss, H. P. Stevens, J. Buchan, I. M. Leigh and D. P. Kelsell (2002). "Diagnosis and confirmation of epidermolytic palmoplantar keratoderma by the identification of mutations in keratin 9 using denaturing high-performance liquid chromatography." Br J Dermatol **146**(6): 952-7.

Rugg, E. L., McLean, W. H., Allison, W. E., Lunny, D. P., Macleod, R. I., Felix, D. H., Lane, E. B., and Munro, C. S. (1995) "A mutation in the mucosal keratin K4 is associated with oral white sponge nevus". Nat Genet **11**:450-2.

Sanchez, A., Bullejos, M., Burgos, M., Jimenez, R., and Diaz, R. (1996) "An alternative to blunt-end ligation for cloning DNA fragments with incompatible ends". Trends Genet **12**:44.

Sanger, F., Nicklen, S., and Coulson, A. R. (1977) "DNA sequencing with chain-terminating inhibitors". Proc Natl Acad Sci U S A **74**:5463-7.

Sawaf, M. H., Ouhayoun, J. P., Shabana, A. H., and Forest, N. (1990) "Cytokeratin expression in human tongue epithelium". Am J Anat **189**:155-66.

Sayama, K., Yamasaki, K., Hanakawa, Y., Shirakata, Y., Tokumaru, S., Ijuin, T., Takenawa, T., and Hashimoto, K. (2002) "Phosphatidylinositol 3-kinase is a key regulator of early phase differentiation in keratinocytes". J Biol Chem **277**:40390-6.

Schweizer, J., P. E. Bowden, P. A. Coulombe, L. Langbein, E. B. Lane, T. M. Magin, L. Maltais, M. B. Omary, D. A. Parry, M. A. Rogers and M. W. Wright (2006). "New consensus nomenclature for mammalian keratins." J Cell Biol **174**(2): 169-74.

Seoane Leston, J. M., Aguado Santos, A., Varela-Centelles, P. I., Vazquez Garcia, J., Romero, M. A., and Pias Villamor, L. (2002) "Oral mucosa: variations from normalcy, part I". Cutis **69**:131-4.

Shieh, D. H., L. C. Chiang and T. Y. Shieh (2003). "Augmented mRNA expression of tissue inhibitor of metalloproteinase-1 in buccal mucosal fibroblasts by arecoline and safrole as a possible pathogenesis for oral submucous fibrosis." Oral Oncol **39**(7): 728-35.

Shore, L., McLean, P., Gilmour, S. K., Hodgins, M. B., and Finbow, M. E. (2001) "Polyamines regulate gap junction communication in connexin 43-expressing cells". Biochem J **357**:489-95.

Smart, J. D. (2004). "Lectin-mediated drug delivery in the oral cavity." Adv Drug Deliv Rev **56**(4): 481-9.

Smith, C., Zhu, K., Merritt, A., Picton, R., Youngs, D., Garrod, D., and Chidgey, M. (2004) "Regulation of desmocollin gene expression in the epidermis: CCAAT/enhancer-binding proteins modulate early and late events in keratinocyte differentiation". Biochem J **380**:757-65.

Soames, J. V., Southam, J. C. (2005). *Oral Pathology*. 4th edition. pp131-186. Oxford.

Soboleski, M. R., Oaks, J., and Halford, W. P. (2005) "Green fluorescent protein is a quantitative reporter of gene expression in individual eukaryotic cells". Faseb J **19**:440-2.

Song, J., Bjarnason, J., and Surette, G. M. (2005) "The identification of functional motifs in temporal gene expression analysis". Evolutionary Bioinformatics **1**:84-96.

Squier, C. A. and G. A. Kammeyer (1983) "The role of connective tissue in the maintenance of epithelial differentiation in the adult." Cell Tissue Res **230**(3): 615-30.

Squier, C. A. and M. J. Kremer (2001). "Biology of oral mucosa and esophagus." J Natl Cancer Inst Monogr(29): 7-15.

Steinert, P. M., Kartasova, T., and Marekov, L. N. (1998) "Biochemical evidence that small proline-rich proteins and trichohyalin function in epithelia by modulation of the biomechanical properties of their cornified cell envelopes". J Biol Chem **273**:11758-69.

Steinert, P. M., and Marekov, L. N. (1999) "Initiation of assembly of the cell envelope barrier structure of stratified squamous epithelia". Mol Biol Cell **10**:4247-61.

Strachan, T., Read, A. P. (2003). *Human Molecular Genetics*, 3rd edition. pp123-127. London and New York. Garland Science.

Sun, T. T., Eichner, R., Nelson, W. G., Tseng, S. C., Weiss, R. A., Jarvinen, M., and Woodcock-Mitchell, J. (1983) "Keratin classes: molecular markers for different types of epithelial differentiation". J Invest Dermatol **81**:109s-15s.

Tobin, D. J. (2006) "Biochemistry of human skin--our brain on the outside". Chem Soc Rev **35**:52-67.

Tomic-Canic, M., Day, D., Samuels, H. H., Freedberg, I. M., and Blumenberg, M. (1996) "Novel regulation of keratin gene expression by thyroid hormone and retinoid receptors". J Biol Chem **271**:1416-23.

Tomic-Canic, M., Komine, I. M. Freedberg and M. Blumenberg (1998). "Epidermal signal transduction and transcription factor activation in activated keratinocytes." J Dermatol Sci **17**(3): 167-81.

Tompa, M., Li, N., Bailey, T. L., Church, G. M., De Moor, B., Eskin, E., Favorov, A. V., Frith, M. C., Fu, Y., Kent, W. J., Makeev, V. J., Mironov, A. A., Noble, W. S., Pavese, G., Pesole, G., Regnier, M., Simonis, N., Sinha, S., Thijs, G., van Helden, J., Vandenbogaert, M., Weng, Z., Workman, C., Ye, C., and Zhu, Z. (2005) "Assessing computational tools for the discovery of transcription factor binding sites". Nat Biotechnol **23**:137-44.

Tong, Q., Tsai, J., Tan, G., Dalgin, G., and Hotamisligil, G. S. (2005) "Interaction between GATA and the C/EBP family of transcription factors is critical in GATA-mediated suppression of adipocyte differentiation". Mol Cell Biol **25**:706-15.

Tudor, D., M. Locke, E. Owen-Jones and I. C. Mackenzie (2004). "Intrinsic patterns of behavior of epithelial stem cells." J Invest Dermatol Symp Proc **9**(3): 208-14.

Vaidya, M. M., Sawant, S. S., Borges, A. M., Naresh, N. K., Purandare, M. C., and Bhisey, A. N. (2000) "Cytokeratin expression in human fetal tongue and buccal mucosa". J Biosci **25**:235-42.

Vassar, R., M. Rosenberg, S. Ross, A. Tyner and E. Fuchs (1989). "Tissue-specific and differentiation-specific expression of a human K14 keratin gene in transgenic mice." Proc Natl Acad Sci U S A **86**(5): 1563-7.

Wang, I. J., E. C. Carlson, C. Y. Liu, C. W. Kao, F. R. Hu and W. W. Kao (2002). "Cis-regulatory elements of the mouse Krt1.12 gene." Mol Vis **8**: 94-101.

Wang, X., Pasolli, H. A., Williams, T., and Fuchs, E. (2008) "AP-2 factors act in concert with Notch to orchestrate terminal differentiation in skin epidermis". J Cell Biol **183**:37-48.

Wang, Y. N., and Chang, W. C. (2003) "Induction of disease-associated keratin 16 gene expression by epidermal growth factor is regulated through cooperation of transcription factors Sp1 and c-Jun". J Biol Chem **278**:45848-57.

Wanner, R., J. Zhang, B. M. Henz and T. Rosenbach (1996). "AP-2 gene expression and modulation by retinoic acid during keratinocyte differentiation." Biochem Biophys Res Commun **223**(3): 666-9.

Wanner, R., Zhang, J., Dorbic, T., Mischke, D., Henz, B. M., Wittig, B., and Rosenbach, T. (1997) "The promoter of the HaCaT keratinocyte differentiation-related gene keratin 4 contains a functional AP-2 binding site". Arch Dermatol Res **289**:705-8.

Waseem, A., Y. Alam, B. Dogan, K. N. White, I. M. Leigh and N. H. Waseem (1998). "Isolation, sequence and expression of the gene encoding human keratin 13." Gene **215**(2): 269-79.

Waseem, A., B. Dogan, N. Tidman, Y. Alam, P. Purkis, S. Jackson, A. Lalli, M. Machesney and I. M. Leigh (1999). "Keratin 15 expression in stratified epithelia: downregulation in activated keratinocytes." J Invest Dermatol **112**(3): 362-9.

Weinmann, A. S., Yan, P. S., Oberley, M. J., Huang, T. H., and Farnham, P. J. (2002) "Isolating human transcription factor targets by coupling chromatin immunoprecipitation and CpG island microarray analysis". Genes Dev **16**:235-44.

Werner, S. and B. Munz (2000). "Suppression of keratin 15 expression by transforming growth factor beta in vitro and by cutaneous injury in vivo." Exp Cell Res **254**(1): 80-90.

Werner, T., Fessele, S., Maier, H., and Nelson, P. J. (2003) "Computer modeling of promoter organization as a tool to study transcriptional coregulation". Faseb J **17**:1228-37.

Whitbread, L. A. and B. C. Powell (1998). "Expression of the intermediate filament keratin gene, K15, in the basal cell layers of epithelia and the hair follicle." Exp Cell Res **244**(2): 448-59.

Whittock, N. V., R. A. Eady and J. A. McGrath (2000). "Genomic organization and amplification of the human keratin 15 and keratin 19 genes." Biochem Biophys Res Commun **267**(1): 462-5.

Whyte, D. A., C. E. Broton and E. J. Shillitoe (2002). "The unexplained survival of cells in oral cancer: what is the role of p53?" J Oral Pathol Med **31**(3): 125-33.

Winning, T. A., and Townsend, G. C. (2000) "Oral mucosal embryology and histology". Clin Dermatol **18**:499-511.

Winter, H., M. Rentrop, R. Nischt and J. Schweizer (1990). "Tissue-specific expression of murine keratin K13 in internal stratified squamous epithelia and its aberrant expression during two-stage mouse skin carcinogenesis is associated with the methylation state of a distinct CpG site in the remote 5'-flanking region of the gene." Differentiation **43**(2): 105-14.

Winter, H., Fink, P., and Schweizer, J. (1994) "Retinoic acid-induced normal and tumor-associated aberrant expression of the murine keratin K13 gene does not involve a promotor sequence with striking homology to a natural retinoic acid responsive element". Carcinogenesis **15**:2653-6.

Workman, J. L., R. G. Roeder and R. E. Kingston (1990). "An upstream transcription factor, USF (MLTF), facilitates the formation of preinitiation complexes during in vitro chromatin assembly." Embo J **9**(4): 1299-308.

Wu, R. L., S. Galvin, S. K. Wu, C. Xu, M. Blumenberg and T. T. Sun (1993). "A 300 bp 5'-upstream sequence of a differentiation-dependent rabbit K3 keratin gene can serve as a keratinocyte-specific promoter." J Cell Sci **105 (Pt 2)**: 303-16.

Wu, X., Quondamatteo, F., Lefever, T., Czuchra, A., Meyer, H., Chrostek, A., Paus, R., Langbein, L., and Brakebusch, C. (2006) "Cdc42 controls progenitor cell differentiation and beta-catenin turnover in skin". Genes Dev **20**:571-85.

Yang, L. C., Ng, D. C., and Bikle, D. D. (2003) "Role of protein kinase C alpha in calcium induced keratinocyte differentiation: defective regulation in squamous cell carcinoma". J Cell Physiol **195**:249-59.

Yano, S., Komine, M., Fujimoto, M., Okochi, H., and Tamaki, K. (2004) "Mechanical stretching in vitro regulates signal transduction pathways and cellular proliferation in human epidermal keratinocytes". J Invest Dermatol **122**:783-90.

Yuki, T., Haratake, A., Koishikawa, H., Morita, K., Miyachi, Y., and Inoue, S. (2007) "Tight junction proteins in keratinocytes: localization and contribution to barrier function". Exp Dermatol **16**:324-30.

Yuspa, S. H., Kilkenny, A., Cheng, C., Roop, D., Hennings, H., Kruszewski, F., Lee, E., Strickland, J., and Greenhalgh, D. A. (1991) "Alterations in epidermal biochemistry as a consequence of stage-specific genetic changes in skin carcinogenesis". Environ Health Perspect **93**:3-10.

Zabel, U., R. Schreck and P. A. Baeuerle (1991). "DNA binding of purified transcription factor NF-kappa B. Affinity, specificity, Zn²⁺ dependence, and differential half-site recognition." J Biol Chem **266**(1): 252-60.

Zhang, G., Gurtu, V., and Kain, S. R. (1996) "An enhanced green fluorescent protein allows sensitive detection of gene transfer in mammalian cells". Biochem Biophys Res Commun **227**:707-11.

Zhang, J. S., Wang, L., Huang, H., Nelson, M., and Smith, D. I. (2001) "Keratin 23 (K23), a novel acidic keratin, is highly induced by histone deacetylase inhibitors during differentiation of pancreatic cancer cells". Genes Chromosomes Cancer **30**:123-35.

Zhao, H., S. Jin, F. Fan, W. Fan, T. Tong and Q. Zhan (2000). "Activation of the transcription factor Oct-1 in response to DNA damage." Cancer Res **60**(22): 6276-80.

Zhou, Q., Cadrin, M., Herrmann, H., Chen, C. H., Chalkley, R. J., Burlingame, A. L., and Omary, M. B. (2006) "Keratin 20 serine 13 phosphorylation is a stress and intestinal goblet cell marker". J Biol Chem **281**:16453-61.

Zhu, Z., Shendure, J., and Church, G. M. (2005) "Discovering functional transcription-factor combinations in the human cell cycle". Genome Res **15**:848-55.

Website addresses

- 1) <http://www.nlm.nih.gov/medlineplus/ency/images/ency/fullsize/8912.jpg>
- 2) <http://137.222.110.150/calnet/A%20Oral%20Cav1/image/looking%20into%20oral%20cavity-features%20seen.jpg>
- 3) <http://en.wikipedia.org/wiki/Image:Skin.jpg>
- 4) http://bioinformatics.wustl.edu/webTools/PAP%20Help1_files/image041.gif
- 5) <http://www.medscape.com/content/2004/00/47/29/472915/art-nrc472915.fig1.gif>
- 6) <http://www.answers.com/topic/keratin>
- 7) <http://carolguze.com/text/102-19-tissuesorgansystems.shtml>

- 8) <http://www.lab.anhb.uwa.edu.au/mb140/corepages/integumentary/Images/skthick0021he.jpg>
- 9) <http://www.med.ufl.edu/biochem/keithr/research.html>
- 10) http://www.floridamarine.org/images/articles/23559/23559_5526.jpg
- 11) <http://www.abdn.ac.uk/staffpages/uploads/bms292/Sat-CMV-EGFP.jpg>
- 12) <http://www.wcb.ed.ac.uk/COIL/Images/Equipment/facs.jpg>
- 13) <http://www.micro.magnet.fsu.edu/cells/intermediatefilaments/intermediatefilaments.html>
- 14) <http://www.ncbi.nlm.nih.gov/Genbank/index.html>
- 15) http://en.wikipedia.org/wiki/Sticky_end#Overhangs_and_sticky_ends
- 16) http://www.mun.ca/biology/scarr/4241_RCMhelix.jpg
- 17) http://images.google.co.uk/imgres?imgurl=http://www.nature.com/embor/journal/v5/n8/images/7400200f4.jpg&imgrefurl=http://www.nature.com/embor/journal/v5/n8/fig_tab/7400200_f4.html&h=400&w=600&sz=13&hl=en&start=4&usg=__i7eR2mCdz2IKY6hCX78wXeKEL3U=&tbnid=eT50qmm2zGipSM:&tbnh=90&tbnw=135&prev=/images%3Fq%3D4%2Bhuman%2Bgenomic%2BDNA%2BAmplified%26gbv%3D2%26hl%3Den%26sa%3DX
- 18) http://en.wikipedia.org/wiki/Intergenic_region
- 19) <http://wwwn.cdc.gov/dls/ila/cd/india/Jan21/2.00-3.00%20Ramesh%20HIV%20Testing%20Technologies.ppt#332,39,Advantages>
- 20) http://en.wikipedia.org/wiki/Laser_capture_microdissection
- 21) http://www.clontech.com/images/pt/dis_vectors/PT3054-5.pdf
- 22) <http://www.pkclab.org/PKC/vector/pDsRed1N1.pdf>

Appendices

Table 7.1: Forward and reverse primer for K13 and K15 promoter sequences

K13 Forward primer	5'-tcccggagGTATACcgatggggtgggctgaaagtc -3' BstZ171
K13 Reverse primer	3'-cacaggtgagacccttctcgCCATGG-5' KpnI
K15 Forward primer	5'-agtggggaGTATACggggagtgcccttacatcctg-3' BstZ171
K15 Reverse primer	3'-tcccatatattctccccctgcactcCTTAAG-5' EcoRI

Table 7.2: primers used to amplify the K15 and K13 gene for quantitative Polymerase chain reaction

Name of primer	Sequence	GC % content	Melting temperature °C	Secondary structure	Primer dimer
K13 PCR-F:	5'-CTC CAC TCA GCT GGG AAG TC-3'	60	64.01	none	no
K13 PCR-R:	3'-CTT GAG ATC CAT CCC CTG AA-5'	50	63.94	none	No
K15 PCR-F:	5'-CTC CAC TCA GCT GGG AAG TC-3'	60	64.01	none	no
K15 PCR-R:	3'-CTT GAG ATC CAT CCC CTG AA-5'	50	63.94	none	No

Table 7.3: The number of molecules in each mole of K13 promoter deletion fragments

SCC25 or HeLa	Promoterless pEGFPN-3B	K13 FL Pro	R1	R2	R3	R4	R5	R6
Insert(bp)	0	-3018	-2540	-1953	-1512	-1017	-670	-289
Insert plus vector (bp)	4117	7135	6567	6070	5629	5134	4787	4406
Molecular weight (g)	2717220	4709100	4334220	4006200	3715140	3388440	3159420	2907960
Avogadro number 6.022×10^{23}	2656500	5134140	4833180	4445760	4153380	3828000	3600300	3348840
Avogadro number 6.022×10^{23} divide by Molecular weight (g)	2.71722	4.69722	4.38108	3.98508	3.70788	3.35148	3.11388	2.87628
Number of Molecules in (1g)	$6.02E+23$	$6.02E+23$	$6.02E+23$	$6.02E+23$	$6.02E+23$	$6.02E+23$	$6.02E+23$	$6.02E+23$
Number of Molecules in (1 μ g)	$6.02E+17$	$6.02E+17$	$6.02E+17$	$6.02E+17$	$6.02E+17$	$6.02E+17$	$6.02E+17$	$6.02E+17$
*Ratio of Promoterless pEGFPN-3B to all fragments	$2.215E+11$	$1.278E+11$	$1.389E+11$	$1.5021E+11$	$1.620E+11$	$1.776E+11$	$1.905E+11$	$2.070E+11$
FACS result	Promoterless pEGFPN-3B 4117	K13Full length Promoter -3018	K13R1 -2540	K13 R2-1953	K13 R3-1501	K13 R4-1017	K13 R5-670	K13 R6-289
The concentration of each K13 promoter construct to take to give same of molecules as promoterless pEGFP-N3B	1	1.73	1.60	1.47	1.37	1.25	1.16	1.07
Average raw FACS data of pEGFP-N3B over pDsRed1-N1	5	19	37	6	19	26	21	15

*The concentration of DNA to take for each of the K13 promoter fragments, to give the same number of molecules as promoterless pEGFP-N3B

Table 7.4: The sequence of K13 promoter fragments

Primer name	Primer length	Cat No/ ID No of Primer	Sequence	Orientation	Purpose
K13-DR1	46	10336-022 H2995G08	AAT GAC TGC GGT CTC CTC CCG TAT ACG TTT CAA GGG AAG GAG CAG C	5' to 3'	SDM of first 374bp
K13-DR2	46	10336-022 H2995G10	TTG CGA GGC CAG GGA TTC AGG TAT ACC CCT GAC CCT GCC CGG CCC T	5' to 3'	SDM of 755bp
K13-DR3	44	10336-022 H3022H06	GAG AAA CTC AGG GAC TAT GTG TAT ACC CTG CCA GAG GGA GCT TC	5' to 3'	SDM of 1100bp
K13-DR4	46	10336-022 H2995H02	CCT TGT ACC TTT TCC CAG TCG TAT ACC TGA CTC CAC ACC CCT GGT G	5' to 3'	SDM of 1593bp
K13-DR5	46	10336-022 H2995H04	AGA GGA AGT GGC CCT GTC CAG TAT ACT AGC GAA TAT TCT CCG AGC C	5' to 3'	SDM of 2039bp
K13-DR6	46	10336-022 H2995H06	TTC ACT GTG CAG GCT CTG AGG TAT ACC CAG TAT TAG AAC GGG ACC T	5' to 3'	SDM of 2623bp

Table 7.5: pEGFP-N3B Vector sequence used for K13 full length and subsequent truncated promoter constructs DNA sequencing

Primer name	Primer length	Cat No/ ID No of Primer	Sequence	Orientation	Purpose
pEGFPs	46	10336-022 H2995G07	GCT GGC CTT TTG CTC ACA TGT T	3' to 5'	For sequencing (Reverse sequence of 4658 to 4678 in pEGFP- N3B vector)

Table 7.6: Standard solution and Media

Reagent	Preparation
Ampicillin (100mg/ml)	2.5g dissolved in 25ml dH ₂ O, aliquoted into 5ml bijous and stored at -70°C or -20°C for long term storage
Buffer P1 (Resuspension buffer)	50mM Tris -HCL pH 8, 10mM EDTA, 100 µl/ml RNase A and store in 2-8% after addition of RNase A.
DNA loading buffer	20mM EDTA, 30% sucrose, 0.1% bromophenol blue, 0.1% xylene cyanol FF, 1M Tris HCL pH 8.0
DNase free RNase-A	100mg dissolved into 10ml of 0.01M sodium acetate at pH 5.3, this was then boiled to 100°C, in 50 ml falcon tubes in a glass beaker containing distilled water on top of busen burner for 15 minutes. This was then allowed to cool, then 1/10 of 10mM Tris HCl at pH 7.4, was added , this mixture was then aliquoted into 1.5ml eppendorf tubes aliquots and stored at -20°C
400ml of E4/F12 containing	75% (v/v) Dulbecco's Modified Eagle's Medium (DMEM), 25% (v/v) Ham's F12 medium.
Epilife medium with calcium	Epidermal growth factor 100ng/ml, hydrocortisone 0.18mg/ml, insulin 2.5mg/ml, transferrin 2.5mg/ml, BPE and PSA in which 1ml of each medium supplement was added to 400ml epilife medium .
E4 medium + insulin (only used for MCF 7 cell line)	400ml DMEM, 40 FCS, 4ml glutamine and 10µl insulin (50µg/ml) passed through 0.22 filter
10mM IPTG (per 10ml)	24mg of isopropyl-1-thio-β-D-galactopyranoside (IPTG), 10ml of sterile distilled water and store at -20°C and to spread 100µl per LB-agar plate
Kanamycin (100mg/ml)	2.5g dissolved in 25ml dH ₂ O, aliquoted into 5ml bijous and stored at -70°C or -20°C for long term storage.

Table 7.7: Standard solution and Media

Reagent	Preparation
LB medium	10g Bacto-trytone (Oxoid), 5g Bacto-yeast (Oxoid), 5g NaCl dissolved in 1L dH ₂ O and autoclaved
LB agar	As LB medium plus 1.5% Bacto agar (Oxoid)
LB-Amp	LB media containing 100µl/ml ampicillin
1 x Lysis buffer:	62mM Tris-HCl pH 6.8 2% w/v SDS 10% glycerol 0.05% β-mercaptoethanol 0.01% bromo-phenol blue
Lysozyme (100mg/ml)	500mg dissolved in 5ml Tris HCL
5M NaCl	292.2g in 1L dH ₂ O autoclaved
3M Na-acetate	246.08g in 1L dH ₂ O, pH adjusted to 5.5 with glacial acetic acid
NZY- Broth (per litre)	10g of NZ amine (Casein hydrolysate) 5g of Yeast Extract, 5g of NaCl add distilled water to a final volume of 950ml and then adjusted pH to 7.5 using NaOH and autoclave. Then added the following filter sterilized supplements prior to use 12.5ml of 1M MgCl ₂ , 12.5ml of 1M Mg SO ₄ , 20ml of 20%(w/v) glucose (or 10ml of 2M glucose)

Table 7.8: Standard solution and Media

Reagent	Preparation
Phosphate Buffered Saline	137mM sodium chloride, 2.7mM KCl 10mM NaHPO ₄ and 2mM KH ₂ PO ₄ made up to 500ml with distilled water.
PPC	Phenol, Phenol chloroform, Chloroform in the ratio of 24:24:1.
Proteinase K buffer	Two times Proteinase K buffer
Proteinase K enzyme	Proteinase K 20mg/ml purchase as lyophilized powder and dissolved at concentration of 20mg/ml in sterile 50mM Tris HCl at pH 8, 1.5 mM calcium acetate, stock was then divided into 1.5ml eppendorf tubes aliquots and stored at -20°C
PBS:	dissolve 1 PBS tablet per 100ml of distilled water
PBS-T:	add 500µl of Tween-20 detergent in 500ml of PBS
PBS-T+5% milk:	dissolve 5g of powder skimmed milk in 100ml of PBS-T.
Ready Mix+ medium	400ml of E4/F12, 4ml of RM+, 40ml of Foetal Calf Serum (10% FCS v/v) and 4ml of glutamine(1% v/v).
4ml 'Ready Mix' concentrate was added to final concentration of :	Hydrosorstine 0.4µg/ml, Cholera Toxin 10 ⁻¹⁰ M, Transferrin 5µg/ml, Liothyronine 2 x 10 ⁻¹¹ M, Adenine 1.8 x 10 ⁻⁴ M, Insulin 5µg/ml, Epidermal growth factor (EGF) 10 ng/ml.
Running Buffer (1L):	Tris Base 3g, Glycine 14.4g, SDS 1g made to 1 litre was distilled water.

Table 7.9: Standard solution and Media

Reagent	Preparation
SOC medium	SOC medium was supplied as 10ml bottle which contained: 2% weight/volume Tryptone, 0.5% weight/volume yeast extract, 10mM NaCl, 2.5mM KCL, 10mM MgCL ₂ , 10mM MgSO ₄ and 20mM glucose (Invitrogen) .
STE	20mM Tris HCL pH 8.0, 50mM EDTA, 8% sucrose made upto 100ml dH ₂ O.
10x TBE	445mM (54g/L) Tris, 445mM (27.5g/L) boric acid, 10mM (3.7g/L) EDTA
Tris HCL	10mM Tris –HCL, 1mM EDTA, autoclaved
Trypsin (0.25% in Versene)	NaCl 2.5g, Na ₂ HPO ₄ 8g, KH ₂ PO ₄ 0.2g, versene (EDTA) 1g, Trypsin 2.5g, phenol red 1.5ml. These ingredients were made up to 1L of distilled water. pH adjusted with NaOH to 7.2. Aliquots were supplied filter sterilized and 15 ml bottled in universals and stored at -20°C until use.
Transfer Buffer (1L)::	25mM Tris, 0.2M glycine, 20% methanol make to 800ml with distilled water then adjusted pH 8.5, added enough distilled water to make 1 litre.
Thiazolyl Blue Tetrazolium Bromide (Sigma) and also known as MTT	0.01grams of Thiazolyl Blue Tetrazolium Bromide into 20ml of appropriate media for the cells being used then container was wrapped with foil and left at 4°C till use.
Versene	NaCl 8g, KCL 0.2g, Na ₂ HPO ₄ 1.2g, KH ₂ PO ₄ 0.2g, Versene (EDTA) 0.2g, phenol red 1.5ml these ingredients were all dissolved and made up to 1L in distilled water. pH adjusted with NaOH to 7.2, and the solution was aliquoted into 16ml universals and autoclaved for 20 minutes prior to storage at 4°C.
2% X-Gal (per 10 ml)	0.2g of 5-bromo-4-chloro-3-indolyl- β-D-galactopyranoside (X-Gal), 10ml of dimethylformide (DMF) and store at -20°C and to spread 100µl per LB-agar plate

Table 7.10: Materials used in the study and company of purchase

dATP, dTTP, dCTP, dGTP (100mM) (Promega).
BIO-X-ACT Long DNA polymerase, 10X OptiBuffer (Bioline, UK).
Human genomic DNA (Promega).
DNA ladder (Promega).
Forward and reverse primers for K13 and K15 promoter amplification (Invitrogen).
Forward and reverse primers site directed mutagenesis of K13 promoter(Stratagene).
Restriction endonucleases and their buffers (New England biolabs UK).
2X quick ligation buffer and T4 DNA Ligase (Invitrogen).
Ampicillian and kanamycin (Sigma, UK).
Topo TA vector cloning kit (Invitrogen) and pEGFP-N3 vector (BD Biosciences).
One shot <i>E.coli</i> competent cells (Invitrogen).
XLI0-Gold ultra competent cells and XLI0-Blue ultra competent cells (Stratagene).
Miniprep and maxipreparation of DNA kits (Qiagen Ltd, Crawley, UK).
Hams F12 and E4 media (cancer research UK).
DMEM and Typsin (Biowest and Gibco).
4 alpha PMA and TPA (Promega).
PI3K and AkT pathway LY294002 inhibitor (Calbiochem).
MEK 1/2 pathway PD98059 inhibitor (Calbiochem).
Trichostatin A (Calbiochem).
Sodium Butyrate (Calbiochem).
Fugene 6 (Roche 6).
Lipofectamine (Invitrogen).

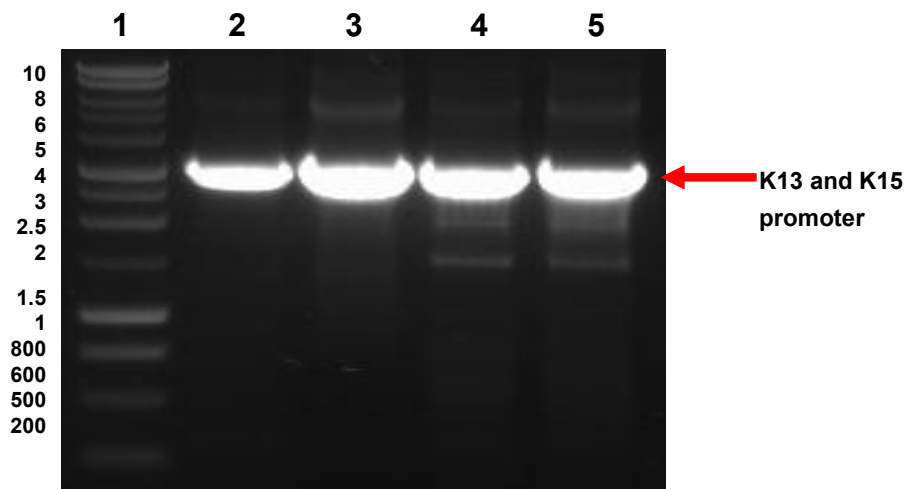


Figure 7.1: Ethidium-bromide stained agarose gel showing results of K13 and K15 promoter PCR product amplified from K13 and K15 promoter pEGFP-N3B construct. Lane 1: 10Kb DNA ladder, Lane 2 and 3: K13 promoter PCR product (3Kb) in absence and presence of enhancer, Lane 4 and 5: K15 promoter PCR product (3Kb) in absence and presence of enhancer. The DNA was analysed on 1.5% agarose containing ethidium bromide.

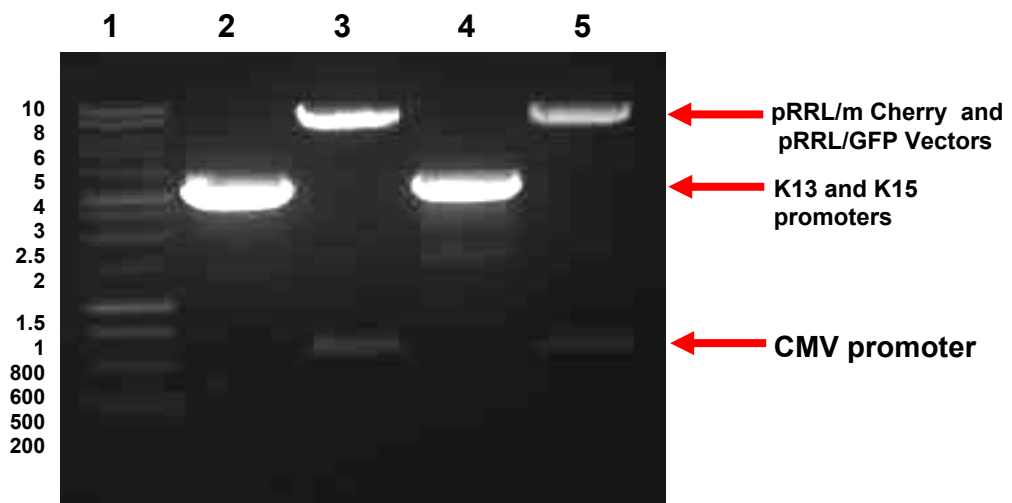


Figure 7.2: Ethidium-bromide stained agarose gel showing results of K13 and K15 promoter PCR product and pRRL/m Cherry and pRRL/GFP vectors digested with XbaI and ClaI prior to ligation. Lane 1: 10Kb DNA ladder, Lane 2: K13 promoter PCR product (3Kb) digested with Xba I and ClaI to linearize the K13 promoter, Lane 3: pRRL/m Cherry vector digested with Xba I and ClaI to remove CMV promoter (562bp), Lane 4: K15 promoter PCR product (3Kb) digested with Xba I and ClaI to linearize the K15 promoter, Lane 5: pRRL/GFP vector digested with Xba I and ClaI to remove CMV promoter (592bp). The DNA was analysed on 1.5% agarose containing ethidium bromide.

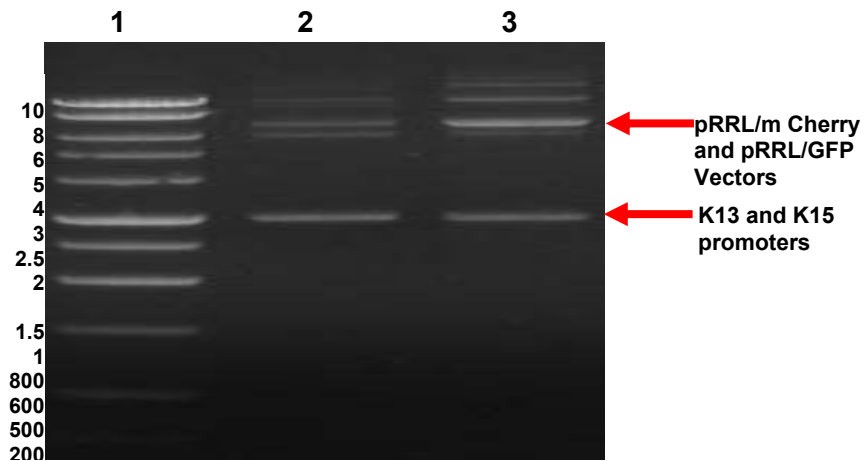


Figure 7.3: Ethidium-bromide stained agarose gel showing results of K13 and K15 promoter PCR product ligated to pRRL/m Cherry and pRRL/GFP vectors digested with XbaI and ClaI. Lane 1: 10Kb DNA ladder, Lane 2: K13 promoter PCR product (3Kb) and pRRL/m Cherry digested with Xba I and ClaI to linearize the K13 promoter, Lane 3: K15 promoter PCR product (3Kb) and pRRL/GFP vectors. The DNA was analysed on 1.5% agarose containing ethidium bromide.

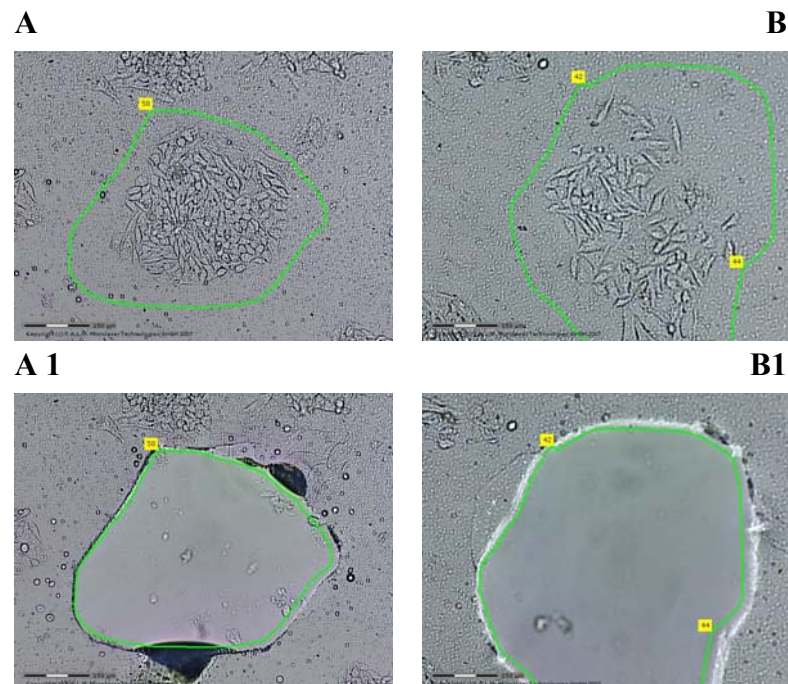


Figure 7.4: K15 promoter construct expression in holoclone (A) and paraclone (B) colony of oral SCC25 cells prior to catapulting (A and B) and after catapulting (A1 and B1) using laser capture software, with a catapulting energy of 50 watts required to lift the cut section of duplex petridish.

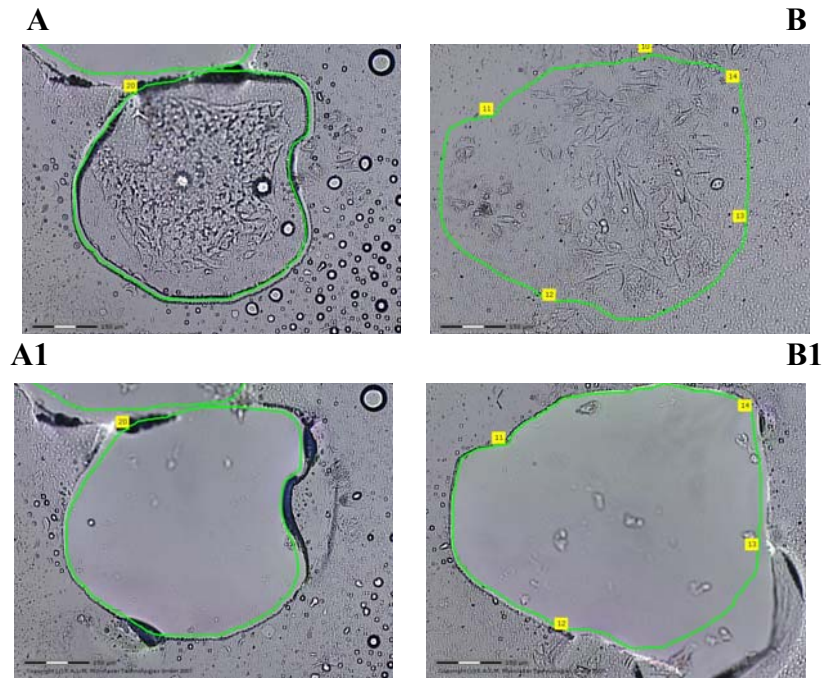


Figure 7.5: K13 promoter construct expression in holoclone (A) and paraclone (B) colony of oral SCC25 cells prior to catapulting (A and B) and after catapulting (A1 and B1) using laser capture software, with a catapulting energy of 50 required to lift the cut section of duplex petridish.

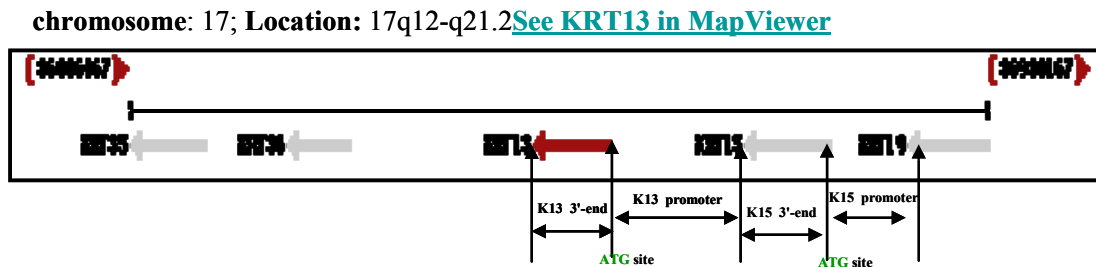


Figure 7.6: Diagram showing the maximum upstream promoter size and the 3'-end downstream size of K13 and K15 gene relative to their gene positions in the chromosome 17: Using the ncbi database the maximum upstream promoter size of K13 and K15 was estimated to be around 8Kb for K13 and 4.6Kb for K15 (picture obtained through extrapolating the ncbi website number 14 in the reference section).

```

-3001 ggacacttttctgtctcagcctggagacctgggaataggggggagggggatggggaaat
-2941 tgaggggaatgccctttcaatcctcgtggtcactcgtggccacttcagctctgttgagcaatc
-2881 cctgtgagtcactctgtccaaactgaggtcaggctgagctgaggttatctccatttccc
-2821 tgatgtgagactaaagctcagagagggagggcgcattaccaaagccgaccagctggt
-2761 aaatgggaaaagaggggtttaaaggttaagctctctgggctccagaccacacccctctccc
-2701 tggcatttccctggggaacaggagaggtgtggggaggttcaaggttgttgagagctca
-2641 ttctccttgtgccctcaaagtctcactatggccctgagggaggtctgtgttaatggccta
-2581 agttaaatcaggaaccaggctcagagaggtgagctctctccactgggctgcactgcc
-2521 tcaattcaagggaaaaagggccagctccacagatggcccccactctggctgcagtgggcaaa
-2461 gtcagaaactggcacagcatcctgggcaggctgctcggggcaggggccgg gsetacaagc
-2401 tgggctggggccagacagagctttatcttcgcaaggccatcccacctggtgctaatgagg
-2341 aggctccgggcccacccagatctggagctcacagttagcgtttggactgaaaccagggga
-2281 tttgtgctggggcagtgaggggggcagctgcccccctggcctgggctgagagatag
-2221 agaaaagccacctcgaagggctgctggagagagtcagggtgcagaaggggatactggctggg
-2161 gtcacagcccttctcaccctgggggtgaaaggcgagtaattgttcttgagttaatctgtgg
-2041 gggccacaatgtctgcagaggcttttaagagctctggatgactgagtttgatattttt
-1981 ctttcggagggaaaagacaataccctcccaccctgagacaaataccacactgtctgtgcc
-1921 agcatggaggccaggctcactgcgaagatggatgagaaggaaccccccaccctctgc
-1861 tggctggcagttccccttgcagccagctcagatgcaggaatattggggtctgcaggaag
-1801 gaacttctccctgtgccctgtttggtgaggggtgaggaacctgttgagctcctggctt
-1741 gcccttaccaggttgccactggccacaagtgtctcactctcccaagttcaaatctca
-1681 ttctttctgaaactctgggtgggggtcaccctctgtgtgagggatgagagggatgagga
-1621 tgcaaaagtctctgttaaatcaaaagtgcagggtagaagtaaaaggtatgctctata
-1561 gcaaaaataagaacctaaagaacaacctgcgttgcacctaggagctggctatggaaagctc
-1501 atgcccttgagcctaaagaacctgctcaggctcacagggtcattctgagccccacaaca
-1441 aaagccctcctggtaggggactcaggccaggtgcccgtcactgcaacctggcccctgca
-1381 tgtctggcaactgggtggggatccaggaagggcaggatgggggctctgggcccaggg
-1321 cttccctggaggtgagaggtgagagggccctctgcacagggaaacagagacttaaaag
-1261 gtaaatgtccacagcttaccatggttaattggtagggtaggattgaaaccagcctca
-1201 cagcttaccatgatattgataaaggcaggatcaaaaccgggctgagggactccaga
-1141 cctctgccacttaccatgctgcaacctgggctaggaactcctcctgagtttctgtga
-1081 agccctggggccaggctccagagggctgagccacacctccaagtggcactgcccacagga
-1021 tcaggtgtccctgaaaggtgtccctgagctggtggccagagaaaaggctcctcgtgag
-961 ttcaactcccctgtgtgtagcaaatgctctggtcttcaagatctccggtgtctccag
-901 cctgctgcccagctctccctctcttcccttccacagcatcaggcacatagagcctctg
-841 cagggccctgccccagccagcactgacagagacagatgggggcaatctggccctgcta
-781 agcagcagcatgctctcctggagaaggcaggggcttccggaaactgcccagccttat
-721 cagcggaggtttgcccacaacatcccagaacagcagaaggttcagcgcctgcaagt
-661 gcaggtgtgggatacatcagtcacccctgtcagtcaccaagcctgctgggctttgtga
-601 ggggtgccaaggaacacaggtggaggatggcagggggggagtagaggtgggagggggag
-541 tccactgcagcaccaggtgagggatgagctggtcctcctggtcactcagctcagctgaa
-481 cactactcaaggtccctggtcctgctcctccactgcccagggggccctgcatcccat
-421 ccccagggctccactctccctgagccctgagctctcactcactcactcactcactca
-361 ttcactcactcactcactcagaggttttgagttggaataacacagcataatgatcgcca
-301 gggactcccaactaaagaacagggagctgctcctctggggagaggtcagggtcgggg
-241 aaagtgaagtcagctgagggcagcagttggcctgagctgctcagtcacagcagaggtc
-181 tggtagctgtgctgtagtagagttgctcctcctgctcctctctggcaatggagagatg
-121 aaactgtaataccaagtttaaaacctgcccctggggaaaaacactataatctgaaatg
-121 tctctttgtgcattaaaaaaaaaataagaagaaaaaacctcactgaccactcaaggt
-61 gtcagggcagctgtgtttgtcaggaagggcagaagggagttgctttgctttagggggagc
-1 gtaggctcccacaacacctctgaagggatataaaggagccccagcgtgagcctggcct
+1 ggtacctcctggcagcactctctgggtttgctgagaactcacgggctccagctaccttggc
+61 ctgcaacacacactctctgcaaaactctctcccaactctggggctggctcaaccgggg
+121 gggtccctcctgctggggaggtgagctttggtgggggagctctctggggaggtgg
+181 aaagcgaagtatctcagctctctctgctaggtttgtctctctcagggctcagggagagata
+241 gggggtgcatgaggtctgtggctttggtggagggctgtaggtgtttctcgtggaag
+301 ctttggagggggcgttggtaggggttttggtagggttttggtaggagcaggtgggtgt
+361 ctctctggcaatgagaaaataaccatgcagaacctcaatgaaccctggcctcctcact
+421 ggacaaggtacgtgccctggaggggccaatgctgacctggaggtggaagatccatgactg
+481 gtcccagaagcagaccccacccagccagcaatgogactacagccaatactccaagaacct
+541 tgaagagctccgggacaaggtgagctcctggatgtcaaaagagggggagcaggtggctgg
+601 taccctgtacacagctctaagtctcaggttactgctgactcaaggaaactcttccctgcc
+661 caggcaatgactgtcgttatgtaactcagcaaaattggaatgcacctgctgtccaggt
+721 gcagagggcagtgacatctctcaacttgggtgctgggggagggagagaggggtctt
+781 gggaatcctggttaggaccaacaggggacaggtgggggcaataataaagaccagagggca
+841 gtagctcacacctgtaataccagctgcttggggggccaaggtgataggttctcgtgtc
+901 caggtttagaggtgcagtgagctatgactgcccactgcaactccggcctaggtgacag
+961 agtggaaacctgtatctaatataaaaaataataaaaaaaaagagcaactcgcctccc
+1021 tacctcatgcccctgagcctctctgcataaagattctcttacctcttttgcagaagt
+1081 ggattggaggtggcctcatgagttccagatgtagaacctctgtcttttccataaag
+1141 aggtctttgtgcccanaagactgttgggtcttaggagacctgggaaactcattacaact
+1201 ctgccaccactcactcaccattttactccctaaagctgggttctcattgttaaaatgc
+1261 ctctttaactgccctccaggttgcctactggctggaatgtctctgagatccatggctgt
+1321 ccaaggtgtgcagggagcagtgacctgagttgtccacagtggggctgggtggaggtctc
+1381 tgagagagctatgtcagagctggctgcaccccactgcccactcctctgggcaacaaat
+1441 tcccacaggaactactgctccttggcttcttgggctggagataaaggaagcagctcc
+1501 tcaaggtgtctcaagaggtggaatgggcaaaaacagaaatggacactgaaagtgaggtc
+1561 ggacttggcccacccagagcctcaagattttgttgggtgctcagaggggtgagtg
+1621 tcagtaggggtgatttcaatgaggggtggccttgggtgcagagcagagagcagcag
+1681 ggagagagagaggtcctctagacaccagctctgctcctcagatcatggccaccacct

```

Figure 7.7: The K15 upstream and downstream nucleotide sequence. The black coloured nucleotide sequence corresponds to the full length -3.018kb K15 promoter. The underlined black nucleotide at the top and bottom respectively correspond to the region where the forward and reverse primers was designed to amplify the 3.018kb K15 promoter. The original K15 promoter sequence (6 nucleotides, underlined in black) does not differ much from the BstZ17I site (GTATAC), so this sequence corresponds to the site where BstZ17I primer was designed, in attempt to retain or minimise change to the BstZ17I sequence. The underlined navy blue 6 nucleotides sequence correspond to the site where EcoRI was designed. The red 3 nucleotides sequence corresponds to the ATG and the yellow (+61-541) highlighted sequence corresponds to the start of coding region (exon 1). The light blue (+541-1681) highlighted sequence corresponds to K15 intron 1.